

MEA Meeting 2022 Abstract Book

The abstract book is compiled in the following order, with 69 poster abstracts followed by 26 oral presentation abstracts.

Presenting author	Title
Sophie Kussauer	Stem Cell- Derived Pacemaker Cells for Drug Testing Applications
Udo Kraushaar	Laser-induced action potential like cardiac action potential recordings on microelectrode array systems for increased predictivity in cardiac safety pharmacology
Michele Dipalo	Long-term recording of cardiac action potentials for chronic cardiotoxicity assessment
Alessio Boschi	A Mirror Virtual Cell for Label-Free, Accurate, and Noninvasive recordings of Action Potentials of Human-Derived Cardiomyocytes
Jihyun Lee	Repeated and on-demand intracellular recording of cardiomyocytes
Barbara Genocchi	Covariance and entropy analysis to better depict astrocytes effects in neuron-astrocyte networks cultured on MEAs.
Kerstin Lenk	Neuronal and astrocytic interactions in schizophrenia: A computational modeling study
Misaki Inaoka	Microelectrode arrays for detection of astrocytic activity
Eva Voogd	Effect of hypoxia and temperature investigated in a human in vitro model of the ischemic penumbra.
João Santiago	Oxygen Gradient Device for the In Vitro Study of Ischemic Stroke
Joose Kreutzer	Device for Studying Acute Ischemic Conditions
Emre Kapucu	Parkinson's-on-Chip Model: Screening the activity and its propagation of hPSC-derived neurons during α -synuclein aggregation on MEA embedded microfluidic chips
Manuela Gries	Functional and electrophysiological changes of the gut and the enteric nervous system in an Alzheimer's and Parkinson's disease model
Clemens Sauter	Electrophysiological characterization of human pluripotent stem cell-derived disease models of hereditary spastic paraplegia type 4 (SPG4)
Sabrina Oerter	A hiPSC-based model of PARK2 copy number variation carriers: Finding the link between adult-onset ADHD, mitochondrial function and NVU impairment
Jenny Wickham	Neocortical Layers 5 and 6 are the Drivers of Baseline Network Activity in Micro-electrode Array Recordings of Epileptic Human Brain Slice Cultures
Mireia Gómez-Budia	Synaptic function in human cortical biopsies from patients with idiopathic normal pressure hydrocephalus
Martina Brofiga	Characterization of the cortical-hippocampal interactions in an in vitro MEA-based model
Francesca Callegari	Towards understanding in vitro brain circuits: a study on cortico-hippocampal and cortico-thalamic cultures
Fabio Poggio	Neuronal heterogeneity as necessary condition to perform pharmacological studies on brain-on-a-chip models
Giulia Parodi	Long-term electrophysiological characterization of excitatory neuronal networks derived from human induced pluripotent stem cells
Stephan Ihle	Inducing stimulation dependent plasticity in topologically constrained small-scale neuronal networks
Gerco Hassink	Synaptic densities are restored in primary neural cultures exposed to electrical stimulation after a period of hypoxia
Xin Hu	Simultaneous Optical and Electrical Recordings of Large-scale Neuronal Network

Daniel Ziesel	Subthreshold electrical stimulation to promote plasticity in neuronal networks
Anouk Heuvelmans	Modelling mTORopathy-related epilepsy in cultured murine hippocampal neurons using the Multi-Electrode Array.
Nruthyathi Nruthyathi	Enhancing the activity of GABAA receptors but not GABAB receptors abolishes pathological oscillations in retinitis pigmentosa mouse model rd10
Miriam Reh	Expression of Channelrhodopsin-2 (ChR2) in retinal cells restores visual responses in blind mouse retina
Nairouz Farah	Investigating the survival and function of retinal ganglion cells in an organotypic culture: An in-vitro model for studying synaptogenesis
Gal Shpun	Fabrication of a 3D high-resolution implant for neural stimulation - challenges and solutions
Andrea Kauth	Analyzing MEA-chip designs for electroporation-based genetic modification in novel retinal implants
Donatella Di Lisa	Electrophysiological recording of a patterned neuronal network realized with ink-jet printing technique
José Mateus	Spontaneous bidirectional signal conduction along axons in vitro
Mahdi Ghazal	Accurate neurons localization in 2D cell cultures by using high performance electropolymerized microelectrode arrays correlated with optical imaging
Marc Heuschkel	A MEA-based in vitro Traumatic Brain Injury Platform
Audrey Sebban	Micro-structured microfluidic devices implemented with a custom MEA for all human neuromuscular junctions
Katarina Vulić	Tailoring neuronal connectivity using PDMS microstructures with nanochannels on MEAs
Bharat Nowduri	Collagen-like gold nanostructures on microelectrodes promote neuronal adhesion and growth
Tobias Ruff	Towards biohybrid brain stimulation using unidirectional PDMS based axon guidance structures
Jens Duru	Compartmentalization of neural networks on CMOS MEAs using PDMS microstructures
Steven Schulte	Long-term monitoring of morphological and functional properties in enteric neuronal networks in vitro using a novel upside-down microelectrode array approach
Tomi Rynnänen	Improving the lifetime of the silicon nitride insulator layer in microelectrode arrays
Dominique Decker	Fabrication of whole-surface-nanostructured MEAs to improve neuronal signal recording
Maximilian Becker	Current response of ferroelectric microelectrodes to sinusoidal voltage signals
Markus Pribyl	Fabrication and functionalization of selective laser etched microfluidic devices
Heinz Wanzenboeck	Direct LCD-3D printing onto MEA substrates
Rasmus Schmidt Davidsen	Pyrolytic and selectively passivated 3D carbon pillar electrodes on interdigitated fingers for local stimulation
Corentin Scholaert	Dendritic-like PEDOT:PSS electrodes for 2D in-vitro electrophysiology
Reem Almasri	Liquid-crystal transducers: Towards a multi-optrode array system for electrophysiology sensing applications
François Ladouceur	All-optical neural interfaces: architecture and scalability
Johannes Gurke	Hybrid fabrication of multimodal intracranial implants for electrophysiology and local drug delivery

Domenic Pascual	Flexible microelectrode arrays for intrapancreatic recording
Thoralf Herrmann	A Test bench for flexible implants
Blandine Clément	Toward the development of a stretchable nerve-on-chip platform to study the role of tensile stress in peripheral neuropathies in vitro
Eashika Ghosh	Concepts for multi-layer flexible microelectrode arrays with active electrode addressing for future epiretinal implants
Aaron Delahanty	Thin CMOS-compatible silicon scaffold for interfacing with 3D cell culture models
Beata Trzpił-Jurgielewicz	Low-distortion CMOS neural preamplifier for high-channel-count neuroelectronic interfaces
Andreas Pickhinke	CMOS-compatible fabrication of vertical nanoneedles for an optimized intracellular in vitro cell contact
Timo Lausen	A Low-Noise CMOS MEA with 4k Recording Sites, 4k Recording Channels, and 1k Stimulation Sites
Onur Toprak	Memristive device integration on CMOS MEA chips for neural activity detection
Hasan Ulasan	Electrochemical Measurement Platform within Multi-functional High-density Microelectrode Array
Raziyeh Bounik	A new CMOS-electrode-array-based impedance sensor integrated into an open microfluidic platform
Tobias Gänswein	Tracking Axon Initial Segment Plasticity using high-density microelectrode arrays: A Computational Study
Xiaohan Xue	High-throughput ground-truth validation of neuronal spike sorting algorithms
Erdem Altuntac	Spatiotemporally Resolved Neurogenic Computational Model
Timo Salpavaara	Understanding electrical signals in volume conductor on MEA
Martina Lamberti	Prediction in in-vitro neural networks
Benedikt Maurer	Studying the information processing of small patterned neural networks in vitro
Gerco Hassink	Interface development to facilitate measurement of neuronal activity using micro electrode arrays
Ellis Meng	Polymer Microelectrode Array Interfaces to the Nervous System
Helen Steins	A Flexible Microelectrode Array for Bioelectronic Interfacing
Ivan Minev	Rapid prototyping of soft electrode arrays for implantable, wearable and cell culture applications
Lucia Wittner	Physiological and pathological synchronisations in the human cortex
Brett Emery	Investigating Multimodal Neurogenesis: Olfactory Bulb and Hippocampal Networks on a High-density Neurochip
Marta Cerina	Neuroprotective role of lactate release from astrocytes in a human in vitro model of the ischemic penumbra
Marta Care	Towards personalized neurostimulation strategies to restore brain function after lesion
Andrey Vinogradov	Openly available MEA dataset from hPSC-derived and rat cortical networks and associated data analysis pipeline
Nina Doorn	In silico modeling to unravel human neuronal network phenotypes on microelectrode arrays
Philipp Hornauer	DeePhys, a machine learning-driven platform for electrophysiological phenotype screening of human stem-cell derived neuronal networks
Diego Ghezzi	Neuroprostheses for artificial vision
Jiri Ehlich	Direct measurement of oxygen reduction reactions at neurostimulation electrodes
Andrea Corna	In-vitro evaluation of artificial vision restoration in the retina using high density micro-electrode arrays

Domingos Leite de Castro	Delayed feedback control as a closed-loop stimulation protocol to disrupt oscillatory network bursting in vitro
Susanna Mierau	Network function in human cerebral organoids as a platform for mechanistic and therapeutic advances in cognitive disorders
Csaba Forro	Kirigami-like mesh-electrode-arrays for integration with human electrogenic organoids
Oramany Phouphetlinthong	Micro Electrode Array for the monitoring of inner electrical activity of cerebral organoids
Anssi Pelkonen	Microelectrode array recording of midbrain organoid slices cultured in air-liquid interface
Donhee Ham	Brain, copy and paste
Hasan Ulasan	Impedance Measurements and Electrophysiological Recordings of Mouse Retinae on a Multifunctional HD-MEA Platform
Pawel Jurgielewicz	Microstimulation in the rat barrel cortex using custom ASIC-based 512-channel system and high-density silicon probes
Rahul Panat	3D Printed Customizable Neural Probes
Paolo Cesare	A multimodal 3D neuro-microphysiological system with neurite-trapping microelectrodes
Ropafadzo Mzezewa	Development of functional in vitro model in Dravet syndrome patient hiPSC-derived cortical neurons
Andrea Kauth	Development of a microelectrode array with embedded microfluidic inputs for electroporation of retinal slices
Giada Cattelan	Evaluation of a novel in vitro neurocardiac cellular model for the study of heart disorders.

Stem Cell- Derived Pacemaker Cells for Drug Testing Applications

Sophie Kussauer^{1,2*}, Patrick Dilk^{1,2}, Moustafa Elleisy^{1,2}, Anne-Marie Galow³, Julia Jung^{1,2}, Andreas Hoeflich³, Robert David^{1,2*}

¹ Department of Life, Light, and Matter of the Interdisciplinary Faculty at Rostock University, 18059 Rostock, Germany

² Reference and Translation Center for Cardiac Stem Cell therapy (RTC), Department of Cardiac Surgery, Rostock University Medical Center, 18057 Rostock, Germany

³ Institute of Genome Biology, Leibniz Institute for Farm Animal Biology (FBN), 18196 Dummerstorf, Germany

* Correspondence: Sophie.Kussauer@med.uni-rostock.de, Robert.David@med.uni-rostock.de

Cardiovascular diseases are the most common cause of death worldwide and therefore require an increased scientific attention. As therapeutic strategies evolve, more and more patients with ischemic heart disease survive but subsequently suffer from cardiac arrhythmias. In addition to disease-related arrhythmias, drug-induced rhythm disturbances also occur as adverse side effects. Hence, there is an urgent need for suitable test systems both for toxicity screening of drugs that have a direct influence on the cardiac conduction system and for the assessment of possible side effects of already approved drugs with and without cardiac indication.

To address this issue, our group developed a protocol for the generation of functional cardiac pacemaker cells from pluripotent stem cells (PSCs)[1]–[4]. Recently, we defined the transcriptome of the cells on single cell level using 10 x Genomics technology, confirming their pacemaker cell identity [5].

Using these cells *in vitro*, we are currently working on transference of cardiac risk assessment relevant for the cardiac conduction system based on micro electrode arrays (MEA). Here we describe long- term cultivation of these cells on the MEA-platform which required a number of crucial optimization steps: our cell clusters resulting from the selection process have a very strong cohesion, are difficult to dissociate and the single aggregates have a very low ability to establish new cell-cell contacts among each other. Nevertheless, these connections are inevitable for obtaining meaningful results from MEA measurements. After developing a suitable protocol, we gained a cell-layer of pure cardiac pacemaker cells on an MEA surface that is viable and electrophysiologically active over several weeks, showing pacemaker specific excitation properties. Responses to known test substances, such as carbachol, isoprenaline and ZD 7288 led to expected influences on beating frequencies and conduction velocities.

To summarize, our system for the first time allows answering cardiac conduction system-relevant questions in a cellular network, both under baseline conditions and after drug exposure.

References

- [1] J. J. Jung *et al.*, “Programming and Isolation of Highly Pure Physiologically and Pharmacologically Functional Sinus-Nodal Bodies from Pluripotent Stem Cells,” *Stem Cell Reports*, vol. 2, no. 5, pp. 592–605, May 2014, doi: 10.1016/j.stemcr.2014.03.006.

- [2] C. Rimbach, J. J. Jung, and R. David, "Generation of Murine Cardiac Pacemaker Cell Aggregates Based on ES-Cell-Programming in Combination with Myh6-Promoter-Selection," *JoVE*, no. 96, p. 52465, Feb. 2015, doi: 10.3791/52465.
- [3] F. Hausburg, J. J. Jung, and R. David, "Specific Cell (Re-)Programming: Approaches and Perspectives," in *Advances in biochemical engineering/biotechnology*, vol. 163, 2017, pp. 71–115. doi: 10.1007/10_2017_27.
- [4] A. Yavari *et al.*, "Mammalian γ 2 AMPK regulates intrinsic heart rate," *Nat Commun*, vol. 8, no. 1, p. 1258, Dec. 2017, doi: 10.1038/s41467-017-01342-5.
- [5] A.-M. Galow *et al.*, "Quality control in scRNA-Seq can discriminate pacemaker cells: the mtRNA bias," *Cell. Mol. Life Sci.*, vol. 78, no. 19–20, pp. 6585–6592, Oct. 2021, doi: 10.1007/s00018-021-03916-5.

Laser-induced action potential like cardiac action potential recordings on microelectrode array systems for increased predictivity in cardiac safety pharmacology

Jasmin Schäfer,^a Timm Danker,^a Karin Gebhardt,^a Udo Kraushaar^{a,*}

a. NMI Natural and Medical Sciences Institute at the University of Tübingen, 72770 Reutlingen, Germany

* udo.kraushaar@nmi.de

Live-threatening drug-induced cardiac arrhythmia is often preceded by a prolonged cardiac action potential (AP), commonly accompanied by small proarrhythmic potential fluctuations. The shape and time course of the repolarizing fraction of the AP can be pivotal for the presence or absence of arrhythmia.

Microelectrode arrays (MEA) allow easy access to cardiotoxic compound effects via extracellular field action potentials (fAP). Although a powerful and well-established tool in research and cardiac safety, the fAP waveform does not allow to infer the original AP shape due to the intrinsic AC filtering of the recording principle.

The newly developed device LUCE by Foresee Biosystems can repetitively open the membrane of cardiomyocytes growing on top of the MEA electrodes at multiple cultivation time points, using a highly focused nanosecond laser beam. The laser poration enables transcellular voltage recordings, resulting in transforming the electrophysiological signal from fAP to intracellular-like APs. This intracellular access allows precise quantification of the AP shape and better classification of proarrhythmic potentials, including early and late afterdepolarizations and ectopic beats (in comparison to regular MEA recordings).

This system is a revolutionary extension to existing electrophysiological methods, permitting accurate evaluation of cardiotoxic effect with all advantages of MEA-based recordings (easy acute and chronic experiments, signal propagation, etc.).

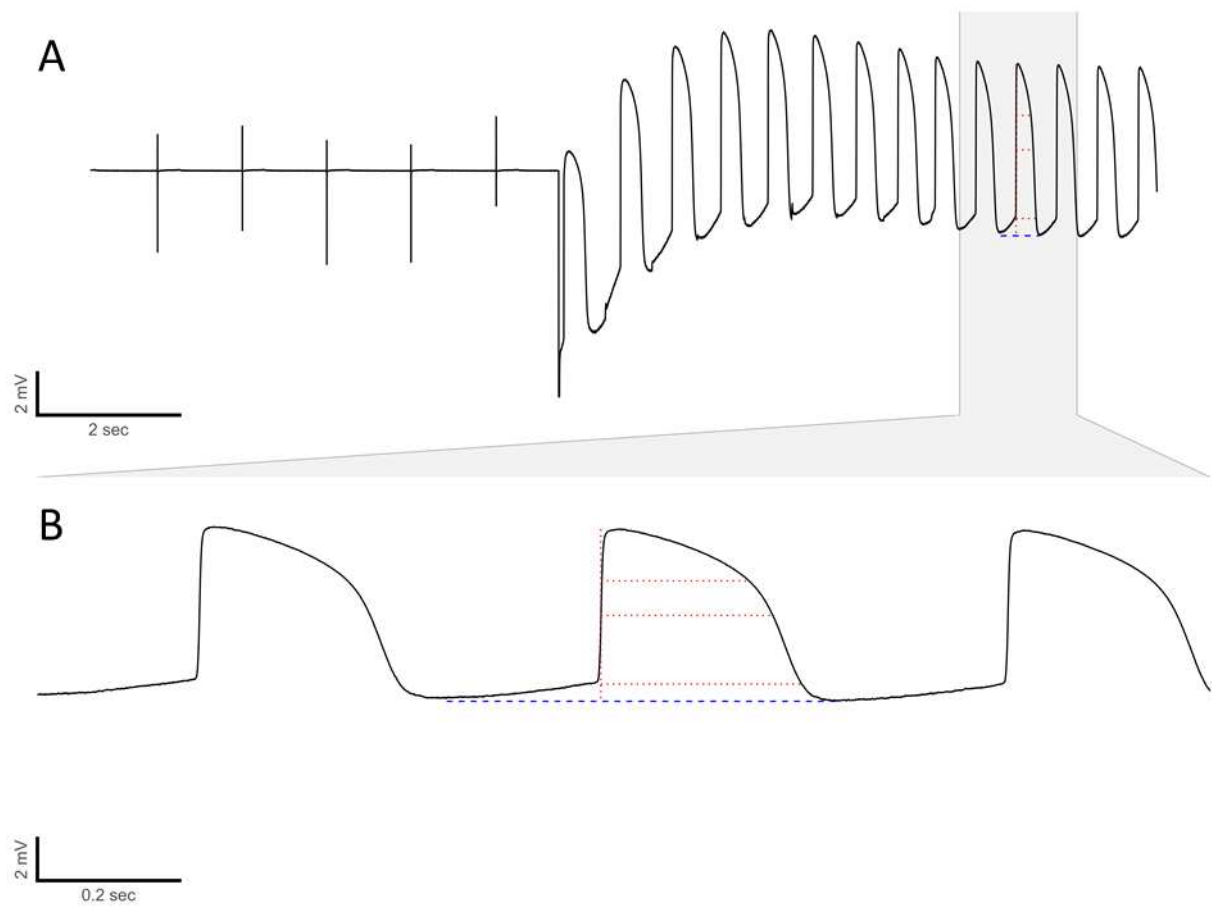


Figure 1: Laser poration transforms fAP signals into intracellular like APs

A Trace of a MEA recording showing the transformation of fAP signals to intracellular like APs of cardiomyocytes after being porated by the highly focused laser beam. B Close-up of the intracellular like action potential shape which allows quantifying different action potential parameters such as the action potential duration (APD, indicated with red horizontal lines), action potential amplitude (APA, indicated with red vertical line) and the interspike interval (ISI, indicated with blue line).

Long-term recording of cardiac action potentials for chronic cardiotoxicity assessment

Giuseppina Iachetta,^a Nicolò Colistra,^b Giovanni Melle,^b Francesco De Angelis,^{a*} Michele Dipalo^{a,*}

- a. Istituto Italiano di Tecnologia, Via Morego 30, Genova, Italy
- b. Foresee Biosystems S.r.l., Via XX Settembre 33/10, Genova, Italy

* michele.dipalo@iit.it, francesco.deangelis@iit.it

The process of drug discovery is an extremely long and expensive one [1], and cardiotoxicity is still the major cause of drug failure and withdrawn from the market [2]. To make drug development more efficient, the reliable identification of chronic cardiotoxic effects during *in vitro* screenings is fundamental for filtering out toxic compounds before *in vivo* animal experimentation and clinical trials. Current techniques such as patch-clamp, voltage indicators, and standard microelectrode arrays (MEAs) do not offer at the same time high sensitivity for measuring transmembrane ion currents and low-invasiveness for monitoring cells over long time. Although MEAs provide non-invasive and long-term measurements of electrical signals from electrogenic cells [3], this technology is limited to record extracellular field potentials (FPs) instead of the intracellular action potentials (APs). Extracellular FPs occur as a biphasic signal, whereas intracellular APs waveforms display the collective activity of several ion channels, providing crucial information about the complex effects of drugs on transmembrane ionic currents. Here, we propose laser-based optoporation [4-6] applied to MEAs to measure intracellular APs from human induced pluripotent stem cells (hiPSC-CMs) for more than 1 continuous month (see Figure 1). Thanks to an automatic optoporation by means of laser scanning, we obtain high-quality intracellular AP recordings from all electrodes of the multiwell 60-electrode commercial MEAs and the individual interval sessions of intracellular APs can last as long as 20-30 minutes. In particular, our approach permits the accurate electrophysiological assessment of cardiac syncytia maturation during time and provides reliable data on chronic cardiotoxic effects caused by known compounds such as pentamidine [7], a hERG channel trafficking inhibitor, and doxorubicin [8], one of the most effective chemotherapy drugs. Our results demonstrate that optoporation may be an effective *in vitro* strategy to detect chronic cardiotoxicity in the early phases of drug development.

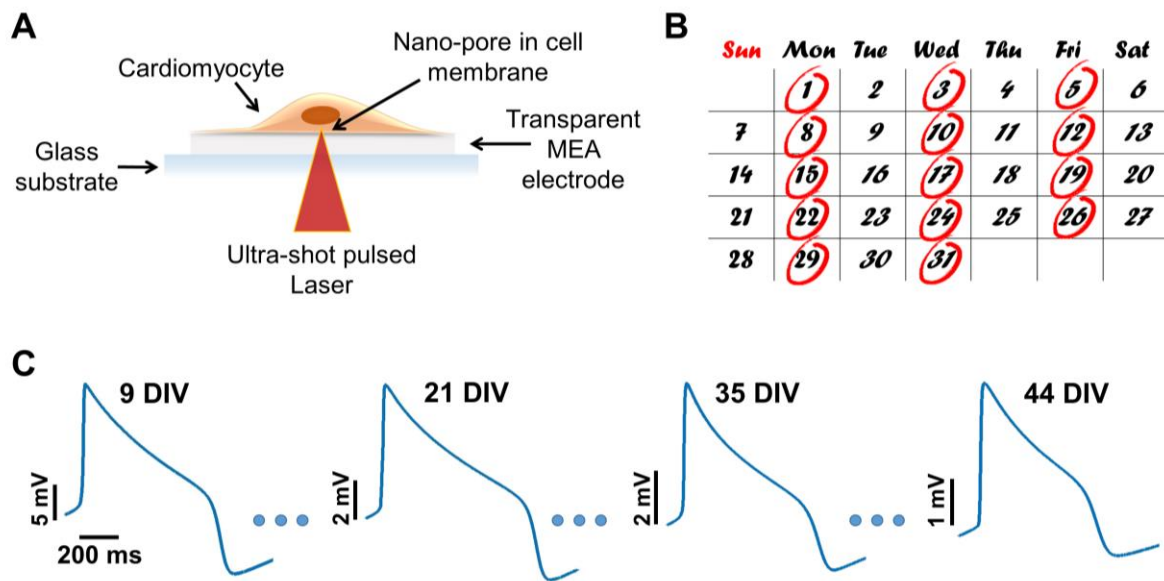


Figure 1: Long-term intracellular action potential recordings from hiPSC-CMs. (A) Representative scheme of laser-based optoporation on MEA device. (B) Time course of APs recording. (C) Action potential mean waveforms of cardiac syncytium at different days in vitro (DIVs).

References

- DiMasi, J.A., Feldman, L., Seckler, A., Wilson, A. (2010). Trends in risks associated with new drug development: success rates for investigational drugs. *Clin Pharmacol Ther* 87(3), 272–277. doi:10.1038/clpt.2009.295.
- McNaughton, R., Huet, G., Shakir, S. (2014). An investigation into drug products withdrawn from the EU market between 2002 and 2011 for safety reasons and the evidence used to support the decision-making. *BMJ Open* 4(1): e004221. doi:10.1136/bmjopen-2013-004221.
- Stett, A., Egert, U., Guenther, E., Hofmann, F., Meyer, T., Nisch, W., Haemmerle, H. (2003). Biological application of microelectrode arrays in drug discovery and basic research. *Anal Bioanal Chem.* 377(3):486-95. doi: 10.1007/s00216-003-2149-x.
- Dipalo, M., Melle, G., Lovato, L., Jacassi, A., Santoro, F., Caprettini, V., Schirato, A., Alabastrri, A., Garoli, D., Bruno, G., Tantussi F., De Angelis, F. (2018). Plasmonic meta-electrodes allow intracellular recordings at network level on high-density CMOS-multi-electrode arrays. *Nat Nanotechnol* 13(10), 965–971. doi:10.1038/s41565-018-0222-z.
- Melle, G., Bruno, G., Maccaferri, N., Iachetta, G., Colistra, N., Barbaglia, A., Dipalo, M., De Angelis, F. (2020). Intracellular Recording of Human Cardiac Action Potentials on Market-Available Multielectrode Array Platforms. *Front Bioeng Biotechnol* 8:66. doi:10.3389/fbioe.2020.00066.
- Iachetta, G., Colistra, N., Melle, G., Deleye, L., Tantussi, F., De Angelis, F., Dipalo, M. (2021). Improving reliability and reducing costs of cardiotoxicity assessments using laser-induced cell poration on microelectrode arrays. *Toxicol Appl Pharmacol*, 418:115480. doi:10.1016/j.taap.2021.115480.
- Dennis, A., Wang, L., Wan, X., Ficker, E. (2007). hERG channel trafficking: novel targets in drug-induced long QT syndrome. *Biochem Soc Trans* 35(5), 1060–1063, doi:10.1042/BST0351060.
- Bozza, W.P., Takeda K., Alterovitz, W-L., Chou C-K., Shen, R-F., Zhang, B. (2021). Anthracycline-Induced Cardiotoxicity: Molecular Insights Obtained From Human-Induced Pluripotent Stem Cell-Derived Cardiomyocytes (hiPSC-CMs). *AAPS J* 23(2):44. doi:10.1208/s12248-021-00576-y.

A Mirror Virtual Cell for Label-Free, Accurate, and Noninvasive recordings of Action Potentials of Human-Derived Cardiomyocytes

Alessio Boschi^{a,b}, Andrea Barbaglia^a, Rosalia Moreddu^a, Giuseppina Iachetta^a, Michele Dipalo^a, Francesco DeAngelis^a

- a. Istituto Italiano di Tecnologia, Via Morego 30, Genova 16136, Italy
- b. Department of Informatics, Bioengineering, Robotics, Systems Engineering (DIBRIS), University of Genova, Genova, Italy

* Francesco.DeAngelis@iit.it

The in-vitro recording of action potentials (APs) from electrogenic cells has a central role in investigating many cellular processes[1]. The accurate measure of APs requires efficient coupling between cell membrane and working electrodes, and often it is necessary to access the intracellular compartment by means of poration. So far, four main techniques allowed direct access to the intracellular compartment: (i) spontaneous poration of the cell-membrane caused by extra sharp nanowires[2], (ii) electrical poration achieved by a sequence of short electrical pulses[3], (iii) plasmonic optoporation obtained at the tip of nano nanopillars excited by laser pulses[4], (iv) perforated patch-clamp techniques. While the quality of measurements has improved in recent years, invasiveness has become the main issue that affect unpredictably the reliability of the measure itself[3,4]. In this work, we present a new approach to record high-quality intracellular signals with minimal invasiveness. We developed a device that converts the cellular ionic currents into mirror currents of charged fluorescence molecules in a microfluidic chamber[7]. This approach allows to record intracellular-like action potentials of cells by monitoring the mirror charge dynamics. Since the mirror charge dynamics is observed by optical read-out, the device provides high spatial resolution down to 5-10 μm and possibility to obtain high parallelization. Moreover, this method does not require poration of cell membrane, proving to be intrinsically non-invasive. We demonstrated this new device is an ideal candidate for the next generation of reliable assessment of cardiotoxicity on human-derived cardiomyocytes. Our results pave the way towards the optimisation process of the device in order to record in-vitro neuronal signals as well.

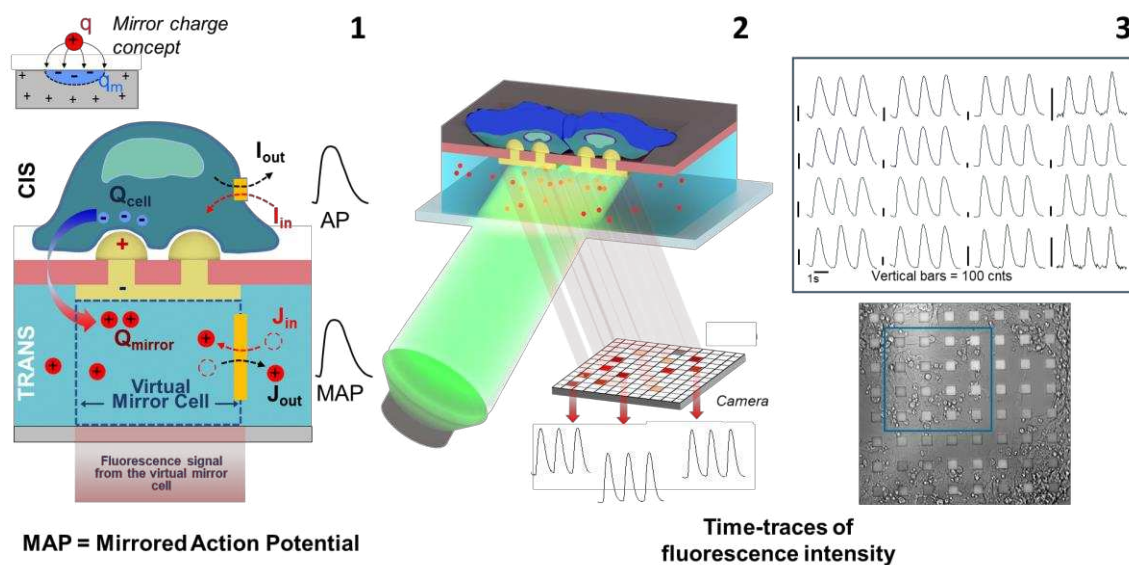


Figure 1: Panel 1 it shows a schematic representation of the concept of mirror charge and a cross-section scheme of the device itself: in the CIS chamber cardiomyocytes are cultured and placed in close contact with gold mushroom micro-electrodes. In the TRANS chamber, fluorophore molecules are dissolved in a solution and are free to move. When the cell fires an action potential (AP), the AP is mirrored through the electrode from the CIS to the TRANS chamber and affects the dynamics of the fluorophores. The variation of the concentration of fluorescent molecules under the electrode implies a variation of fluorescent signal: the lower the concentration the lower the fluorescence. The panel 2 shows a scheme of the principle of the optical read-out of the device: the fluorescent dyes are excited by a fluorescent lamp and the signal is acquired by a CMOS camera. On the top of panel 3 it is shown an example of optical signal from 16 single electrodes. On the bottom right, it is highlighted the area containing the respective 16 electrodes from which we obtained the signals above.

References

- [1] R. Chen, A. Canales, and P. Anikeeva, "Neural recording and modulation technologies," *Nat. Rev. Mater.*, vol. 2, no. 2, p. 16093, 2017, doi: 10.1038/natrevmats.2016.93.
- [2] R. Liu *et al.*, "Ultra-Sharp Nanowire Arrays Natively Permeate, Record, and Stimulate Intracellular Activity in Neuronal and Cardiac Networks," *Adv. Funct. Mater.*, vol. 32, no. 8, p. 2108378, 2022, doi: <https://doi.org/10.1002/adfm.202108378>.
- [3] Z. C. Lin, C. Xie, Y. Osakada, Y. Cui, and B. Cui, "Iridium oxide nanotube electrodes for sensitive and prolonged intracellular measurement of action potentials," *Nat. Commun.*, vol. 5, no. 1, p. 3206, 2014, doi: 10.1038/ncomms4206.
- [4] M. Dipalo *et al.*, "Intracellular and Extracellular Recording of Spontaneous Action Potentials in Mammalian Neurons and Cardiac Cells with 3D Plasmonic Nanoelectrodes.," *Nano Lett.*, vol. 17, no. 6, pp. 3932–3939, Jun. 2017, doi: 10.1021/acs.nanolett.7b01523.
- [5] F. Pei and B. Tian, "Nanoelectronics for Minimally Invasive Cellular Recordings," *Adv. Funct. Mater.*, vol. 30, no. 29, p. 1906210, 2020, doi: <https://doi.org/10.1002/adfm.201906210>.
- [6] J. Abbott *et al.*, "A nanoelectrode array for obtaining intracellular recordings from thousands of connected neurons," *Nat. Biomed. Eng.*, vol. 4, no. 2, pp. 232–241, 2020, doi: 10.1038/s41551-019-0455-7.
- [7] A. Barbaglia *et al.*, "Mirroring Action Potentials: Label-Free, Accurate, and Noninvasive Electrophysiological Recordings of Human-Derived Cardiomyocytes," *Adv. Mater.*, vol. 33, no. 7, p. 2004234, 2021, doi: <https://doi.org/10.1002/adma.202004234>.

Repeated and on-demand intracellular recording of cardiomyocytes

Jihyun Lee^{a,*}, Tobias Gänswein^a, Hasan Ulasan^a, Vishalini Emmenegger^a, Ardan M. Saguner^b, Firat Duru^{b,c}, Andreas Hierlemann^a

- a. Department of Biosystems Science and Engineering, ETH Zurich, 4058 Basel, Switzerland
- b. Department of Cardiology, University Heart Center Zurich, 8091 Zurich, Switzerland
- c. Center for Integrative Human Physiology, University of Zurich, 8091 Zurich, Switzerland

* jihyun.lee@bsse.ethz.ch

Pharmaceutical compounds, besides having a desired on-target mechanism of action, may have cardiotoxic properties, which sometimes result in life-threatening off-target effects in the heart, a major cause for drug withdrawals from the market. For example, doxorubicin, a topoisomerase II inhibitor, used for chemotherapy of malignant cancers, is known to cause cardiomyopathy and arrhythmia, which may endanger the life of the patient and preclude a successful completion of the treatment. Thus, there is a need to study and to detect the risks of cardiotoxic effects at an early stage in drug development. To investigate proarrhythmic effects of drugs, the patch clamp technique has been used as the gold standard for characterizing the electrophysiology of cardiomyocytes *in vitro*; however, low-throughput and the intense training that is needed for applying patch clamp techniques limit their application. Recently, studies have shown that microelectrode arrays (MEAs) can be used to obtain intracellular-like signals from multiple cells at the same time [1]. The use of MEA-based techniques requires the fabrication of 3D-structured electrodes [1,2] or the integration of an optical system [3].

In this study, we used high-density MEAs with porous Pt-black electrodes [4] to repeatedly obtain intracellular signals from hundreds of cardiomyocytes derived from human induced pluripotent stem cells (iPSCs). Transient intracellular signals were attained by means of electroporation, after which the cell membrane resealed over time. The intracellular waveforms of cardiomyocytes were analyzed using specific features of action potential waveforms and machine learning-based feature extraction techniques. We found that the intracellular signal waveforms remain unchanged throughout repeated electroporations, indicated by similarities of waveforms and extracted features. Moreover, the electroporation success rate increased during repetitions to up to 95%. We thus conclude that our high-throughput technique to record intracellular signals in combination with human iPSC-derived cardiomyocytes has the potential to serve as an *in vitro* platform for cardiotoxicity screening.

Acknowledgements

This project is supported by Personalized Health and Related Technologies initiative of the ETH Domain (Project No. PHRT-iDoc 2018-329) and the Swiss National Science Foundation under contract 205320_188910 / 1.

References

1. Abbott, J., Ye, T., Ham, D., Park, H. (2018). Optimizing Nanoelectrode Arrays for Scalable Intracellular Electrophysiology. *Acc. Chem. Res.* 51, 3, 600-608. doi: 10.1021/acs.accounts.7b00519
2. Desbiolles, B.X.E., de Coulon, E., Maïno, N., Bertsch, A., Rohr, S., Renaud, P. (2020). *Microsystems & Nanoengineering* 6:67. doi: /10.1038/s41378-020-0178-7

3. Dipalo, M., Melle, G., Lovato, L., Jacassi, A., Santoro, F., Caprettini, V., Schirato, A., Alabastri, A., Garoli, D., Bruno, G., Tantussi, F., De Angelis, F. (2018). Plasmonic meta-electrodes allow intracellular recordings at network level on high-density CMOS-multi-electrode arrays. *Nat Nano* 13, 965-971. doi: 10.1038/s41565-018-0222-z
4. Ballini, M., Muller, J., Livi, P., Yihui, C., Frey, U., Stettler, A., Shadmani, A., Viswam, V., Jones, I.L., Jackel, D., Radivojevic, M., Lewandowska, M.K., Gong, W., Fiscella, M., Bakkum, D.J., Heer, F., Hierlemann, A. (2014). A 1024-Channel CMOS Microelectrode Array With 26,400 Electrodes for Recording and Stimulation of Electrogenic Cells In Vitro, *IEEE J. Solid-State Circuits* 49:11, 2705–2719. doi: 10.1109/JSSC.2014.2359219

Covariance and entropy analysis to better depict astrocyte effects in neuron-astrocyte networks cultured on MEAs.

Barbara Genocchi,^a Annika Ahtainen,^a Annika Niemi,^a Jarno M. A. Tanskanen,^a Michael T. Barros,^b Kerstin Lenk,^{c,d} Jari Hyttinen,^a Narayan Puthanmadam Subramaniyam^{a,*}

- a. Faculty of Medicine and Health Technology, Tampere University, Tampere, Finland
 - b. School of Computer Science and Electronic Engineering, University of Essex, Colchester, UK
 - c. Institute of Neural Engineering, Graz University of Technology, Graz, Austria
 - d. BioTechMed, Graz, Austria
- * narayan.subramaniyam@tuni.fi

Astrocytes control neuronal electrical activity [1]. However, more research on the effects of astrocytes is still needed. For traditional analysis methods, signals recorded with microelectrode arrays (MEAs) are often converted to binary strings to account for spike. Subsequently, spike and burst analyses are normally conducted [2]. Spike train synchronicity is often calculated from the inter-burst intervals (IBIs) [3]. However, to study how the astrocytes interact with and control the neuronal activity, also the raw signal characteristics are of interest. We co-cultured rat cortical neurons and astrocytes on 60-electrode MEAs with different neuron/astrocyte ratios from “pure” neuronal cultures (NS) to co-cultures containing 50% neurons and 50% astrocytes (referred as 50/50 co-cultures). The number of neurons plated was kept constant and the number of astrocytes was adjusted based on the desired ratio (see [1] for further details on the protocol). We combined spike and burst rate (SR and BR, respectively) analysis with techniques often used in signal analysis. Therefore, we analyzed: i) the cross-covariance between the signals of each pair of MEA channels; and ii) the degree of complexity and entropy in the signals [4, 5].

At all time points (in days *in vitro* (DIV)), the co-cultures exhibited lower SRs and BRs compared to the NS cultures (Fig. 1 A-B), which indicates that astrocytes downregulated neuronal activity. At 28 DIV, NS cultures showed high SR levels, comparable to hyperactivity; this was not found in co-cultures. The BR development (Fig. 1 B) for NS did not change notably from 14 DIV to 19 DIV, and slightly increased for 28 DIV. The differences between 19 DIV and 28 DIV were not statistically significant. For co-cultures, the bursting was almost not present at 14 DIV, but developed at a later stage (19 DIV). The differences between the three time points (14, 19, and 28 DIV) were not statistically significant. The IBIs decreased from 14 DIV to 28 DIV in all the cultures (Fig. 1 C) in accordance with the increased BR (Fig. 1 B).

The empirical cumulative distribution function (CDF) of the covariance shifted towards higher values with the network development (14-19-28 DIV, Fig.1 D-E-F). At 14 DIV, the 80/20 and 50/50 cultures did not exhibit any correlated channels, resulting in the absence of the relative CDFs. At the end of the experiment at 28 DIV, when the networks were considered fully developed, the covariance had decreased with the increased number of astrocytes. Lastly, we analyzed the complexity and the entropy of the signals using complexity-entropy causality plane [5] based on ordinal patterns. At 14 DIV, the entropies were relatively high for all the cultures, indicating sparseness in the signals [4] (Fig. 1 G). From 19 DIV, the NS cultures started to develop repetitiveness in the channel signals, and the entropies decreased (Fig. 1 H). At 28 DIV, the co-cultures still showed higher entropy, especially for 50/50 co-cultures, suggesting randomness and thus desynchronization (Fig. 1 I). These latter analyses better capture the regularity of the signal behavior compared to mere IBI analysis (Fig. 1 C); this is due to the analyses utilizing relative information contents rather than mere spike/spike train statistics. For the co-cultures, the use of empirical CDFs for the covariances between channels clearly showed lower levels of covariance for the majority of the correlated channels and less covarying channels. This indicates desynchronization of the network activity, which may be caused by the astrocytes bringing synapse level and local control to the network. Our work illustrates that the adoption of techniques commonly used in various neuroscience applications can enhance the understanding of how the astrocytes shape and control neuronal activity.

Acknowledgment: The project has received funding from the European Union's Horizon 2020 research and innovation programme, grant agreement No. 824164.

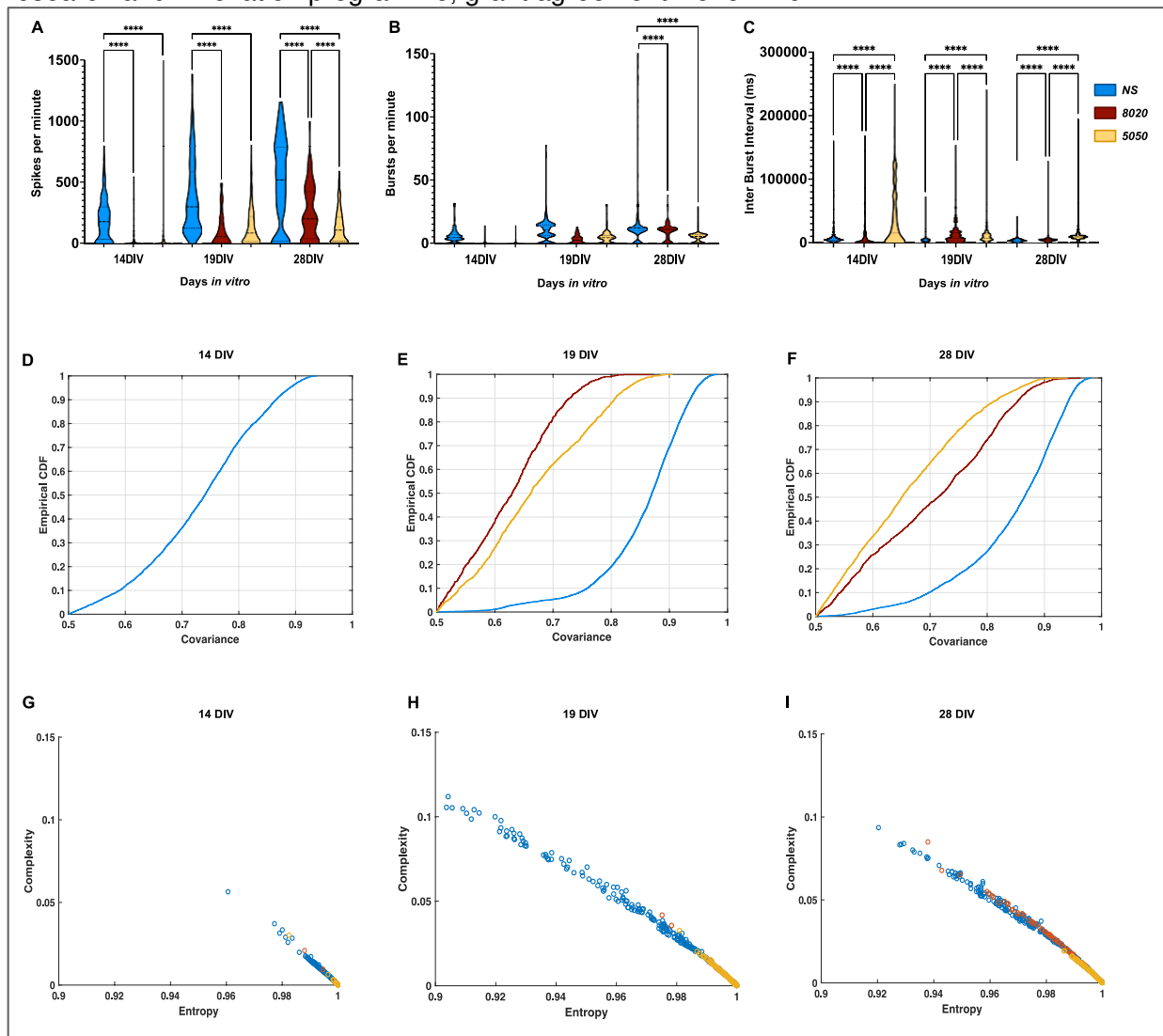


Figure 1: A-C) Traditional spike and burst analysis per channel for the different cultures. A) SRs. B) BRs. C) IBIs. D-F) Empirical CDFs of the covariances at 14, 19, and 28 DIV. D) At 14 DIV, only the NSs exhibited covarying channels (thus, no results for the 80/20 and 50/50). G-I) Complexity-entropy causality planes at 14, 19, and 28 DIV. * $p < 0.05$, ** $p < 0.01$, *** $p < 0.001$, **** $p < 0.0001$. The numbers of MEAs: 4 for NS, 2 for 80/20, and 6 for 50/50.

References

1. Ahtainen, A., Genocchi, B., Tanskanen, J. M. A., Barros, M. T., Hyttinen, J. A. K., and Lenk, K. (2021). Astrocytes exhibit a protective role in neuronal firing patterns under chemically induced seizures in neuron–astrocyte co-cultures. *Int J Mol Sci* 22, 12770. doi:10.3390/ijms222312770.
2. Cotterill, E., Charlesworth, P., Thomas, C. W., Paulsen, O., and Eglén, S. J. (2016). A comparison of computational methods for detecting bursts in neuronal spike trains and their application to human stem cell-derived neuronal networks. *J Neurophysiol* 116, 306–321. doi:10.1152/jn.00093.2016
3. Välikki, I., Lenk, K., Mikkonen, J. E., Kapucu, F. E., and Hyttinen, J. (2017). Network-wide adaptive burst detection depicts neuronal activity with improved accuracy. *Front Comput Neurosci* 11, Article 40. doi:10.3389/fncom.2017.00040.
4. Subramaniyam, N. P., Donges, J. F., and Hyttinen, J. (2015). Signatures of chaotic and stochastic dynamics uncovered with ϵ -recurrence networks. *Proc R Soc A* 471, 20150349. doi:10.1098/rspa.2015.0349.
5. López-Ruiz R., Mancini H. L., and Calbet X. (1995) A statistical measure of complexity. *Phys Lett A* 209, 321–326. doi:10.1016/0375-9601(95)00867-5.

Neuronal and astrocytic interactions in schizophrenia: A computational modeling study

Lea Fritschi^a, Johanna Lindmar^b, Florian Scheidl^c, Kerstin Lenk^{d,*}

- a. ETH Zurich, Department of Mathematics, Zurich, Switzerland
- b. ETH Zurich, Institute of Neuroinformatics, Zurich, Switzerland
- c. ETH Zurich, Department of Computer Science, Zurich, Switzerland
- d. Graz University of Technology, Institute of Neural Engineering, Graz, Austria

* kerstin.lenk@tugraz.at

Astrocytes have been associated with psychiatric disorders such as schizophrenia in several studies. However, there are several different hypotheses regarding the pathological mechanisms of neurons and astrocytes in schizophrenia. Computer models can increase knowledge of biophysical processes, especially when experiments are not feasible or too expensive. In Lenk et al. [1], we developed a mathematical neuron-astrocyte network model to investigate the influence of astrocytes on neuronal activity. The neurons and astrocytes were thereby distributed over a virtual multielectrode array.

Here [2], we use the model by Lenk et al. [1] to investigate several hypotheses about schizophrenia. In our simulations, reducing the number of astrocytes or neurons leads to decreased glutamate concentration in astrocytes and reduced neuronal network activity. Increased release of ATP (adenosine triphosphate) by astrocytes toward postsynaptic neurons also decreases neuronal activity (Figure 1A) but temporarily increases the glutamate concentration in astrocytes (Figure 1B). A reduction in the release of the neurotransmitter glutamate and the decreased glutamate uptake by astrocytes, respectively, results in increased network activity. Also, the increase in synaptic weights, i.e., the coupling strength, of excitatory and inhibitory neurons, respectively, leads to this result.

Schizophrenia is expressed by distinct dysregulations and malfunctions in neurons and astrocytes. Our simulations suggest, that the interaction of neurons and astrocytes in schizophrenia should be further investigated in more detail.

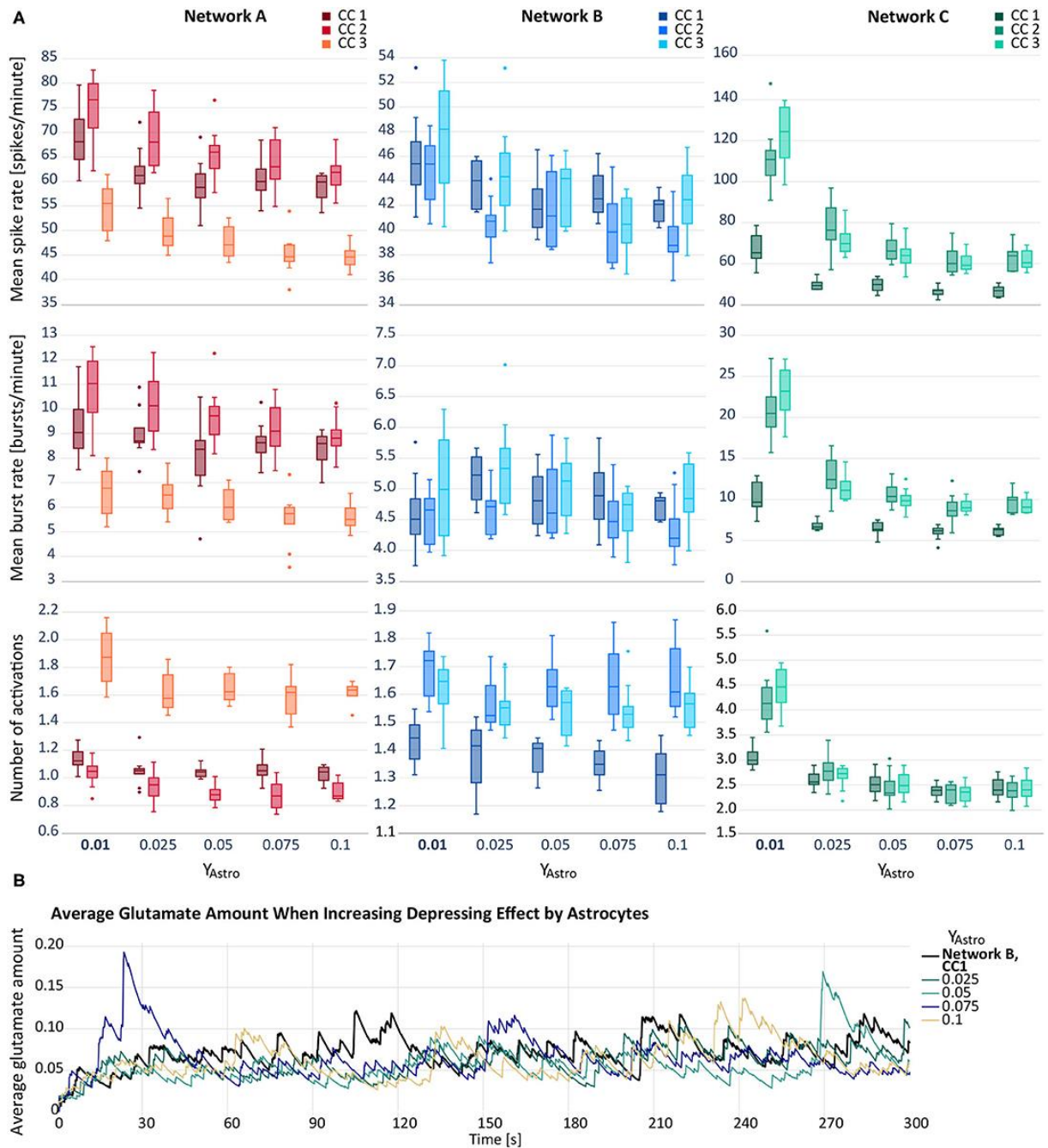


Figure 1: (A) Mean spike rate (top), mean burst rate (middle), and mean number of activations per astrocyte (bottom) resulting from the networks with increased astrocytic depression compared to the default networks A–C including connectivity configurations CC 1, 2, 3 with $y_{Astro} = 0.01$ (bold). Note that the y-axes differ for each subfigure. (B) Average glutamate amount in astrocytes when applying a depressive effect on the postsynapse by releasing ATP from the astrocyte (y_{Astro}). The black line resembles the baseline activity from network B, CC 1. The remaining lines represent deviating values of y_{Astro} (figure taken from [2], CC BY license).

References

1. Lenk, K., Satuvuori, E., Lallouette, J., Ladrón-de-Guevara, A., Berry, H., Hyttinen, J.A.K. A Computational Model of Interactions Between Neuronal and Astrocytic Networks: The Role of Astrocytes in the Stability of the Neuronal Firing Rate. *Front Comput Neurosci* 2020, 13:92.
2. Fritschi, L., Lindmar, J.H., Scheidl, F., Lenk, K. Neuronal and Astrocytic Regulations in Schizophrenia: A Computational Modelling Study. *Front Cell Neurosci* 2021, 15:718459.

Microelectrode arrays for detection of astrocytic activity

Misaki Inaoka,^a Sagnik Middy,^{a,b} Ana Fernández-Villegas,^b Gabriele S. Kaminski Schierle,^b and George G. Malliaras^{a,*}

- a. Electrical Engineering Division, Department of Engineering, University of Cambridge, 9 JJ Thomson Ave, Cambridge, CB3 0FA, United Kingdom
- b. Department of Chemical Engineering and Biotechnology, University of Cambridge, Philippa Fawcett Dr, CB3 0AS, United Kingdom

* gm603@cam.ac.uk

Astrocytes, a type of glial cell, actively interact with neurons and thus play an essential role in brain information processing [1,2]. The discovery of this fact, which has long been overlooked since the rise of neuronal research, has led to a significant reconsideration of the importance of astrocytes in the overall understanding of the brain. To date, single-cell electrophysiological activity using patch-clamp and calcium concentration using Ca^{2+} imaging have been investigated in astrocytes. To further elucidate astrocyte function, it is necessary to develop electrophysiological tools to capture the low-amplitude, slow oscillations generated from astrocytes at the network level to complement existing observation methods.

We have developed 64-channel *in vitro* microelectrode arrays (MEAs) (see Figure 1). This device consists of 100 μm diameter Au electrodes coated with PEDOT:PSS, a conducting polymer with excellent properties as an interface material between tissue and device [3]. The devices, fabricated by lift-off of PEDOT:PSS (see Figure 2), were found to have stable electrical properties with low impedance, allowing reliable fabrication and mass production even in highly channel-dense MEAs, for example, without losing any electrodes during fabrication. Furthermore, the structure of the device ensures that the electrodes do not interfere with cell elongation, resulting in both device stability and biocompatibility. Further *in vitro* recording of astrocytic electrophysiology will be carried out using this device.

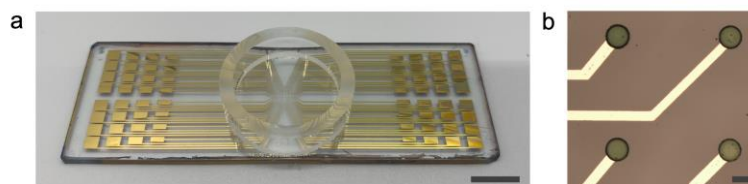


Figure 1: a) Image of 64-channel *in vitro* MEAs. b) Enlarged view of the electrode section. Scale bars: left 1 cm; right 100 μm .

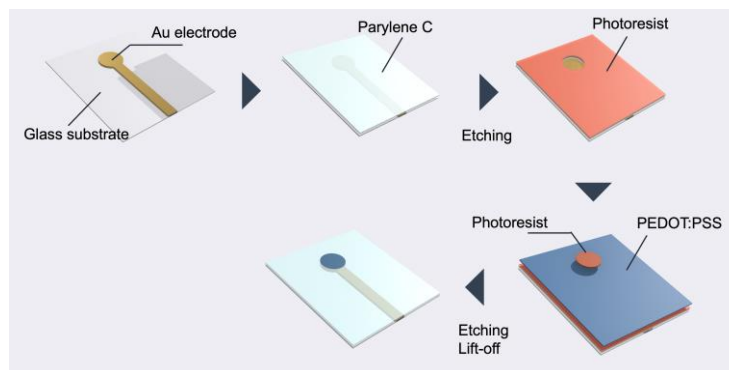


Figure 2: Fabrication process of the device.

References

1. Pannasch, U. and Rouach, N. (2013). Emerging role for astroglial networks in information processing: from synapse to behavior. *Trends Neurosci* 36, 405–417. doi: 10.1016/j.tins.2013.04.004
2. Araque, A., Parpura, V., Sanzgiri, R. P., and Haydon, P. G. (1999). Tripartite synapses: glia, the unacknowledged partner. *Trends Neurosci* 22, 208–215. doi: 10.1016/s0166-2236(98)01349-6
3. Zeglio, E., Rutz, A. L., Winkler, T. E., Malliaras, G. G., and Herland, A. (2019). Conjugated Polymers for Assessing and Controlling Biological Functions. *Adv Mater* 31, 1806712. doi: 10.1002/adma.201806712

Effect of hypoxia and temperature investigated in a human *in vitro* model of the ischemic penumbra.

Voogd, E.J.H.F.^{a*} Thijs, M.^a, Levers, M.R.^a, Hofmeijer, J.^a & Frega, M.^a

- a. Department of clinical neurophysiology, University of Twente, Drienerloolaan 5 Enschede, The Netherlands.

* e.j.h.f.voogd@utwente.nl

Ischemic stroke is one of the leading causes for death and disability worldwide. Currently the treatment strategies for ischemic stroke are very limited. While over 2000 studies into neuroprotective agents conducted in animals were beneficial, they failed to be translated to the clinic [1]. This problem could be partly related to strategy, where only a specific neuronal receptor or signaling pathway is targeted. These strategies might not be sufficient enough to battle the extensive pathophysiological cascade that follows acute ischemic stroke [2]. Therefore, strategies affecting multiple signaling pathways and cell types could be beneficial for ischemic stroke patients. In particular, the rising evidence that hypothermia could be a neuroprotective strategy in animal models and clinical trials is promising, by ameliorating brain damage through inhibition of multiple pathways i.e. oxidative stress [3] and cell death pathways [4]. Here we represent a human *in vitro* model of the ischemic penumbra and studied the effect of hypoxia on neuronal functioning and treatment strategies such as hypothermia.

To generate a human *in vitro* model of the ischemic penumbra, neurons were differentiated from human induced pluripotent stem cells (hiPSCs) and cultured on micro-electrode arrays (MEAs) containing 12 electrodes and glass coverslips [5]. Controlled hypoxia proportional to penumbral oxygen levels and temperature were achieved by computer-controlled climate chambers. Outcome measures included electrophysiological activity (mean firing rate (MFR), network burst rate (NBR) and network burst duration (NBD)) recorded through MEAs, cell viability (live dead assay including apoptosis) and quantification of synaptic puncta, and were investigated during and after hypoxia, in normothermia (37 °C) or hypothermia (34 °C).

We first showed that normothermia during 48h of hypoxia (hereafter referred to as not treated cultures) led to complete loss of MFR and NBR (fig. 1). The results of a live dead assay showed that number in apoptotic cells increased, followed by an increase in the number of dead cells during hypoxia. Secondly, we showed that neuronal cultures subjected to hypothermia during 48h of hypoxia showed an overall lower MFR compared to not treated cultures (fig.1 A). The NBR of hypothermia treated cultures increased and synchronous activity was longer lasting compared to not treated cultures (fig. 1B). The duration of synchronous events (NBD) in hypothermia treated cultures was shorter compared to not treated cultures (fig. 1C). When reoxygenation and re-establishment of normothermia is achieved, hypothermia treated cultures recover to baseline levels of random (MFR) and synchronous activity (NBR), while in not treated cultures recovery was not present. However, after reoxygenation the baseline levels of NBD in hypothermia treated cultures are not recovered.

This study showed that hiPSCs derived neurons exposed to hypoxia can serve as a human *in vitro* model of the penumbra. This study also showed that hypothermia seemed to be neuroprotective in hiPSCs neurons, since recovery after re-oxygenation and re-establishment of normothermia was observed.

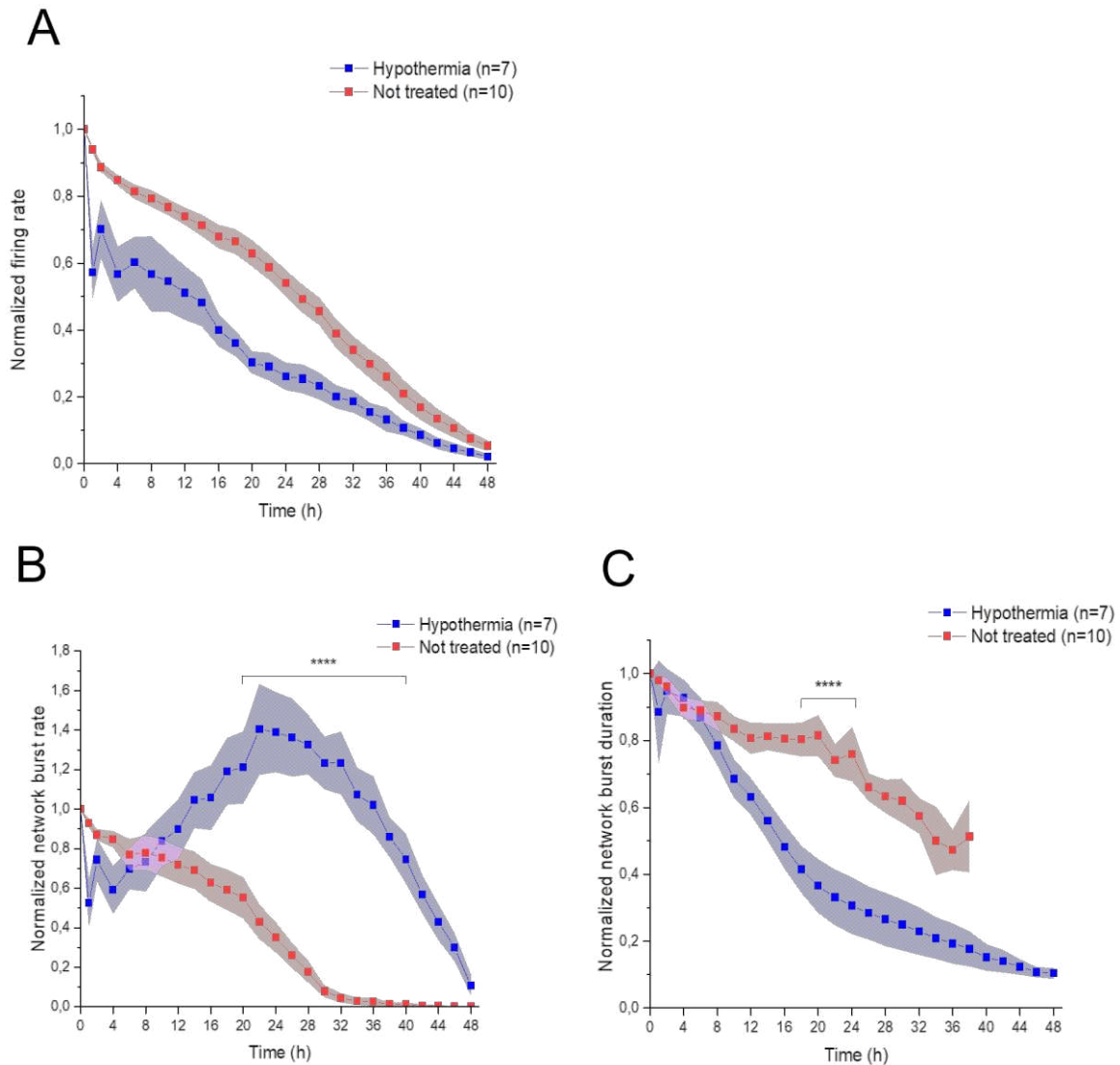


Figure 1: Graphs showing the effect of hypoxia on not treated cultures (red) and hypothermia treated cultures (blue) on (A) mean firing rate, (B) network burst rate and (C) network burst duration. **** = $p < 0.0001$

References

1. Ginsberg M.D. (2008). Neuroprotection for ischemic stroke: past, present and future. *Neuropharmacology* 55(3):363-89. doi: 10.1016/j.neuropharm
2. Lee J.H., Zhang J., Yu S.P. (2017). Neuroprotective mechanisms and translational potential of therapeutic hypothermia in the treatment of ischemic stroke. *Neural Regen Res* 12(3):341-50. doi: 10.4103/1673-5374.202915.
3. Katz L.M., Young A.S., Frank J.E., Wang Y., Park K. (2004). Regulated hypothermia reduces brain oxidative stress after hypoxic-ischemia. *Brain Res* 1017(1-2):85-91. doi: 10.4103/1673-5374.202915
4. hoi K.E., Hall C.L., Sun J.M., Wei L., Mohamad O., Dix T.A., et al. (2012). A novel stroke therapy of pharmacologically induced hypothermia after focal cerebral ischemia in mice. *FASEB J* 26(7):2799-810. doi: 10.1096/fj.11-201822
5. Frega M., van Gestel S.H., Linda K., van der Raadt J., Keller J., Van Rhijn J.R., et al. (2017). Rapid Neuronal Differentiation of Induced Pluripotent Stem Cells for Measuring Network Activity on Micro-electrode Arrays. *J Vis Exp* 119. doi: 10.3791/54900

Oxygen Gradient Device for the In Vitro Study of Ischemic Stroke

João Santiago¹, Joose Kreutzer², Pasi Kallio² and Joost le Feber^{1,*}

1. Clinical Neurophysiology, University of Twente, PO Box 217 7500AE, Enschede, The Netherlands
2. Micro and Nanosystems Research Group, Faculty of Medicine and Health Technology, Tampere University, Tampere, Finland

* j.lefeber@utwente.nl

In the core of a brain infarct perfusion is severely impeded and neuronal death occurs within minutes [1]. In the penumbra, an area with some remaining perfusion that surrounds the core, cells initially remain viable, but activity is significantly impeded. In principle the penumbra can be saved if reperfusion is established in time, making it a promising target for treatment [2]. In vitro models with cultured neurons on microelectrode arrays (MEAs) have been used to investigate how ischemic stroke affects neuronal functioning [3] [4], and suggest that stimulation may be beneficial [6]. These were uniform models, focusing on the isolated penumbra, with no adjacent regions like a core and unaffected regions (normal perfusion) [5]. However, processes in these regions may affect neuronal functioning and survival in the penumbra, possibly influencing the hypothesized beneficial effect of therapeutic stimulation.

We designed, fabricated, and characterized a biocompatible device to impose an oxygen gradient on *in vitro* neuronal cultures, to better simulate ischemic stroke, mimicking core, penumbra, and healthy tissue. The device consists of three parts: a silicone-made culture chamber, a tailored O₂ gradient lid assembly containing two inserts to conduct gas flows of controlled composition, and a metal lid lock (see Figure 1a). It is attachable to the MEA to allow cell culturing and continuous long-term recordings under controlled conditions. To characterize the oxygen gradient, a small Platinum Tetrakis (Pentafluorophenyl) Porphyrin (PtTFPP) sensor array was used to calibrate the device. To form the gradient, two known gas mixtures (95% N₂ + 5% CO₂ and 95% air with 5% CO₂) were supplied through two inserts, which were separated by a 3.5 mm gap between them. The effect of the device was tested on cell cultures obtained from brain cortices of newborn Wistar rats. Main readouts included the rate and shape of action potentials detected, recorded fraction of artifacts, and the noise captured by electrodes. Viability of the cultures was evaluated in follow-up experiments, 1-3 days after exposure to the device.

The oxygen sensors were calibrated using a Stern-Volmer approach and indicated that the device formed a stable and reproducible gradient within 30 minutes (see Figure 1b), extending from 17.6% to 4.7% of oxygen. Oxygen concentrations at the extremes are in principle adjustable within this (physiologically relevant) range. The established gradient did not have a perpendicular component. The environmental O₂ concentration did not affect the established gradient. Application of the device did not negatively affect electrophysiological recordings: mean action potential showed to be consistent in shape and amplitude for all active electrodes, noise levels did not change, and the device did not generate additional artifacts. In follow-up experiments cultures were still viable, thus confirming biocompatibility of the device. In conclusion, the developed device works well and seems a promising tool for *in vitro* models of ischemic stroke.

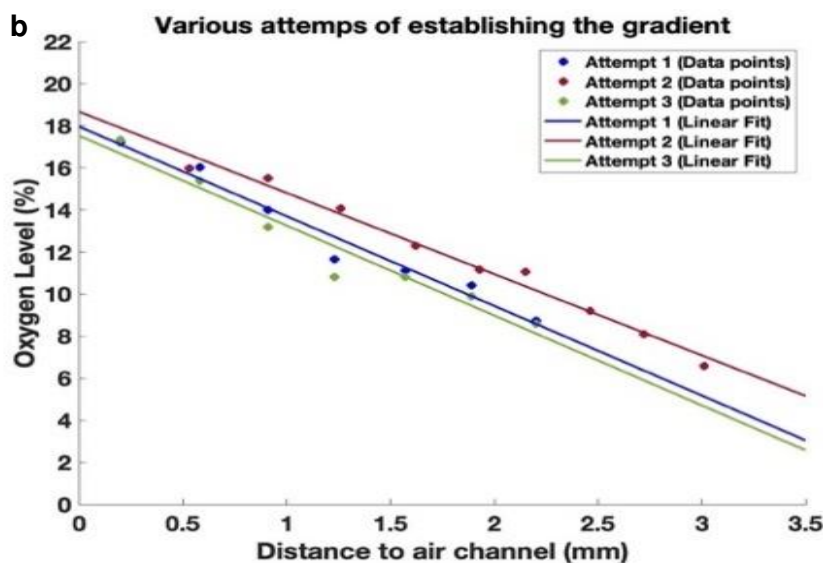
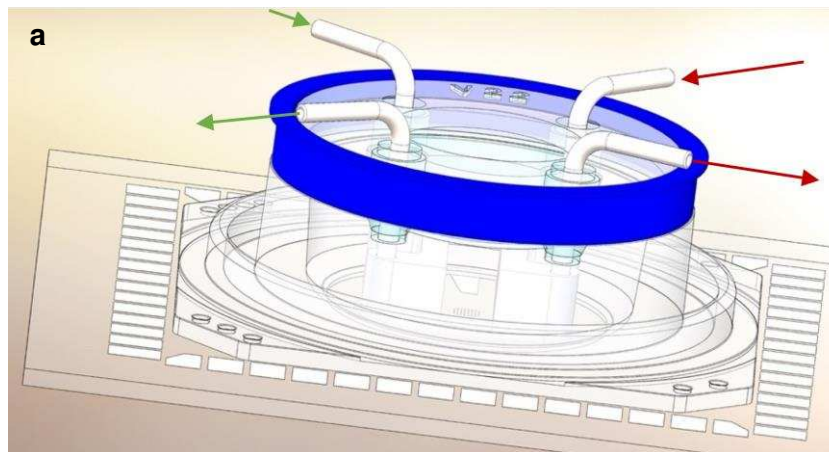


Figure 1: a) 3D impression of the device: placed on top of the MEA with a PDMS ring and sealed with a ring (blue); gas mixtures flow through the inserts of the device (red arrows: 95% N₂ + 5% CO₂; green arrows: 95% Air + 5%CO₂). b) O₂ gradients observed in three experiments with the respective linear fits for each gradient showing its reproducibility.

References

1. Lakhan, S. E., Kirchgessner, A., & Hofer, M. (2009). Inflammatory mechanisms in ischemic stroke: Therapeutic approaches. *Journal of Translational Medicine*, 7, 1–11. <https://doi.org/10.1186/1479-5876-7-97>
2. Hakim, A. M. (1987). The Cerebral Ischemic Penumbra. *Canadian Journal of Neurological Sciences / Journal Canadien Des Sciences Neurologiques*, 14(4), 557–559. <https://doi.org/10.1017/S0317167100037355>
3. Le Feber, J., Erkamp, N., Van Putten, M. J. A. M., & Hofmeijer, J. (2017). Loss and recovery of functional connectivity in cultured cortical networks exposed to hypoxia. *Journal of Neurophysiology*, 118(1), 394–403. <https://doi.org/10.1152/jn.00098.2017>
4. Fedorovich, S., Hofmeijer, J., van Putten, M. J. A. M., & le Feber, J. (2017). Reduced synaptic vesicle recycling during hypoxia in cultured cortical neurons. *Frontiers in Cellular Neuroscience*, 11, 32. <https://doi.org/10.3389/FNCEL.2017.00032/BIBTEX>
5. Le Feber, J., Pavlidou, S. T., Erkamp, N., Van Putten, M. J. A. M., & Hofmeijer, J. (2016). Progression of neuronal damage in an in vitro model of the ischemic penumbra. *PLoS ONE*, 11(2), 1–19. <https://doi.org/10.1371/journal.pone.0147231>
6. Muzzi, L., Hassink, G., Levers, M., Jansman, M., Frega, M., Hofmeijer, J., Van Putten, M., & Le Feber, J. (2020). Mild stimulation improves neuronal survival in an in vitro model of the ischemic penumbra. *Journal of Neural Engineering*, 17(1). <https://doi.org/10.1088/1741-2552/ab51d4>

Device for Studying Acute Ischemic Conditions

Joose Kreutzer,^{ab*} Jenna Suoranta,^b Hannu Välimäki,^a Pasi Kallio^a

- a. Micro- and Nanosystems Research Group, Faculty of Medicine and Health Technology, Tampere University, Tampere, Finland
 - b. BioGenium Microsystems Ltd, Tampere, Finland
- * joose.kreutzer@tuni.fi

In the human body, acute ischemic condition occurs locally in the tissue when blood flow is suddenly limited or fully blocked. Limited or blocked blood flow produces hypoxic conditions for the cells due to the lack of oxygen supply within the flow. This condition might lead to life-threatening issues such as stroke or heart attack within seconds to minutes after the loss of blood flow [1]. Ischemic stroke is the third leading cause of death in industrialized countries [1] and ischemic heart disease is the leading cause of death worldwide [2]. However, pathophysiology of these acute diseases is not yet fully understood. To gain this understanding, it is essential to create novel and innovative tools and devices for the researchers in the field.

We have developed a mini-incubator (See Figure 1A) that provides controlled environment for prolonged hypoxia, physoxia, and standard-like 5% CO₂ “normoxia” studies during the MEA recordings on MEA amplifier (See Figure 1B) or outside the incubator [3,4,5]. The mini-incubator maintains the pH, temperature, and constant gas concentration for normoxia, physoxia, and/or hypoxia conditions. The acute ischemic conditions can be modelled utilizing the novel “Acute lid” design. The lid is replaceable part on top of the 1-well assembly on the MEA plate (See Figure 1A). The lid is closed with the Lid lock that seals the chamber to avoid evaporation. The lid includes gas permeable membrane that allows rapid change of oxygen partial pressure for the cells due to the close proximity of the membrane to the cells. 1-well assembly on MEA is closed with the Chamber cover and supplied with 5ml/min gas supply of dry gas.

The performance of the Acute lid under the operation was characterized by measuring the dynamics of the oxygen partial pressure without cells and determining the evaporation. A step response from 19 kPa to 1 kPa pO₂ was measured and a fall time (time between 90% and 10% of the step) and time constant of the step response was calculated (See Figure 1C). Oxygen step response measurements were performed with a custom-made oxygen sensor platform [6]. Addition to step response, the 2D oxygen map was determined from the bottom of the plate. Furthermore, the evaporation rate through the thin membrane was determined to demonstrate the compatibility of the lid to be used with dry gas mixture supply (this is an important aspect as no humidification of gas supply is needed). Evaporation was compared to incubator conditions.

As the result, evaporation of mini-incubator with Acute lid assembly under 5ml/min flow rate of dry gas supply is $1.2 \pm 0.3 \mu\text{l/h}$ (n=6), which is much less than similar culture wells inside the humidified incubator with evaporation rate as high as $4.7 \pm 0.4 \mu\text{l/h}$ (n=6). Low evaporation rate enables long-term experiments on MEA amplifier outside the humid incubator [4,5]. Furthermore, Acute lid provides rapid change of oxygen partial pressure for the cells. Calculated fall time and time constant for the step response of oxygen partial pressure are 2.0 min and 1.3 min, respectively. Similar dynamics are provided for step response from 1 kPa to 19 kPa pO₂ (data not shown here). Additionally, the 2D map of oxygen shows equal distribution of oxygen on the plate (data not shown here).

As conclusion, the mini-incubator with Acute lid provides novel tool to study acute ischemic conditions on MEA. With this assembly, truly hypoxic conditions can be maintained for the cells also on prolonged time on the MEA. In addition, the same mini-incubator can be utilized in other research such as in microscopy to maintain physiological environment during the experiments. Therefore, the mini-incubator is perfect tool for the long-term cell culture outside an incubator.

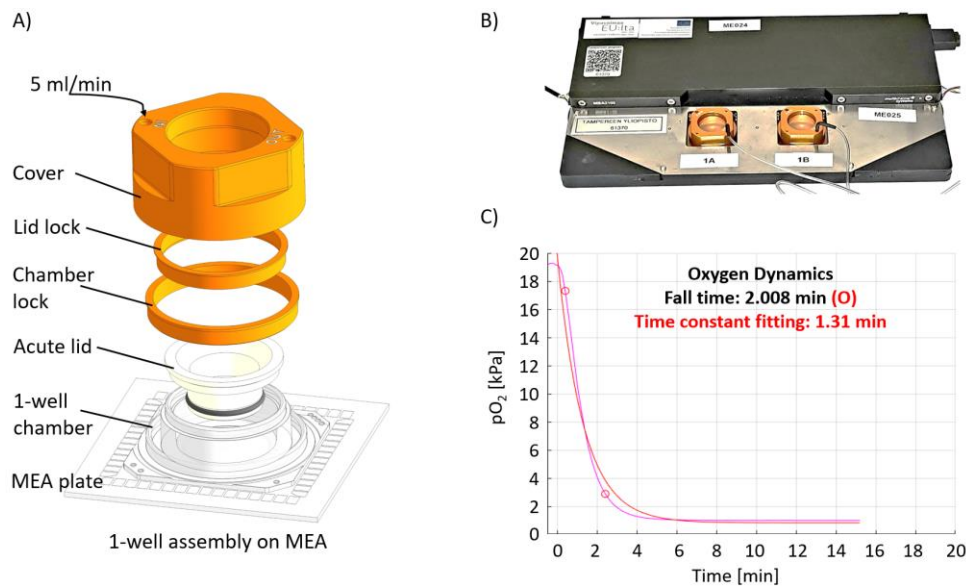


Figure 1: A) Mini-incubator assembled on the MEA plate with Acute lid. 5ml/min gas supply (dry gas) is enough to maintain the hypoxic condition for long period of time. B) 1-well assembly on MEA amplifier. C) Oxygen dynamics measured with custom-made oxygen sensor demonstrating fast dynamics for step response of oxygen partial pressure from 19 kPa to 1 kPa.

References

1. Lakhan, S. E., Kirchgessner, A., & Hofer, M. (2009). Inflammatory mechanisms in ischemic stroke: therapeutic approaches. *J. transl. med.*, 7, 97. <https://doi.org/10.1186/1479-5876-7-97>
2. Khan, M. A., Hashim, M. J., Mustafa, H., Baniyas, M. Y., Al Suwaidi, S., AlKatheeri, R., Alblooshi, F., Almatrooshi, M., Alzaabi, M., Al Darmaki, R. S., & Lootah, S. (2020). Global Epidemiology of Ischemic Heart Disease: Results from the Global Burden of Disease Study. *Cureus*, 12(7), e9349. <https://doi.org/10.7759/cureus.9349>
3. Gaballah, M., Penttinen, K., Kreutzer, J., Mäki, A.-J., Kallio, P., and Aalto-Setälä, K. (2022). Cardiac Ischemia On-a-Chip: Antiarrhythmic Effect of Levosimendan on Ischemic Human-Induced Pluripotent Stem Cell-Derived Cardiomyocytes. *Cells*, 11(6), 1045. <https://doi.org/10.3390/cells11061045>
4. Häkli, M., Kreutzer, J., Mäki, A. J., Välimäki, H., Lappi, H., Huhtala, H., Kallio, P., Aalto-Setälä, K. and Pekkanen-Mattila, M. (2021). Human induced pluripotent stem cell-based platform for modeling cardiac ischemia. *Sci. Rep*, 11(1), 1–13. <https://doi.org/10.1038/s41598-021-83740-w>
5. Kreutzer, J., Ylä-Outinen, L., Mäki, A. J., Ristola, M., Narkilahti, S., and Kallio, P. (2017). Cell culture chamber with gas supply for prolonged recording of human neuronal cells on microelectrode array. *J. Neurosci. Met.*, 280, 27–35. <https://doi.org/10.1016/j.jneumeth.2017.01.019>
6. Välimäki, H., Verho, J., Kreutzer, J., Kattiparambil Rajan, D., Ryyänen, T., Pekkanen-Mattila, M., Ahola, A., Tappura, K., Kallio, P., and Leikkala, J. (2017) Fluorimetric oxygen sensor with an efficient optical read-out for in vitro cell models. *Sens. Act. B Chem.* 249, 738–746, <https://doi.org/10.1016/j.snb.2017.04.182>

Parkinson's-on-Chip Model: Screening the activity and its propagation of hPSC-derived neurons during α -synuclein aggregation on MEA embedded microfluidic chips

Fikret Emre Kapucu,^{a,*} Lisa Tujula,^a Oskari Kulta^a, Susanna Narkilahti^a

a. Faculty of Medicine and Health Technology, Tampere University, Finland

* emre.kapucu@tuni.fi

A well-known pathological feature of Parkinson's disease (PD) is the accumulation of misfolded assemblies of a specific protein, i.e., α -synuclein. In PD, the pathologic α -synuclein assemblies can spread along the interconnected neuronal networks (circuits) in a "prion-like" manner promoting the spread of pathology [1,2]. Aggregated forms of α -synuclein travel through the axons anterogradely or retrogradely [3]. The formed malicious strains of α -synuclein are also transferred to other neurons via different routes in which they behave as seeds to initiate the same pathological process. Recently, to initiate this cascade, preformed α -synuclein amyloid fibrils (PFFs) are used as seeds in several in vivo and in vitro studies [4]. Previously, the effects of extracellularly added α -synuclein monomers [5] and PFFs [6] on the neuronal spontaneous firing and Ca^{2+} oscillations were observed to cause reduced synaptic functionality.

Parkinson's-on-chip model is an ongoing multidisciplinary project introducing the state-of-the-art tools from the cell biology, sensory technologies, microfluidics and biomedical signal analysis to obtain novel information in synucleopathies, particularly in PD. In the project, previously developed custom chip models are utilized [7,8]. MEMO chip used in the project has 3 separate compartments each of which has 24 electrodes. Tunnels between the compartments have also 8 electrodes each. Thus, both axonal and neuronal network level (dys)functionality are monitored and temporally defined in relation to disease progression. An example work from the project which utilizes MEMO chip [7] is described in Figure 1.

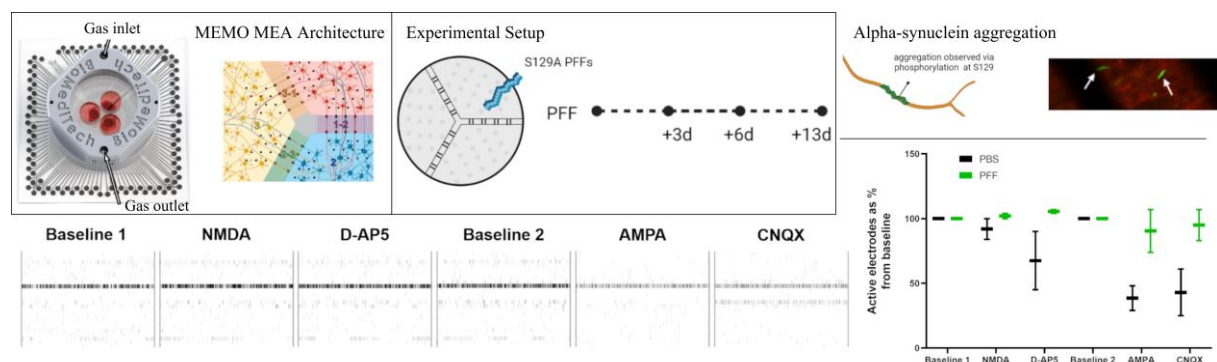


Figure 1: The application of α -synuclein PFFs on the selected compartment of 3-compartment MEMO chip [7]. Aggregation of recruited forms of α -synuclein is followed via labeling the phosphorylation at S129 residue of α -synuclein. Samples are fixed on the endpoint days. Endpoint recordings are obtained at the 3rd, 6th and 13th day of PFF treatment. An exemplary recording from day six of the PFF applied compartment is presented as raster plots. Created with BioRender.com

References

1. Kordower, J., Chu, Y., Hauser, R. et al. (2008). Lewy body-like pathology in long-term embryonic nigral transplants in Parkinson's disease. *Nat Med* 14, 504–506. <https://doi.org/10.1038/nm1747>
2. Guo, J., Lee, V. (2014). Cell-to-cell transmission of pathogenic proteins in neurodegenerative diseases. *Nat Med* 20, 130–138. <https://doi.org/10.1038/nm.3457>

3. Uchihara, T., Giasson, B.I. (2016). Propagation of alpha-synuclein pathology: hypotheses, discoveries, and yet unresolved questions from experimental and human brain studies. *Acta Neuropathol* 131, 49–73. <https://doi.org/10.1007/s00401-015-1485-1>
4. Bieri, G., Gitler, A. D. & Brahic, M. (2018). Internalization, axonal transport and release of fibrillar forms of alpha-synuclein. *Neurobiology of Disease* 109, 219–225. <https://doi.org/10.1016/j.nbd.2017.03.007>
5. Alhebshi, A. H., Odawara, A., Gotoh, M. et al. (2014). Thymoquinone protects cultured hippocampal and human induced pluripotent stem cells-derived neurons against α -synuclein-induced synapse damage. *Neuroscience Letters* 570, 126–131. <https://doi.org/10.1016/j.neulet.2013.09.049>
6. Gribaudo, S., Tixador, P., Bousset, L., et al. (2019). Propagation of α -Synuclein Strains within Human Reconstructed Neuronal Network. *Stem Cell Reports* 12, 230–244. <https://doi.org/10.1016/j.stemcr.2018.12.007>
7. Pelkonen, A., Mzezewa, R., Sukki, L. et al. (2020). A modular brain-on-a-chip for modelling epileptic seizures with functionally connected human neuronal networks. *Biosens. Bioelectron.* 168, 112553. <https://doi.org/10.1016/j.bios.2020.112553>
8. Ristola, M., Fedele, C., Hagman, S. et al. (2021). Directional Growth of Human Neuronal Axons in a Microfluidic Device with Nanotopography on Azobenzene-Based Material. *Advanced Materials Interfaces*, 8(11). <https://doi.org/10.1002/admi.202100048>

Functional and electrophysiological changes of the gut and the enteric nervous system in an Alzheimer's and Parkinson's disease model

Manuela Gries,^a Steven Schulte,^a Anne Christmann,^a Stephanie Rommel,^a Bharat Nowduri,^a Monika Saumer^a, Karl-Herbert Schäfer^{a,b*}

- a. Department of Informatics and Microsystems and Technology, University of Applied Sciences Kaiserslautern, Working Group Enteric Nervous System, 66482, Zweibrücken, Germany.
- b. Department of Pediatric Surgery, Medical Faculty Mannheim, University of Heidelberg, 68167, Mannheim, Germany.

* karlherbert.schaefer@hs-kl.de

The number of patients suffering from neurodegenerative diseases like Alzheimer's or Parkinson's disease rises with increasing life expectancy. Unfortunately, these disorders do not become clinically apparent until a significant neural damage already occurred, whereby a therapeutic treatment is nearly impossible [1]. Since there is growing evidence that the onset and course of neurodegenerative diseases might be influenced by or even start in the gastrointestinal tract, its intrinsic nervous system, the enteric nervous system, might be an ideal target for both early diagnosis and treatment [2]. To evaluate the impact of the neuropathological peptide of Alzheimer's disease on gastrointestinal motility, we performed mesenteric beta-amyloid perfusions of the murine gut using an ex vivo organ bath. The perfusion experiments lead to significantly decreased gut diameters and an altered gut peristaltic, thus, delivering evidences for functional changes of the gut by interacting directly with the enteric nervous system. There is a lack of appropriate models to study modifications in neural activity, the features of intercellular signaling, or the effects of drugs on the functional activity of neurons during Alzheimer's and Parkinson's disease development in the gut. In this work, however, we established an acute experimental model of amyloid- and synucleinopathy, respectively, using primary enteric neurons. We employed live-cell imaging to detect intracellular calcium levels and multi-electrode arrays to measure the action potential activity and the spiking rates of the cells. After acutely exposing enteric cultures to the relevant neuropathological peptides in both, Alzheimer's and Parkinson's disease, beta-amyloid and A30P alpha-synuclein respectively, we found for both peptides significant calcium increases as well as elevated and dose-dependent spike numbers (Fig. 1) compared with the basic activity of the cells. In conclusion, our results highlight a prominent role of both, beta-amyloid and A30P alpha-synuclein, in the modulation of calcium activity in enteric neurons whose specific functioning is crucial for the corroboration and modulation of synaptic function.

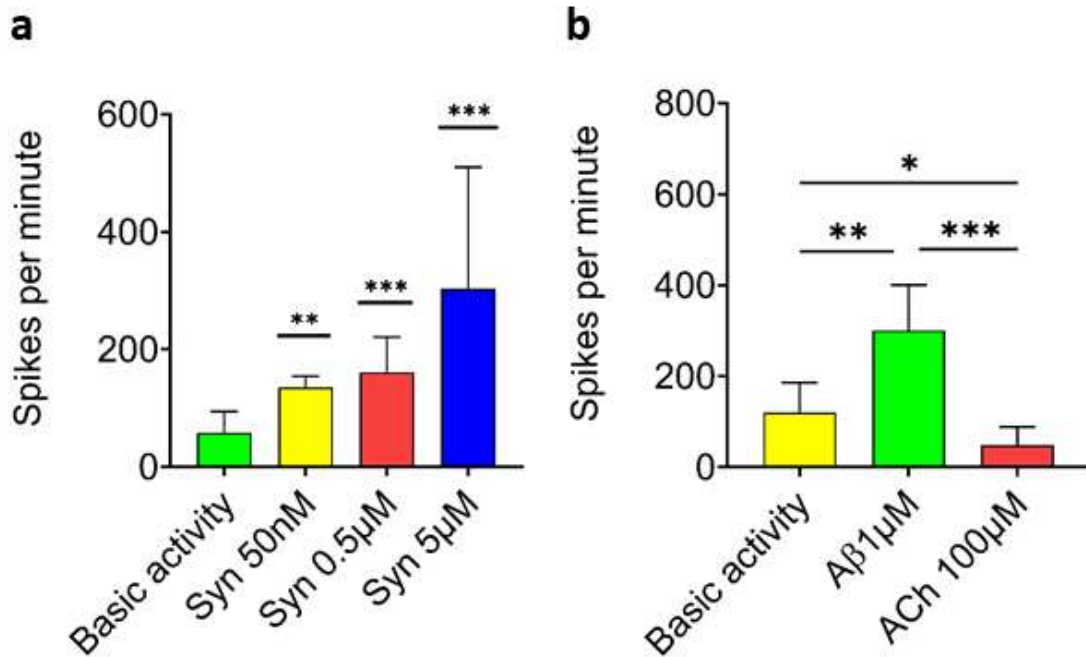


Figure 1: Multi-Electrode-Array measurements of isolated enteric neurons after (a) A30P-alpha-synuclein and (b) beta-amyloid/acetylcholine exposure. * $p \leq 0.05$ ** $p \leq 0.01$ and *** $p \leq 0.001$ using ANOVA.

1. Postuma R.B., Berg D., Stern M., Poewe W., Olanow C.W., Oertel W., Obeso J., Marek K., Litvan I., Lang A.E., Halliday G., Goetz C.G., Gasser T., Dubois B., Chan P., Bloem B.R., Adler C.H., Deuschl G. MDS clinical diagnostic criteria for Parkinson's disease. *Mov Disord.* 2015 Oct;30(12):1591-601. doi: 10.1002/mds.26424. PMID: 26474316.

2. Braak H., de Vos R.A., Bohl J., Del Tredici K. Gastric alpha-synuclein immunoreactive inclusions in Meissner's and Auerbach's plexuses in cases staged for Parkinson's disease-related brain pathology. *Neurosci Lett.* 2006 Mar 20;396(1):67-72. doi: 10.1016/j.neulet.2005.11.012. Epub 2005 Dec 5. PMID: 16330147.

Electrophysiological characterization of human pluripotent stem cell-derived disease models of hereditary spastic paraplegia type 4 (SPG4)

Clemens Sauter^{a,b,c}, Milena Korneck^{a,b,c}, Linus Wiora^{a,b,c}, Jacob Helm^{a,b,c}, Jasmin Treu^a, Fulya Ersoy^d, Matthijs van der Moolen^d, Betül Uysal^b, Carolin Fischer^b, Melanie Kraft^b, Paolo Cesare^d, Ludger Schöls^{a,b}, Stefan Hauser^{a,b}

- a. German Center for Neurodegenerative Diseases (DZNE), 72076 Tübingen, Germany
- b. Hertie Institute for Clinical Brain Research, University of Tübingen, 72076 Tübingen, Germany
- c. Graduate School of Cellular and Molecular Neuroscience, University of Tübingen, 72076 Tübingen, Germany
- d. NMI Natural and Medical Sciences Institute at the University of Tübingen, 72770 Reutlingen, Germany

* Clemens.Sauter@uni-tuebingen.de

Hereditary spastic paraplegia (HSP) is a heterogeneous group of neurodegenerative diseases of the spinal cord going along with progressive degeneration of upper motor neurons. Mutations in *SPAST* (SPG4) are the most common cause of HSP, which encodes spastin, a microtubule severing protein. A precise mechanistic understanding of SPG4 pathology remains unclear, partly because multiple perturbed disease pathways likely integrate into a more complex pathomechanism.

While most *in vitro* models of HSP appear to reflect only specific aspects of the disease, neuronal-glia co-cultures grant an exciting opportunity to investigate autonomous and non-cell autonomous effects of SPG4 in a more comprehensive approach. Taking advantage of iPSC-derived neural cell types, we analyzed electrophysiological properties using microelectrode arrays (MEAs). This provides a suitable platform to identify potential disease-relevant functional abnormalities in SPG4 neural networks with specific focus on synaptic connectivity. To this end, human iPSC-derived cortical neurons from controls and isogenic heterozygous and homozygous *SPAST* knockouts were cultivated together with primary mouse astrocytes on Multiwell-MEAs. A range of parameters describing spiking, bursting and network activity was extracted and compared across cell lines. Long-term co-culture experiments revealed pro-maturational effects of astrocytes upon cortical neuronal networks.

The implementation of disease-specific iPSC-derived astrocytes will facilitate further investigations into neuron-glia interactions, while providing a fully human culture system that enables to investigate non-cell autonomous effects and the role of astrocytes in the pathology of HSP.

A hiPSC-based model of *PARK2* copy number variation carriers: Finding the link between adult-onset ADHD, mitochondrial function and NVU impairment

Sabrina Oerter,^{a,b*} Markus Glaser,^b Zora Schickardt,^c Rhiannon McNeill,^c Carolin Koreny,^c Erhard Wischmeyer,^d Sarah Kittel-Schneider,^c and Antje Appelt-Menzel^{a,b}

- a. Fraunhofer Institute for Silicate Research ISC, Würzburg, Germany
- b. Chair Tissue Engineering and Regenerative Medicine, University Hospital Würzburg, Würzburg, Germany
- c. Department of Psychiatry, Psychosomatics and Psychotherapy, University Hospital Würzburg, Würzburg, Germany
- d. Department of Cellular Neurophysiology, University of Bielefeld, Bielefeld, Germany

* sabrina.oerter@isc.fraunhofer.de

Copy number variations (CNVs) in the *PARK2* gene have been shown to be associated with attention deficit hyperactivity disorder (ADHD) [1]. Thus, genetic variants in *PARK2* might result in protein dysfunction, thereby impacting mitochondrial (Mt) stability. In addition, disruption of the blood-brain barrier (BBB) has been suggested to play a role in ADHD [2], leading to changes in BBB functionality and metabolic activity, and thus to barrier opening and a disrupted microenvironment, thereby affecting neuronal physiology. In previous studies, we developed a cell model from ADHD patient-derived fibroblast (carriers and non-carriers of a *PARK2* CNV previously associated with ADHD) which were reprogrammed to induced pluripotent stem cells (hiPSC) and differentiated into neuronal cells. In those fibroblasts and neuronal cells we could find preliminary evidence for Mt dysfunction. Furthermore, we could show that the hiPSC-derived neurons were electrophysiological active and small changes in synaptic activity were observed between *PARK2* CNV carriers suffering from ADHD versus cells from healthy controls (Figure 1). Taken together, there appears to be a link between ADHD, mitochondrial and neuronal dysfunction, which has not previously been investigated.

In this project, our first findings will further be validated in an advanced isogenic *in vitro* test system of the neurovascular unit (NVU) combining the BBB with the adjacent central nervous system to recapitulate ADHD-related cellular and molecular, as well as functional changes (Figure 2). For the development of NVU models, patient-specific brain capillary endothelial cells and cortical neurons will be co-cultured in static transwell-based setups and subsequently under microfluidic culture conditions. Compared to respective monoculture, complex crosstalk between both cell types and cellular impairment are examined.

Our NVU model will provide a standardized platform for screening in ADHD treatment and can be used to replicate and explore gene-environment interactions by simulating ADHD-associated risk factors. Furthermore, therapeutic approaches will be validated to restore mitochondrial and cellular function.

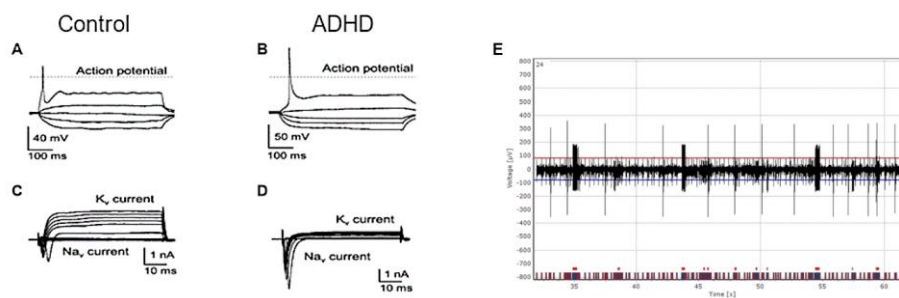


Figure 1: Whole-cell patch-clamp recording of hiPSC-derived cortical neurons (control and ADHD patient) upon depolarizing pulses from -100 to +20 mV inducing single action potentials (A,B), voltage-clamp recording showing typical neuronal voltage-gated sodium and potassium currents (C,D). (E) Functional analysis of hiPSC-derived neurons of a healthy patient based on local field potential trace of an individual microelectrode (MEA system).

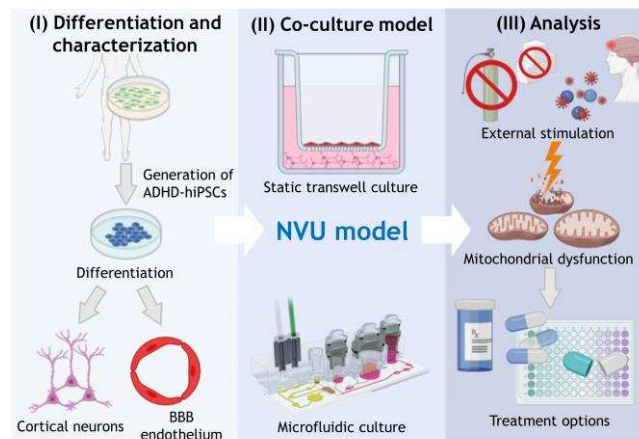


Figure 2: Project concept to generate ADHD-specific *in vitro* models of the NVU with subsequent analysis of mitochondrial and cellular function under ADHD-related stress conditions and after treatment.

References

1. Jarick, I., Volckmar, A. L., Pütter, C., Pechlivanis, S., Nguyen, T. T., Dauvermann, M. R., Beck, S., Albayrak, Ö., Scherag, S., Gilsbach, S., Cichon, S., Hoffmann, P., Degenhardt, F., Nöthen, M. M., Schreiber, S., Wichmann, H. E., Jöckel, K. H., Heinrich, J., Tiesler, C. M., Faraone, S. V., ... Hinney, A. (2014). Genome-wide analysis of rare copy number variations reveals PARK2 as a candidate gene for attention-deficit/hyperactivity disorder. *Molecular psychiatry*, 19(1), 115–121. <https://doi.org/10.1038/mp.2012.161>
2. Leffa, D. T., Torres, I., & Rohde, L. A. (2018). A Review on the Role of Inflammation in Attention-Deficit/Hyperactivity Disorder. *Neuroimmunomodulation*, 25(5-6), 328–333. <https://doi.org/10.1159/000489635>

Neocortical Layers 5 and 6 are the Drivers of Baseline Network Activity in Micro-electrode Array Recordings of Epileptic Human Brain Slice Cultures

Jonas Ort^{a,b,d,*}, Jenny Wickham^c, Aniella Bak^d, Andrea Corna^{c,g}, Julia Schmierer^c, Thomas Wuttke^{e,f}, Niklas Schwarz^f, Hans Clusmann^a, Yvonne Weber^d, Daniel Delev^{a,b}, Günther Zeck^{c,g}, Henner Koch^d

- a. Department of Neurosurgery, RWTH Aachen University, Medical Faculty, Aachen, Germany
 - b. Neurosurgical Artificial Intelligence Lab Aachen (NAILA), RWTH Aachen University Hospital, Aachen, Germany
 - c. Neurophysics, Natural and Medical Sciences Institute, University of Tübingen, Reutlingen, Germany
 - d. Department of Epileptology, Neurology, RWTH Aachen University, Medical Faculty, Aachen, Germany
 - e. Department of Neurosurgery, University of Tübingen, Germany
 - f. Department of Neurology and Epileptology, Hertie Institute for Clinical Brain Research, University of Tübingen, Germany
 - g. Institute of Biomedical Electronics, TU Wien, Austria
- * jort@ukaachen.de

Objective

Epilepsy is a condition hallmarked by synchronized depolarizations of groups of neurons resulting in seizures.¹ The underlying conditions can vary extensively ranging from structural pathologies to trauma. However, the electrophysiological and micro-anatomical correlates of seizures are yet to be described. Here, we leverage novel culturing methods for human brain slices and spatio-temporal electrophysiological recordings using micro-electrode arrays (MEA) to investigate for the features of synchronized network activities to describe epileptic discharges on a micro-network-level.^{2,3}

Methods

Neocortical human brain tissue samples from resective epilepsy surgeries were cultured using human cerebrospinal fluid (hCSF) as described. MEA recordings were performed using a 256-MEA with artificial CSF (aCSF) and hCSF. Data analysis was performed using custom Python scripts including the libraries numpy and scipy. In short, spikes were extracted using a mean absolute deviation threshold-based approach. Network activities were defined as episodes of elevated activity with the mean moving average firing rate (FR) exceeding the mean FR of the whole recording. For each of these network events ($n = 6043$), we extracted a total of 62 features including interspike-interval distributions, layer specific mean FR, and channels specific bursting times. Scipy's Pearsonr-method was used to calculate correlations.

Results

Mean length of network activities was 1.765 seconds with a mean FR of 616.18 Hz. We found a strong correlation between the FR of layers 5 and 6 and the network FR ($r = 0.993$, $p < 0.001$). This was not found for any other neocortical layer (layer 1: $r = -0.125$, $p < 0.001$, layer 2 and 3: $r = 0.222$, $p < 0.001$, layer 4: $r = 0.541$, $p < 0.001$). For layers 5 and 6, this effect was observed for experiments in hCSF and aCSF, which indicates a network-modulating role of these layers. Layers 2 and 3 only showed a strong correlation with the network burst FR for hCSF ($r = 0.85$, $p < 0.001$) but not for aCSF ($r = 0.063$, $p < 0.001$).

Conclusion

Our finding suggests a distinct role of layers 5 and 6 in the emergence of highly synchronized network spiking activity. Although the differentiation between electrophysiological equivalent of interictal discharges and physiological network activity remains difficult, our results may help to understand epilepsy as network disease with spatially distributed layer-specific properties.

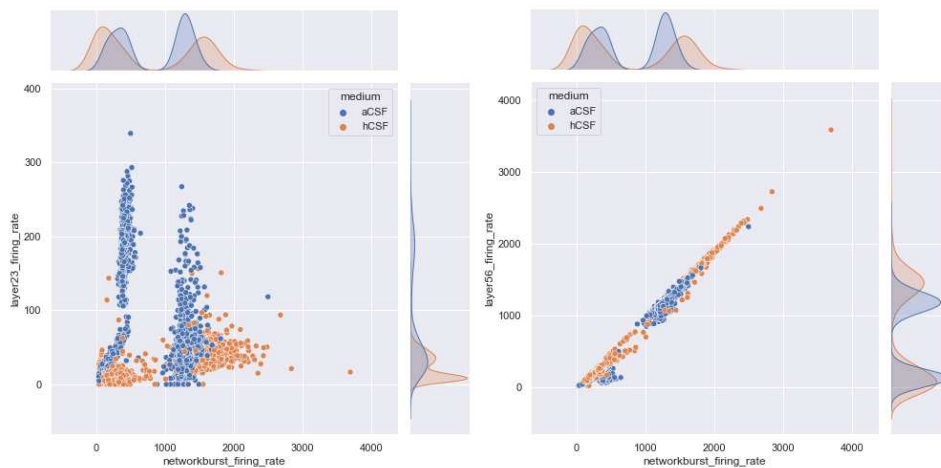


Figure 1: Firing rate of networkbursts compared to specific firing rates of Layers 2/3 (left) and Layers 5/6 (right). Each dot represents one network bursting event.

References

1. Duncan, J. S., Sander, J. W., Sisodiya, S. M. & Walker, M. C. Adult epilepsy. *The Lancet* **367**, 1087–1100 (2006).
2. Schwarz, N. *et al.* Long-term adult human brain slice cultures as a model system to study human CNS circuitry and disease. *eLife* **8**, e48417 (2019).
3. Wickham, J. *et al.* Human Cerebrospinal Fluid Induces Neuronal Excitability Changes in Resected Human Neocortical and Hippocampal Brain Slices. *Front. Neurosci.* **14**, (2020).

Synaptic function in human cortical biopsies from patients with idiopathic normal pressure hydrocephalus

Mireia Gómez-Budia^{a#}, Antonios Dougalis^{a#}, Anssi Pelkonen^a, Ville Leinonen^{b,c, #}, Tarja Malm^{a, #, *}

- a. A. I. Virtanen Institute for Molecular Sciences, Faculty of Health Sciences, University of Eastern Finland, Neulaniementie 2, 70211 Kuopio, Finland
- b. Department of Neurosurgery, Kuopio University Hospital, 70029 KYS, Finland
- c. Neurosurgery, Institute of Clinical Medicine, Faculty of Health Sciences, University of Eastern Finland, 70210 Kuopio, Finland

#, # equal contribution

* tarja.malm@uef.fi

The function of cortical synapses is mostly studied in animal models and human induced pluripotent stem (hiPSC) derived cultures. However, the animal models are functionally different from their human counterparts [1] and the hiPSC-derived models do not represent the fully mature neurons and synapses in the human brain, especially those in aged individuals [2]. Data on the function of human cortical neurons can be obtained from large (0.5-1cm³) biopsies from patients with intractable epilepsy or brain tumors. There is also an option for obtaining biopsies from the human cortex unaffected by epilepsy or cancer: small volume (~10-20 mm³) Broadman area 8 biopsies excised from elderly patients undergoing shunt operation for idiopathic normal pressure hydrocephalus (iNPH) [2,3]. iNPH is characterized by accumulation of excess cerebrospinal fluid to ventricles [3]. The shunt tube drains the excess CSF to the abdominal cavity, and the biopsy can be obtained from shunt implantation site with minimally invasive methods. Our novel aim was to establish whether these biopsies can provide functional microelectrode array (MEA) data of synaptic function in the human cortex.

The shunt surgeries are performed at the Kuopio University Hospital where biopsies are obtained from 1-2 patients/week. The use of biopsies has been approved by The Research Ethics Committee of the Northern Savo Hospital District (decision No 276/13.02.00/2016) and all patients have given their informed consent according to the declaration of Helsinki. The biopsies are collected to ice-cold artificial CSF (aCSF) and embedded in 2 % agarose and sliced into 350 µm sections containing all cortical layers within 1 h of collection. In addition to electrophysiology, slices from the same biopsy are collected for spatial transcriptomics, proteomics, electron microscopy and diagnostic evaluation for signs of other neurodegenerative diseases with immunohistochemistry (Fig.1). In addition, blood and CSF samples are obtained from the same patients. MEA recordings are performed using the MEA2100-Mini-60-System (Multichannel Systems [MCS], Germany) under constant perfusion. The responsiveness to pharmacological stimuli was studied by treatments with carbachol (50 µM, 5 min) and N-methyl-D-aspartate (NMDA; 200 µM, 2 min) on sample penetrating MEAs (60-3DMEA250/12/100iR-Ti, MCS). For initiating long-term potentiation, the slices were treated with 100 µM picrotoxin and subjected to theta-burst stimulation (TBS). The LTP experiments were performed on sample penetrating MEAs and MEAs with planar electrodes (60MEA200/30iR-Ti, MCS).

The iNPH biopsies can be maintained with moderate yield as acute slices. Carbachol and NMDA caused reversible, layer-dependent cortical activation. LTP could be induced in the samples and analysed, even though the analysis was hampered by the overlap of the stimulation-artefact and synaptic response. We conclude that this unique iNPH patient cortical biopsies are a physiologically relevant model of synaptic function in aged human neurons.

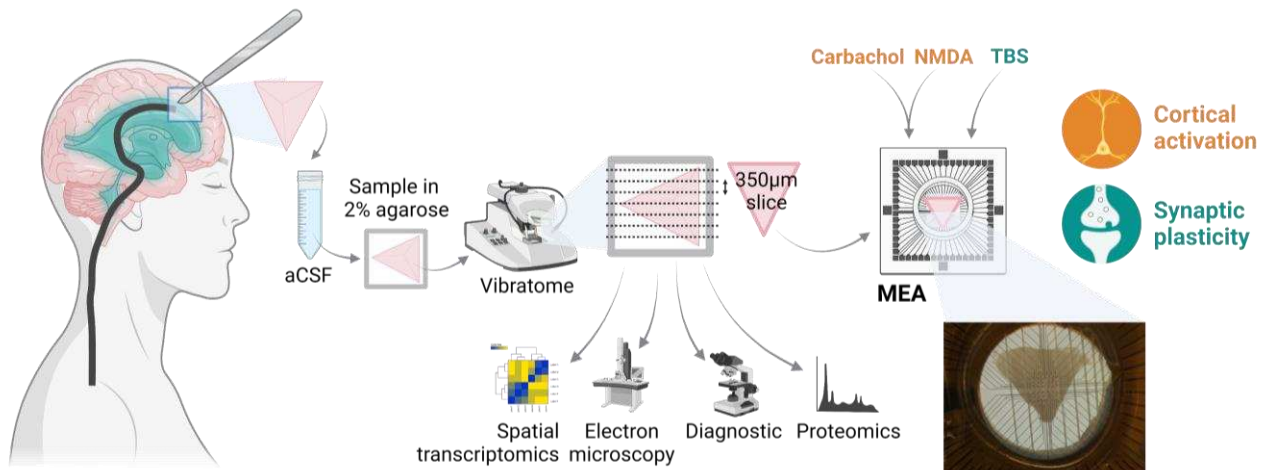


Figure 1. A small biopsy from an iNPH patient is collected into aCSF. In the laboratory, it is embedded in agarose and sliced with a vibratome obtaining 350µm slices. They are used for spatial transcriptomics, electron microscopy, diagnostics and proteomics. More importantly, one or two slices are destined to electrophysiological MEA experiments in order to unravel, using pharmacological or electrical stimuli, the cortical activation and synaptic plasticity of these unique samples.

References

1. Hodge, R.D.; Bakken, T.E.; Miller, J.A.; Smith, K.A.; Barkan, E.R.; Graybuck, L.T.; Close, J.L.; Long, B.; Johansen, N.; Penn, O.; et al. Conserved cell types with divergent features in human versus mouse cortex. *Nature* **2019**, *573*, 61–68, doi:10.1038/s41586-019-1506-7.
2. Pelkonen, A.; Pistono, C.; Klecki, P.; Gómez-Budia, M.; Dougalis, A.; Konttinen, H.; Stanová, I.; Fagerlund, I.; Leinonen, V.; Korhonen, P.; et al. Functional Characterization of Human Pluripotent Stem Cell-Derived Models of the Brain with Microelectrode Arrays. *Cells* **2021**, *11*, doi:10.3390/cells11010106.
3. Leinonen, V.; Koivisto, A.M.; Savolainen, S.; Rummukainen, J.; Tamminen, J.N.; Tillgren, T.; Vainikka, S.; Pyykkö, O.T.; Mölsä, J.; Fraunberg, M.; et al. Amyloid and tau proteins in cortical brain biopsy and Alzheimer's disease. *Ann. Neurol.* **2010**, *68*, 446–453, doi:10.1002/ana.22100.

Characterization of the cortical-hippocampal interactions in an *in vitro* MEA-based model

Martina Brofiga^{a,b}, Mariateresa Tedesco^c, Marietta Pisano^{a,b}, Paolo Massobrio^{a,d,*}

- a. Department of Informatics, Robotics, and Systems Engineering (DIBRIS), University of Genova, Genova (Italy)
- b. ScreenNeuroPharm s.r.l, Sanremo (Italy)
- c. 3Brain GmbH, Wädenswil, (Switzerland)
- d. National Institute for Nuclear Physics (INFN), Genova (Italy)

* paolo.massobrio@unige.it

The human brain is the most complex organ of our body. It gives rise to all our thoughts, actions, memories, feelings, and experiences. However, since such high complexity, understanding human physiology, as well as pathogenesis, is not straightforward. Most of our knowledge about neural signal processing and transmission among different cell assemblies derives from computational models [1]. These models make simplistic assumptions about the biophysical properties of neurons that can modify their real nature and properties. To overcome this problem, we recreated an *in vitro* network consisting of interconnected sub-populations of dissociated rat neurons coupled to Micro-Electrode Arrays (MEAs) keeping three fundamental properties of the real brain: heterogeneity, three dimensionality (3D), and modularity [2]. In this work, we focused on the functional and dynamical interactions between interconnected cortical and hippocampal assemblies.

To reproduce *in vitro* such properties, we developed polydimethylsiloxane (PDMS)-based masks reversible bonded with the area of MEAs. We used pre-sterilized and pre-coated glass microbeads (40 μm diameter) [3] in order to realize a packed scaffold where neuronal networks can spread their connections recreating a 3D connectivity. The polymeric devices were fabricated by conventional soft lithographic molding technique. Regarding the polymeric mask, we developed devices with two (Figure 1A) and three (Figure 1B) interconnected compartments. In the first case, the two compartments (4x2 mm) are separated by 25 parallel microchannels. In the second one, the larger compartment displays a width of 6.5 mm and a length of 4.3 mm. The smaller ones have a diameter of 3.4 mm. Every compartment is connected with the other through 20 micro-channels. In both mask the micro-channels are equally spaced at interval of 50 μm and present a width of 10 μm , length of 200 μm and a height of 5 μm .

We investigated the propagation of the network activity originated by the interactions of the different populations in 2D and 3D configuration during the networks' development. Moreover, we correlated functional and structural connectivity to the recorded dynamics. The main finding is that the coexistence of the two neuronal types (i.e., cortical and hippocampal neurons) modulated the features of the functional connections (excitation vs. inhibition), changing the patterns of electrophysiological activity. We observed over a wide dataset of cultures that hippocampal neurons preferentially project inhibitory connections towards the cortical counterpart acting on the temporal scale of the network bursts. On the contrary, cortical neurons establish a larger amount of intra-population connections, suggesting a high degree of clusterization. When the two populations are interconnected in a 3D fashion, we observed variation both in terms of spiking and bursting activity: a wider dynamics repertory similarly to what found *in vivo* can be appreciated [4].

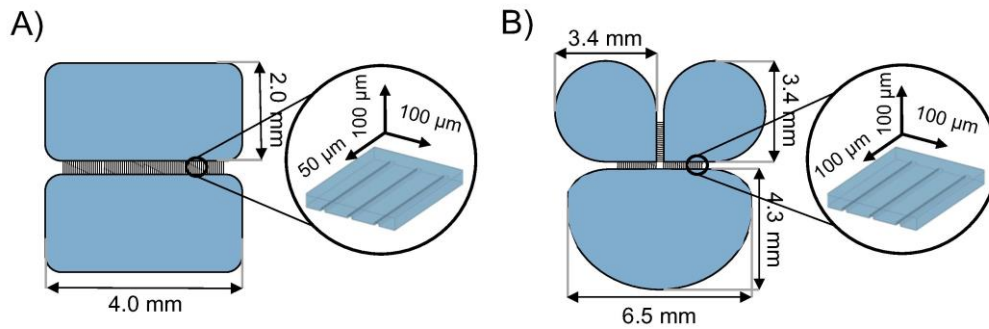


Figure 1: Sketch of the polymeric device used. A) Dual-compartment mask. B) Three-compartment map.

References

- [1] H. Markram, "The Blue Brain Project," *Nature Reviews Neuroscience* 2006 7:2, vol. 7, no. 2, pp. 153–160, Feb. 2006, doi: 10.1038/nrn1848.
- [2] M. Brofiga, M. Pisano, R. Raiteri, and P. Massobrio, "On the road to the brain-on-a-chip: a review on strategies, methods, and applications," *Journal of Neural Engineering*, vol. 18, no. 4, p. 041005, Aug. 2021, doi: 10.1088/1741-2552/AC15E4.
- [3] S. Pautot, C. Wyart, and E. Isacoff, "Colloid-guided assembly of oriented 3D neuronal networks," *Nature Methods*, vol. 5, pp. 735–740, 2008, doi: 10.1038/nmeth.1236.
- [4] X. Leinekugel, R. Khazipov, R. Cannon, H. Hirase, Y. Ben-Ari, and G. Buzsáki, "Correlated bursts of activity in the neonatal hippocampus in vivo," *Science*, vol. 296, no. 5575, pp. 2049–2052, Jun. 2002, doi: 10.1126/science.1071111.

Towards understanding *in vitro* brain circuits: a study on cortico-hippocampal and cortico-thalamic cultures

Francesca Callegari,^a Martina Brofiga,^{ab} Paolo Massobrio,^{ac*}

- a. Department of Informatics, Bioengineering, Robotics, Systems Engineering (DIBRIS), University of Genova, Genova, Italy
 - b. ScreenNeuroPharm
 - c. National Institute for Nuclear Physics (INFN), Genova, Italy
- * paolo.massobrio@unige.it

One of the biggest challenges of today's neuroscience is to understand how circuits of neurons compute, a problem that, according to some, we should be able to solve in the next 50 years [1]. Cracking the code of single neuronal circuits should help to understand even harder unsolved issues, from the basic principle of memory and brain computation, up to what gives rise to pathological conditions. The scientific question behind the present work fits in this framework. Our aim was to study and compare two different brain circuits, the cortico-hippocampal (Cx-Hp) and the cortico-thalamic (Cx-Th) ones (Figure 1a). To emulate these circuits, we exploited an *in vitro* model made up of polymeric microfluidic masks and Micro-Electrode Arrays (MEAs) to create interconnected heterogeneous networks. Spontaneous spiking and bursting activities were detected with the methods described in [2] and [3]. Then, we identified the excitatory and inhibitory functional connections and evaluated the synchronization level of the spiking activity. In particular, statistical interdependence between neuron pairs was obtained identifying the local maxima and minima in cross-correlograms [4]. Finally, the synchronization was evaluated by means of the Coincidence Index (CI_0) defined on the cross-correlation function.

Our results suggest that the modulation of the cortical activity is highly dependent on the physiological input it receives, as is evident from the spontaneous activity of the examined configurations and the cortical control (Figure 1b). Hippocampal neurons drove a more sustained and packed cortical activity and a reshaping of its functional connectivity. The hippocampal afferents induced a change in the distribution of the inhibitory connections, which resulted in a decrease in the amount of inhibitory information exchanged between the two populations (Figure 1c, *top*). Considering the role of GABAergic neurons in the synchronization of networks [5] and our findings on connectivity, we investigated the synchronization level to find a possible interplay between connectivity and dynamics. We observed a significant increase in the intra-compartment CI_0 with respect to the inter-compartment one (Fig. 1e, *top*). Such a behaviour can be explained by the altered distribution of the strongest functional connections, as fewer of them are established between the compartments in the Cx-Hp configuration (Figure 1e, *top*). This suggests the formation of internal microcircuit which could justify the higher intra-compartment synchronization. Instead, Thalamic neurons induced a more random and scattered cortical activity. The change in cortical activity was supported by a strong redistribution of the functional inhibitory links. No inhibitory information was exchanged between the compartments (Figure 1c and e, *bottom*). Moreover, the synchronization level increased under thalamic influence (Fig. 1d, *bottom*). The higher intra-compartment synchronization may be sustained by the different distribution of the inhibitory links [5], which are segregated in the originating compartment. To better assess the thalamic population's role in the synchronicity of the network, its activity was chemically silenced. In this condition, the CI_0 was lower than in the Cx-Th configuration but still significantly higher than in the controls (Fig. 1d, *bottom*). This result demonstrated that when the thalamic population projected afferences to the cortical sub-population, it strongly drove the activity of the cortical network, forcing its rhythm on the whole culture.

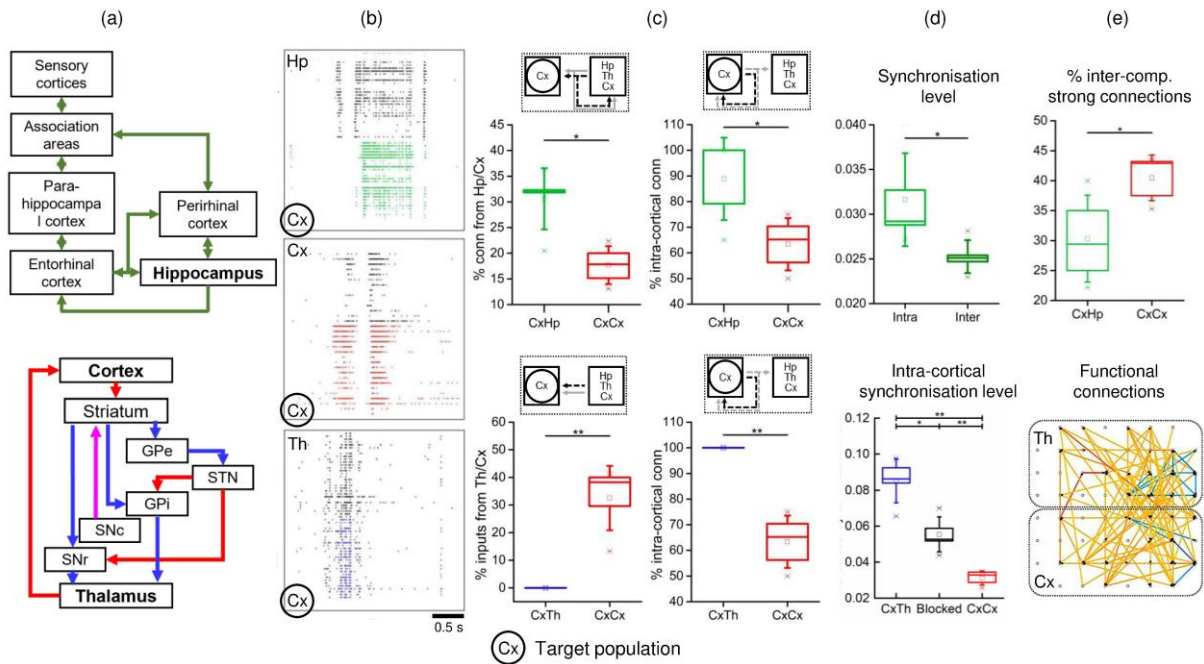


Figure 1: a) Diagram of the cortico-hippocampal (top) and cortico-thalamic (bottom) circuits. b) Raster plots of 3 seconds of spontaneous activity from a Cx-Hp (top), Cx-Cx (middle), and Cx-Th (bottom) representative population. c) Percentages of inhibitory connections within and between the compartments, in particular: connections from the source (top left) and from the target (top right) compartments in Cx-Hp configuration (green) and relative cortical control (red); inputs to (bottom left) and connections from (bottom right) the target compartment in the Cx-Th configuration (blue) and relative cortical control (red). d) Synchronization level: comparison between intra- and inter-compartment Cl_0 in Cx-Hp configuration (top); intra-cortical Cl_0 in Cx-Th and Cx-Cx configuration. e) Functional connections: percentage of inter-compartment strong connections in Cx-Hp configuration and relative control (top); map of the strongest detected links on MEA in Cx-Th configuration (bottom)

References

1. Adolphs R. (2015). The unsolved problems of neuroscience. *Trends Cogn Sci*, 19(4):173. doi: 10.1016/J.TICS.2015.01.007.
2. Maccione A., Gandolfo M., Massobrio P., Novellino A., Martinoia S., Chiappalone M. (2009). A novel algorithm for precise identification of spikes in extracellularly recorded neuronal signals. *J Neurosci Methods*, 177:241–9. doi: 10.1016/j.jneumeth.2008.09.026.
3. Chiappalone M., Novellino A., Vajda I., Vato A., Martinoia S., van Pelt J. (2005). Burst detection algorithms for the analysis of spatio-temporal patterns in cortical networks of neurons. *Neurocomputing*, 65–66(SPEC. ISS.):653–62. doi: 10.1016/j.neucom.2004.10.094.
4. De Blasi S., Ciba M., Bahmer A., Thielemann C. (2019). Total spiking probability edges: A cross-correlation based method for effective connectivity estimation of cortical spiking neurons. *J Neurosci Methods*, 312:169–81. doi: 10.1016/j.jneumeth.2018.11.013.
5. Bonifazi P., Goldin M., Picardo M. A., Jorquera I., Cattani A., Bianconi G., et al. (2009). GABAergic hub neurons orchestrate synchrony in developing hippocampal networks. *Science*, 326(5958):1419–24. doi: 10.1126/science.1175509.

Neuronal heterogeneity as necessary condition to perform pharmacological studies on brain-on-a-chip models

Fabio Poggio^a, Martina Brofiga^{a,b}, Francesca Callegari^a, Paolo Massobrio^{a,c,*}

- a. Department of Informatics, Bioengineering, Robotics, and Systems Engineering (DIBRIS), University of Genova, Via All'Opera Pia, 15, 16145 Genova GE, Italy.
- b. ScreenNeuroPharm s.r.l, Sanremo (Italy)
- c. National Institute for Nuclear Physics (INFN), Genova (Italy)

* paolo.massobrio@unige.it.

The brain is a complex system characterized by different neuronal populations (e.g., cortical, hippocampal, thalamic neurons) that interact following well-defined principles of connectivity [1]. Furthermore, neurons exhibit a rich range of spatiotemporal patterns and dynamic states [2]. *In vitro* models, where dissociated neurons are chronically coupled to Micro-Electrode Arrays (MEAs), allow to study many neuronal network properties taking into account such complexity [3]. Dissociated neuronal networks coupled to MEAs have been used as *in vitro* model for several applications like the investigation of the spontaneous dynamics [4], [5], the modulation of their response by delivering electrical stimulation [6], and the induction of synaptic plasticity [7], and to perform pharmacological studies by using different neuronal types. However, most of the works made use of too simplified systems with only one type of neuronal cell (homogeneous) and did not consider the intrinsic modularity features of the brain [8]. Such shortcomings could lead to underestimate or overestimate the effect of a drug.

In the light of the above considerations, interacting sub-populations (modularity) of different types of neurons (heterogeneity) could be a valid tool to investigate chemical modulation of the electrophysiological activity [9].

In this work, we used both heterogeneous and homogeneous *in vitro* engineered neuronal assemblies made up of interacting sub-populations of cortical and hippocampal neurons as a tool to investigate how this specific neuronal circuit responds to the delivery of bicuculline (BIC), a competitive antagonist of GABA_A receptors [10].

In order to guarantee the structural segregation of the different neuronal populations and mutual interconnections between them, we used a two-chamber polymeric mask made up of polydimethylsiloxane (PDMS) [9].

Comparing the spiking activity of homogeneous and heterogeneous networks, we observed that the effects of BIC turn out to be relevant for a smaller dose on the cortical-hippocampal networks. Indeed, the heterogeneous hippocampal sub-population ($1.04 \pm 1.20 \mu\text{M}$) showed a reduction of 92% (p-value = 0.03, see Figure 1 *red*) in the average IC₅₀ with respect to the hippocampal controls ($12.86 \pm 13.92 \mu\text{M}$). Regarding the cortical cultures, the average IC₅₀ is $0.75 \pm 0.68 \mu\text{M}$ in the heterogeneous configuration, and $16.49 \pm 15.86 \mu\text{M}$ in the cortical controls, with a reduction of 95% (p-value = 0.006, see Figure 1 *green*). Additionally, the effect of the BIC is significantly more reproducible on the heterogeneous networks, in fact the heterogeneous hippocampal and cortical Fano Factors values are 91% and 96% lower than the corresponding homogeneous ones, respectively.

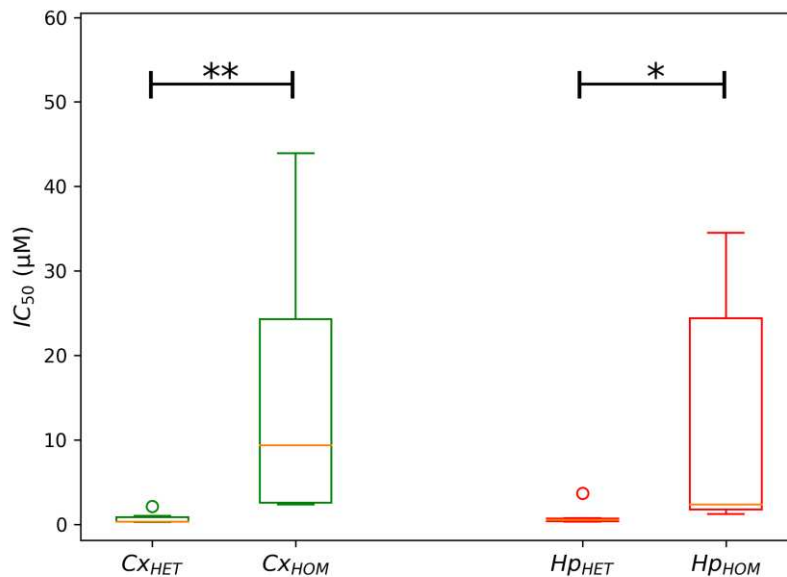


Figure 1: IC_{50} boxplots showing the four considered categories, i.e., hippocampal (Hp_{HET}) and cortical (Cx_{HET}) sub-populations of the heterogeneous networks, hippocampal (Hp_{HOM}) and cortical (Cx_{HOM}) homogeneous assemblies (* refers to $p < 0.05$, and ** to $p < 0.01$ Kruskal-Wallis non-parametric test).

References

- [1] T. T. Kanagasabapathi *et al.*, "Functional connectivity and dynamics of cortical-thalamic networks co-cultured in a dual compartment device," *J. Neural Eng.*, vol. 9, no. 3, 2012, doi: 10.1088/1741-2560/9/3/036010.
- [2] C. Forró *et al.*, "Modular microstructure design to build neuronal networks of defined functional connectivity," *Biosens. Bioelectron.*, vol. 122, 2018, doi: 10.1016/j.bios.2018.08.075.
- [3] M. Brofiga, M. Pisano, R. Raiteri, and P. Massobrio, "On the road to the brain-on-a-chip: A review on strategies, methods, and applications," *Journal of Neural Engineering*, vol. 18, no. 4, 2021, doi: 10.1088/1741-2552/ac15e4.
- [4] V. Pasquale, P. Massobrio, L. L. Bologna, M. Chiappalone, and S. Martinoia, "Neuronal Avalanches In Networks Of Neurons Cultured In Vitro," 2008.
- [5] G. J. Brewer, M. D. Boehler, A. N. Ide, and B. C. Wheeler, "Chronic electrical stimulation of cultured hippocampal networks increases spontaneous spike rates," *J. Neurosci. Methods*, vol. 184, no. 1, 2009, doi: 10.1016/j.jneumeth.2009.07.031.
- [6] D. Poli and P. Massobrio, "High-frequency electrical stimulation promotes reshaping of the functional connections and synaptic plasticity in in vitro cortical networks," *Phys. Biol.*, vol. 15, no. 6, 2018, doi: 10.1088/1478-3975/aae43e.
- [7] M. Chiappalone, P. Massobrio, and S. Martinoia, "Network plasticity in cortical assemblies," *Eur. J. Neurosci.*, vol. 28, no. 1, 2008, doi: 10.1111/j.1460-9568.2008.06259.x.
- [8] M. Frega *et al.*, "Cortical cultures coupled to Micro-Electrode Arrays: A novel approach to perform in vitro excitotoxicity testing," *Neurotoxicol. Teratol.*, vol. 34, no. 1, 2012, doi: 10.1016/j.ntt.2011.08.001.
- [9] M. Brofiga, M. Pisano, M. Tedesco, R. Raiteri, and P. Massobrio, "Three-dimensionality shapes the dynamics of cortical interconnected to hippocampal networks," *J. Neural Eng.*, vol. 17, no. 5, 2020, doi: 10.1088/1741-2552/abc023.
- [10] R. Razet *et al.*, "Use of bicuculline, a GABA antagonist, as a template for the development of a new class of ligands showing positive allosteric modulation of the GABA(A) receptor," *Bioorganic Med. Chem. Lett.*, vol. 10, no. 22, 2000, doi: 10.1016/S0960-894X(00)00514-X.

Long-term electrophysiological characterization of excitatory neuronal networks derived from human induced pluripotent stem cells

Giulia Parodi ^a, Monica Frega ^b, Sergio Martinoia ^{a,*}

a. Department of Informatics, Bioengineering, Robotics, Systems Engineering (DIBRIS), University of Genoa, Via All'Opera Pia 13, 16145, Genova (GE)

b. Department of Clinical neurophysiology, University of Twente, 7522 NB Enschede, Netherlands.

* giulia.parodi@edu.unige.it

In vitro neuronal models on micro-electrodes arrays (MEAs) have become an important tool to investigate the complex behaviour of healthy and diseased neuronal circuits [1]. MEAs proved to be a valid and widely used tool to record activity from different neuronal culture systems, mostly from rodent origin [7]. However, rodent models can only be partially compared to the processes of the human brain, and several human disorders cannot be reproduced with rodent cultures [6]. Human induced pluripotent stem cells (hiPSCs) technology allows the network phenotyping with systems that most closely resembles the human brain [3, 5, 9], increasing the popularity of MEA technology [2, 3]. Nevertheless, MEA technology is not always used to its full potential to investigate hiPSC-derived neuronal network as the latter have not been benchmarked as extensively as rodent neuronal cultures. Many studies often quantify the general neuronal network activity by a single or a few parameters [3, 8], particularly the mean firing rate (MFR) and the mean burst rate (MBR), not addressing the complex network characteristics. The purpose of this study is to perform a long-term electrophysiological characterization of *in vitro* hiPSC-derived neuronal networks generated through one of the most widely used differentiation protocols (i.e., Ngn2 induction [4, 10], see Figure 1), with a wide set of non-standard parameters, similarly to a previous study [9]. HiPSCs were obtained from fibroblasts derived from skin biopsies of healthy subjects and reprogrammed into stem cells. Cells were differentiated into cortical excitatory neurons (iNeurons) through Ngn2 overexpression, induced with the introduction of doxycycline into the culture medium, obtaining early-stage neurons cultures. After 3 days, we moved the cultures on MEAs pre-coated with poly-L-ornithine hydrobromide (Sigma-Aldrich) (50 $\mu\text{g}/\text{mL}$) and human laminin (BioLamina) (20 $\mu\text{g}/\text{mL}$), obtaining networks composed of excitatory iNeurons and rat astrocytes to ensure proper support to the cells and to promote neuronal growth and maturation. We then recorded the basal activity (15 minutes at 10 kHz) every week to thoroughly evaluate the maturation of the culture. We started the recordings from the day in vitro (DIV) 35, time at which the network start to show relevant activity. We performed data analysis with custom-made tools developed in MATLAB (MathWorks, Natick, MA, USA) and with the software package SpyCode [11]. We computed standard (i.e., MFR, MBR) and non-standard parameters (e.g., peak amplitude, rise time, and decay time of network bursts, spike time histogram) to describe the spontaneous network activity. The choice of these new parameters is aimed at identifying peculiar characteristics of the phenotype. Here we first demonstrated the stability of the networks with respect to standard (see Figure 2) and to non-standard parameters. The identified parameters can later be used as a comparison to detect features of diseased neuronal networks phenotypes, highlighting differences or affinities that were previously hidden. In this study we therefore wanted to provide a robust and widely standardized tool, offering a reliable resource to advance the hiPSC field toward the use of MEAs to distinguish disease phenotypes and for drug discovery.

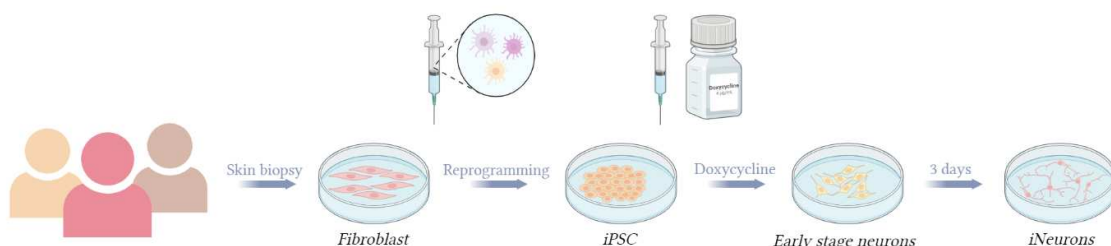


Figure 1: Generation of iPSC-derived human neuronal network starting from healthy subjects.

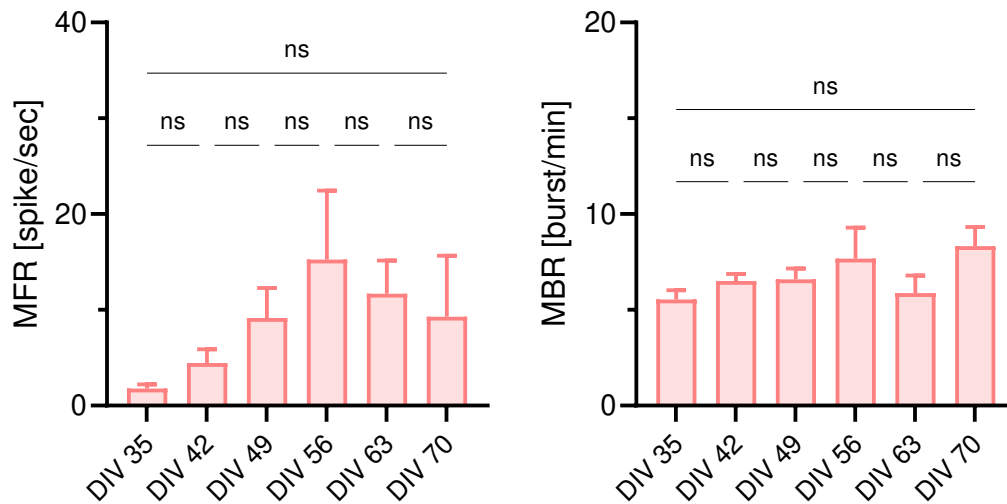


Figure 2: Comparison of the MFR and MBR among weeks. The analysis has been performed only on active electrodes. The plots show the mean parameters of the networks (mean \pm standard error of the mean). One-way ANOVA Kruskal-Wallis test with Dunn's correction for multiple testing was used to compare temporal steps. DIV, days in vitro; ns, not significant.

References

- Pelkonen, A., Pistono, C., Klecki, P., Gómez-Budia, M., Dougalis, A., Kontinen, H., ... & Malm, T. (2021). Functional Characterization of Human Pluripotent Stem Cell-Derived Models of the Brain with Microelectrode Arrays. *Cells*, 11(1), 106.
- Deneault, E., Faheem, M., White, S.H., Rodrigues, D.C., Sun, S., Wei, W., Piekna, A., Thompson, T., Howe, J.L., Chalil, L., et al. (2019). CNTN5 $-/+$ or EHMT2 $-/+$ human iPSC-derived neurons from individuals with autism develop hyperactive neuronal networks. *eLife* 8,1–26.
- Frega, M., Linda, K., Keller, J.M., Guñmuˆxs-Akay, G., Mossink, B., van Rhijn, J.R., Negwer, M., Klein Gunnewiek, T., Foreman, K., Kompier, N., et al. (2019). Neuronal network dysfunction in a model for Kleefstra syndrome mediated by enhanced NMDAR signaling. *Nat. Commun.* 10, 1–15.
- Frega, M., van Gestel, S.H.C., Linda, K., van der Raadt, J., Keller, J., Van Rhijn, J.-R., Schubert, D., Albers, C.A., and Nadif Kasri, N. (2017). Rapid neuronal differentiation of induced pluripotent stem cells for measuring network activity on micro-electrode arrays. *J. Vis. Exp.* 119, 1–10.
- Kayama, T., Suzuki, I., Odawara, A., Sasaki, T., and Ikegaya, Y. (2018). Temporally coordinated spiking activity of human induced pluripotent stem cell-derived neurons co-cultured with astrocytes. *Biochem. Biophysical Res. Commun.* 495, 1028–1033.
- Keller J.M., Frega M. (2019) Past, Present, and Future of Neuronal Models In Vitro. In: Chiappalone M., Pasquale V., Frega M. (eds) *In Vitro Neuronal Networks. Advances in Neurobiology*, vol 22. Springer, Cham
- McConnell, E.R., McClain, M.A., Ross, J., LeFev, W.R., and Shafer, T.J. (2012). Evaluation of multi-well microelectrode arrays for neurotoxicity screening using a chemical training set. *NeuroToxicol.* 33, 1048–1057.
- Mertens, J., Marchetto, M.C., Bardy, C., and Gage, F.H. (2016). Evaluating cell reprogramming, differentiation and conversion technologies in neuroscience. *Nat. Rev. Neurosci.* 17, 424–437.
- Mossink, B., Verboven, A. H., van Hugte, E. J., Gunnewiek, T. M. K., Parodi, G., Linda, K., & Frega, M. (2021). Human neuronal networks on micro-electrode arrays are a highly robust tool to study disease-specific genotype-phenotype correlations in vitro. *Stem cell reports*, 16(9), 2182-2196.
- Zhang, Y., Pak, C.H., Han, Y., Ahlenius, H., Zhang, Z., Chanda, S., Marro, S., Patzke, C., Acuna, C., Covy, J., et al. (2013). Rapid single-step induction of functional neurons from human pluripotent stem cells. *Neuron* 78, 785–798.
- Bologna, L. L., Pasquale, V., Garofalo, M., Gandolfo, M., Baljon, P. L., Maccione, A., ... & Chiappalone, M. (2010). Investigating neuronal activity by SPYCODE multi-channel data analyzer. *Neural Networks*, 23(6), 685-697.

Inducing stimulation dependent plasticity in topologically constrained small-scale neuronal networks

Stephan J. Ihle,^a Sophie Girardin,^a Benedikt Maurer,^a Tobias Ruff,^a Jens Duru,^a János Vörös^{a,*}

- a. Laboratory of Biosensors and Bioelectronics, Institute for Biomedical Engineering, University and ETH Zurich, Gloriastrasse 35, 8092, Zurich, Switzerland

* janos.voros@biomed.ee.ethz.ch

How learning and memory is achieved in the brain is arguably one of the most fundamental questions that the field of neuroscience is aiming to solve. Even though it is of such high significance, its answer remains for the most part elusive. In order to answer this question we believe it is necessary to observe neuronal activity from the bottom-up instead of investigating the brain as a whole. In bottom-up neuroscience, individual neurons are studied in-vitro. We propose using multi-electrode arrays (MEAs) that can be used to stimulate and record neurons extracellularly from multiple locations in parallel with high spatial resolution.

By placing polydimethylsiloxane (PDMS) microstructures on top of a MEA it is possible to constrain the growth of neurites of a neuron [1]. This is done by physically confining the location at which cell soma can be placed and where the neurites can grow in order to guide in a circular fashion with high accuracy [2,3]. Doing so allows us to compartmentalize a MEA into multiple independent networks, where each network covers 4 electrodes of a 60-electrode MEA. Therefore, a total of 15 independent networks can be investigated in parallel on a single MEA. The microstructure of a network is shown in Figure 1A.

We created 4-node networks of primary rat hippocampal neurons (E18). A fluorescent stained network is presented in Figure 1B. Plasticity is manifested as changes in the spiking response of such well-defined neural networks to certain electrical stimuli. Electrical stimuli were applied periodically every 250 ms for 10 min followed by a 10 min recovery period without any stimulus. The spiking responses of a network was then plotted as a raster plot, where the horizontal axis encodes the time (latency) after a stimulus was applied, while the vertical axis encodes the experimental time. We have recently shown that a network spike-time response stays remarkably reproducible under such a stimulation paradigm [3]. The consistency of the spiking response is reflected by spike bands appearing in the raster plots. We present the spiking responses of a network to four 10 minutes stimulation intervals in Figure 1C.

Plasticity effects can be characterized into two categories. Firstly, spike bands can either appear or disappear in the raster plot over time, which corresponds to at least one neuron in a node starting or stopping to spike over time, respectively. Secondly, the exact timing of a spike can change over time, corresponding to a bent spike band. In this work we investigated the second category of network plasticity. We found that approximately 20% of the spike bands expressed a delayed spiking response (depression), while 5% started to occur earlier over time (potentiation). While the number of depressed spike responses significantly increased over time, there was no significant change in the frequency of potentiated spike bands. In Figure 1D, the percentages of potentiating and depressing bands is presented.

These results show that topologically constrained neuronal networks can be used to observe plasticity effects. In the future, we will investigate the exact mechanisms of these effects further by using tools that can increase the quality of over our neural networks. These tools encompass induced pluripotent stem cells to have better control over the exact cell type [4], nanostructures that can guide neuritic growth with more control [5], and high-density CMOS-MEAs that grant higher spatial resolution [6].

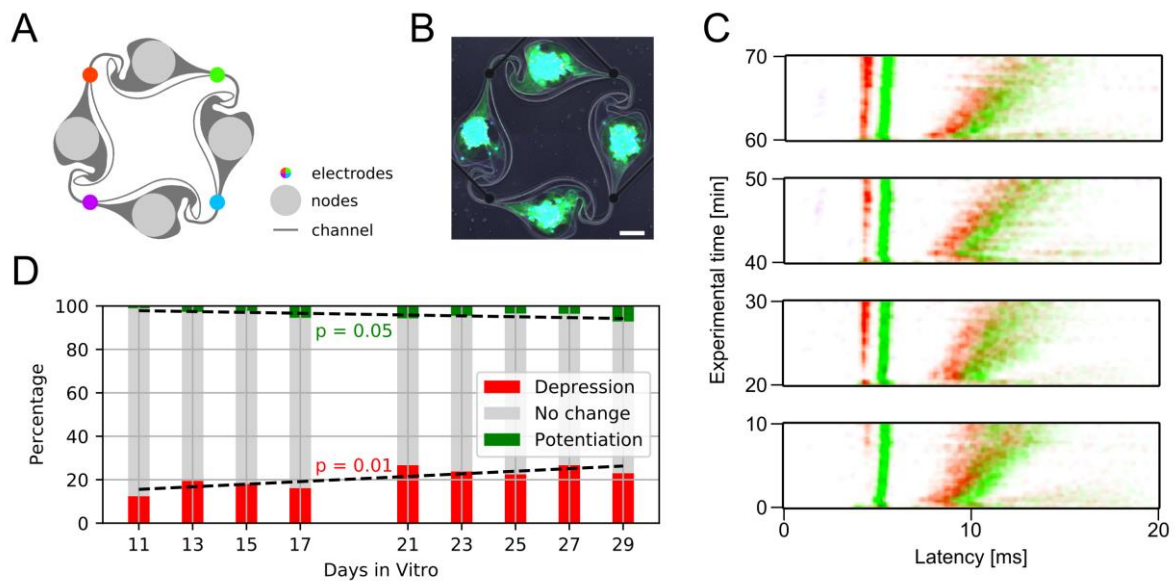


Figure 1: Reproducible plasticity in topologically constrained neuronal networks. (A) PDMS Microstructure used in this work. Cell soma are located in the nodes (light gray), while neurites can grow in the channel (dark gray). Each network covers four electrodes. Subfigure adapted from [3]. (B) Fluorescent image of an exemplary neuronal network. Stains: calcein AM (green), hoechst (blue), ethidium homodimer-1 (red). Scalebar: 100 μm . Subfigure adapted from [3]. (C) Raster plot of a network that has been stimulated repeatedly every 250 ms at the top left (red) electrode for 10 min followed by 10 min of no stimulation. Spike bands can be observed on the red and green electrode. Each of the two electrodes have a band that experiences a depressing spike timing effect at a latency of around 10 ms. (D) Percentage of bands that experience a depressing and potentiating effect for different days in vitro.

References

- Renault, R., Durand, J. B., Viovy, J. L., and Villard, C. (2016). Asymmetric axonal edge guidance: a new paradigm for building oriented neuronal networks. *Lab on a Chip*, 16(12), 2188-2191.
- Forró, C., Thompson-Steckel, G., Weaver, S., Weydert, S., Ihle, S., Dermutz, H., ... and Vörös, J. (2018). Modular microstructure design to build neuronal networks of defined functional connectivity. *Biosensors and Bioelectronics*, 122, 75-87.
- Ihle, S. J., Girardin, S., Felder, T., Ruff, T., Hengsteler, J., Duru, J., ... and Vörös, J. (2022). An experimental paradigm to investigate stimulation dependent activity in topologically constrained neuronal networks. *Biosensors and Bioelectronics*, 201, 113896.
- Girardin, S., Clément, B., Ihle, S. J., Weaver, S., Petr, J. B., Mateus, J. C., ... and Vörös, J. (2022). Topologically controlled circuits of human iPSC-derived neurons for electrophysiology recordings. *Lab on a Chip*.
- Mateus, J. C., Weaver, S., van Swaay, D., Renz, A., Hengsteler, J., Aguiar, P., and Vörös, J. (2021). Nanoscale patterning of in vitro neuronal circuits.
- Duru, J., Küchler, J., Ihle, S. J., Forró, C., Bernardi, A., Girardin, S., ... and Ruff, T. (2022). Engineered biological neural networks on high density CMOS microelectrode arrays. *Frontiers in neuroscience*, 16.

Synaptic densities are restored in primary neural cultures exposed to electrical stimulation after a period of hypoxia

G.C. Hassink^a, M. Levers^a, J. Kreutzer^b, P. Kallio^b, J. Hofmeijer^a, and J. le Feber^{a*}

- a. Clinical Neurophysiology, Technical Medical Centre, University of Twente, Enschede, the Netherlands,
- b. Micro- and Nanosystems Research Group, Faculty of Medicine and Health Technology, Tampere University, Tampere, Finland

* j.lefeber@utwente.nl

Worldwide, fifteen Million people suffer from brain ischemia of any cause yearly [1]. Prolonged ischemia leads to necrosis of neurons and glial cells, but shorter periods, e.g. due to cardiac arrest followed by resuscitation [2], initially allows for cell survival. Here, synaptic failure often strongly reduces neural activity and cells may either recover or further deteriorate and die. Earlier work of our group indicated that 6-24h of hypoxia significantly reduced network activity [3-4], as well as synapse densities [5] in cultured cortical networks. Ghrelinergic stimulation, which mildly activated networks, was shown to increase survival and to restore synaptic density [6]. Electrical stimulation of neurons after a period of mild hypoxia had a similar effect on cell survival [7] and recovery of synapses [8]. In the current report we extended this dataset, applied and investigated whether synapses that disappeared during hypoxia were degraded or internalized.

Flat MEAs were mounted with removable silicone culture chambers, developed by (BioGenium Microsystems Ltd; Fig 1A) [9,10] and seeded with dissociated rat cortical cultures. After validation of stimulus responses (Fig 1C) and a baseline recording of spontaneous activity, 21-28 days old cultures were exposed to 6h of hypoxia (10% of normoxia; $pO_2 \approx 20\text{mmHg}$; Fig 1B). To mimic the time needed to reach the hospital, electrical stimulation was applied 3h after the hypoxic period (Fig 1B). Cultures were stimulated for 6h (single biphasic pulses, 200 μs per phase, 1500 mV) in 3 groups of 19-20 electrodes each with 30s intervals between pulses (figure 1B & C). Then, cultures were fixed and micro-graphs were taken at 60x. Synapses (synaptophysin staining) were automatically counted by an algorithm in polygons that were drawn manually around areas that contained soma of neurons.

During exposure of cultures to 6h hypoxia, network firing dropped to $\sim 50\%$ of baseline, with slight recovery during 3h reoxygenation and an increase during 6h electrical stimulation. Hypoxia treatment followed by 9h recovery significantly (40-60%) reduced synapse densities in $n=5$ cultures, compared to normoxic controls ($n=5$, Fig 1D, left and middle bar). Synapse densities significantly re-increased following 6h of electrical stimulation ($n=6$; $p<0.05$), to pre-hypoxic values (Fig 1D, right bar). Reduced synapse density may result from redistribution of synaptic proteins over the axolemma, or to protein degradation. To discriminate between these possible mechanisms, we used quantitative western blots to determine the total amount of synaptophysin in lysates of cultures exposed to hypoxia ($n=24$) and control cultures ($n=24$). Fluorescence intensities were corrected for possible differences in total protein to account for possibly different total numbers of cells. We found no significant differences in levels of Synaptophysin between hypoxia treated and control cultures (Fig 1E, $p>0.05$). However, besides synaptophysin monomers ($\sim 50\%$), blots showed substantial formation of dimers ($\sim 30\%$) and oligomers (Fig 1E, right panel), which may have obscured results.

In conclusion, synaptic density decreased during hypoxia. Synaptic proteins were probably not degraded but most likely internalized. Electrical stimulation after a period of mild hypoxia restores synaptic density in neurons *in vitro*, supporting the hypothesis that synaptic activity is beneficial for recovery of synapses after hypoxia.

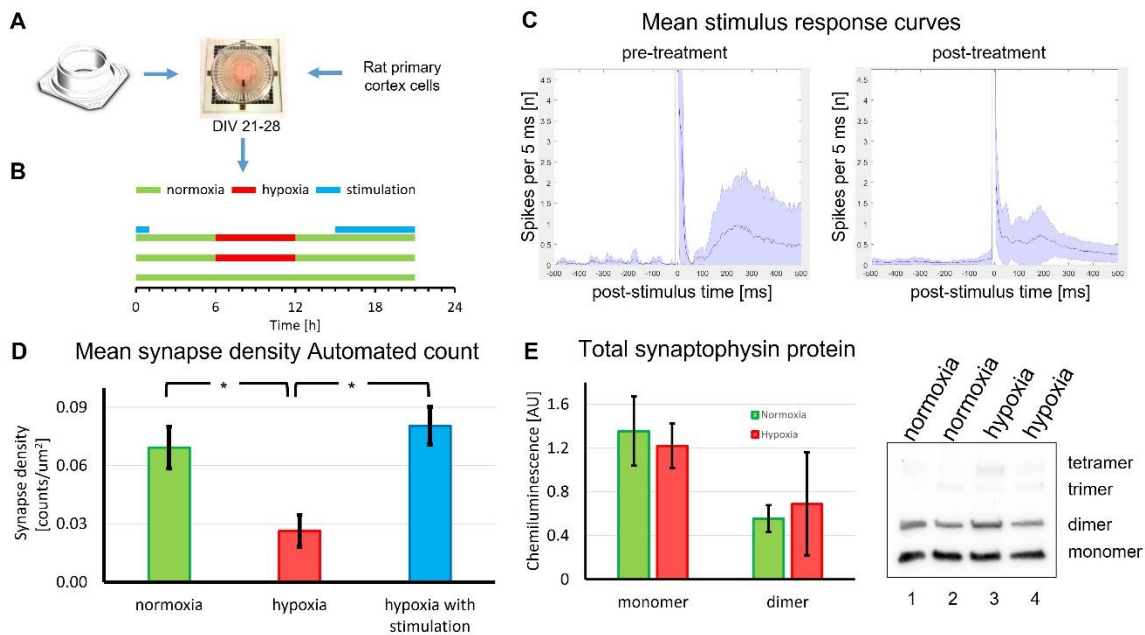


Figure 1: Overview of the experiment. Flat MEAs were mounted with removable silicone culture chambers as in A. cultures were exposed to the conditions as in B using the stimulation as described. Stimulus response curves were recorded and displayed pre-hypoxia (C left panel) and post-hypoxia (C right panel). The curves are showing histograms of the average number of recorded spikes within time bins of 5 ms, given a stimulation at $t=0$. Mean synapse densities as counted by synaptophysin positive puncta were determined under conditions indicated in (D). Data represent the mean of $n=140-200$ images, taken from six independent experiments per condition. Total synaptophysin normalized for total protein was measured by quantitative western blots (E). Western blot data represent the mean of 12 wells per condition, each blotted in duplicate (6 and 36 μl). p values < 0.05 (T-test) are indicated with *. Error bars represent 95% confidence intervals.

References

1. J. J. Guilbert (2003). "The world health report 2002 - reducing risks, promoting healthy life.," *Educ. Health (Abingdon)*, vol. 16, no. 2, p. 230, doi: 10.1080/1357628031000116808.
2. R. L. C. Vogels, P. Scheltens, J. M. Schroeder-Tanka, and H. C. Weinstein (2007). "Cognitive impairment in heart failure: A systematic review of the literature," *Eur. J. Heart Fail.*, vol. 9, no. 5, pp. 440–449, doi: 10.1016/j.ejheart.2006.11.001.
3. J. Hofmeijer, A. T. B. Mulder, A. C. Farinha, M. J. A. M. vanPutten and J. le Feber (2014). "Mild hypoxia affects synaptic connectivity in cultured neuronal networks." *Brain Res* 1557: 180-189.
4. J. le Feber, S. Tzafi Pavlidou, N. Erkamp, M. J. A. M. van Putten and J. Hofmeijer (2016). "Progression of Neuronal Damage in an In Vitro Model of the Ischemic Penumbra." *PLoS One* 11(2): e0147231.
5. J. le Feber, A. Dummer, G.C. Hassink, M.J.A.M. van Putten, J. Hofmeijer (2018). "Evolution of Excitation-Inhibition Ratio in Cortical Cultures Exposed to Hypoxia." *Front Cell Neurosci.*, 12:183. doi: 10.3389/fncel.2018.00183.
6. I. Stoyanova, J. Hofmeijer, M. J. A. M. van Putten, and J. Le Feber (2015) "Acyl Ghrelin Improves Synapse Recovery in an In Vitro Model of Postanoxic Encephalopathy," *Mol. Neurobiol.*, doi: 10.1007/s12035-015-9502-x.
7. L. Muzzi, G.C. Hassink, M. Levers, M. Jansman, M. Frega, J. Hofmeijer, M. van Putten and J. le Feber (2019). "Mild stimulation improves neuronal survival in an in-vitro model of the ischemic penumbra." *J Neural Eng* 7(1): 016001.
8. G.C. Hassink, M. Levers, S. Kamphuis, I. Born, J. Hofmeijer, and J. Le Feber (2018). "Synaptic densities in hypoxia exposed and electrically stimulated primary neural cultures," *Cell. Neurosci. Arch.*, vol. 12, no. 00057, doi: 10.3389/conf.fncel.2018.38.00057
9. J. Kreutzer, L. Ylä-Outinen, P. Kärnä, T. Kaarela, J. Mikkonen, H. Skottman, S. Narkilahti, and P. Kallio (2012) "Structured PDMS Chambers for Enhanced Human Neuronal Cell Activity on MEA Platforms," *J. Bionic Eng.*, vol. 9, no. 1, pp. 1–10, doi: 10.1016/S1672-6529(11)60091-7.
10. M. Häkli, Kreutzer, J., Mäki, A. J., Välimäki, H., Lappi, H., Huhtala, H., Kallio, P., Aalto-Setälä, K., and Pekkanen-Mattila, M. (2021). "Human induced pluripotent stem cell-based platform for modeling cardiac ischemia." *Scientific Reports*, 11(1), 1–13., doi.org/10.1038/s41598-021-83740-w

Simultaneous Optical and Electrical Recordings of Large-scale Neuronal Network

Sara Pecoraro^a, Xin Hu^a, Diana Klütsch^a, Hayder Amin^{a,*}

- a. German Center for Neurodegenerative Diseases (DZNE), Dresden, Germany
Biohybrid Neuroelectronics Lab (BIONICS)

* Corresponding author: hayder.amin@dzne.de

The mammalian brain performs its complex cognitive functions by the coordinated activity of densely interconnected neuronal networks. Thus, the representation of brain activity patterns has been strongly suggested to encode and process dynamical information about the world [1]. In turn, the equilibrium in activity and stability of brain computations is mediated by the coregulation of excitatory and inhibitory incoming information [2]. Therefore, manipulating and monitoring the coordinated spatiotemporal activity across large-scale populations of neurons is essential to understanding the operating principles of brain functions and requires advanced optical/electrical approaches and mathematical models. Calcium (Ca^{+2}) imaging is currently a predominant optical technique to study the intracellular activity of large neuronal populations with cell-type specificity, though it represents a slow, nonlinear measuring of the underlying spiking activity, which requires additional denoising and deconvolution steps to reveal the neural activity [3]. In parallel, recently, a new generation of high-density microelectrode arrays based on CMOS technology (i.e., HD-neurochip) have become the state-of-the-art in recording direct spiking activity simultaneously from thousands of neurons in healthy and disease neuronal networks [4], [5]. Identifying the excitatory/inhibitory network balance regulated by the firing features of Glutamatergic/GABAergic neuronal populations in a large-scale network remain widely unexplored, and related studies have been limited to small-scale networks [6]. To address this significant challenge, we here report a multimodal platform of Ca^{+2} imaging and HD-neurochip to allow simultaneous intra-extracellular measurements of large-scale hippocampal spiking activity and neuronal structural population identity at single-cell resolution (**Figure 1**). Our experimental-computational approach, including the analytical toolbox, allows; **i**) identifying simultaneous intra-extracellular activity and morphological information of a very large-scale neuronal network ($\sim 7 \text{ mm}^2$ image size); **ii**) Implementing a deconvolution computation to compare Ca^{+2} spiking activity occurrence with the single-unit activity of HD-neurochip; **iii**) characterizing location-specific feature of neuronal population (i.e., Glutamatergic/GABAergic) obtained with automated algorithm and spike sorting method; **iv**) providing further quantification of advanced functional connectivity and network synchrony of intra-extracellular information to decipher multiscale neural code complexity.

Our study provides a systematic approach to monitoring very large-scale neuronal components with a neuronal identity that may help categorize multiple layers of neural firing variability. Indeed, it also supports the dynamical and functional mapping of multiscale mechanisms underlying drugs targeting specific neuronal populations in physiological and pathological conditions.

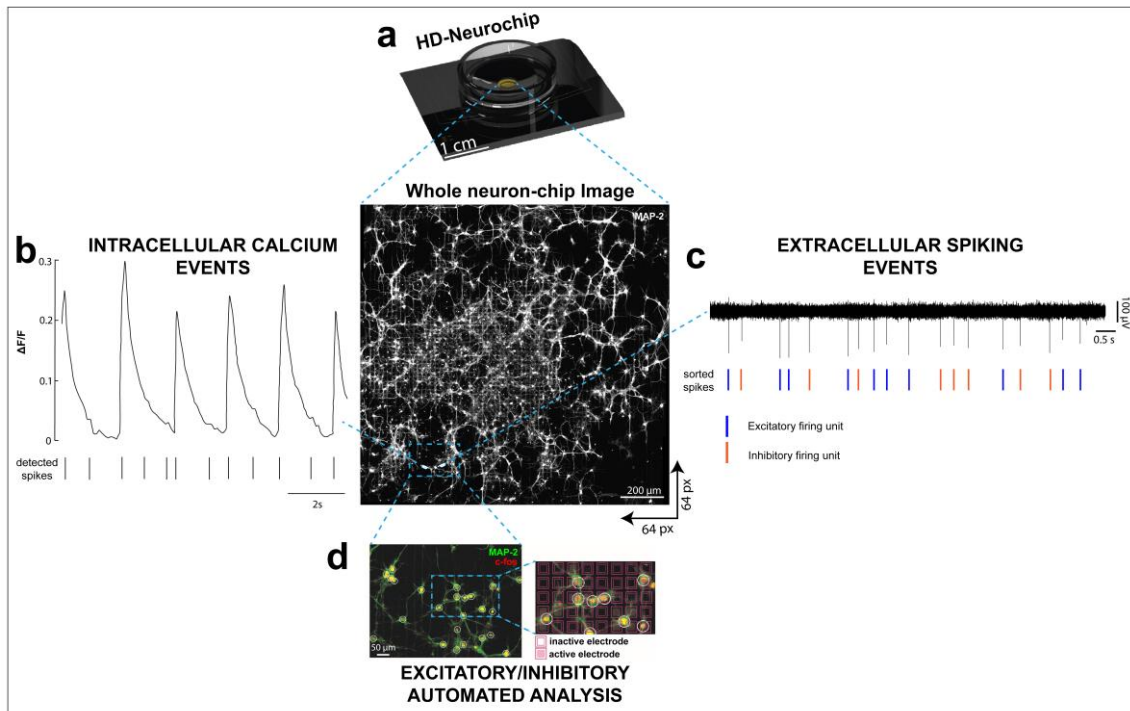


Figure 1: Large-scale optical-electrical biosensing platform. a) Graph showing the high-density neurochip integrated with 4096 electrodes with a hippocampal neuronal network (DIV24) identified by MAP-2 staining for the dendritic connections. b) Optical readout of intracellular Ca^{+2} signal from a single segmented and identified neurons in the network (a) and detected spikes with the deconvolution method. c) Electrical readout of extracellular spiking activity sorted for two units (excitatory/inhibitory) that were structurally and functionally identified with our automated detection tool shown in (d).

References

- [1] N. Kriegeskorte and J. Diedrichsen, "Peeling the Onion of Brain Representations," *Annu. Rev. Neurosci.*, vol. 42, pp. 407–432, 2019, doi: 10.1146/annurev-neuro-080317-061906.
- [2] M. Okun and I. Lampl, "Instantaneous correlation of excitation and inhibition during ongoing and sensory-evoked activities," *Nat. Neurosci.*, vol. 11, no. 5, pp. 535–537, 2008, doi: 10.1038/nn.2105.
- [3] C. Grienberger and A. Konnerth, "Imaging Calcium in Neurons," *Neuron*, vol. 73, no. 5, pp. 862–885, Mar. 2012, doi: 10.1016/J.NEURON.2012.02.011.
- [4] H. Amin, A. Maccione, F. Marinaro, S. Zordan, T. Nieuws, and L. Berdondini, "Electrical responses and spontaneous activity of human iPS-derived neuronal networks characterized for 3-month culture with 4096-electrode arrays," *Front. Neurosci.*, vol. 10, no. 121, pp. 1–15, 2016, doi: 10.3389/fnins.2016.00121.
- [5] H. Amin, T. Nieuws, D. Lonardoni, A. Maccione, and L. Berdondini, "High-resolution bioelectrical imaging of A β -induced network dysfunction on CMOS-MEAs for neurotoxicity and rescue studies," *Sci. Rep.*, vol. 7, no. 1, p. 2460, Dec. 2017, doi: 10.1038/s41598-017-02635-x.
- [6] A. Becchetti, F. Gullo, G. Bruno, E. Dossi, M. Lecchi, and E. Wanke, "Exact distinction of excitatory and inhibitory neurons in neural networks: A study with GFP-GAD67 neurons optically and electrophysiologically recognized on multielectrode arrays," *Front. Neural Circuits*, vol. 6, no. AUGUST 2012, pp. 1–11, 2012, doi: 10.3389/fncir.2012.00063.

Review on subthreshold electrical stimulation to promote plasticity in neuronal networks

Daniel Ziesel^{a,*}, Kerstin Lenk^b, Gernot R. Müller-Putz^{b,c}, Karin Kornmueller^d, Susanne Scheruebel^d, Rainer Schindl^d, Muammer Üçal^e, Aleksandar Opančar^f, Vedran Đerek^f, Christian Baumgartner^{a,c}, Theresa Rienmüller^{a,c}

- a. Institute of Health Care Engineering with European Testing Center of Medical Devices, Graz University of Technology, Austria
- b. Institute of Neural Engineering, Graz University of Technology, Austria
- c. BioTechMed Graz, Austria
- d. Gottfried Schatz Research Center, Chair of Biophysics, Medical University of Graz
- e. Research Unit of Experimental Neurotraumatology, Department of Neurosurgery, Medical University of Graz, Austria
- f. Department of Physics, Faculty of Science, University of Zagreb, Croatia

* daniel.ziesel@tugraz.at

Motivation

Subthreshold electrical stimulation (STES) has the potential to induce plasticity in neuronal networks at relatively low stimulation intensities compared to suprathreshold stimulation. Since lower intensity stimulation affects smaller areas of tissue, STES has a better spatial resolution and side effects are less likely, while the lower energy consumption of STES makes it optimal for low-power applications in e.g. implantable devices [1]. Here, we want to investigate a variety of subthreshold pulse protocols utilized in current literature that can be used as a potential treatment to promote recovery e.g. after stroke or traumatic brain injury.

Materials and Methods

A review on studies utilizing STES to promote plasticity and functional recovery was carried out. Three studies describing distinct efficacious stimulation protocols were finally selected and compared. This research serves as a basis for further in-vitro experiments on subthreshold stimulation with neuronal cell cultures on multielectrode arrays (MEAs).

Results

While STES cannot induce action potentials *per se*, it can facilitate neuronal firing by complementing physiological subthreshold excitatory postsynaptic potentials, and thereby increasing synaptic weight. It was shown that this leads to causal activation between neurons, resulting in synaptic remapping and enhanced plasticity in a rat stroke model starting at low intensities of 30 % of the action potential threshold [1]. Continuous subthreshold stimulation with 20 Hz square-wave pulses applied directly after facial nerve crush injury in rabbits was shown to facilitate functional recovery by improving the conduction velocity in injured nerves at about 70 % stimulation intensity [2]. When STES is applied to CA3 neurons in hippocampal slice cultures with patch clamp electrodes, their intrinsic firing patterns can be modified, adapting the pattern of the conditioning stimuli leading to long-lasting changes in neuronal behavior [3].

Discussion

Multiple studies have shown that STES can effectively induce plasticity in neuronal networks at a reduced energy cost compared to suprathreshold stimulation. While STES has rarely been used in conjunction with MEAs [4], we will investigate different subthreshold stimulation protocols and characterize their effect on neuronal cell cultures and network activity in greater detail.

Acknowledgements

This research was funded in part by the Austrian Science Fund (FWF) [ZK 17].

References

1. K. Kim *et al.*, "Subthreshold electrical stimulation as a low power electrical treatment for stroke rehabilitation," *Sci. Rep.*, vol. 11, no. 1, Art. no. 1, Jul. 2021, doi:

10.1038/s41598-021-93354-x.

2. J. Kim, S. J. Han, D. H. Shin, W.-S. Lee, and J. Y. Choi, "Subthreshold continuous electrical stimulation facilitates functional recovery of facial nerve after crush injury in rabbit," *Muscle Nerve*, vol. 43, no. 2, pp. 251–258, Feb. 2011, doi: 10.1002/mus.21840.
3. S. Soldado-Magraner *et al.*, "Conditioning by subthreshold synaptic input changes the intrinsic firing pattern of CA3 hippocampal neurons," *J. Neurophysiol.*, vol. 123, no. 1, pp. 90–106, Jan. 2020, doi: 10.1152/jn.00506.2019.
4. M.-G. Liu *et al.*, "Long-term potentiation of synaptic transmission in the adult mouse insular cortex: multielectrode array recordings," *J. Neurophysiol.*, vol. 110, no. 2, pp. 505–521, Jul. 2013, doi: 10.1152/jn.01104.2012.

Modelling mTORopathy-related epilepsy in cultured murine hippocampal neurons using the Multi-Electrode Array.

A.M. Heuvelmans^{a,b}, Y. Elgersma^{a,b}, G.M. van Woerden^{a,b,c*}

- a. Department of Clinical Genetics, Erasmus Medical Center, Rotterdam, 3015 CN, The Netherlands
- b. The ENCORE Expertise Center for Neurodevelopmental Disorders, Rotterdam, 3015 CN, The Netherlands
- c. Department of Neuroscience, Erasmus Medical Center, Rotterdam, 3015 CN, The Netherlands

[*g.vanwoerden@erasmusmc.nl](mailto:g.vanwoerden@erasmusmc.nl)

The mechanistic target of rapamycin complex 1 (mTORC1) signaling pathway is a ubiquitous cellular pathway involved in the regulation of cell metabolism, growth, proliferation and survival. Its activity is critically regulated by multiple upstream proteins. mTORopathies is a group of disorders, caused by hyperactivity of the mTORC1 pathway. Many pathogenic variants have been identified in various genes coding for proteins upstream of mTORC1, causing a mTORopathy, often with profound impact on the nervous system [1]. mTORC1 is directly activated by Ras-Homologue Enriched in Brain (RHEB), which in turn is inhibited by the Tuberous Sclerosis Complex (TSC) protein complex. Indeed, gain of function mutations in *RHEB* and loss of function mutations in *TSC1* or *TSC2*, both have been shown to cause mTORC1 hyperactivity. One of the most debilitating symptoms of mTORopathies is the often drug-resistant epilepsy, urging the need for a better understanding of disease mechanisms and screening methods for new anti-epileptic drug treatments [1,2]. To this end, we make use of a *Tsc1*-KO mouse model and overexpression of a gain of function RHEBp.P37L mutation, both of which were shown to cause seizures in mice [3,4].

In this study, we culture *Tsc1*-KO and RHEBp.P37L overexpressing mouse primary hippocampal neurons on the Multi-electrode array (MEA) to explore changes in network activity in response to mTORC1 hyperactivity. Finding an epilepsy-like phenotype in this system allows a more high-throughput initial screen for new anti-epileptic drugs before moving on to more elaborate in vivo studies.

We show that hyperactivity of the mTORC1 pathway through either a loss of function of the TSC-complex, or a gain of function mutation in the RHEB protein, leads to aberrant network activity. Besides a previously identified increase in mean firing rate in TSC-models [5,6], we find changes in burst characteristics, such as a decreased burst rate and increased burst duration in both models. These phenotypes are normalized to control upon treatment with rapamycin, an mTORC1-inhibitor. These results suggest that using the MEA system, we can model epilepsy-like activity in *Tsc1*-KO and RHEBp.P37L-overexpression hippocampal neurons, and that this can be used as a high-throughput screening method for potential drug treatments.

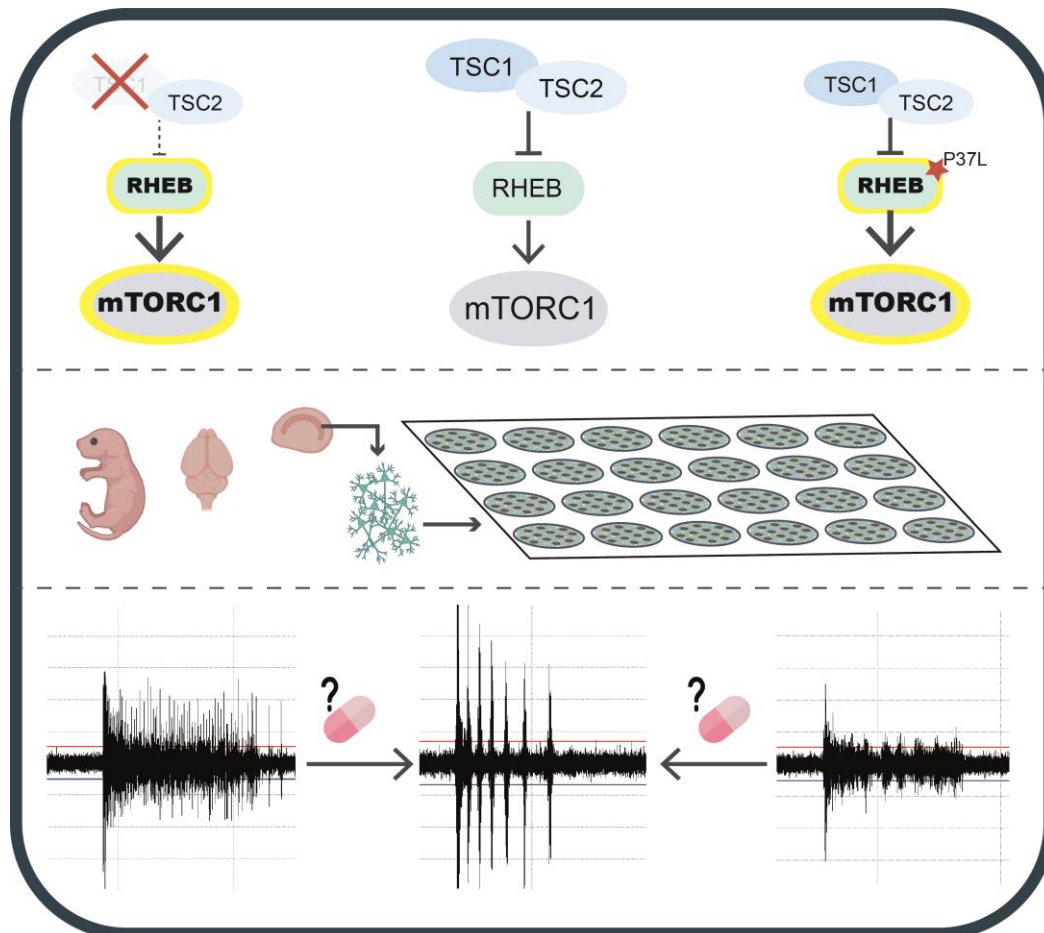


Figure 1: Aberrant network activity as a result of mTORC1-hyperactivity through either a loss of function of TSC-complex activity (left) or a gain of function mutation in RHEB (right).

References

1. Karalis, V., Bateup, H.S. (2021) Current approaches and future directions for the treatment of mTORopathies. *Dev Neurosci* 43, 143-158. doi:10.1159/000515672
2. Overwater, I.E., Bindels-de Heus, K., Rietman, A.B., ten Hoopen, L.W., Vergouwe, Y., Moll, H.A., de Wit, M.Y. (2015). Epilepsy in children with tuberous sclerosis complex: Chance of remission and response to antiepileptic drugs. *Epilepsia* 56, 1239-1245. doi:10.1111/epi.13050
3. Koene, L.M.C., van Grondelle, S.E., Proietti Onori, M, Wallaard, I, Kooijman, N.H.R.M., van Oort, A, Schreiber, J, Elgersma, Y. (2019). Effects of antiepileptic drugs in a new TSC/mTOR-dependent epilepsy mouse model. *Ann Clin Transl Neurol* 6, 1273-1291. doi:10.1002/acn3.50829
4. Proietti Onori, M, Koene, L.M.C., Schäfer, C.B., Nellist, M., de Brito van Velze, M., Gao, Z., Elgersma, Y., van Woerden, G.M. (2021). RHEB/mTOR hyperactivity causes cortical malformations and epileptic seizures through increased axonal connectivity. *PLoS Biol.* 19, e3001279. doi:10.1371/journal.pbio.3001279
5. Bateup, H.S., Johnson, C.A., Denefrio, C.L., Saulnier, J.L., Kornacker, K., Sabatini, B.L. (2013) Excitatory/inhibitory synaptic imbalance leads to hippocampal hyperexcitability in mouse models of tuberous sclerosis. *Neuron* 78, 510-22. doi:10.1016/j.neuron.2013.03.017
6. Winden, K.D., Sundberg, M., Yang, C., Wafa, S.M.A., Dwyer, S., Chen, P.F., Buttermore, E.D., Sahin, M. (2019) Biallelic Mutations in TSC2 Lead to Abnormalities Associated with Cortical Tubers in Human iPSC-Derived Neurons. *J Neurosci* 39, 9294-9305. doi:10.1523/JNEUROSCI.0642-19.2019

Enhancing the activity of GABA_A receptors but not GABA_B receptors abolishes pathological oscillations in retinitis pigmentosa mouse model *rd10*

Nruthyathi^{*}, Jana Gehlen, Frank Müller

Institute of Biological Information Processing, Molecular and Cell Physiology, IBI-1,
Forschungszentrum Jülich, Germany
^{*}n.nruthyathi@fz-juelich.de

Purpose: In retinitis pigmentosa mouse model *rd10*, an intrinsic oscillatory activity is observed upon retinal degeneration. These oscillations are shown to compromise efficiency of electrical stimulation by retinal prostheses [1]. In this study we tested whether GABA_B receptor agonists could abolish these pathological oscillations in the retina.

Methods: *In vitro* recordings of local field potentials (LFPs) and spiking activity of retinal ganglion cells (RGCs) from the retina of 5-6 month old wt and *rd10* mice were obtained using multi electrode arrays. The effect of pharmacological drugs on the oscillatory activity and stimulation efficiency was determined. RGCs were stimulated with a single biphasic current pulse and stimulation efficiency was determined as the ratio of post stimulus action potential rate to pre stimulus action potential rate in the presence and absence of the drug.

Results: In *rd10* retina, the oscillatory activity is seen at a frequency of 3-6Hz in the LFPs and RGC firing. Oscillations can be abolished concomitant with an increase in stimulation efficiency by the inhibitory neurotransmitters GABA and glycine and by GABA_A receptor modulators like benzodiazepines. But benzodiazepines are known to cause various side effects and a prolonged use in patients is not advisable. Therefore, in this study we extend this investigation to other GABAergic drugs that might present lesser side effects.

Baclofen, a clinically approved agonist at a different GABA receptor – the GABA_B receptor - was tested. At all concentrations, baclofen reduced the frequency of the oscillation but did not abolish it completely. The stimulation efficiency was not improved significantly.

Discussion: Targeting GABA_B receptors with baclofen did not abolish oscillations. This shows that pathways comprising GABA_B receptors are not involved or play a minor role in the generation/propagation of the oscillations as compared to pathways with GABA_A receptors. Other drugs that would have a similar effect as GABA and benzodiazepines like GABA reuptake blockers or GABA catabolism inhibitors that would potentially abolish oscillations need to be tested in future experiments.

Acknowledgement: Funded by the Deutsche Forschungsgemeinschaft (DFG, German Research Foundation), GRK2610/1 - project number 424556709.

Reference:

1. Gehlen, J., Esser, S., Schaffrath, K., Johnen, S., Walter, P., and Müller, F. (2020). Blockade of Retinal Oscillations by Benzodiazepines Improves Efficiency of Electrical Stimulation in the Mouse Model of RP, *rd10*. *Investigative ophthalmology & visual science* 61(13), 37. doi:10.1167/iovs.61.13.37

Expression of Channelrhodopsin-2 (ChR2) in retinal cells restores visual responses in blind mouse retina

Miriam Reh,^{a,b} Meng-Jung Lee,^{b,c} Günther Zeck,^{b,d} *

- a. Institute for Ophthalmic Research University Tübingen
AG Schwarz, Adaptive Optics, Elfriede-Aulhorn-Str. 7, 72076 Tübingen, Germany
- b. NMI Naturwissenschaftliches und Medizinisches Institut an der Universität Tübingen,
Markwiesenstr. 55, 72770 Reutlingen, Germany
- c. Bernstein Center Freiburg, Neurobiology and Neurotechnology, Hansastr. 9a, 79104
Freiburg, Germany
- d. Institute of Biomedical Electronics, TU Wien, Gußhausstrasse 27, 1040 Vienna,
Austria

* Miriam.reh@uni-tuebingen.de

Depending on the state of retinal degeneration, several retinal cells are promising targets for optogenetic vision restoration approaches [1]. Here, we investigate the optogenetic approach on two genetically modified mouse models: rd10 mouse-line expressing ChR2 in either retinal ganglion cells (RGCs) (rd10-ChR2) [2] or in rod bipolar cells (rBCs) (rd10-pcp2-ChR2) [3]. Achieved spatial and temporal resolution were assessed through ex vivo mouse retina recordings, where the retina was placed RGC side down on a CMOS-based micro-electrode array (MEA) [4] for recording of RGC activity and an objective was located above to project light stimulation patterns onto the retina from the degenerated photoreceptor side (*see Figure 1*). To estimate the temporal resolution, a gaussian white noise (gwn) stimulus sequence was presented to the retina, and the RGC output was used to calculate the spike triggered average (STA), where the detected zero crossing represents an estimate for the response latency of the cell.

Figure 1 compares the derived STAs for optogenetic versus visual photoreceptor stimulation. It is observed, that temporal filter shapes derived from optogenetic stimulation in rd10-ChR2 retina results in only ON- behavior STAs that are notably shortened for optogenetic compared to photoreceptor stimulation (7.5 ms compared to 100 ms), as direct stimulation of RGCs overcomes synaptic retinal transmission and phototransduction. When stimulating rBCs, measured response latencies are about a factor of 8 larger than those of direct RGC stimulation, enabling a detection of visual stimuli close to healthy vision.

Spatial resolution describes the ability to discriminate fine patterns and to resolve the details in a visual scene. To achieve an estimate for spatial resolution, an alternating grating stimulus [5] was used and a logistic regression model was applied on the two phases of the alternating grating to estimate if the respective grating width is resolved by the brain. Here, we achieved accuracies > 95% for grating stripe widths of 10 μm (1.75 cpd) for direct optogenetic RGC stimulation, while for rBC stimulation, we observed a decreased spatial resolution (0.175 cpd). This results most likely from the observed bursting activity triggered by the network activation of All amacrine cells [6] following optogenetic stimulation of rBCs. Thus, expression of ChR2 in rBCs leads to a trade-off between having both ON and OFF polarity responses after vision restoration and a reduced spatial resolution accuracy.

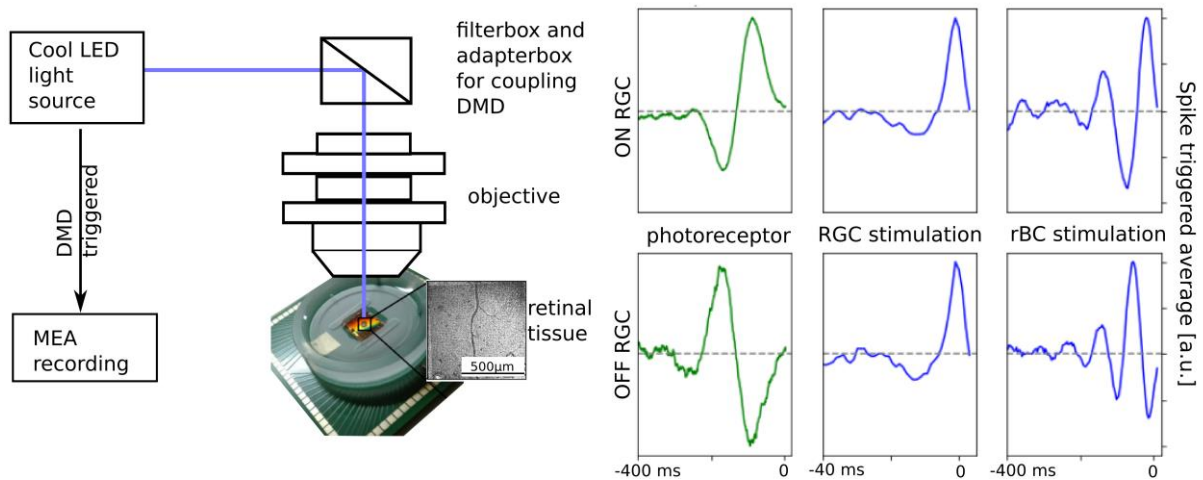


Figure 1: Experimental setup for recording RGC activity in *rd10* mice expressing ChR2. The light emitted from LEDs of the CoolLED system is coupled into the digital mirror device (DMD), where the temporal and spatial stimulation pattern is created and projected onto the retinal sample, located on a CMOS-MEA. Temporal gwn stimulation allows for estimation of the STA, giving an estimate for the achievable temporal resolution.

References

1. Hulliger, Elmar Carlos, Simon Manuel Hostettler, and Sonja Kleinlogel (2020). Empowering retinal gene therapy with a specific promoter for human rod and cone ON-bipolar cells. *Molecular Therapy-Methods & Clinical Development*.
2. Miriam Reh, Meng-Jung Lee, Julia Schmierer, et al. (2021). Spatial and temporal resolution of optogenetically recovered vision in ChR2-transduced mouse retina. *Journal of Neural Engineering*. url: <http://iopscience.iop.org/article/10.1088/1741-2552/abe39a>.
3. Reh, M., Lee, M. J., & Zeck, G. (2022). Expression of Channelrhodopsin-2 in Rod Bipolar Cells Restores ON and OFF Responses at High Spatial Resolution in Blind Mouse Retina. *Advanced Therapeutics*, 2100164.
4. Bertotti, G., Velychko, D., .. & Thewes, R. (2014, October). A CMOS-based sensor array for in-vitro neural tissue interfacing with 4225 recording sites and 1024 stimulation sites. *2014 IEEE Biomedical Circuits and Systems Conference (BioCAS) Proceedings* (pp. 304-307).
5. Abdeljalil, Jellali et al. (2005). The optomotor response: a robust first-line visual screening method for mice. *Vision research* 45.11, pp. 1439–1446.
6. Trenholm, Stuart and Gautam B Awatramani (2015). Origins of spontaneous activity in the degenerating retina. *Frontiers in cellular neuroscience* 9, p. 277.

Investigating the survival and function of retinal ganglion cells in an organotypic culture: An in-vitro model for studying synaptogenesis

Nairouz Farah^{1,2}, Efrat Simon³, Aviad Slotky¹, Amos Markus¹, Yossi Mandel^{1,2}

(1) School of Optometry and Vision Science, Bar-Ilan University, Ramat-Gan, Israel.

(2) Institute for Nanotechnology and Advanced Materials (BINA), Bar-Ilan University, Ramat Gan, Israel.

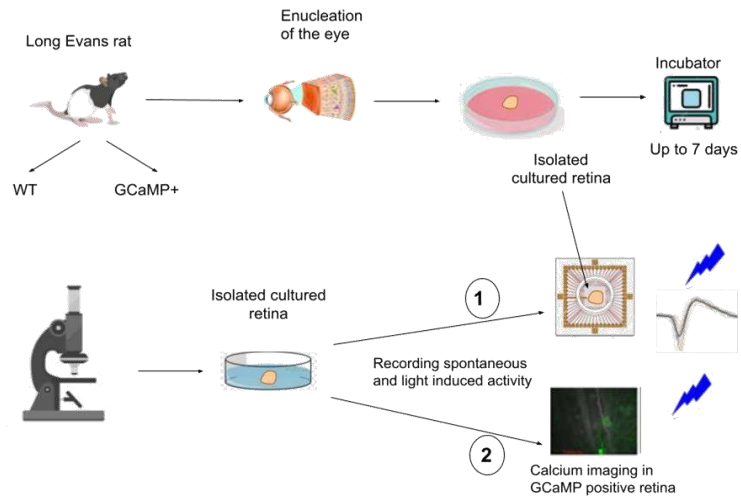
(3) The Gonda Brain Research Center, Bar-Ilan University, Ramat Gan, Israel.

Background: Stem cells replacement therapy is becoming a promising pursued avenue for vision restoration in people with degenerative diseases of the outer retina. However, the integration and survival of the transplanted cells and the formation of fully functioning synapses remain challenge. Our aim is to develop an ex-vivo experimental paradigm which will allow us to address these issues while working under experimentally controlled conditions and avoiding immune system reactions faced in-vivo. In the current report we describe our effort for monitoring the retinal viability and function using both optical and electrophysiological measures.

Methods: We are utilizing organotypic retinal cultures (similarly to Alarautalahti et al 2019) from either WT or transgenic rats expressing the calcium indicator GCaMP6f while monitoring the survival of the retinal ganglion cells (RGCs) using both extracellular recordings (multi electrode arrays), and calcium imaging at various time points. The RGCs survival is inferred through either electrical or light (470nm LED-12 μ W/mm²) induced responses. Moreover, these investigations are complemented by morphological analysis obtained through confocal microscopy and TUNEL imaging for the quantification of apoptosis occurring throughout the culturing

Results: Our calcium imaging revealed robust spontaneous activity of the RGCs up to 72hrs, albeit decreasing throughout culturing period. We observe a decrease in the percentage of spontaneously active RGCs from 4.26% in acute preparations to 2.09% in 96hrs culture. Concurrently with these experiments, we have successfully established the system for extracellular investigation of RGC electrical properties incorporating flexible light pattern stimulation and multiunit analysis of the light induced responses over 60 channels. We were able to observe various RGCs types e.g., ON, OFF, ON-OFF identified by 1sec flashes applied at 0.2Hz. Moreover, through the well-known white Gaussian noise stimulus combined with spike triggered averaging we generated RGCs receptive field maps obtaining the expected results both spatial (160 μ m FWHM) and temporally. Both light and electrically induced responses were observed in retinal cultures up to 48hrs post culturing as visible through calcium imaging as well as electrophysiological recording. These results are in agreement with confocal imaging of retinal cryosections stained with the live dead assay TUNEL revealing the relatively preserved RGC layer with significant cell death occurring in the Outer Nuclear Layer (containing the photoreceptors).

Conclusions: The experimental paradigm presented here can serve as a useful tool for monitoring retinal cells survival and functional viability during organotypic retinal cultures. Future work will explore the use of organotypic retinal cultures described here for the investigation of pluripotent cell derived photoreceptor integration with the host retina, a main obstacle towards successful cell replacement vision restoration approaches.



A schematic illustration of the electrophysiological investigations setup

References

1. Virpi Alarautalahti, Symantas Ragauskas, Jenni J. Hakkarainen, Hannele Uusitalo-Järvinen, Hannu Uusitalo, Jari Hyttinen, Giedrius Kalesnykas, Soile Nymark (2019); Viability of Mouse Retinal Explant Cultures Assessed by Preservation of Functionality and Morphology. *Invest. Ophthalmol. Vis. Sci.* ;60(6):1914-1927. doi: <https://doi.org/10.1167/iovs.18-25156>.

Fabrication of a 3D high-resolution implant for neural stimulation - challenges and solutions

Gal Sphun^{a,b,c}, Nairouz Farah^{b,d}, Amos Markus^{b,d}, Doron Gerber^d, Zeev Zalevsky^{a,c} and Yossi Mandel^{*,b,c,d,e}

- a. The Alexander Kofkin Faculty of Engineering, Bar Ilan University, Ramat Gan, 5290002, Isreal.
 - b. Faculty of Life Sciences, School of Optometry & Visual Science, Bar Ilan University, Ramat Gan, 5290002, Isreal.
 - c. Bar Ilan Institute for nanotechnology & advanced materials (BINA), Bar Ilan University, Ramat Gan, 5290002, Isreal.
 - d. The Mina and Everard Goodman Faculty of Life Sciences Bar-Ilan University, Ramat-Gan 52900, Israel
 - e. The Gonda Multidisciplinary Brain Research Center, Bar-Ilan University
- * Author for correspondence Tel.: +972-3738-4234; yossi.mandel@biu.ac.il

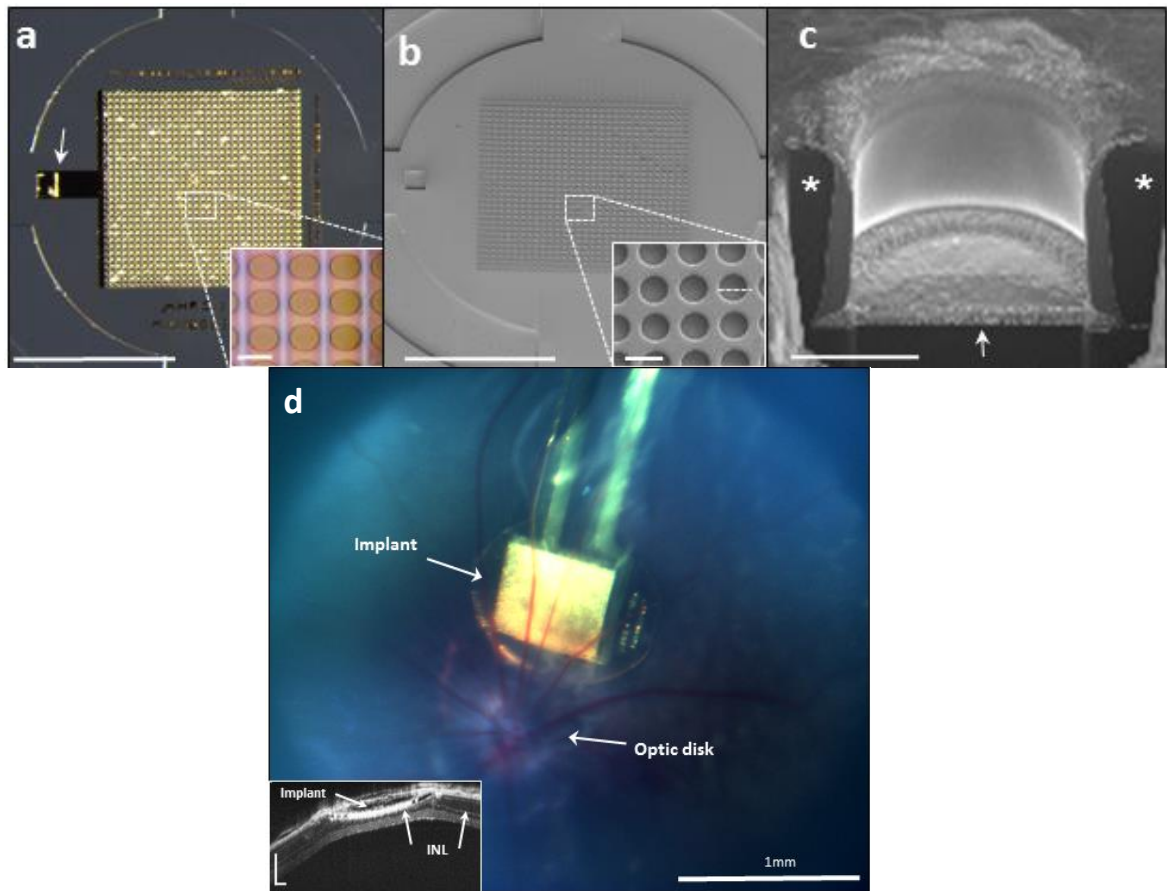
Abstract:

Objective - Tissue integrated microelectronic devices for neural stimulation hold great potential in restoring the functionality of degenerated organs, specifically, retinal prostheses which are aimed at vision restoration [1,2]. Such devices require 3D structures with high resolution, high aspect-ratio (AR), biocompatibility, and suitable mechanical properties. However, the fabrication process of such 3D polymer-metal devices is very complex and is faced with many challenges impairing their functionality [3,4].

Approach - As a model for the optimization process we describe here the fabrication of a bio-functionalized 3D 1mm circular subretinal implant composed of SU-8 polymer integrated with dense gold microelectrodes (23 μ m pitch) passivated with 3D micro-well-like structures (20 μ m diameter, 3 μ m resolution). Toward this end, a nickel (Ni) evaporated silicon (Si) wafer was sequentially spin-coated with SU-8 and photolithographed layer-by-layer, with sharp electrode formation achieved through a two-step bi-layer lift-off process using LOR/AZ followed by Cr/Au thin-layer sputter deposition to increase adhesion. Next, the device was released by overnight Ni wet-etching using nitric acid, after which it was bio-functionalized with N₂ plasma treatment and the addition of the bio-adhesion molecule arginine-glycine-aspartic acid (RGD).

Main results - SEM and FIB cross section examinations revealed good structural design with high resolution (3 μ m resolution) and high aspect ratio (6.6), strong solid gold-SU8 adherence with sharp electrode configuration. *In-vivo* studies showed good integration of the device in the rat sub-retinal space and cell migration into the wells. Moreover, *in-vitro* examination of the bio-functionalization revealed the promotion of cell adhesion to the electrode surface using the RGD bio-molecule as well as the improvement of cell attachment to the SU-8 surface following dry plasma treatment and the feasibility to stimulate the retina.

Significance - The reported process and optimization steps described here in detail can aid in the design and fabrication of neural implants, characterized by high resolution and aspect ratio aiming toward neural stimulation at a single-cell resolution.



Images of a completed retinal implant (1mm in diameter) with gold electrodes array. a) Color image top view of full SU-8-gold retinal implant, scale bar 0.5mm. Insert is a zoom in on the area demarcated by the rectangle (scale bar 20 μ m). b) SEM images top view of the implant as in a. scale bar 0.5mm. In the insert, zoom-in on the area demarcated by the rectangular, scale bar 20 μ m. c) A FIB/SEM cross section imaging of the 3D well-like structure encapsulating the electrode, scale bar 10 μ m. The black pillars are the SU-8 micro-wells walls (*) and gold electrode (white arrow). Scale bar 5 μ m. d) Fundus image of the implanted device (white arrow) demonstrates the good placement near the optic disk, scale bar 1mm. In the inset, an Optical coherence tomography cross section image revealing good integration of the implant in the sub-retinal space under the inner nuclear layer (INL, white arrows), scale bar 200 μ m.

References

- [1] G.A. Goetz, D. V Palanker, Electronic approaches to restoration of sight., *Rep. Prog. Phys.* 79 (2016) 096701. <https://doi.org/10.1088/0034-4885/79/9/096701>.
- [2] R. Feiner, T. Dvir, Tissue-electronics interfaces: From implantable devices to engineered tissues, *Nat. Rev. Mater.* 3 (2017). <https://doi.org/10.1038/natrevmats.2017.76>.
- [3] A. Gadre, M. Kastantin, S.L.S. Li, R. Ghodssi, An integrated BioMEMS fabrication technology, in: 2001 Int. Semicond. Device Res. Symp. Symp. Proc. (Cat. No.01EX497), IEEE, Washington, DC, USA, 2001: pp. 5–8. <https://doi.org/10.1109/ISDRS.2001.984471>.
- [4] B.Y.P. and M.J.M. Rabih Zaouk, Introduction to Microfabrication Techniques, in: S.D. Minteer (Ed.), *Microfluid. Tech. - Rev. Protoc.*, Humana Press Inc., Totowa, NJ, 2006: pp. 5–15. <https://doi.org/10.1385/1-59259-997-4:3>.

Analyzing MEA-chip designs for electroporation-based genetic modification in novel retinal implants

Andrea Kauth,¹ Lena Hegel,¹ Sandra Johnen,² Sven Ingebrandt^{1,*}

1. Institute of Materials in Electrical Engineering 1, RWTH Aachen University, Sommerfeldstr. 24, 52074 Aachen
 2. Department of Ophthalmology, RWTH Aachen University, Pauwelsstr. 30, 52074 Aachen
- * ingebrandt@iwe1.rwth-aachen.de

The concept of retinal prostheses is to restore vision to patients suffering from degenerative diseases such as Retinitis Pigmentosa. Established approaches focused on a replacement of the degenerated photoreceptors by either subretinal or epiretinal stimulation of the remaining intact neurons in the retina [1]. Following the epiretinal approach, our interdisciplinary group developed several generations of implants. In these implants, microelectrode arrays (MEAs) were used to stimulate the retinal ganglion cells to produce phosphene-based vision [2,3]. However, these earlier versions of retinal prostheses did not consider that during disease progression, the photoreceptor layer degenerates, and a functional re-organization of the remaining neuronal network occurs. This re-organization had a direct impact on the stimulation efficiency of the implants [4,5]. In our next-generation implant concepts in the interdisciplinary research-training-group InnoRetVisionⁱ (GRK2610), we aim to integrate additional functions into the retinal implants. For this purpose, we investigate if MEA-based genetic modification of the remaining retinal cells could be used to improve the stimulation efficiency and to protect the ganglion cell layer from further degeneration.

Electroporation is one of several different approaches to genetically modify cells or tissue. Here, short electrical pulses are applied to the cells and, as a response, the cell membrane temporarily forms reversible pores. Through these pores, plasmid DNA-encoding genes or therapeutic sequences can enter the cell. Transfection efficiency as well as cell survival are directly affected by the electric field strength [6]. Since retinal prostheses already utilize MEAs, we focus on electroporation to combine genetic modification and retinal stimulation in one platform.

In a previous project, simulations via COMSOL (COMSOL Multiphysics version 5.1, Stockholm, Sweden) revealed how the electrode shape and distance can be optimized to generate the most homogeneous electrical field strength possible. In this former project, only two MEA chips per 4" wafer could be fabricated.

In this study, we present an optimized MEA fabrication process that allows the fabrication of 40 MEA chips in parallel on a 4-inch glass wafer. We used the flip-chip technique to encapsulate the MEA chips onto printed circuit board (PCB) carriers (Figure 1-A), which are compatible with our homemade MEA amplifier system or with the MEA2100-system (Multichannel Systems, Reutlingen, Germany). In our fabrication process, we vary the electrode material (IrOx, TiN, Au and ITO) (Figure 1-B) and the electrode shape (circular, squared and cloverleaf shaped) to analyze the impact of these parameters on electroporation efficiency.

First electroporation experiments using pMAX GFP (from Cell Line Nucleofector™ Kit V, Lonza) revealed a successful transfection of HEK293 cells cultivated on IrOx MEAs, as seen in Figure 1-C.

With this study, we aim to lay the foundation of a next generation of retinal implants for genetic modification and functional adaptation during retinal degeneration.

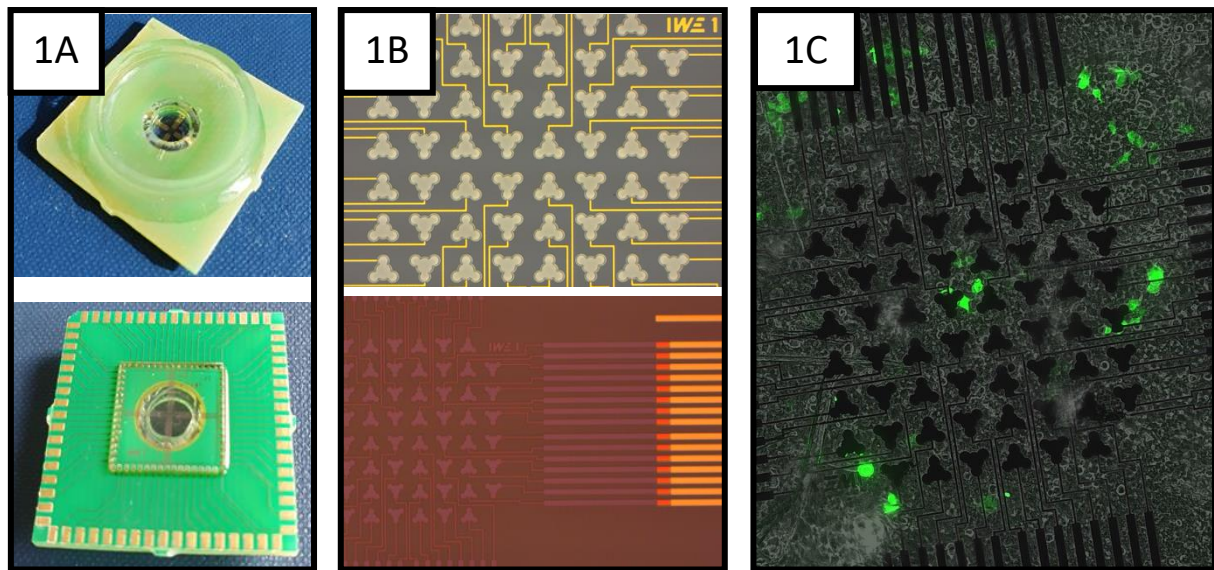


Figure 1: A) Encapsulated MEA-Chips (1cm x 1cm), flip-chipped to PCBs (2.54 cm x 2.54 cm). B) Microscopy images of different electrode materials (IrOx on top image, ITO on bottom image). C) Inverse microscopy image of transfected HEK293 cells on IrOx electrodes.

References

1. Chader, G.J., Weiland, J., and Humayun, M.S. (2009). Artificial vision: needs, functioning, and testing of a retinal electronic prosthesis. *Prog Brain Res* 175, 317-332. doi:10.1016/S0079-6123(09)17522-2.
2. Waschkowski, F., Hesse, S., Rieck, A.C. et al. (2014). Development of very large electrode arrays for epiretinal stimulation (VLARS). *BioMed Eng OnLine* 13(11). doi:10.1186/1475-925X-13-11.
3. Mokwa, W., Goertz, M., Koch, C., Krisch, I., Trieu, H.K., and Walter, P. (2008). Intraocular epiretinal prosthesis to restore vision in blind humans. *30th Annual International Conference of the IEEE Engineering in Medicine and Biology Society*, 5790-5793. doi:10.1109/IEMBS.2008.4650530.
4. Haselier C., Biswas S., Rösch S., Thumann G., Müller F., and Walter P. (2017). Correlations between specific patterns of spontaneous activity and stimulation efficiency in degenerated retina. *PLoS ONE* 12(12). doi:10.1371/journal.pone.0190048.
5. Biswas S., Haselier C., Mataruga A., Thumann G., Walter P., and Müller F. (2014). Pharmacological Analysis of Intrinsic Neuronal Oscillations in rd10 Retina. *PLoS ONE* 9(6). doi:10.1371/journal.pone.0099075.
6. Jain T., and Muthuswamy J. (2008). Microelectrode array (MEA) platform for targeted neuronal transfection and recording. *IEEE Trans. Biomed. Eng.* 55, 827-832. doi:10.1109/TBME.2007.914403.

Electrophysiological recording of a patterned neuronal network realized with ink-jet printing technique

Andrea Andolfi¹, Donatella Di Lisa¹, Pietro Arnaldi¹, Alberto Lagazzo², Sara Pepe³,
Monica Frega⁴, Anna Fassio³, Sergio Martinoia¹, Laura Pastorino¹

Corresponding Author: laura.pastorino@unige.it

¹Department of Informatics, Bioengineering, Robotics and Systems Engineering (DIBRIS),
University of Genoa, Genoa, Italy

²Department of Civil, Chemical and Environmental Engineering (DICCA), University of
Genoa, Genoa, Italy

³Department of Experimental Medicine, University of Genoa, Genoa, Italy

⁴Department of Clinical Neurophysiology, University of Twente, Enschede, The Netherlands

One of the main questions in neuroscience concerns the recurrent relationship between the structure and function of a neuronal network. Thanks to a simplified and easily controllable environment, *in vitro* studies remain one of the most helpful tools to investigate physiological and pathological behaviors. In particular, two-dimensional neuronal cultures on microelectrode array (MEA) represent a gold standard for studying neuronal activity [1]. The versatility of these systems, thanks to the large recording area, made them essential in the study of the relationship between the functional activity of neuronal networks and their structural organization [2]. Different fabrication methods are used to obtain engineered networks, involving physical and/or chemical approaches in order to favor and guide cellular attachment and development. Among all patterning techniques, inkjet printing has gained considerable interest thanks to a direct-write allowing efficient deposition of material without the use of physical masters, leading to significant savings in both time and cost [3]. In this work, we propose an easy, fast, and low-cost method for the realization of patterned neuronal cultures on a MEAs device using drop-on-demand (DOD) inkjet technology. The ink used is based on chitosan (CHI), a copolymer well known for its low-cost, biocompatibility, biodegradability, muco-adhesiveness, antibacterial activity, and bioaffinity [4]. The scheme in figure 1 describes the main steps for the realization of patterned cell culture, where the pattern is designed, modified, and printed in a few minutes, thanks to the software provided by the printer. Furthermore, thanks to a print resolution comparable to the microelectrode size, it's possible to realize in a precise way both patterns that covered the active area of the MEA (i.e., full pattern) and patterns for just the connection of the microelectrodes (i.e., grid pattern). Our preliminary results demonstrate how neurons follow the spatial organization suggested by the patterned substrate and how their electrophysiological activity can be recorded. In particular, guided neuronal network development was characterized by contrast phase microscopy and by immunostaining using fluorescence microscopy. Microtubule-associated protein (MAP-2) and Dapi were used to label dendritic arborization and neurons nuclei, respectively. Figure 2a shows how the cell culture remains confined within the active area of the MEA, thanks to the full pattern printed on the device. Figure 2b shows how cell culture can be organized even with more complicated geometries. Finally, in figure 3c is possible to observe a set of waveforms of an example MEAs electrode.

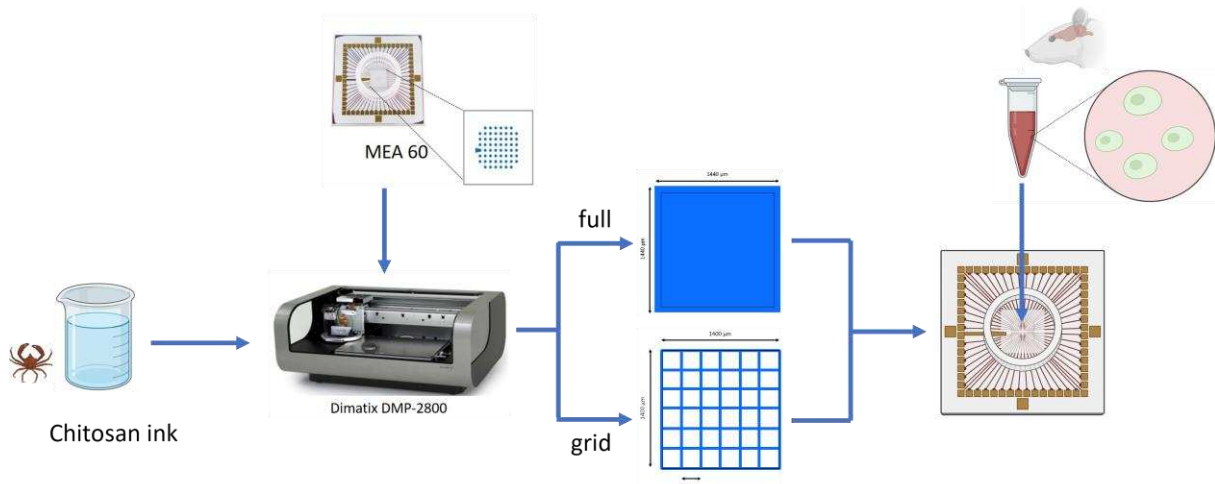


Figure 1: scheme of the main steps to realize patterned cell culture.

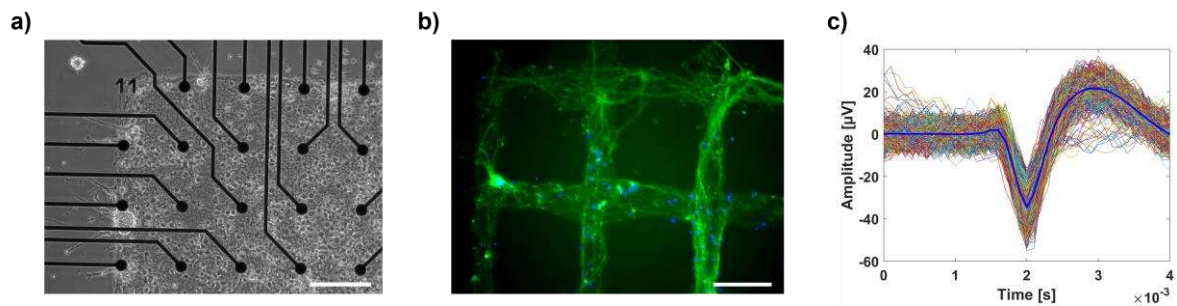


Figure 2: **a)** contrast phase image of 19 DIV rodent hippocampal patterned neuronal network on MEA device with a full pattern (scalebar: 200 μm). **b)** Immunochemistry staining images of 15 DIV rodent hippocampal neuronal on a grid patterned substrate, labeled for MAP2 (green) and DAPI (blue). **c)** Set of waveforms of a patterned neuronal network at 19 DIV of an example MEA electrode.

References

1. M. Chiappalone et al. Networks of neurons coupled to microelectrode arrays: a neuronal sensory system for pharmacological applications, *Biosensors and Bioelectronics*, Volume 18, Issues 5–6, 2003, Pages 627-634, ISSN 0956-5663, [https://doi.org/10.1016/S0956-5663\(03\)00041-1](https://doi.org/10.1016/S0956-5663(03)00041-1).
2. E. Tibau et al., Interplay activity-connectivity: dynamics in patterned neuronal cultures. In *AIP Conference Proceedings* (Vol. 1510, No. 1, pp. 54-63). American Institute of Physics (2013, January).
3. E. Tekin et al., Inkjet printing as a deposition and patterning tool for polymers and inorganic particles, *Soft Matter*, 4, 703-713, 2008.
4. V. I. Scanga et al., Biomaterials for neural-tissue engineering — Chitosan supports the survival, migration, and differentiation of adult-derived neural stem and progenitor cells. *Canadian Journal of Chemistry*, 2010.

Spontaneous bidirectional signal conduction along axons *in vitro*

Mateus JC^{a,d}, Lopes CDF^{a,#}, Aroso M^a, Costa AR^b, Gerós A^{a,e}, Meneses J^{f,g}, Faria P^f, Neto E^c, Lamghari M^c, Sousa MM^b, Aguiar P^{a*}

- a. Neuroengineering and Computational Neuroscience Lab, i3S- Instituto de Investigação e Inovação em Saúde, Universidade do Porto, Porto, Portugal
 - b. Nerve Regeneration Lab, i3S- Instituto de Investigação e Inovação em Saúde, Universidade do Porto, Porto, Portugal
 - c. Neuro & Skeletal Circuits Lab, i3S- Instituto de Investigação e Inovação em Saúde, Universidade do Porto, Porto, Portugal
 - d. ICBAS- Instituto de Ciências Biomédicas Abel Salazar, Universidade do Porto, Porto, Portugal
 - e. FEUP – Faculdade de Engenharia da Universidade do Porto, Porto, Portugal
 - f. CDRSP-IPL - Centre for Rapid and Sustainable Product Development – Instituto Politécnico de Leiria, Marinha Grande, Portugal
 - g. IBEB - Instituto de Biofísica e Engenharia Biomédica, Faculdade de Ciências, Universidade de Lisboa, Lisboa, Portugal
- # present address: IBEC – Institute for Bioengineering of Catalonia, Barcelona, Spain

* Corresponding author: pauloaguiar@i3s.up.pt

Embedded in the canonical perspective on how neurons communicate is the idea of stereotypical and unidirectional axonal conduction. However, recent technological advances are revealing the complex physiology of the axon and challenging long-standing assumptions [1]. Namely, while most action potential (AP) initiation occurs at the axon initial segment in CNS neurons, initiation in distal parts of the axon has been shown to occur [2]–[5]. Such ectopic AP activity has not been reported yet in studies using *in vitro* neuronal networks and its functional role, if exists, is still not clear.

Taking advantage of microElectrode array and microFluidic (μ EF) devices to assess axonal conduction in neuronal cultures [6], we have recently reported that a significant fraction of the conducted APs does not come from the canonical synapse-dendrite-soma signal flow, but instead originates at the distal axon [7]. We demonstrate that spontaneous bidirectional (orthodromic and antidromic) AP conduction occurs in both hippocampal and dorsal root ganglion cultures, reshaping our understanding of how information flows *in vitro*. We investigate and characterize this bidirectional conduction in physiological conditions, after distal axotomy, and after pharmacological modulation. High-temporal resolution recordings have revealed that conduction velocity is asymmetrical, with antidromic conduction being slower than orthodromic. Via computational modeling and super-resolution microscopy, we show that the experimental difference can be explained by axonal morphology. Importantly, antidromic APs may carry information and have a functional impact on the neuron, as they consistently depolarize the soma. Thus, plasticity or gene transduction mechanisms triggered by soma depolarization can be affected by antidromic activation [8].

With neuronal cultures being used extensively in conditions where axonal conduction plays an important role (e.g., neural circuits, axonal transport), acknowledging this prevalence of bidirectional axonal conduction is of fundamental importance. Moreover, with the recent finding that dopamine axons can generate APs distally, and independently of somatodendritic activity, to control dopamine release *in vivo* [4], this work raises the question if spontaneous distal activation is an important mechanism in other physiological and pathological contexts. We believe that μ EF devices can be a powerful tool to answer these important questions.

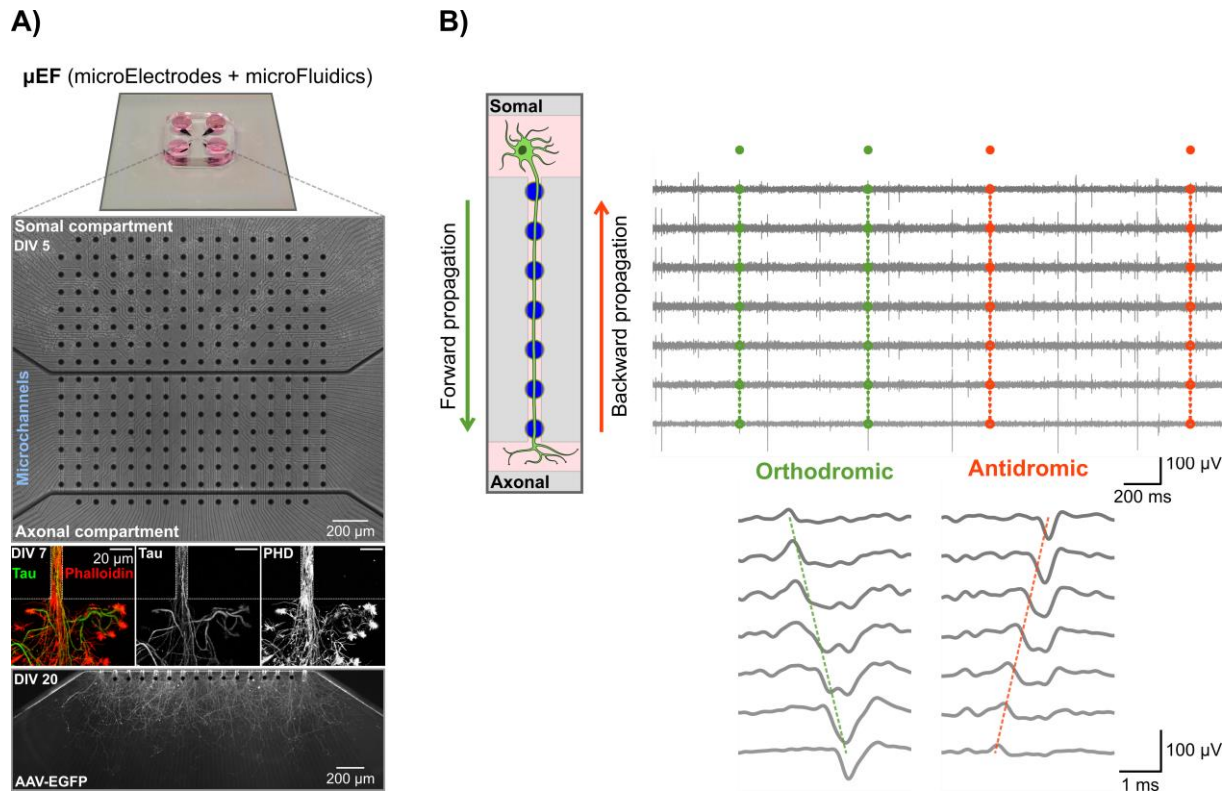


Figure 1 – A) Photograph of a μ EF and phase-contrast microscopy image mosaic of a hippocampal mono-culture at five days in vitro (DIV). The whole 252 MEA active area is shown. A microfluidic device composed of 16 microchannels (10 μ m width; 700 μ m minimum length) is aligned to include seven microelectrodes each. Below, an axonal compartment of a hippocampal culture (expressing EGFP) at 20 DIV and the exit of a single microchannel at 7 DIV (stained for Tau and phalloidin) are shown. **B)** Schematized μ EF concept and representation of the two possible direction flows of signal propagation. Example traces of 3 s of activity within a microchannel of a dorsal root ganglia culture at 11 DIV. Detected orthodromic and antidromic propagating events are marked as green and orange, respectively.

References

- [1] P. Alcamí and A. El Hady, "Axonal Computations," *Front. Cell. Neurosci.*, vol. 13, p. 413, Sep. 2019, doi: 10.3389/fncel.2019.00413.
- [2] T. Dugladze, D. Schmitz, M. A. Whittington, I. Vida, and T. Gloveli, "Segregation of Axonal and Somatic Activity During Fast Network Oscillations," *Science (80-.)*, vol. 336, no. 6087, pp. 1458–1461, Jun. 2012, doi: 10.1126/science.1222017.
- [3] M. E. J. Sheffield, T. K. Best, B. D. Mensh, W. L. Kath, and N. Spruston, "Slow integration leads to persistent action potential firing in distal axons of coupled interneurons," *Nat. Neurosci.*, vol. 14, no. 2, pp. 200–207, Feb. 2011, doi: 10.1038/nn.2728.
- [4] C. Liu *et al.*, "An action potential initiation mechanism in distal axons for the control of dopamine release," *Science (80-.)*, vol. 375, no. 6587, pp. 1378–1385, 2022, doi: 10.1126/science.abn0532.
- [5] C. Thome, F. C. Roth, J. Obermayer, A. Yanez, A. Draguhn, and A. V. Egorov, "Synaptic entrainment of ectopic action potential generation in hippocampal pyramidal neurons," *J. Physiol.*, vol. 596, no. 21, pp. 5237–5249, Nov. 2018, doi: 10.1113/JP276720.
- [6] C. D. F. Lopes, J. C. Mateus, and P. Aguiar, "Interfacing Microfluidics with

Microelectrode Arrays for Studying Neuronal Communication and Axonal Signal Propagation,” *J. Vis. Exp.*, no. 142, pp. 1–8, 2018, doi: 10.3791/58878.

- [7] J. C. Mateus *et al.*, “Bidirectional flow of action potentials in axons drives activity dynamics in neuronal cultures,” *J. Neural Eng.*, vol. 18, no. 6, p. 066045, Dec. 2021, doi: 10.1088/1741-2552/AC41DB.
- [8] O. Bukalo, E. Campanac, D. A. Hoffman, and R. D. Fields, “Synaptic plasticity by antidromic firing during hippocampal network oscillations,” *Proc Natl Acad Sci U S A*, vol. 110, no. 13, Mar. 2013, doi: 10.1073/pnas.1210735110.

Acknowledgements

This work was partially financed by FEDER - Fundo Europeu de Desenvolvimento Regional funds through the COMPETE 2020 - Operational Programme for Competitiveness and Internationalisation (POCI), Portugal 2020, and by Portuguese funds through FCT - Fundação para a Ciência e a Tecnologia in the framework of the projects PTDC/EMD-EMD/31540/2017 (POCI-01-0145-FEDER-031540) and PTDC/MED-NEU/28623/2017 (NORTE-01-0145-FEDER-028623). JCM was supported by FCT (PD/BD/135491/2018) in the scope of the BiotechHealth PhD Program.

Accurate neurons localization in 2D cell cultures by using high performance electropolymerized microelectrode arrays correlated with optical imaging

Mahdi Ghazal,^a Corentin Scholaert,^a Camille Lefebvre,^b Nicolas Barois,^d Sebastien Janel,^d Mehmet Cagatay Tarhan,^a Morvane Colin,^b Luc Buée,^b Sophie Halliez,^b Sebastien Pecqueur,^a Yannick Coffinier,^a Fabien Alibert,^{a,e} Pierre Yger^{b,c,*}

- a. Institut d'Électronique, Microélectronique et Nanotechnologie (IEMN), CNRS, UMR 8520, F-59652 Villeneuve d'Ascq, France Department 2, University 2, Address 2
- b. Lille Neurosciences & Cognition (IiNCog) – U1172 (INSERM, Lille), Univ Lille, CHU Lille 59045 Lille, France
- c. Sorbonne Université, INSERM, CNRS, Institut de la Vision, F-75012 Paris, France
- d. Univ. Lille, CNRS, Inserm, CHU Lille, Institut Pasteur Lille, U1019 - UMR 9017 - CIIL - Center for Infection and Immunity of Lille, F-59000 Lille, France.
- e. Laboratoire Nanotechnologies & Nanosystèmes (LN2), CNRS, Université de Sherbrooke, J1X0A5, Sherbrooke, Canada

* pierre.yger@inserm.fr

The development of electronic devices such as microelectrode arrays (MEAs), used to record extracellularly simultaneous electrical activity of large populations of neurons is blooming [1]. To enhance the quality of the recordings, the use of electrode made of conducting polymer such as PEDOT has recently emerged for optimizing the performance of microelectrodes due to its mixed ionic electronic conduction, biocompatibility and low impedance [2]. However, the extent to which these new interfaces can help the algorithmic pipelines of spike sorting [3], i.e. turning extracellular potentials into individual spike trains remains unexplored. To address this issue, we checked if the physical positions of the neurons could be reliably inferred from extracellular electrical recordings obtained by MEAs, and thus be exploited by downstream spike sorting algorithms. To do so, we combine high resolution images of neuronal tissues and dense recordings performed via high performant electropolymerized electrodes based MEAs.

Firstly, we report the use of EDOT electropolymerization to tune post-fabrication material and geometrical parameters of passive microelectrodes. The process optimizes the cell/electrode interface by decreasing its impedance and improving its affinity with neurons: results demonstrate a better biocompatibility and improved signal-to-noise ratio (SNR) (up to 40 dB). Thanks to the higher SNR, we were able to detect more cells in comparison with gold electrodes from the same neural network by using spike sorting. Hence, the higher number of cells detected will lead into more accurate analysis of the localization of the active neurons on top of MEA. Secondly, by using these high performant MEAs, we investigated the possibility to accurately estimate the positions of the neurons solely from extracellular recordings by studying the correlation between electrical activity (obtained via spike sorting), optical imaging (Fluorescent) and Scanning Electron Microscopy (SEM) of neural networks cultured on MEAs. By using the SpykingCircus software [4] to spike sort the extracellular recordings, we estimated the positions of the neurons either by using the center of mass of their electrical signatures, or by inferring the positions assuming cells would behave as monopoles [5]. By superposition of the fluorescent and the SEM images, we compared the observed physical positions of the neurons with the ones predicted by the two aforementioned methods. This approach showed the high accuracy of the monopole hypothesis compared to the center of mass.

In this work, we showed how the use of a material engineering technique for optimizing state of art MEAs can enhance the quality of the recordings. Hence, the correlation of these high quality recordings with optical imaging paves the way towards new algorithmic possibilities for spike sorting algorithms that could make use of a more reliable estimation of neuronal positions.

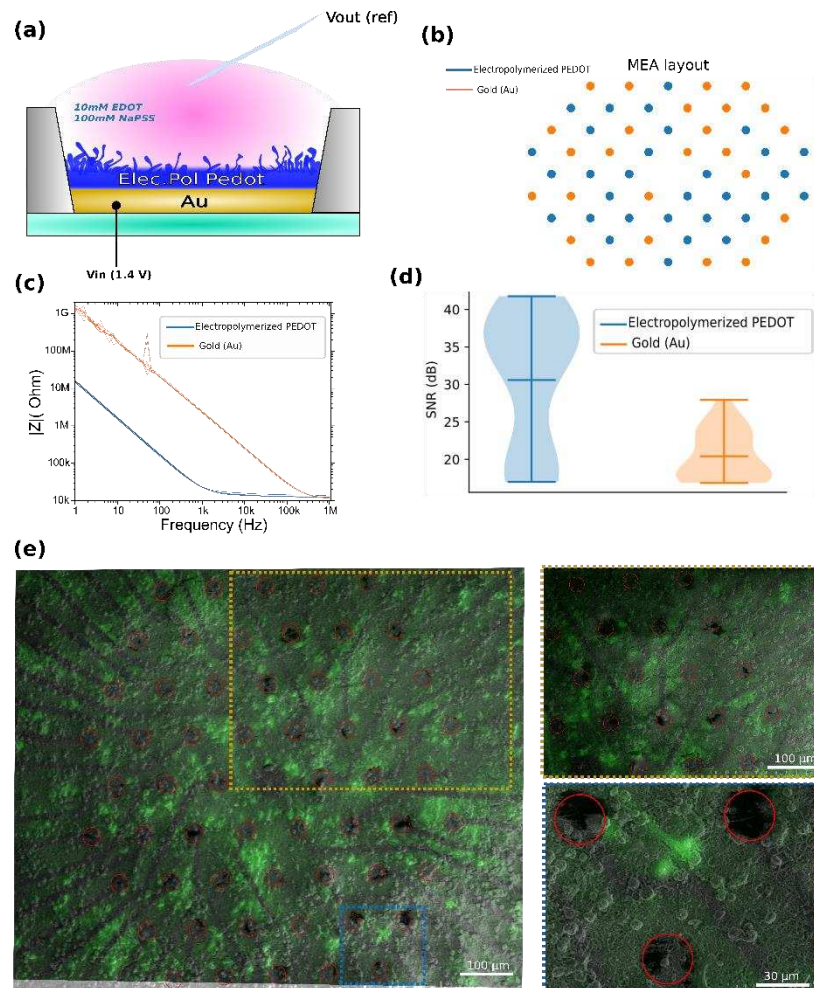


Figure 1 Methodological procedure. (a) Electropolymerization setup. (b) MEA layout with both gold and Electropolymerized electrodes, its impedance Bode plot (c) and SNR of its recordings from same MEA (d). (e) Superposition of SEM and Fluorescent images. Red circles are the positions of the electrodes.

References:

- [1] M. E. J. Obien, "Revealing neuronal function through microelectrode array recordings," *Frontiers in Neuroscience*, p. 30, 2015.
- [2] P. Fattahi, G. Yang, G. Kim, and M. R. Abidian, "A Review of Organic and Inorganic Biomaterials for Neural Interfaces," *Adv. Mater.*, vol. 26, no. 12, pp. 1846–1885, 2014, doi: <https://doi.org/10.1002/adma.201304496>.
- [3] B. Lefebvre, P. Yger, and O. Marre, "Recent progress in multi-electrode spike sorting methods," *Journal of Physiology-Paris*, vol. 110, no. 4, pp. 327–335, Nov. 2016, doi: 10.1016/j.jphysparis.2017.02.005.
- [4] P. Yger *et al.*, "A spike sorting toolbox for up to thousands of electrodes validated with ground truth recordings in vitro and in vivo," *eLife*, vol. 7, p. e34518, Mar. 2018, doi: 10.7554/eLife.34518.
- [5] J. Bussard, E. Varol, H. D. Lee, N. Dethé, and L. Paninski, "Three-dimensional spike localization and improved motion correction for Neuropixels recordings," *Neuroscience*, preprint, Nov. 2021. doi: 10.1101/2021.11.05.467503.

A MEA-based *in vitro* Traumatic Brain Injury Platform

Marc O. Heuschkel^a, Luc Stoppini^a, Loris Gomez Baisac^a, Yoan Neuenschwander^c, Denis Prim^b, Cédric Schmidt^c, Marc E. Pfeifer^b, Jérôme Extermann^c, Adrien Roux^{a,*}

- a. Tissue Engineering Laboratory, HEPIA HES-SO University of Applied Sciences and Arts Western Switzerland, 1202 Geneva, Switzerland
- b. Diagnostic Systems Research Group, Institute of Life Technologies, School of Engineering, University of Applied Sciences and Arts Western Switzerland (HES-SO Valais-Wallis), 1950 Sion, Switzerland.
- c. Micro-Nanotechnology group, HEPIA HES-SO University of Applied Sciences and Arts Western Switzerland, 1202 Geneva, Switzerland

* adrien.roux@hesge.ch

Mild traumatic brain injury (mTBI) is a neurological injury, resulting in an alteration of mental status, such as confusion or amnesia. To better understand the pathophysiology of this type of trauma, we are developing an *in vitro* model of mTBI based on human 3D neuronal tissues derived from iPS cells [1]. This mTBI *in vitro* model is intended to reproduce some key events leading to acute and long-term consequences on brain parenchyma damages.

To induce the trauma, a microvalve (Fritz Gyger AG, Switzerland) is positioned at a precise distance above the 3D neuronal tissue and culture medium is ejected with controlled velocity, and amount to induce an instant compression of the neuronal tissue, mimicking a concussion event (see Figures 1A&1B). We induced repetitive mTBI assaults on the tissue to assess if physiologic vulnerabilities might be exacerbated by repeated mild injuries within specific time windows between injuries. The validation of this model is achieved by using complementary read-out modalities, i.e., electrical monitoring, measurement of biomarkers released into the surrounding medium via a multiplex immunoassay [2], confocal imaging, and optical projection tomography.

The functional electrophysiological monitoring of the 3D neuronal tissues is performed using proprietary Strip-MEA Biochips [3] designed to monitor neuronal activity at an air-liquid interface. This experimental setup is well suited for very long-term follow-up because it maintains 3D neuronal tissues in best possible survival conditions. These capabilities are made possible by the Strip-MEA Biochip based on four flexible and porous polyimide membranes incorporating eight platinum black microelectrodes in each (see Figures 1C&1D). Electrophysiological activity at control (before), during, and after the induction of the mTBI is compared to evaluate mTBI effects on the 3D neuronal tissues. Preliminary results show that immediately following impacts, a complete and immediate abolition of spike activities as well as induction of burst activities can be observed (see Figure 2). mTBI recovery data is recorded as early as 3 hours after the event and is also compared to control activity. Measured biomarker levels (see Figure 3) indicate a significant concentration increase after induced injury of glial proteins (GFAP and S100 β), as also observed clinically *in vivo* for (m)TBI patients. Further studies to expand the panel of monitored biomarkers and to investigate the release kinetics of neuron-specific biomarkers such as h-FABP and NSE are ongoing. Traumatized neuronal tissues are stained with propidium iodide and DRAQ5TM fluorescent dyes, embedded in agarose gel and mounted in capillary tubes for Optical Projection Tomography (OPT) and confocal microscopy. 3D fluorescence imaging of the entire tissue allows spatial localisation of the impact region (see Figure 3E) and quantification of apoptosis as a function of injury level.

Following the obtained results, this new approach enables to study complex mechanisms involved during brain trauma and may become a useful tool to test potential neuroprotection protocols toward therapeutical recovery from mTBI.

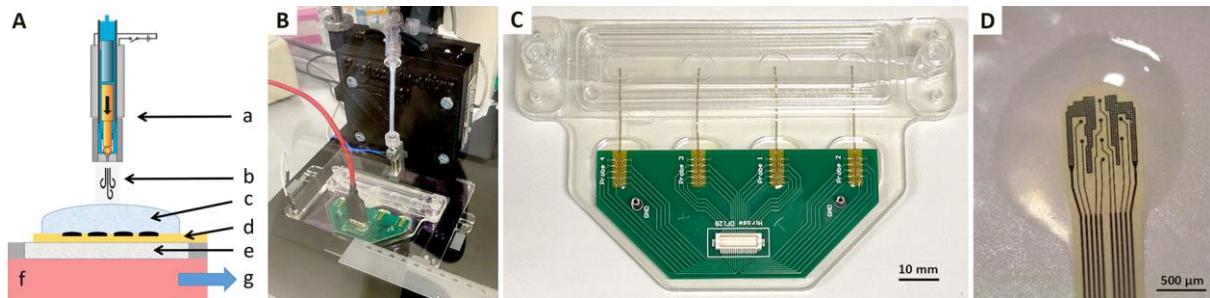


Figure 1: A: Schematic of a Strip-MEA Biochip mounted on the mTBI induction platform: (a) microvalve, (b) ejected liquid medium, (c) 3D neuronal tissue, (d) Strip-MEA recording area, (e) porous membrane, (f) circulating medium, (g) biomarkers analysis. B: Picture of the mTBI setup based on a strip-MEA Biochip placed below a microvalve allowing ejection of medium on the 3D neuronal tissues. C: Strip-MEA Biochip consisting of 4 recording sites with 8 platinum black electrodes on each. D: Porous flexible Strip-MEA on a 3D neuronal tissue at air-liquid interface.

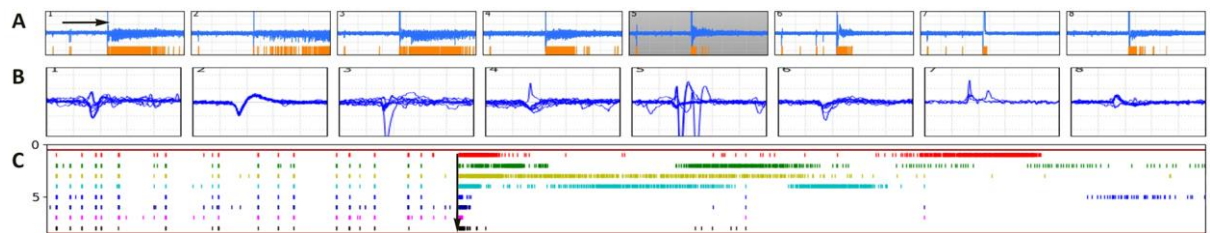


Figure 2: Representative experiment of one 3D neuronal tissue after mTBI induction (black arrow) recorded with 8 strip-MEA electrodes (Duration=25s, Amplitude= $\pm 250\mu V$). A: Raw data of the spontaneous activity on 8 electrodes. B: Corresponding spike cut-outs (Duration=5ms, Amplitude= $\pm 250\mu V$). C: Raster plot of the same 8 electrodes showing the spike timestamps over time before and after the mTBI induction (Displayed duration=5m45s).

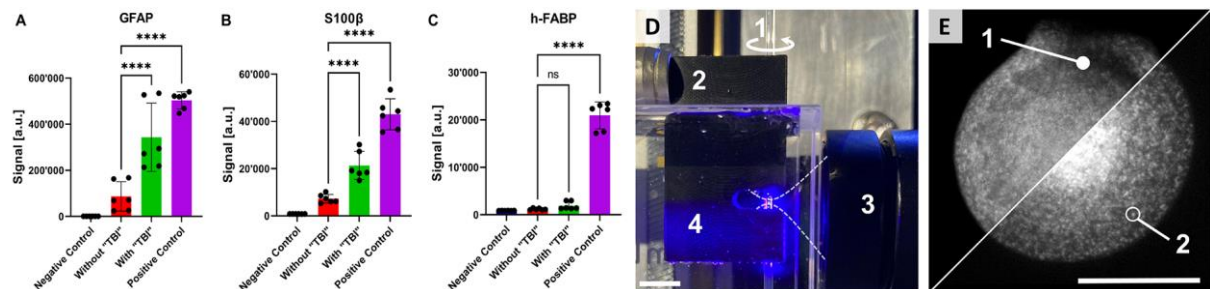


Figure 3: Preliminary A: GFAP, B: S100 β , and C: h-FABP biomarker levels measured without (red bar) or with (green bar) "TBI-type" induced injury. It was observed that 3D neuronal tissues experiencing a "TBI" pulse exhibited increased signals for glial biomarkers (GFAP and S100 β) as compared to neuron-specific biomarkers (h-FABP). Each condition was measured on three independent tissues ($n=3$) and in duplicates ($m=2$). D: Picture of high-resolution Optical Projection Tomography (OPT) setup. A blue LED excites the tissue fluorescence from the right. 1) A FEP tube embedding the 3D neuronal tissue in agarose gel is rotated in front of the imaging system (3) using a step motor, 2) mechanical support that guides the FEP tube over rotation, 4) water cell allowing optical index matching between agarose, FEP tube and the objective lens (Scale=10mm). E: Optical projection of 3D neuronal tissues with and without trauma. ROI 1 indicates the reduced signal intensity region surrounding the trauma. ROI 2 shows a typical sane single neuron (Scale=300 μm).

References

- Govindan, S., Batti, L., Osterop, S. F., Stoppini, L., Roux, A., (2021). Mass Generation, Neuron Labelling, and 3D Imaging of Minibrains. *Front. Bioeng. Biotechnol.* 8:582650 doi:10.3389/fbioe.2020.582650.
- Jović, M., Prim, D., Saini, E., Pfeifer, M.E., (2022). Towards a Point-of-Care (POC) diagnostic platform for the Multiplex Electrochemiluminescent (ECL) sensing of Mild Traumatic Brain Injury (mTBI) biomarkers. *Biosensors* 12, 172. doi:10.3390/bios12030172.
- Ferlauto, L., D'Angelo, A. N., Vagni, P., Airaghi Leccardi, M. J. I., Mor, F. M., Cuttaz, E. A., Heuschkel, M. O., Stoppini, L., and Ghezzi, D. (2018). Development and Characterization of PEDOT:PSS/Alginate Soft Microelectrodes for Application in Neuroprosthetics. *Front Neurosci* 12, 648. doi:10.3389/fnins.2018.00648

Micro-structured microfluidic devices implemented with a custom MEA for all human neuromuscular junctions

Pauline Duc^{a,e}, Audrey Sebban^{b,e}, Gilles Carnac^{c,e}, Michel Vignes^{d,e}, Gérald Hugon^{c,e}, Benoît Charlot^{b,e} and Florence Rage^{a,e}

- a. IGMM, Institute of molecular genetics, CNRS, Montpellier, France
 - b. IES, Institut d'Electronique et des Systèmes UMR 5214 CNRS, Montpellier, France
 - c. PhyMedExp, U1046 INSERM, UMR9214 CNRS, Montpellier, France.
 - d. IBMM, Institute of Biomolecules, UMR5247 CNRS, Montpellier, France
 - e. University of Montpellier, Montpellier, France
- * Benoit.charlot@umontpellier.fr

This work presents the development of a Micro Electrode Array (MEA) coupled with a compartmentalized microfluidic circuit (Figure 1(a)) for the study of all human reconstructed motor neuron / muscle junctions. In the neuromuscular system, signal transmission from motor neurons to innervated muscle fibers is crucial for their synaptic function, viability, and maintenance. In order to better understand human neuromuscular junction (hNMJ) functionality, and especially in pathologic cases, it is important to be able to reconstruct such neuronal junctions in vitro together with the ability to stimulate, record and observe the cells.

To investigate this motoneuron/muscle junctions at a subcellular level, microfluidic platforms integrated with custom microelectrode arrays are useful to grow different cell types in isolated compartments[1][2][3]. Such devices have already been developed to study in vitro neuronal circuitry. Here, we combined these systems with inductive pluripotent stem cells (iPSC) on a specific pattern of electrodes to stimulate pre-synaptic axons and record post-synaptic muscle activity.

Micromachining was used to create structurations (Figure 1(b,c,d)) with broken lines configuration to guide muscle growth above electrodes, but also to promote an optimal innervation of the muscle cells by axons from the neuronal chamber that have grown through microchannels, therefore optimizing the effectiveness of activity recording. Electrodes were also arranged to best fit the microfluidic chambers in order to specifically stimulate axons that were growing between the two compartments. Isolation of the two cell types allows for the selective treatment of neurons or muscle fibers to assess NMJ functionality hallmarks. Altogether, this microfluidic/microstructured/MEA platform allowed mature and functional in vitro hNMJ modelling.

We demonstrate that electrical activation of motor neurons can trigger recordable extracellular muscle action potentials that can be recorded both with electrodes and by calcium imaging using genetically encoded calcium indicators (Figure 1(e,f)). This study provides evidence for a physiologically relevant model to mimic a hNMJ that will in the future be a powerful tool to better understand and characterize NMJs and their disruption in neurodegenerative diseases.

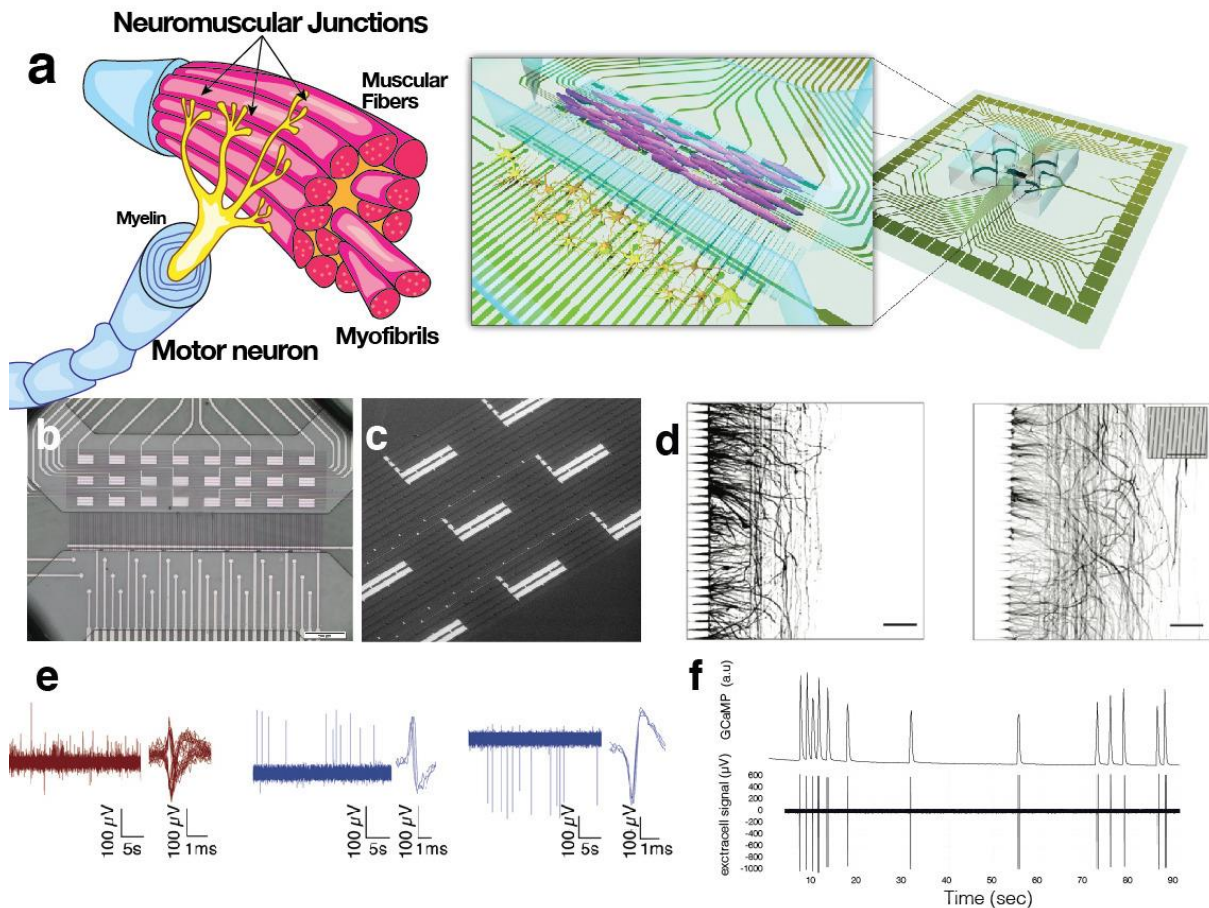


Figure 1: Schematic illustration of a neuromuscular junction and its integration within an *in vitro* microfluidic - MEA system. (b) Microphotograph of the superposition of a compartmentalized microfluidic circuit bonded over a specific microelectrode array and (c) SEM picture of an array of microgrooves made on top of microelectrodes. (d) Microstructure optimization for motoneuron invasion. Staining of axons using anti-Smi32 antibody to visualize their growth in the muscle compartment containing either continuous lines (left) or broken lines (right). (e) examples depicting spiking activity and superimposed traces of spikes recorded in axon (left) and muscle electrodes (middle and right). Note that both positive and negative ongoing signals were recorded by axon electrodes since one electrode record a dozen of microchannel-containing axons. (f) simultaneous recordings of Intracellular Ca^{2+} increases in axons of GCaMP-6f labelled myocyte and extracellular signal through microelectrodes.

References

- [1] E. Moutaux, B. Charlot, A. Genoux, F. Saudou, and M. Cazorla, "An integrated microfluidic/microelectrode array for the study of activity-dependent intracellular dynamics in neuronal networks," *Lab Chip*, vol. 18, no. 22, pp. 3425–3435, Nov. 2018, doi: 10.1039/C8LC00694F.
- [2] P. Duc *et al.*, "Human neuromuscular junction on micro-structured microfluidic devices implemented with a custom micro electrode array (MEA)," *Lab Chip*, vol. 21, no. 21, pp. 4223–4236, Oct. 2021, doi: 10.1039/D1LC00497B.
- [3] E. E. Zahavi, A. Ionescu, S. Gluska, T. Gradus, K. Ben-Yaakov, and E. Perelson, "A compartmentalized microfluidic neuromuscular co-culture system reveals spatial aspects of GDNF functions," *J Cell Sci*, vol. 128, no. 6, pp. 1241–1252, Mar. 2015, doi: 10.1242/jcs.167544.

Tailoring neuronal connectivity using PDMS microstructures with nanochannels on MEAs

Katarina Vulić,^a Sean Weaver,^a Jose Mateus,^b Yu-Yang Oon,^a Stephan Ihle,^a Jens Duru,^a Paulo Aguiar,^b János Vörös^{a,*}

- a. Laboratory of Biosensors and Bioelectronics, Institute for Biomedical Engineering, University and ETH Zurich, Switzerland
- b. Neuroengineering and Computational neuroscience Lab, Institute for Research and Innovation in Health (i3S), University of Porto, Portugal
- * janos.voros@biomed.ee.ethz.ch

The mechanisms behind information storage and processing among neurons in the brain remain one of the major enigmas in neuroscience. The attempts to isolate and characterize a single functional network *in vivo* often result in vast amount of interference with adjacent networks as well as in irreproducibility of the acquired data. We believe that a different, bottom-up approach which includes low-density networks with controlled topology can help overcoming these challenges. Thus, we have developed a simple yet robust experimental platform that has proven fruitful in investigating network connectivity with high spatiotemporal resolution [1,2,3].

To study the relationship between connectivity and synaptic transfer efficiency, we designed a PDMS microstructure consisting of two input nodes with axons guided symmetrically around the output node (see Figure 1). To control the number and location of synaptic connections, the nodes are interconnected with nanochannels that are too narrow for axons but permit the growth of dendritic spines enabling synapse formation [4]. We placed the microstructures on top of microelectrode arrays (MEAs) and used a combination of stimulation and recording to analyze the efficiency of synaptic transfer. Additionally, we used functional imaging to achieve a high spatial resolution for analyzing signal propagation. In parallel, we are developing an *in silico* equivalent that will help us understand and explain the signal transmission properties we observed *in vitro*. Based on the experimental activity we will tune the model parameters and use it to give predictions we can directly test *in vitro*.

We believe that simplifying network topology in combination with electrophysiological and optical activity manipulation and recording could unravel the fundamental concepts of synaptic transmission and information flow between the neurons.

References

1. Duru, J. et al (2022) *Engineered biological neural networks on high density CMOS microelectrode arrays*, Front. Neurosci. 16:829884
2. Girardin S. et al. (2022). *Topologically controlled circuits of human iPSC-derived neurons for electrophysiology recordings*. Lab Chip, 2022, Advance Article
3. Ihle S. et al. (2021). *An experimental paradigm to investigate stimulation dependent activity in topologically constrained neuronal networks*. Biosensors and Bioelectronics 201: 11389
4. Mateus, J. et al. *Nanoscale patterning of in vitro neuronal circuits*, bioRxiv 2021.12.16.472887; doi: <https://doi.org/10.1101/2021.12.16.472887>

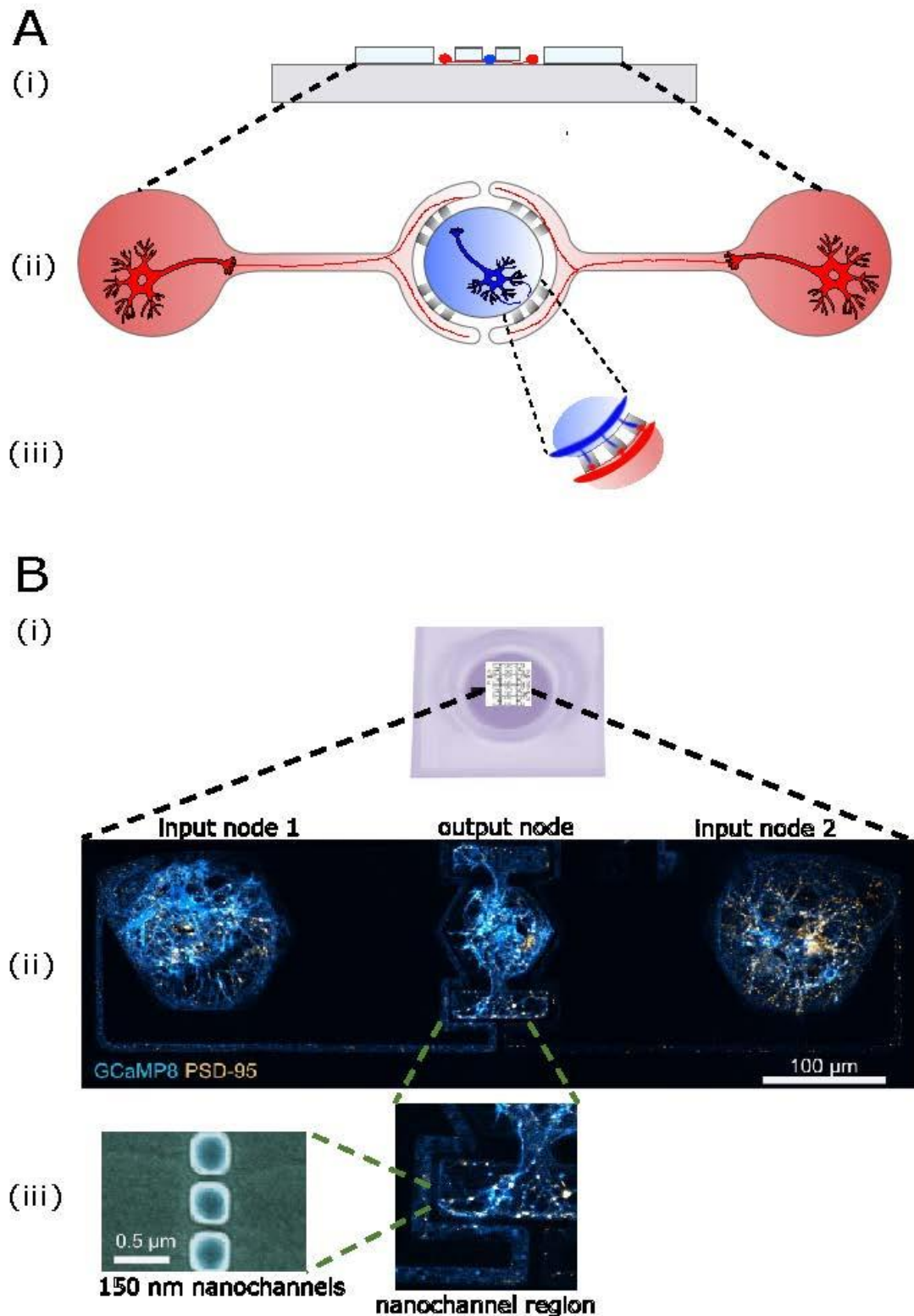


Figure 1: A: Schematic representation of the experimental setup. (i) PDMS microstructures with open landing-spots and closed axon-guiding channels are placed on MEAs. (ii) The channel design assured spatial separation between the input-node neurons that grow in the red compartments from output-node neurons that are placed in the blue compartment. The channel length of the red compartment assures that only the long axons reach the connecting area with the output node. (iii) Nanochannels between the red and blue zones allow for formation of axodendritic synapses, enabling feed-forward connections from input to output. Their dimensions are chosen such that while axons are not able to cross, dendritic spines can form through them. Their size and number can be freely tailored enabling the tailoring of connection strength between input and output. B: (i) Microstructure on top of a thin MEA to electrically and optically stimulate and record activity. (ii) Example of a full circuit consisting of two input nodes and one output node. Neurons are labeled with calcium indicator GCaMP8 and PSD-95 to locate putative synapses. (iii) SEM micrograph of 150 nm wide nanochannels that connect the two compartments.

Collagen-like gold nanostructures on microelectrodes promote neuronal adhesion and growth

Bharat Nowduri, Steven Schulte, Dominique Decker, Manuela Gries, Holger Rabe, Karl-Herbert Schäfer, Monika Saumer*

Department of Informatics and Microsystem Technology, University of Applied Sciences
Kaiserslautern, Amerikastraße 1, 66482 Zweibrücken, Germany

* monika.saumer@hs-kl.de

Microelectrode surfaces coated with natural nanostructures derived from the extracellular matrix proteins (e.g. collagen, laminin, fibronectin etc.) have illustrated substantial improvement in neuronal adhesion. A tighter neuron-electrode coupling subsequently results in enhancement in cell growth, differentiation and proliferation, which in turn promotes extra- and intracellular activity of the neuronal network [1]. Despite the immense beneficial effects of the natural nanostructures, they suffer from two major disadvantages. Firstly, the hydrocarbon composition of the biomolecules amplifies the impedance at the junction between the neuron and microelectrode, which reduces the signal-to-noise ratio of the extracellular recordings [2]. Secondly the natural biomolecules are vulnerable to denaturation in extreme conditions (such as temperature and pH) and at the same time cannot easily be replicated. Micro- and nanostructuring of the microelectrode surface with durable materials (such as metals and ceramics) is a widely used method to replicate the natural nanorough interface of the basement membrane. Therefore, in this study we present a nanostructure fabrication process for microelectrodes mimicking the random structural features of collagen fiber network with nanoimprint lithography and gold electroplating [3]. We then evaluated the neuron adhesion with seal impedance measurements at 1 kHz frequency and neuron-glia cell growth with appropriate neuronal and glial markers (Chicken-anti-PGP9.5 for neurons and Rabbit-anti-S100 β for glial cells).

Nanostructured microelectrodes were fabricated on glass wafers with evaporated gold as the electrode layer. Bovine Achilles tendon collagen type I spin-coated on a silicon wafer was used as the master stamp for nanoimprint lithography (see figure 1a). Neurons from myenteric plexus of post-natal mice were used for evaluation of growth and adhesion on nanostructured surfaces. The proposed process line enables the reproducible fabrication of biomimetic nanostructures on microelectrodes surfaces. SEM analysis show that the longitudinal dimension of these collagen-like gold fibers range between 100 nm and 3 μ m (see Figure 1b), while the lateral dimension is approximately 50 nm. Adhesion analysis with seal impedance calculations illustrated a tighter coupling of the neurons to the nanostructures, when compared to unstructured microelectrodes (see figure 2a). Immunofluorescence analysis showed significant improvement in cell growth on nanostructured gold in comparison to unstructured gold surfaces for both neurons and glial cells (see figure 2b and 2c). Enhanced neuron coupling with nanostructures would definitely suggest robust action potential signal transmission within the neuron network, which could be measured in future experiments with extracellular recordings or intracellular activity with patch clamp methods.

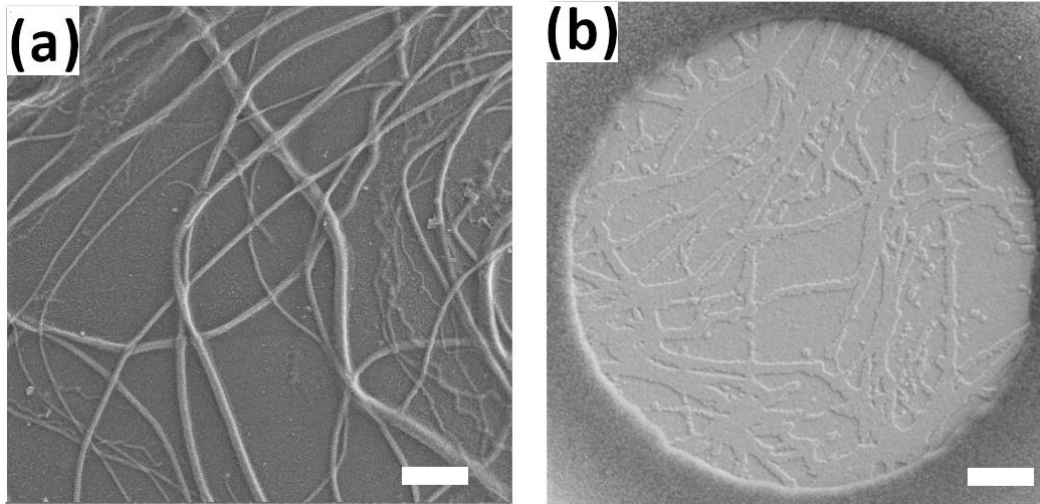


Figure 1: SEM images of (a) collagen fibers coated on silicon wafer, which was used as the stamp for nanoimprint lithography process and (b) microelectrode structured with collagen-like gold nanostructures. (inset scale bars: 2 μm).

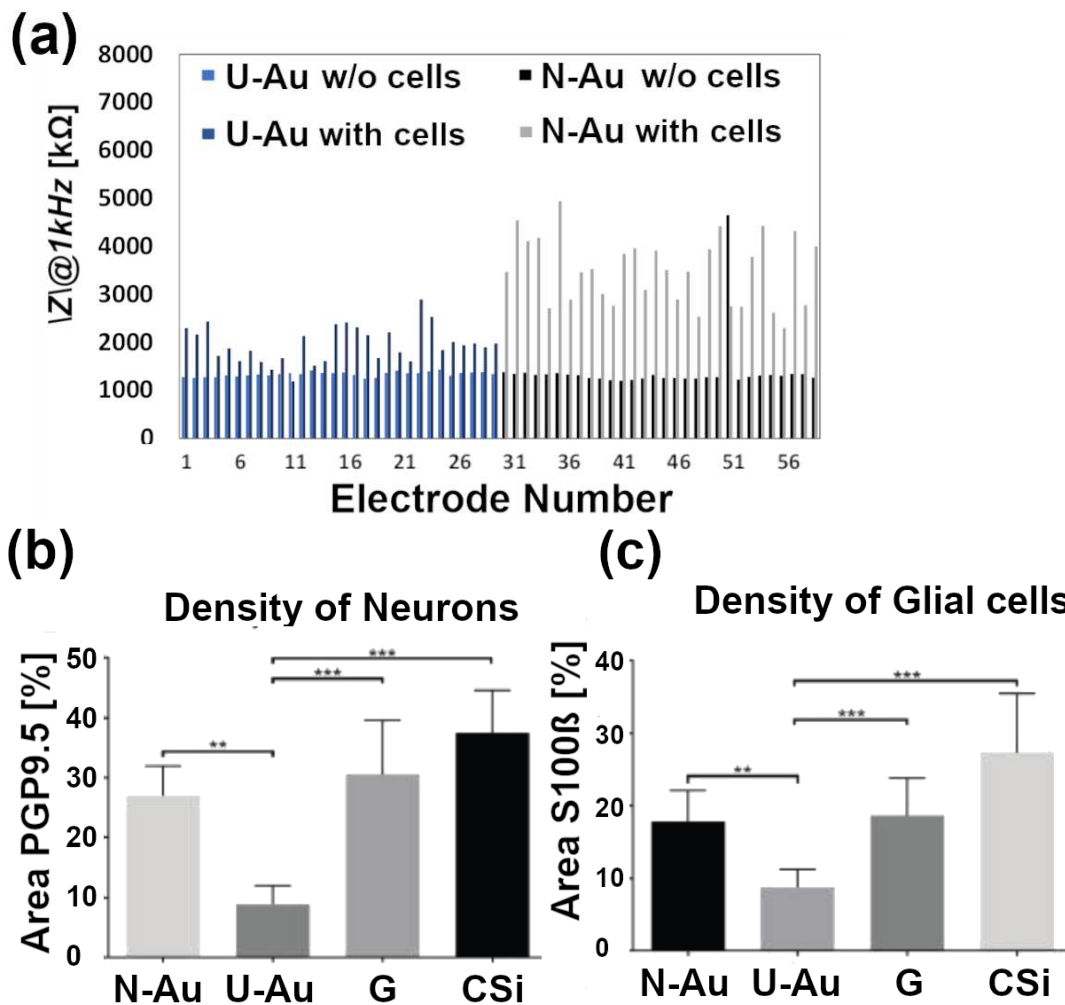


Figure 2: (a) Seal impedance measurements of collagen-like gold nanostructured electrodes N-Au and unstructured electrodes U-Au at 1 kHz frequency with and without enteric neurons cultured on the surface. (b) PGP9.5 and (c) S100β signal to whole picture area as a measure of the amount of neuronal and glial cells on nanostructured surfaces N-Au, unstructured surfaces U-Au, glass G and collagen coated silicon CSi.

1. Sheng, L., Leshchyns'ka, I. and Sytnyk, V. (2013). Cell adhesion and intracellular calcium signaling in neurons. *Cellular communications and signaling* 11, 94. doi:10.1186/1478-811X-11-94.
2. Decker, D., Hempelmann, R., Natter, H., Pirrung, M., Rabe, H., Schäfer, K. H., Saumer, M. (2019). 3D Nanostructured Multielectrode Arrays: Fabrication, Electrochemical Characterization, and Evaluation of Cell–Electrode Adhesion. *Advanced Materials Technologies* 4, 1800436. doi:10.1002/admt.201800436
3. Nowduri, B., Schulte, S., Decker, D., Schäfer, K.-H., Saumer, M. (2020). Biomimetic Nanostructures Fabricated by Nanoimprint Lithography for Improved Cell-Coupling. *Advanced Functional Materials* 30, 2004227. doi:10.1002/adfm.202004227.

Towards biohybrid brain stimulation using unidirectional PDMS based axon guidance structures

T. Ruff^a, L. Sifringer^a, S.J. Ihle^a, S. Steffens^a, T. Delipinar^a, A. Beltraminelli^a, J. Duru^a, T. Zhang^a, E. Ceylan^a, S. Weaver^a, S. Girardin^a, B. Clément^a, S. Madduri^c, B. Roska, J. Vörös^{b,*}

- a. Laboratory of Biosensors and Bioelectronics, ETH Zurich, Institute for Biomedical Engineering, Switzerland
 - b. Institute of Molecular and Clinical Ophthalmology Basel, Switzerland
 - c. Center for Bioengineering and Regenerative Medicine, University of Basel, Switzerland
- * janos.voros@biomed.ee.ethz.ch

Current deep brain stimulation electrodes have a very limited spatial resolution which limits their application for targeted single neuron stimulation. To overcome this limitation, we propose a living biohybrid electrode in which we exploit real neurons as relays to transmit information from a stretchable microelectrode array (MEA [1]) to a neuronal target structure. Our goal is to develop a biohybrid implant that enables single neuron synaptic stimulation of neuronal target structures such as the dLGN for the specific application of vision restoration.

To achieve this goal we are establishing a PDMS microstructure based *in vitro* co-culture system mounted on conventional glass MEAs in which we can seed embryonic rat retinal and thalamus spheroids at defined locations within the PDMS microstructure and guide the axons unidirectionally [2] across electrodes through few μm sized channels towards the target. We optimize the design for reliable unidirectional multichannel stimulation of the target tissue.

We show that retinal neurons grow several mm long axons within the PDMS axon guidance structures to innervate the thalamic target spheroids. We compare how different structural elements enhance unidirectional axon merging, growth speed, channel crosstalk and efficiency to stimulate thalamic target structures.

References

1. Renz, A., Lee, J., Tybrandt, K., Brzezinski, M., Lorenzo, D.A., Cheraka, M.C., Lee, J., Helmchen, F., Vörös, J., Lewis, C.M. (2020). Opto-E-Dura: A Soft, Stretchable ECoG Array for Multimodal, Multiscale Neuroscience. *Adv. Healthc. Mater.* 2000814, 1–11
2. Forró, C., Thompson-Steckel, G., Weaver, S., Weydert, S., Ihle, S., Dermutz, H., Aebersold, M.J., Pilz R., Demkó, L., Vörös, J. (2018) Modular microstructure design to build neural structures with defined functional connectivity. *Biosensors and Bioelectronics*, 10.1016, 75-78

Compartmentalization of neural networks on CMOS MEAs using PDMS microstructures

Jens Duru^a, Joël Küchler^a, Stephan J. Ihle^a, Csaba Forró^b, Aeneas Bernardi^a, Sophie Girardin^a, Benedikt Maurer^a, Julian Hengsteler^a, Robert John^a, János Vörös^a, Tobias Ruff^{a,*}

- a. Laboratory of Biosensors and Bioelectronics, Institute for Biomedical Engineering, ETH Zürich, 8092 Zürich, Switzerland
- b. Stanford University, Cui Laboratory, 290 Jane Stanford Way, Stanford, CA, USA

*Correspondence: toruff@ethz.ch

How ensembles of neurons, like those found in the brain, process and store information remains an unsolved question. Despite a vast amount of technical possibilities, we still have a very poor understanding of such fundamental neuroscience concepts, mainly due to the high complexity of the brain, which renders the isolation of functional circuits *in vivo* impossible.

In order to further progress in neuroscience, we require a new approach, in which functional circuits of only a few neurons and their connections are assembled *in vitro*, providing a platform with highly reduced complexity. In this approach, termed “bottom-up neuroscience”, we make use of polydimethylsiloxane (PDMS) microstructures that confine and direct the growth of neurons and neurites¹. These 200 μm high PDMS microstructures are manufactured externally using a soft-lithography process and were previously implemented with high success on low-density 60-channel glass MEAs with an electrode pitch of 500 μm ^{2,3}. We have developed a method to transfer this technology to complementary metal-oxide-semiconductor (CMOS) MEAs, that provide up to 26,400 microelectrodes with an electrode pitch of only 17.5 μm ⁴. The non-planar surface of the CMOS MEAs required a finely-tuned gluing step in order to seal the microstructure on the chip surface without impairing the guidance capacity of the PDMS microstructures⁵.

We show that we can maintain engineered neural networks of primary rat neurons on CMOS MEAs for several weeks *in vitro*. We can record from the network from both axonal as well as somatic locations across the whole extent of the microstructure. Furthermore, we are able to track the propagation of action potentials within the microstructure with high spatio-temporal resolution.

Having electrical access to the network at a (sub-)cellular level will enable to study the input-output relationship of such engineered neural networks with unprecedented levels of detail.

References

1. Forró et al. (2018). *Modular microstructure design to build neuronal networks of defined functional connectivity*. Biosensors and Bioelectronics, 122, 75–87.
2. Ihle et al. (2021). *An experimental paradigm to investigate stimulation dependent activity in topologically constrained neuronal networks*. Biosensors and Bioelectronics 201: 113896
3. Girardin et al. (2022). *Topologically controlled circuits of human iPSC-derived neurons for electrophysiology recordings*. Lab Chip, 2022, Advance Article
4. Müller et al. (2015). *High-resolution CMOS MEA platform to study neurons at subcellular, cellular, and network levels*. Lab Chip, 15, 2767-2780.3
5. Duru et al. (2022). *Engineered Biological Neural Networks on High Density CMOS Microelectrode Arrays*. Front. Neurosci. 16:829884

Long-term monitoring of morphological and functional properties in enteric neuronal networks *in vitro* using a novel upside-down microelectrode array approach

Steven Schulte^a, Manuela Gries^a, Anne Christmann^a, Dominique Decker^a, Bharat Nowduri^a, Monika Saumer^a, Karl-Herbert Schäfer^{a,b,*}

- a. Department of Informatics and Microsystems and Technology, University of Applied Science Kaiserslautern, 66482 Zweibrücken, Germany.
- b. Department of Pediatric Surgery, Medical Faculty Mannheim, University of Heidelberg, 68167 Mannheim, Germany.

* karlherbert.schaefer@hs-kl.de

Understanding the function of the nervous system and its pathophysiology largely involves comprehending the interplay of its components in the light of its electrogenic properties. To investigate spontaneous neuronal activity or the effect of pharmaceutical substances onto neural networks, the microelectrode array (MEA) technique stands out providing a way of non-destructive analysis of spontaneous and evoked neuronal activity, combined with high spatiotemporal resolution [1] and the possibility to implement long-term recordings [2]. MEA recordings aim to detect changes in the extracellular field potential and hence can be used to examine the electrical activity of neural tissue and to model neurological diseases *in vitro* [3].

However, isolated primary neurons need time to rebuild a network and restore their set of receptors after being seeded, thus delaying the onset of measurements for up to weeks. Moreover, the insulator material of the MEA is continuously etched when being exposed to the culture medium [4], thus the overall recording time is limited. To overcome these restrictions, we developed an alternative approach in cultivating cells on glass samples with photolithographically fabricated distance holders, allowing to measure them upside-down on the MEAs in an acute mode (see figure 1). By applying small weights, cell-to-electrode contact can be enhanced (see figure 2). In addition, to record the impact of chemicals of interest onto electrical activity in long-term experiments, we developed an appropriate microfluidic system for constant exchange of culture medium. The recorded signals differ from the signals obtained from conventional cultures but allow reproducible measurements.

Culturing isolated cells of murine myenteric plexus upside-down, i.e., under the influence of gravity and hypoxic conditions, also alters growth and behavior of these cells (see figure 3), especially regarding geometry and lifespan of the culture. The number of dead cells during the culture was significantly decreased and the neural networks were less impaired by oxidative stress. The architecture of upside-down cultures showed higher resemblance to the structure of the murine myenteric plexus *in vivo*, while conserving electrical activity.

Overall, our results indicate that the upside-down approach not only offers an effective way of enhancing electrophysiological measurements but may also be regarded as a new model for culturing and studying the enteric nervous system. This would not only allow to investigate the impact of neurological diseases *in vitro* but could also offer insights into growth and development of the enteric nervous system under conditions much closer to the *in vivo* environment.

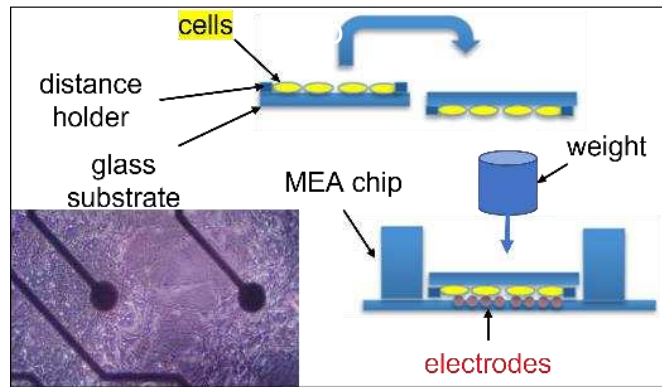


Figure 1: Schematic illustration of upside-down recording of cells grown on glass substrates with distance holders.

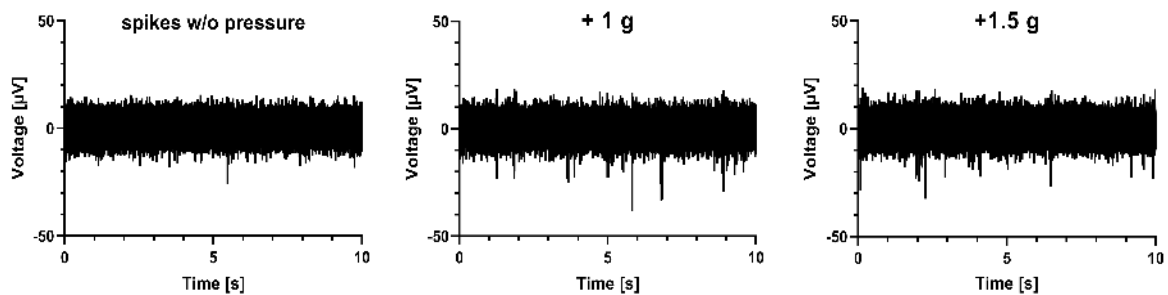


Figure 2: Upside-down MEA recordings without weights vs. increasingly higher amounts. Frequency and amplitude increase adding 1 g and are reduced again with 1.5 g of weight.

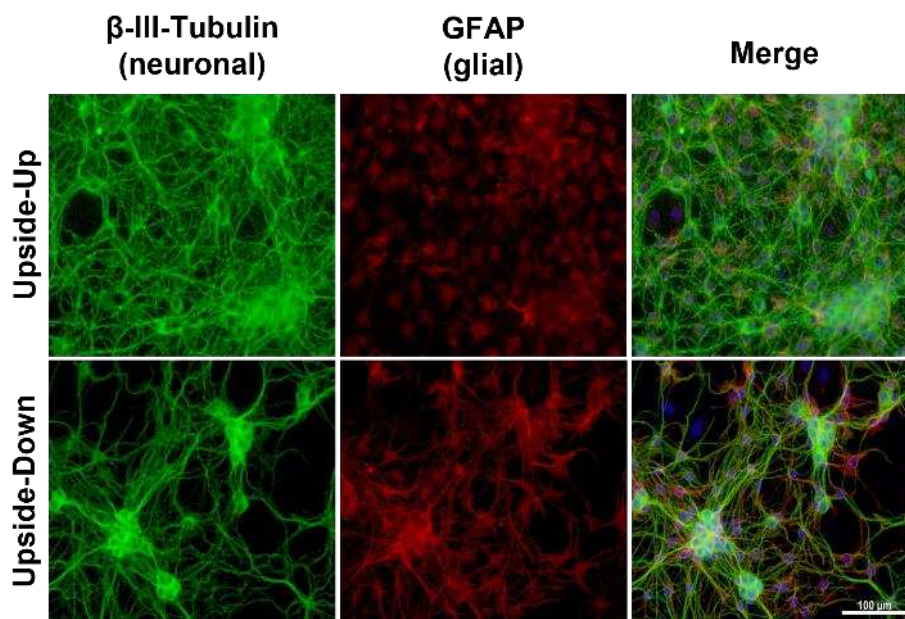


Figure 3: Immunocytochemical staining of myenteric cultures on glass substrates with distance holders (10 μ m), grown Upside-Up vs. Upside-Down after 7 days in vitro, neuronal (β -III-Tubulin, green) and glial structures (GFAP, red) plus Merge (cell nuclei in blue (DAPI)). Magnification 200x, scale bar 100 μ m.

References

1. Ness T V, Chintaluri C, Potworowski J, et al. Modelling and Analysis of Electrical Potentials Recorded in Microelectrode Arrays (MEAs). *Neuroinformatics*. 2015; 13:403–426. <https://doi.org/10.1007/s12021-015-9265-6>

2. Killian NJ, Vernekar VN, Potter SM, Vukasinovic J. A device for long-term perfusion, imaging, and electrical interfacing of brain tissue in vitro. *Front Neurosci.* 2016; 10:1–14. <https://doi.org/10.3389/fnins.2016.00135>
3. Jones IL, Livi P, Lewandowska MK, et al. The potential of microelectrode arrays and microelectronics for biomedical research and diagnostics. *Anal Bioanal Chem.* 2011; 399:2313–2329. <https://doi.org/10.1007/s00216-010-3968-1>
4. G. Schmitt, J.-W. Schultze, F. Faßbender, G. Buß, H. Lüth, M.J. Schöning, “Passivation and corrosion of microelectrode arrays,” *Electrochimica Acta*, Vol. 44, No. 21-22, 1999, pp. 3865-3883. [https://doi.org/10.1016/S0013-4686\(99\)00094-8](https://doi.org/10.1016/S0013-4686(99)00094-8)

Improving the lifetime of the silicon nitride insulator layer in microelectrode arrays

Tomi Ryyänen^{a,b,*}, Antti Karttu^a, Timo Salpavaara^a, Lotta Mäkinen^a, Anna-Mari Moilanen^a, Susanna Narkilahti^a, Pasi Kallio^a

a. Faculty of Medicine and Health Technology, Tampere University, Finland

b. Tampere Institute for Advanced Study, Tampere University, Finland

* tomi.ryynanen@tuni.fi

Throughout the history of the *in vitro* microelectrode arrays (MEAs), silicon nitride (SiN) has been maybe the most common insulator layer material in MEAs, utilized both in commercial products and in-house made MEAs by the academic groups. Motivation for using SiN has mainly been that it is a well-known insulator from integrated circuit industry. Moreover, most of the microfabrication facilities have a plasma-enhanced chemical vapor deposition (PECVD) system needed for the easy fabrication of the SiN thin films, as well as reactive ion etchers (RIE) needed to etch the electrode openings. However, long-term stability of the insulator layer has been a known, but often ignored issue already since the early days of MEAs [1]. As many cell experiments last only a few hours or days, plenty of experiments have been performed successfully. However, some cell experiments may last several weeks or months, and even until a year. Especially in those cases, there is a severe risk that the insulator layer corrodes by the cell culture medium, the cells, or the cleaning procedures between the reuses of MEAs. The corrosion has been reported both for MEAs from a leading commercial manufacturer [2-4], in-house made MEAs [3], and also in general MEA insulator studies [5]. The factors affecting the corrosion rate have been speculated to be related e.g. to the stress [5] or the hydrogen content [6] in the SiN thin film. Even if some manufacturers say their MEAs to last certain number of reuses, it is just a rough generalization, not applicable for all type of experiments. Especially, if the same MEA has been reused several times in long term experiments with aggressive medium, it is possible that the insulator layer disappears even completely earlier than the promised microelectrode life-time. After that, one cannot know anymore whether the measured signal comes from the electrode or from the revealed tracks. The corrosion, already in partial form, will, naturally, also affect the signal amplitudes and the noise levels [3] as the parasitic capacitance between the tracks and medium changes. These all may lead to lost signal details and wrong interpretation of the recorded data.

We have studied how different PECVD deposition parameters affect the cell culture medium tolerance of the SiN insulator layer, and also how the corrosion rate differs between various cell culture media. The results suggest that the default recipe used for the SiN deposition in a microfabrication lab may not necessarily be the optimal one for the MEA use. For example, increasing the deposition temperature, ammonia concentration, or post-annealing the thin film improves SiN layer's corrosion resistance significantly (Figure 1). With badly chosen deposition parameters, the typical 500 nm SiN layer may be completely lost already after less than two weeks' exposure for a medium. As another solution, we propose a method to reduce the SiN corrosion rate to a practically negligible level by a thin protective coating [4]. On the other hand, our studies confirmed also huge differences in how aggressively different cell culture media or the common model medium, DPBS, corrode the SiN layer. Thus, the corrosion rate may be reduced not only by improved engineering but also by the medium selections made by the biologists.

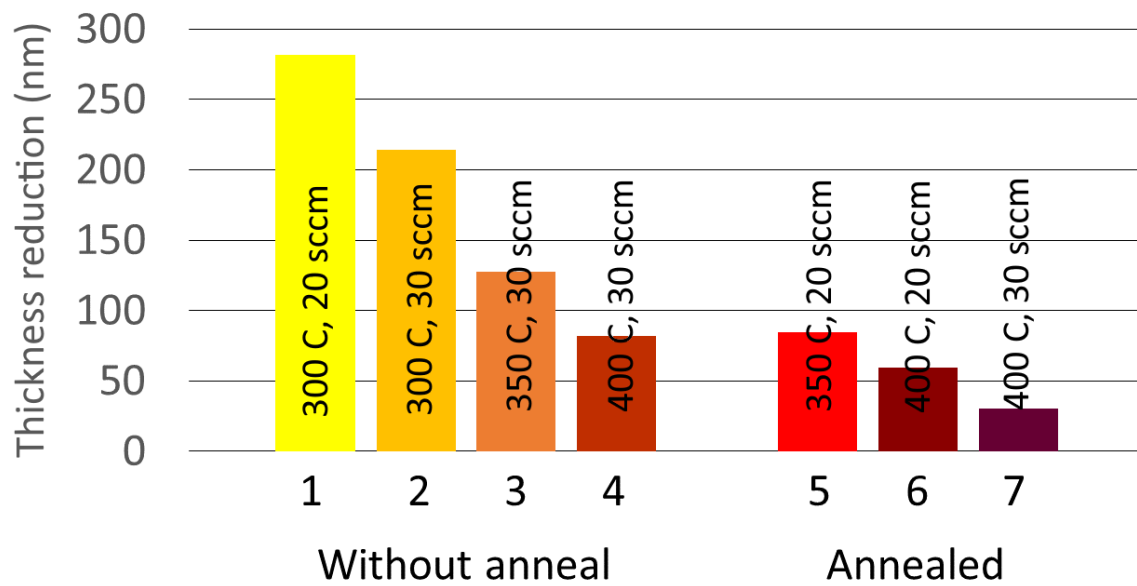


Figure 1: Thickness reduction of the SiN insulation layers after 8 days in a commercial cell culture medium. Deposition temperatures and ammonia concentrations are shown in the bars. The annealing temperature was 450 deg C.

References

1. Thomas, C. A., Springer, P. A., Loeb, G. E., Berwald-Netter, Y., and Okun, L. M. (1972). A miniature microelectrode array to monitor the bioelectric activity of cultured cells. *Experimental Cell Research* 74, 61–66. doi:10.1016/0014-4827(72)90481-8.
2. Wagenaar, D. A., Pine, J., and Potter, S. M. (2004). Effective parameters for stimulation of dissociated cultures using multi-electrode arrays. *J. Neurosci. Methods* 138, 27–37. doi: 10.1016/j.jneumeth.2004.03.005.
3. Ryyänen, T., Toivanen, M., Salminen, T., Ylä-Outinen, L., Narkilahti, S., and Lekkala, J. (2018). Ion Beam Assisted E-Beam Deposited TiN Microelectrodes—Applied to Neuronal Cell Culture Medium Evaluation. *Front. Neurosci.* 12:882. doi: 10.3389/fnins.2018.00882.
4. Karttu, A., et al. (2022). Corrosion and protection of silicon nitride insulators with microelectrode arrays in cell applications. Submitted.
5. Schmitt, G., Schultze, J.W., Faßbender, F., Buß, G., Lüth, H., and Schöning, M.J. (2000). Passivation and corrosion of microelectrode arrays. *Materials and Corrosion* 51, 20. doi: 10.1002/(SICI)1521-4176(200001)51:1<20::AID-MACO20>3.0.CO;2-Q.
6. Chow, R., Langford, W.A., KeMing, W., and Rosler, R.S. (1982). Hydrogen content of a variety of plasmadeposited silicon nitrides. *J. Appl. Phys.* 53, 5630–5633. doi: 10.1063/1.331445.

Fabrication of whole-surface-nanostructured MEAs to improve neuronal signal recording

Dominique Decker, Bharat Nowduri, Steven Schulte, Karl-Herbert Schäfer, Monika Saumer*

Department of Informatics and Microsystem Technology, Kaiserslautern University of Applied Sciences, Amerikastraße 1, 66482 Zweibrücken, Germany

* monika.saumer@hs-kl.de

Micro- or nanostructuring of electrodes is a promising and often successful approach to improve the recording capabilities of multielectrode arrays. Besides of decreasing the input impedance and therefore diminishing the thermal noise of the electrodes, a further important aspect of improving the signal-to-noise ratio correlates with cell adhesion. The closer the cells attaches to the surfaces of the electrodes, the smaller are the signal losses through the culture medium. In our previous work we already demonstrated that the type of nanostructure localized on the electrode plays a significant role regarding tight or loose adhesion of the investigated cells [1]. We also showed that collagen-like gold nanostructures promote the growth of myenteric neurons compared to unstructured gold electrodes [2]. Moreover, by using impedance measurements we were able to estimate an increase in cell adhesion by a factor of four. In general, only a set of electrodes within the array shows significant signal. In order to increase the number of active electrodes during signal recordings, a dense and tightly attached cell network has to be established on the whole surface of the MEA chip. By solely structuring the sensing electrodes, only approx. 1 % of the total chip area contributes to an improved cell attachment, leaving 99 % of the chip area unchanged and thus not increasing the cell adhesion. To obtain an overall improvement of cell adhesion, the nanostructures should cover the chip area completely. Therefore, the current work presents a technique to fabricate whole-surface-nanostructured MEA chips based on collagen nanostructures, fabricated with a novel two-stage nanoimprint lithography process to mimic the topography of the collagen. The collagen structures are copied into a polymer foil, followed by structuring the insulation layer, using the polymer foil as a template. This process results in collagen nanostructures with the same orientation as the original (see figure 1). Scanning electron microscopy as well as impedance measurements are used to monitor the quality of the fabrication process. Signal recordings with myenteric neurons will be performed to compare the number of active electrodes and the recorded signals of whole-surface-nanostructured chips and electrode-only-nanostructured chips to reveal a possible improvement in cell adhesion. In future, also further components of the extracellular matrix could be transferred to the MEA surface in order to investigate the individual influence of these structure geometries in comparison to their biological counterparts. The technology presented might result in a reproducible and durable ECM-like layer which does not limit signal transfer and that might lead to a complete replacement of the highly variable ECM coatings prior to cell seeding.

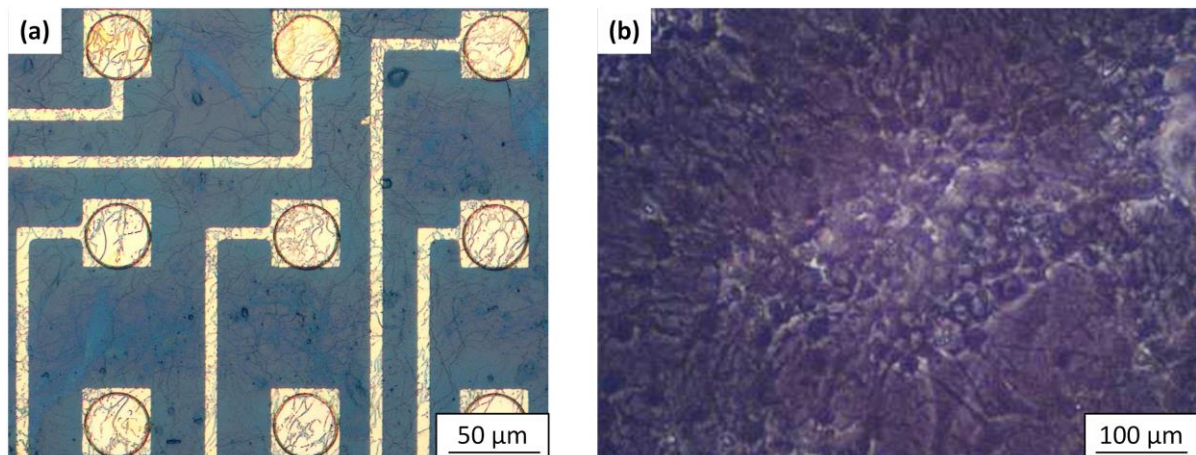


Figure 1: Microscope pictures showing (a) nanostructured electrodes embedded in nanostructured insulator and (b) a network of myenteric neurons cultured on nanostructured insulation after five days in vitro.

References

1. Decker, D., Hempelmann, R., Natter, H., Pirrung, M., Rabe, H., Schäfer, K.-H., Saumer, M. (2019). 3D Nanostructured Multielectrode Arrays: Fabrication, Electrochemical Characterization, and Evaluation of Cell–Electrode Adhesion. *Advanced Materials Technologies* 4,1800436. doi:10.1002/admt.201800436.
2. Nowduri, B., Schulte, S., Decker, D., Schäfer, K.-H., Saumer, M. (2020). Biomimetic Nanostructures Fabricated by Nanoimprint Lithography for Improved Cell-Coupling. *Advanced Functional Materials* 30, 2004227. doi:10.1002/adfm.202004227.

Current response of ferroelectric microelectrodes to sinusoidal voltage signals

Maximilian T. Becker ^{a,*}

- a. Department of Materials Science & Metallurgy, University of Cambridge, 27 Charles Babbage Road, CB3 0FS Cambridge, United Kingdom

* mtb57@cam.ac.uk

The concept of ferroelectric microelectrodes [1] is introduced by analyzing the extracellular stimulation current of microelectrodes coated with an insulating layer to prevent toxic electrochemical effects in bioelectronic applications. It is shown for a microelectrode coated with an insulating ferroelectric layer that the ferroelectric polarization current contributes to the extracellular stimulation current. Depending on the remanent polarization of the ferroelectric, the charge injection capacity (CIC) of ferroelectric microelectrodes can be increased by up to two orders of magnitude as compared to the commonly used extracellular capacitive stimulation [2] with microelectrodes that are coated with a dielectric layer. Here, we simulated the stimulation current and the CIC of a ferroelectric microelectrode based on $\text{Hf}_{0.5}\text{Zr}_{0.5}\text{O}_2$ in response to sinusoidal voltage signals. We then compared our results to the capacitive stimulation current and the CIC provided by microelectrodes based on dielectric $\text{TiO}_2/\text{ZrO}_2$ [3] and conductive TiN [4], which have been recently utilized for sinusoidal stimulation of retinal neurons with state-of-the-art complementary metal-oxide semiconductor (CMOS) microelectrode arrays. Moreover, a comparison is made to recent experimental results on the current response of ferroelectric BaTiO_3 thin films in electrolyte—ferroelectric—semiconductor (EFS) configuration for ferroelectric microelectrode applications [5]. The concept of ferroelectric microelectrodes solves the long-standing problem of low CIC provided by insulated microelectrodes and represents a first step towards future neuroprosthetic devices based on ferroelectric--neural interfaces.

References

1. Becker, M. T. (2021). Charge injection capacity of ferroelectric microelectrodes for bioelectronic applications. *AIP Advances* 11, 065106. doi: 10.1063/5.0049202
2. Fromherz, P., and Stett, A. (1995). Silicon-Neuron Junction: Capacitive Stimulation of an Individual Neuron on a Silicon Chip. *Phys. Rev. Lett.* 75, 1670 – 1673. doi: 10.1103/PhysRevLett.75.1670
3. Bertotti, G. *et al.*, (2014). A CMOS-based sensor array for in-vitro neural tissue interfacing with 4225 recording sites and 1024 stimulation sites. 2014 IEEE Biomedical Circuits and Systems Conference (BioCAS) Proceedings, 304-307. doi: 10.1109/BioCAS.2014.6981723.
4. Corna, A., Ramesh, P., Jetter, F., Lee, M.-J., Macke, J. H., and Zeck, G. (2021). Discrimination of simple objects decoded from the output of retinal ganglion cells upon sinusoidal electrical stimulation. *J. Neural Eng.* 18, 046086. doi: 10.1088/1741-2552/ac0679
5. Becker, M. T., Oldroyd, P., Strkalj, N., Müller, M. L., Malliaras, G. G., and Driscoll, J. L. (2022). Ferroelectricity and resistive switching in BaTiO_3 thin films with liquid electrolyte top contact for bioelectronic devices. *unpublished*

Fabrication and functionalization of selective laser etched microfluidic devices

Markus Pribyl^a, Philipp Taus^a, Sonia Prado-López^a, Heinz D. Wanzelboeck^{a,*}

a. Institute of Solid State Electronics, TU Wien, Gusshausstrasse 25a, 1040 Wien, Austria

* heinz.wanzelboeck@tuwien.ac.at

Microelectrode arrays have been in use for many years for different applications including bioelectronic measurements such as the recording of action potentials [1] or recording of bioimpedance signals [2]. The signals can be derived directly from different biological cells, e.g. neurons, muscle cells, cardiac muscle cells, or from the impedance of non-electrically active cells. The electrical signals can provide insight about the signal propagation along neuronal fibers, the electrical potential of single cells or can be used for bioimpedance tomography [3]. To record a signal with a low noise level different conditions, need to be controlled, like the medium, the shape and material of the MEA electrodes, the signal processing and the fixation of the cell on the MEA [4]. It has been shown that, suction pores can be utilized to provide a better contact between the cells and the MEA [5]. These MEA devices have been in production for many years; e.g. the Beta-Screen-System © from Multi Channel Systems GmbH, Germany, or the Port-a-Patch © system from Nanion Technologies GmbH, Germany to name a few. These systems mostly employ functionalized membranes with integrated pores, and therefore are relatively fragile.

Here, we present a novel and flexible fabrication process where a glass microfluidic chip and a MEA are combined (see Figure 1a). The microfluidic chip has been fabricated from fused silica which was etched with a Selective Laser Etching (SLE) process. The substrates were procured from an external source. This technique allows for the fabrication of transparent substrates. In addition, the SLE fabrication process is flexible to accommodate different designs, e.g. membranes, single pores, open or closed microfluidic channels (see Figure 1b). Closed microfluidic channels can be used for fixation of cells or microtissue samples through suction, drug delivery to the samples, or collection of metabolites for further analysis. The microfluidic substrates were patterned with Au leads and passivated with a SiN layer to generate a functional MEA for recordings. We will discuss the fabrication process of the SLE-MEA system, the potential and shortcoming of the fixation of cells and bioelectronic measurements.

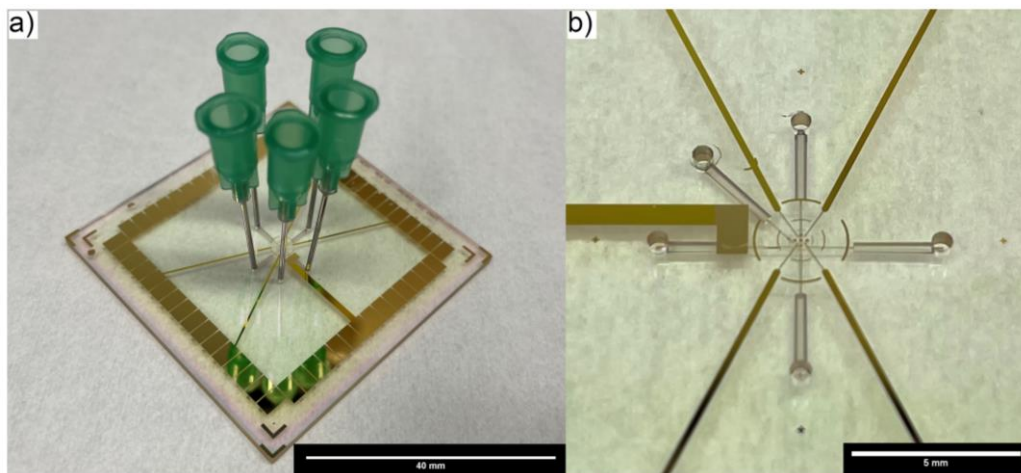


Figure 1: A selective laser etched microfluidic substrate is depicted. a) The MEA chip with cannula interconnects for low pressure connections are shown. b) A detail of the microfluidic ports and the MEA leads are depicted.

References

1. M. E. Spira and A. Hai, "Multi-electrode array technologies for neuroscience and cardiology," *Nat. Nanotechnol.*, vol. 8, no. 2, pp. 83–94, Feb. 2013, doi: 10.1038/nnano.2012.265.
2. Tissue characterization by impedance: a multifrequency approach. Rigaud B, Hamzaoui L, Chauveau N, Granié M, Scotto Di Rinaldi JP, Morucci JP. *Physiol Meas.* 1994 May;15 Suppl 2a:A13-20. doi: 10.1088/0967-3334/15/2a/002.
3. D. J. Bakkum et al., "Tracking axonal action potential propagation on a high-density microelectrode array across hundreds of sites," *Nat. Commun.*, vol. 4, no. 1, p. 2181, Oct. 2013, doi: 10.1038/ncomms3181.
4. M. E. J. Obien, K. Deligkaris, T. Bullmann, D. J. Bakkum, and U. Frey, "Revealing neuronal function through microelectrode array recordings," *Front. Neurosci.*, vol. 8, Jan. 2015, doi: 10.3389/fnins.2014.00423.
5. J. M. Nagarah, A. Stowasser, R. L. Parker, H. Asari, and D. A. Wagenaar, "Optically transparent multi-suction electrode arrays," *Front. Neurosci.*, vol. 9, Oct. 2015, doi: 10.3389/fnins.2015.00384.

Direct LCD-3D printing onto MEA substrates

Philipp Taus^a, Julia Linert^b, Markus Pribyl^a, Sonia Prado-López^a, Michael J. Haslinger^c, Michael Mühlberger^c, Elena Guillén^c, Heinz D. Wanzenboeck^{a*}

- a. Institute of Solid State Electronics, TU Wien, Gusshausstrasse 25a A-1040 Vienna
 - b. Institute of Applied Physics, TU Wien, Wiedner Hauptstrasse 8-10 A-1040 Vienna
 - c. PROFACTOR GmbH, Im Stadtgut D1 A-4407 Steyr-Gleink
- * heinz.wanzenboeck@tuwien.ac.at

Microfluidic systems and chips bridge the gap of the biological micro world to our accessible macro world, creating the interface between e.g. an organoid on a chip to the reservoirs and pumps. Prototype and low volume lab scale microfluidic devices have traditionally been realized by soft lithography [1]. While this process allows for quick adaptation and customization, offers high-fidelity replication of the mould, it is also a highly manual process. Furthermore, it is mostly limited to 2D and 2.5D structures due to the required demoulding step. This work demonstrates directly 3D printing microfluidic structures onto a microstructured Micro Electrode Array glass substrate. Recently rapid prototyping of microfluidic devices using direct 3D printing has become widely available [2]. Inexpensive desktop-sized tools allow to 3D print microfluidic components [3]. Usually the 3D printed parts are either stand-alone systems requiring only fluidic connections, or they need to be attached to a rigid chip encompassing further analysis and processing capabilities, after printing. The attachment of a finished 3D printed part to a rigid surface is possible [4], but requires a manual alignment and handling step, or expensive automation.

We demonstrate a process for direct printing of microfluidic attachments onto inhouse fabricated multi electrode arrays. (borosilicate glass substrate 263Teco, with sputtered gold electrodes defined by a lift-off process using the Merck AZ 5214 e image reversal resist). The process uses a desktop-sized LCD resin printer (Photon mono X, Anycubic) and commercially easily available resins (Color mix basic, 3DJake and Aqua resin 4K grey, Phrozen) to directly print onto an adhesion modified substrate.

The process uses a fixed frame build-plate for medium accuracy alignment of prints onto the substrate, allowing for quick and easy prototyping of sub-mm aligned prints to the substrate. Furthermore, we will report on biocompatibility of the used commercial resin obtained from fibroblast culturing on fully UV light cured dummy prints.

The process shows sub-mm printing of grooves (Figure 1 Top) without additional modifications of the STL file. By employing different printing settings, we will also show, that higher resolution prints are achievable down to 200 µm channel width. We also show a functional liquid tight print onto a MEA featuring sub-mm channels (Figure 1 Bottom).

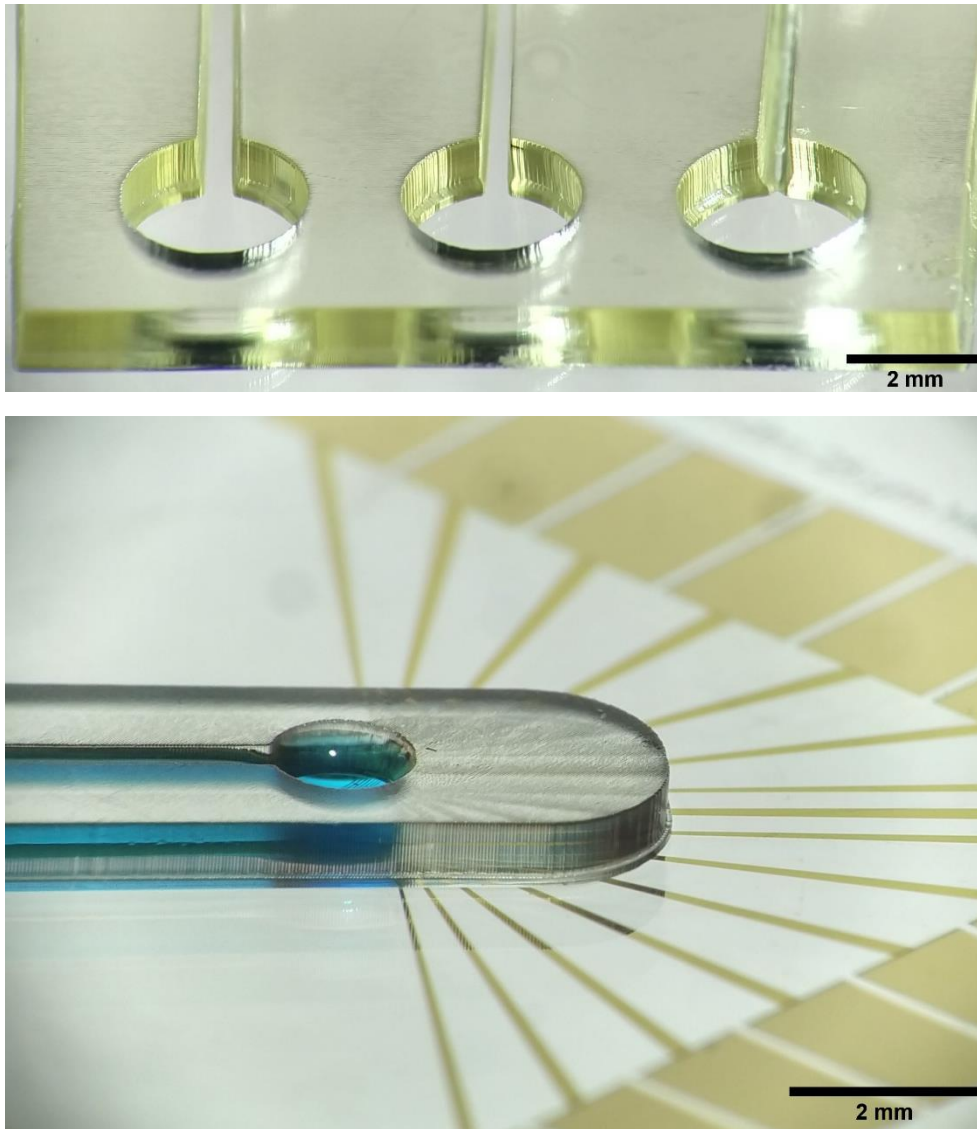


Figure 1: Top: Resolution test of directly on glass printed open microfluidic channels from nominal width left to right: 500 μm , 400 μm , 300 μm . We will demonstrate strategies to extend the possible fully open channel widths down to 200 μm . Bottom: Microfluidic channel printed onto inhouse fabricated MEA. The large rectangles around the perimeter are the contact pads, the 20x20 μm gold recording electrodes are situated below the fluidic channel.

References

1. Qin, D. et al., Soft Lithography for Micro- and Nanoscale Patterning. Nat Protoc 2010, 5, 491–502.
2. Bhattacharjee, N et al., The Upcoming 3D-Printing Revolution in Microfluidics. Lab Chip 2016, 16, 1720–1742.
3. Pagac, M., et al.,. A Review of Vat Photopolymerization Technology: Materials, Applications, Challenges, and Future Trends of 3D Printing. Polymers 2021, 13, 598.
4. Kecili, S.; Tekin, H.C. Adhesive Bonding Strategies to Fabricate High-Strength and Transparent 3D Printed Microfluidic Device. Biomicrofluidics 2020, 14, 024113

Pyrolytic and selectively passivated 3D carbon pillar electrodes on interdigitated fingers for local stimulation

Rasmus Schmidt Davidsen,* ^{a,b} Pratik Kusumanchi ^a, Babak Rezaei ^a, Stephan S. Keller ^a

a. DTU Nanolab, Technical University of Denmark

b. Department of Electrical and Computer Engineering, Aarhus University

* rasda@dtu.dk

We present a novel approach for selective passivation of three-dimensional pyrolytic carbon microelectrodes via electrochemical polymerization of a non-conductive polymer (polydopamine, PDA) onto the surface of carbon electrodes, followed by a selective laser ablation. First, 284 micropillars on a circular 2D carbon base layer were fabricated [1] by pyrolysis of lithographically patterned negative photoresist SU-8 [2,3]. As a second step, dopamine was electropolymerized onto the electrode by cyclic voltammetry (CV) to provide an insulating layer at its surface. The CV parameters, such as the scan rate and the number of cycles, were investigated and optimized to achieve a reliable and uniform non-conductive coating on the surface of the 3D pyrolytic carbon electrode. Finally, the polydopamine was selectively removed only from the tips of the pillars, by using localized laser ablation. The selectively passivated electrodes were characterized by scanning electron microscopy, cyclic voltammetry and electrochemical impedance spectroscopy. The charge transfer resistance was measured to $1.46 \pm 0.2 \text{ k}\Omega$ for the bare electrode, $321 \pm 2.59 \text{ k}\Omega$ after the PDA deposition and $18.86 \pm 6.2 \text{ k}\Omega$ after laser ablation. **Based on CV data, the bare electrodes have charge storage capacity in the range 4.5-6.6 mC/cm².** Due to the use of biocompatible materials, such as pyrolytic carbon and polydopamine, these 3D electrodes are particularly suited for biological applications, such as electrochemical monitoring of cells or retinal implants [4], where highly localized electrical stimulation of neurons is beneficial. Secondly, we also present a chip design for studying local stimulation or MEA measurements, consisting of similar 3D carbon pillars on interdigitated carbon fingers as base. Large Au pads connected to each side of the interdigitated finger design enables probing and measuring from every other finger. The nature of this design enables stimulation or measurement of local regions, **i.e. the two sets of fingers are individually addressable.** with various pillar density towards in-vitro and ex-vivo testing with biological tissue for various applications e.g. retinal prosthesis. Figure 1 shows the selectively passivated pillars (left) and the interdigitated finger design (right).

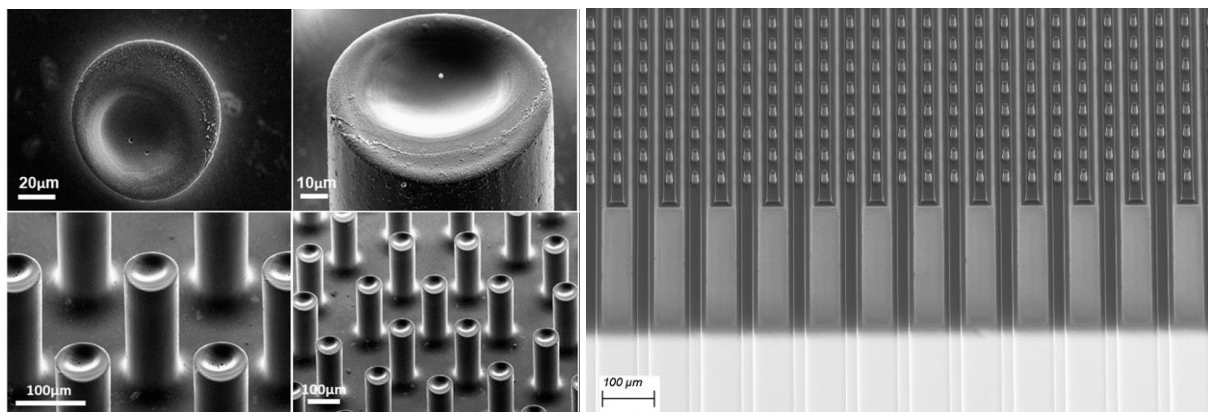


Figure 1: (left) Scanning electron micrographs of carbon pillars selectively passivated by polydopamine. (right) Carbon pillars on interdigitated fingers. Bright area in the bottom is evaporated Au contact pads enabling measurement or stimulation from every other finger.

References

1. Rezaei, B., Saghir, S., Pan, J.Y., Davidsen, R.S., Keller, S.S. (2022). Selective Passivation of Three-Dimensional Carbon Microelectrodes by Polydopamine Electrodeposition and Local Laser Ablation. *Micromachines* 13, 371, doi: 10.3390/mi13030371
2. L. Amato, A. Heiskanen, C. Caviglia, F. Shah, K. Zór, M. Skolimowski, M. Madou, L. Gammelgaard, R. Hansen, E.G. Seiz, M. Ramos, T.R. Moreno, A. Martinez-Serrano, S. S. Keller, J. Emnéus, "Pyrolysed 3D-Carbon Scaffolds Induce Spontaneous Differentiation of Human Neural Stem Cells and Facilitate Real-Time Dopamine Detection" *Advanced functional materials*, **24** 44 (2014) 7042-7052, doi: [10.1002/adfm.201400812](https://doi.org/10.1002/adfm.201400812)
3. R.S. Davidsen, S. Hemanth, S.S. Keller, T. Bek, O. Hansen, "Evaluation of the capacitive behavior of 3D carbon electrodes for sub-retinal photovoltaic prosthesis" *Micro and Nano Engineering* **2** (2019) 110-116, doi: [10.1016/j.mne.2019.02.003](https://doi.org/10.1016/j.mne.2019.02.003)
4. K. Mathieson, J. Loudin, G. Goetz, P. Huie, L. Wang, T. I. Kamins, L. Galambos, R. Smith, J. S. Harris, A. Sher, D. Palanker "Photovoltaic retinal prosthesis with high pixel density" *Nature photonics* **6** (2012) 391-397. doi:10.1038/nphoton.2012.104

Dendritic-like PEDOT:PSS electrodes for 2D in-vitro electrophysiology

Corentin Scholaert,^{a,*} Kamila Janzakova,^a Mahdi Ghazal,^a Michel Daher Mansour,^a Camille Lefebvre,^b Sophie Halliez,^b Yannick Coffinier,^a Sébastien Pecqueur,^a and Fabien Alibart,^{a,c}

- a. Institut d'Électronique, Microélectronique et Nanotechnologie (IEMN), CNRS, UMR 8520, F-59652 Villeneuve d'Ascq, France
- b. Univ. Lille, Inserm, CHU Lille, U1172 - LiNCog - Lille Neuroscience & Cognition, F-59000 Lille, France
- c. Laboratoire Nanotechnologies & Nanosystèmes (LN2), CNRS, Université de Sherbrooke, J1X0A5, Sherbrooke, Canada

* corentin.scholaert.etu@univ-lille.fr

Over the past few years, organic electronics - and especially organic mixed ionic electronic conductors (OMIECs) - has taken bio sensing and neuromorphic applications to a whole new level. However, one of the major limitations of the mainstream technologies today is that electronic circuits need to be pre-shaped according to the intended use and the expected outcome. This top-down approach, far from being flexible/adaptive, does not really make the most of the resources at hand, as it is hard to predict precisely where cells will be located. To counter that, we can either choose to increase the density and the number of electrodes, so that the entire area would be mapped, or shift from a top-down to a bottom-up approach which would allow for a more enlightened decision-making process.

Recently, the electrodeposition of PEDOT:PSS has been explored as a novel technique to grow conducting polymer films and fibers on non-conductive substrates [1]. The work of Janzakova and coworkers [2] took that concept a step further by using electropolymerization of EDOT as a way to create freestanding dendritic-like conductive fibers in a 3D environment, paving the way for in operando material modification, and in fine bottom-up fabrication routes that would be more adaptive and allow for more flexibility. Moreover, it was lately showed that these objects could work as Organic Electrochemical Transistors (OECTs) [3].

Here, we explore the possibility of growing dendritic-like PEDOT fibers on Multielectrode Arrays (MEAs) via electropolymerization of EDOT. Electrophysiological measurements are based on the capacitive coupling between cells and the electrode material. In comparison with local electrodes, the dendritic objects present spatially distributed impedance due to the extensions of their dendritic branches interacting with the biological environment. We investigate the relation between morphology and impedance in these dendritic-like fibers by using a non-conventional Electrochemical Impedance Spectroscopy (EIS) setup that will allow us to apply a potential difference between the two ends of the dendrites, thus studying how biasing them can affect their behavior.

Moreover, it appears that dendritic fibers can be considered both as passive electrodes as well as active devices. We explore the use of these two strategies in the context of electrophysiological measurements.

Finally, the ability to record biological signals results from the interaction between cells and an electrode. Unconventional objects such as dendrites present spatio-temporal filtering properties that could affect the recording of such signals. We investigate how tuning the impedance of a dendrite might be used to record efficiently bio-signals.

References

- [1] Watanabe, T., Ohira, M., Koizumi, Y., Nishiyama, H., Tomita, I., and Inagi, S. (2018). In-Plane Growth of Poly(3,4-ethylenedioxythiophene) Films on a Substrate Surface by Bipolar Electropolymerization. *ACS Macro Lett.*, vol. 7, n° 5, p. 551-555, doi: 10.1021/acsmacrolett.8b00170.
- [2] Janzakova, K., *et al.* (2021). Analog programming of conducting-polymer dendritic interconnections and control of their morphology. *Nat. Commun.*, vol. 12, n° 1, Art. n° 1, doi: 10.1038/s41467-021-27274-9.
- [3] Janzakova, K., Ghazal, M., Kumar, A., Coffinier, Y., Pecqueur, S., and Alibart, F. (2021). Dendritic Organic Electrochemical Transistors Grown by Electropolymerization for 3D Neuromorphic Engineering. *Adv. Sci.*, 8, 2102973, doi: 10.1002/advs.202102973.

Liquid-crystal transducers: Towards a multi-optrode array system for electrophysiology sensing applications

Reem M. Almasri,^{a,*} Amr Al Abed,^a Josiah Firth,^c François Ladouceur,^b Nigel H. Lovell^a.

- a. Graduate School of Biomedical Engineering, UNSW, Sydney, Australia.
- b. School of Electrical Engineering and Telecommunications, UNSW, Sydney, Australia.
- c. Australian National Fabrication Facility, UNSW, Sydney, Australia.

* r.almasri@unsw.edu.au

The application of multi-electrode arrays (MEAs) to electrophysiological studies has gained particular recent prominence with many groups aiming to build next generation brain machine interfaces. Research has been focused on enabling high spatiotemporal recording and modulation of cell activity. While many studies have been done to improve tissue interfacing as well as the signal quality, few of them managed to demonstrate large-scale, densely packed MEAs to record tissue activity and then it was only achievable by way of complex circuit designs [1]. Over the past decade optical techniques have emerged that seek to replace or complement the traditional electrical recordings and imaging of neural and cardiac cell activity; these include voltage-sensitive dye imaging and calcium imaging. However, the concerns regarding the pharmacological consequences, signal to noise ratio, and spatial resolution that are associated with these approaches have highlighted the need for label-free techniques.

Herein, our work leverages the electro-optical transduction properties of liquid crystals (LCs), which are typically used in industrial displays, to design an optrode – i.e., an optical electrode – that passively senses and quantifies biological signals [2]. Sensing systems can then be fabricated as a single optrode channel or as a multi-optrode array (MOA) for large-scale sensing applications. The MOA design does not need interconnecting tracks to sensing electronics, giving an advantage over a conventional MEA in terms of impedance levels and dense configurations. This is because our tests have shown that the system ‘input’ impedance automatically scales with the geometrical area of the sensing interface [3]. Thus, the impedance mismatch and signal loss are kept to a minimum and the input to total system impedance is constant across different sensing areas, allowing in principle to miniaturize the sensing area down to micron scales. We have demonstrated the feasibility of single channel optrode recording from cardiac tissue *ex vivo* and nerves *in vivo*. Furthermore, our preliminary results also show the practicability of recording sinusoidal voltage waveforms from MOAs through a confocal microscope system.

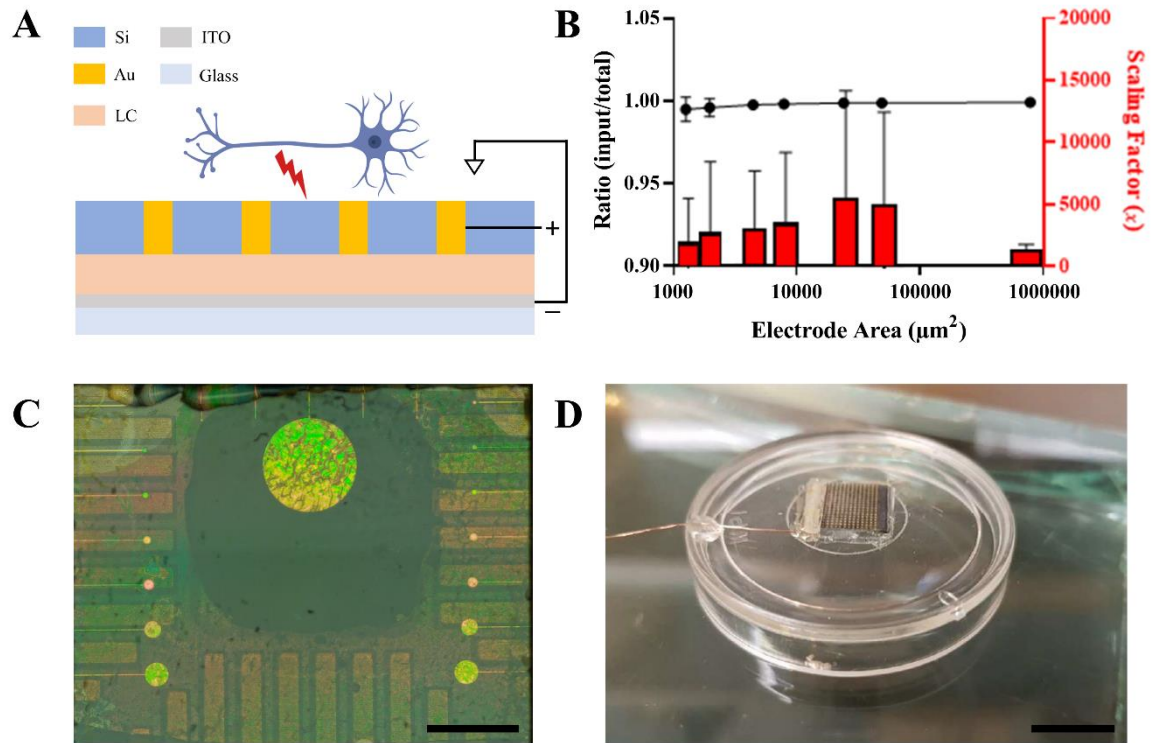


Figure 1: A) A schematic of the MOA's structure. B) The mean scaling factor of impedance values and input to total impedance ratio across all frequencies for different geometrical areas. C) An image showing the different recording sites' diameters. Scale bar is 1 mm. D) Image of MOA showing ground-wire and mirrors as viewed through glass, indium tin oxide (ITO), and LC layer. In practice, the tissue is placed on top of the MOA recording sites and readout is done from the bottom. Scale bar is 1 cm.

References

1. Tsai, D., Sawyer, D., Bradd, A. et al. (2017). A very large-scale microelectrode array for cellular-resolution electrophysiology. *Nat Comm* 8, 1802. <https://doi.org/10.1038/s41467-017-02009-x>
2. Al Abed, A., Srinivas, H., Firth, J. et al. (2018). A biopotential optrode array: operation principles and simulations. *Sci Rep* 8, 2690. <https://doi.org/10.1038/s41598-018-20182-x>
3. Almasri, R.M., Al Abed, A., Wei, Y., Wang, H., Firth, J., Poole-Warren, L., Ladouceur, F., Lehmann, T. and Lovell, N.H. (2021). Impedance Properties of Multi-Optrode Biopotential Sensing Arrays. *IEEE Transactions on Biomedical Engineering*. doi: 10.1109/TBME.2021.3126849

All-optical neural interfaces: architecture and scalability

François Ladouceur,^a* Torsten Lehman,^a Amr Al Abed,^b Nigel H. Lovell^b.

- a. School of Electrical Engineering and Telecommunications, UNSW, Sydney, Australia.
- b. Graduate School of Biomedical Engineering, UNSW, Sydney, Australia.

* f.ladouceur@unsw.edu.au

Recent experimental work has confirmed the viability of all-optical neural interfaces using liquid-crystal transducers [1] and we published earlier their operation principles [2] when integrated to form sensing arrays (see Figure 1). Using photonics technologies, the proposed approach has the potential to scale up to thousands of channels essentially avoiding heat-dissipation and impedance-matching issues [3] that plague standard (electrical domain) implementations of multi-electrode arrays.

Integrating such transducers onto a (potentially conformable) planar substrate requires a means to address each transducer individually. This can be done in a number of ways using addressing techniques developed in the context of optical networks. Of particular relevance is wavelength division multiplexing (WDM) which can be implemented on-chip using entirely passive components. This addressing scheme, coupled with vertical grating couplers provide a complete architecture that would enable the development of high throughput, high density arrays such as the one illustrated in Figure 2.

We discuss herein potential architectures that would support the development of this new class of arrays, namely multi-optrode arrays. Doing so, we will review the *in-vivo* and *ex-vivo* experiments done so far using single channel transducers, discuss impedance matching properties enabling high density arrays, provide examples of potential architectures for a future all-optical neural interface and discuss its scalability. Finally, we will spell out the future challenges that need to be overcome in terms of noise reduction, fabrication, conformability and biocompatibility.

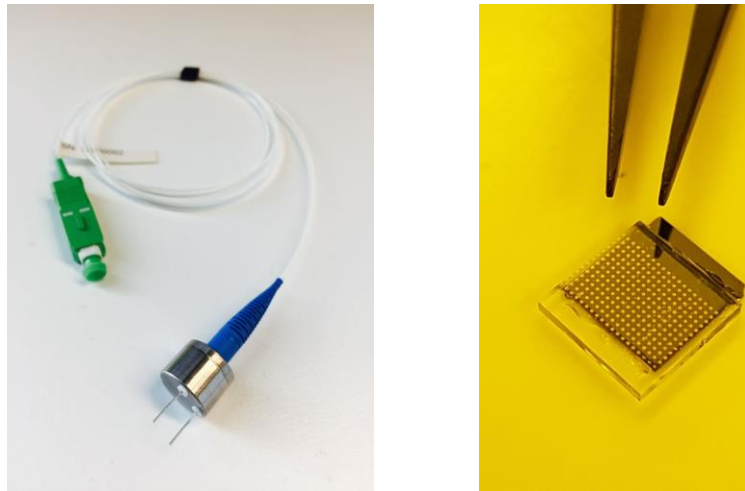


Figure 1: **Left.** Single channel liquid crystal transducer as developed at UNSW Sydney and successfully used to measure neural signals. **Right.** First generation multi-optrode array providing a proof-of-principle integrating 216 transducers onto a single silicon/glass substrate.

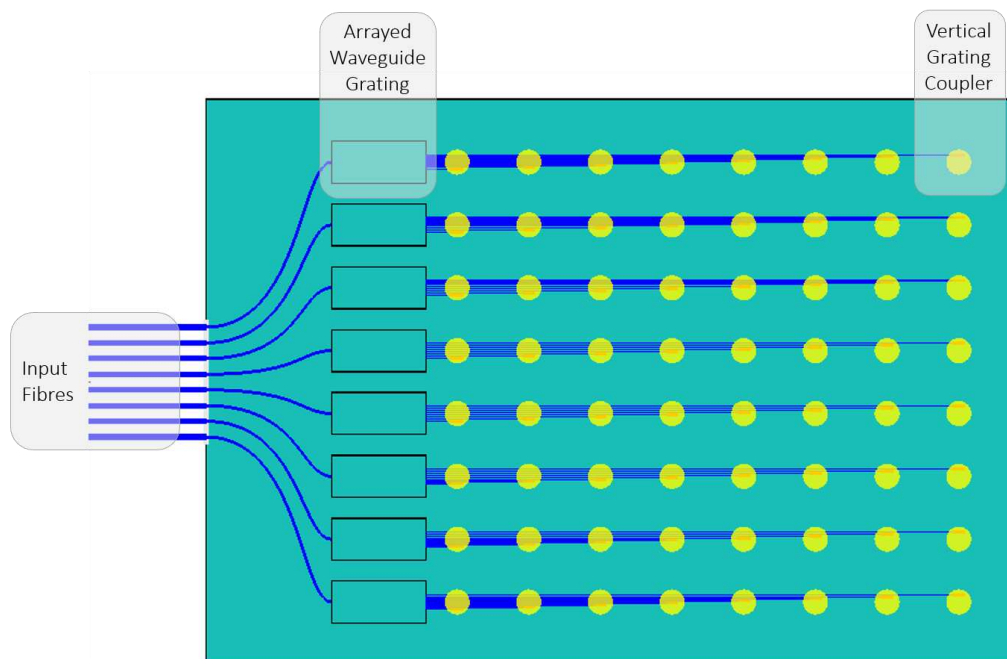


Figure 2: Top view of the integrated chip. A number of optical fibers each carry a broadband signal which is demultiplexed into 8 distinct waveguides by an arrayed waveguide grating. The signal carried by each waveguide is then coupled vertically into a specific liquid-crystal transducer (yellow disc) using a vertical grating coupler. The reflected signal from each transducer follows the reciprocal path to the detection system via the same optical fiber.

References

1. Brodzeli, Z., Silvestri, L. Michie, A., Guo, Q., Pozhidaev, E.P., Chigrinov, V. and Ladouceur, F. (2013) Sensors at your fibre tips: A novel liquid crystal-based photonic transducer for sensing systems, *J. Lightwave Technol.* 31, 2940-2946
2. Al Abed, A., Srinivas, H., Firth, J. et al. (2018). A biopotential optrode array: operation principles and simulations. *Sci Rep* 8, 2690. <https://doi.org/10.1038/s41598-018-20182-x>
3. Almasri, R.M., Al Abed, A., Wei, Y., Wang, H., Firth, J., Poole-Warren, L., Ladouceur, F., Lehmann, T. and Lovell, N.H. (2021). Impedance Properties of Multi-Optrode Biopotential Sensing Arrays. *IEEE Transactions on Biomedical Engineering*. doi: 10.1109/TBME.2021.3126849

Hybrid fabrication of multimodal intracranial implants for electrophysiology and local drug delivery

J. Gurke,^{a,b*} T. Naegele,^b S. Hilton,^b R. Pezone,^b V.F. Curto,^b D. G. Barone,^b E. List-Kratochvil,^c A. Carnicer-Lombarte,^b G. Malliaras^b

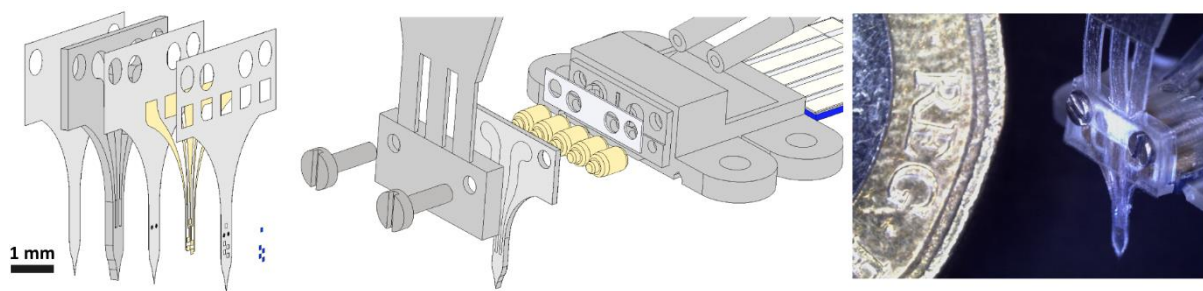
^a Institute of Chemistry, University of Potsdam, Karl-Liebknecht-Str. 24-25, 14476 Potsdam, German

^b Electrical Engineering Division, University of Cambridge, 9 JJ Thomson Ave, Cambridge CB3 0FA, United Kingdom.

^c Department of Chemistry and of Physics and IRIS Adlershof, Humboldt-Universität zu Berlin, Zum Großen Windkanal 2, 12489 Berlin, Germany

* Johannes.gurke@uni-potsdam.de

New fabrication approaches for mechanically flexible materials hold the key to advancing the applications of bioelectronics in fundamental neuroscience and the clinic. By combining the high precision of microfabrication of a thin-film bioelectronic array with the versatility of additive manufacturing of microfluidic systems, we are showing a new, straight-forward approach for the fabrication of intracranial probes capable of multichannel local field recordings and convection-enhanced drug delivery. The process makes use of state-of-the-art parylene-based device architecture and a commercial VAT polymerizable elastomer, combining to produce a flexible implant. The mechanical and electrical properties of the implant are characterised, and its function is validated in an in vivo rodent model. We show that the implant can pharmaceutically modulate neuronal activity in the hippocampus through local drug delivery, while simultaneously recording local field potentials by its electrodes. Chronic implantation tests show good implant stability and minimal tissue response one-week post-implantation. Our work shows the potential of hybrid neuronal probes combining different manufacturing technologies – lithography-based printing and thin-film microfabrication – and paves the way for a new approach to multimodal probes combining the capabilities of both.



Hybrid Fabrication

Heterogeneous Integration

Final Device

Figure 1: The figure shows an explosion schemata of the hybrid fabricated device, its heterogeneous integration, and a microscopic picture of the final device with a one-pound coin for scale.

Flexible microelectrode arrays for intrapancreatic recording

Domenic Pascual,^a Lisa Brauns,^a Matthias Tisler,^b Udo Kraushaar,^a Peter D. Jones^a

- a. NMI Natural and Medical Sciences Institute at the University of Tübingen, Markwiesenstraße 55, 72770 Reutlingen, Germany
- b. Eberhard Karls Universität Tübingen, Geschwister-Scholl-Platz, 72074 Tübingen
- * Peter.Jones@nmi.de

Diabetes mellitus type 2 is one of the most common diseases in the world and is listed by the WHO as the 8th leading cause of death. As the disease progresses, the beta cells in the pancreas lose their ability to secrete insulin. Drug therapy with insulin requires a high level of compliance from the patient by monitoring blood glucose levels. Noncompliance is associated with high comorbidity, including cardiovascular disease, neuropathy, and infectious diseases. Therefore, pancreatic research and new innovative therapeutic approaches are urgently needed.

The pancreatic beta-cells generate an electrical signal during the exocytosis of insulin granules. Schönecker et al. were able to measure this electrical activity of pancreatic islet cells in vitro with an amplitude of 20 μ V. [1]

By a histological examination we found that the beta-cells in a porcine pancreas start only at about 1 mm below the organ's surface. Due to this depth, it is not possible to record the electrical signal of the islets at the organ's surface. In order to obtain evaluable signals, an intrapancreatic recording seems necessary although the tissue in the pancreas contains digestive enzymes that can cause pancreatitis in case of injury.

We introduce a flexible 63-electrode microelectrode array (MEA) that can be implanted in the pancreas and is designed to evade a pancreatic immune response [2]. The flexible mesh-MEA is made out of a 12 μ m thick polyimide. To reach a high signal-to-noise ratio, the TiN electrodes have a diameter of 30 μ m. The implant's width starts at 740 μ m and tapers to 45 μ m at its tip.

To implant the MEA into the porcine pancreas, it is attached to a tungsten needle using polyethylene glycol (PEG). Once the tungsten needle is inserted into the pancreas, the PEG dissolves. Thereafter, the needle can be pulled out of the pancreas and the MEA remains inside. Figure 1 shows the implantation concept, while Figure 2 shows preliminary results in a hydrogel. We will present results from ex vivo implantations towards the goal of acute porcine experiments.

Acknowledgements

This work was financed by the German Federal Ministry of Education and Research (BMBF) in the project PanaMEA (grant 13GW0397D). The work received financial support from the State Ministry of Baden-Wuerttemberg for Economic Affairs, Labour and Housing Construction. The PanaMEA project builds on the results of the "innBW Implant" project (7-4332.62-NMI/49), which was funded by the Ministry of Finance of Baden-Württemberg (MFW).

References

1. Schönecker, S., Kraushaar, U., Guenther, E., Gerst, F., Ullrich, S., Häring, H.-U., . . . Krippeit-Drews, P.(2015). Human Islets Exhibit Electrical Activity on Microelectrode Arrays (MEA). *Experimental and Clinical Endocrinology & Diabetes*, 123(05), 296–298. doi:10.1055/s-0035-1547217

2. Hong, G., Yang, X., Zhou, T. & Lieber, C. M. (2018). Mesh electronics: a new paradigm for tissue-like brainprobes. *Current Opinion in Neurobiology*, 50, 33–41. doi:10.1016/j.conb.2017.11.0

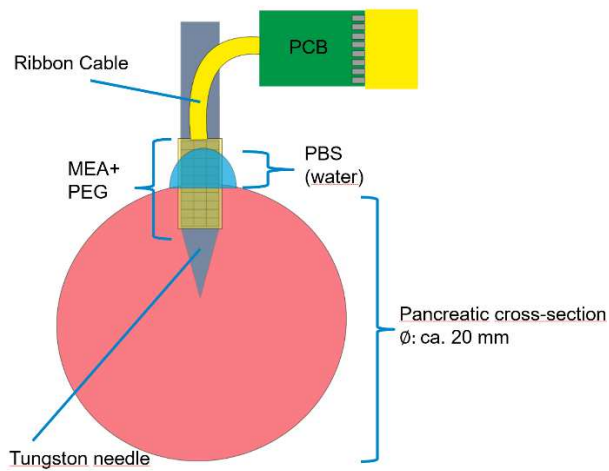


Figure 1: Concept of shuttle-implantation of our Mesh-MEA.

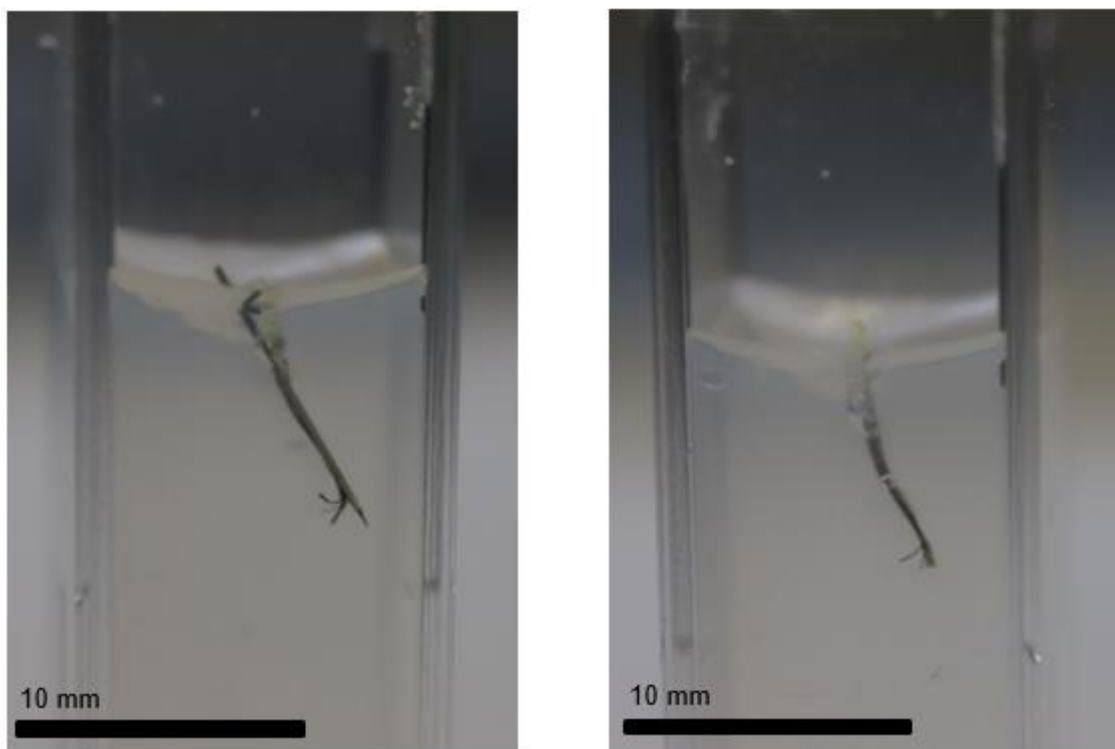


Figure 2: Implantation of polyimide dummies into an agarose hydrogel. Tungsten needle coated with PEG serves as shuttle for the MEA-dummy (left). After PEG dissolved, the tungsten needle can be explanted (right).

A test bench for flexible implants

Thoralf Herrmann^{a*}, Lisa Brauns^a, Helen Steins^a, Michael Mierzejewski^a, Peter D. Jones^a

- a. NMI Natural and Medical Sciences Institute at the University of Tübingen, Reutlingen, Germany

* therrmann@nmi.de

Flexible implants, including microelectrode arrays, exposed to thermal and mechanical stress and affected by electrochemical processes when placed in the human body. Encapsulation is crucial for long term stability and safe device operation, while electrochemical damage to microelectrodes or physical damage. Test engineering is critical for achieving clinical success of bioelectronic implants.

We have developed a test bench for evaluation of bioelectronic devices, which can test complete implants, specific components, or test specimens. Here, we will report on using the test bench for investigating encapsulation of electrical components (thin film traces and wire-bonded connectors) by different polymeric coating systems. The specimens are mounted on a motor driven spindle and moved in physiological saline at a controlled temperature to mimic physiological conditions. Electrical elements are stressed by externally applied voltages to simulate implant function. Four-wire measurements and impedance spectra are taken regularly to monitor the electrical properties of the specimen throughout the observation period (currently up to 15 months).

The observed changes in the measured impedance and resistance (see Figure 1) of samples with different coatings were compared to the optical condition and could be assigned to corrosive effects indicating encapsulation failure.

As implantable devices are subject to strict regulations and need to fulfill defined requirements prior to medical application, these results help saving time and money by defining promising candidates for stable encapsulations at an early stage of implant development. We will also report on limitations of our test bench and developments that will be required towards accredited testing of clinical implants.

Acknowledgements

This work was financed by the German Federal Ministry of Education and Research (BMBF) in the projects Neptun (13GW0271) and Sealant (01QE2039B). The work received financial support from the State Ministry of Baden-Wuerttemberg for Economic Affairs, Labour and Tourism.

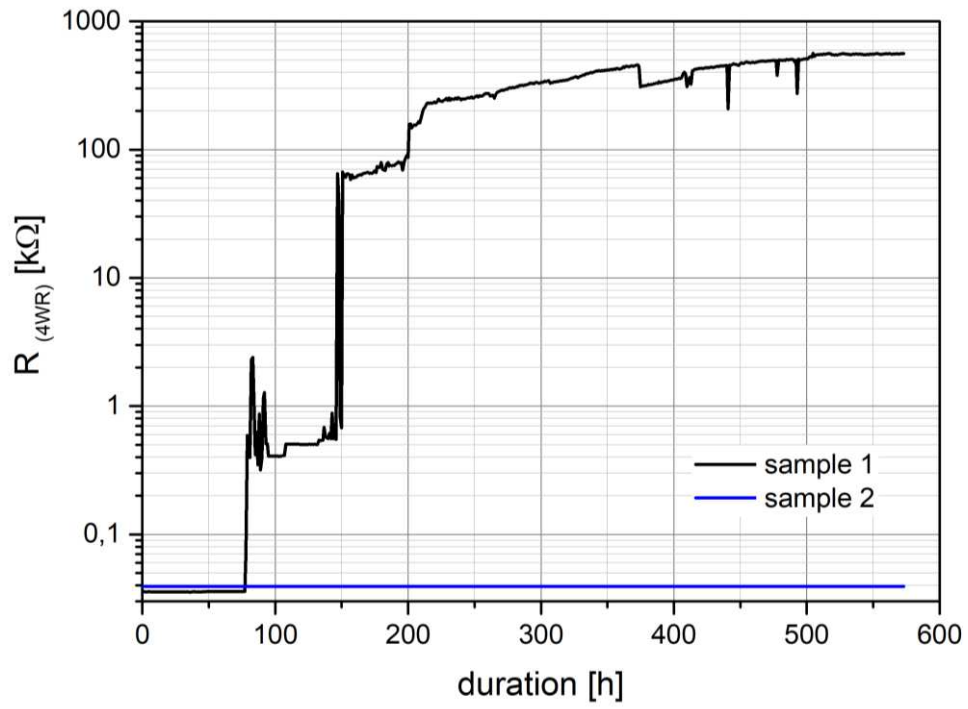


Figure 1: Resistance over time of meander structures at sustained on-load operation. Corrosive effects after 77 hours of operation are only visible at sample 1 (black arrow).

Toward the development of a stretchable nerve-on-chip platform to study the role of tensile stress in peripheral neuropathies *in vitro*

Blandine Clément^a, Tobias Ruff^a, Léo Sifringer^a, Sophie Girardin^a, Sean Weaver^a, Simon Steffens^a, János Vörös^{a,*}

a. Laboratory of Biosensors and Bioelectronics, Institute for Biomedical Engineering, ETH Zürich, 8092 Zürich

* janos.voros@biomed.ee.ethz.ch

Peripheral Neuropathy (PN) is a disease of nerves that can be induced by tensile and compressive stress. Neuropathies are still an irreversible condition as available therapies are limited to symptomatic treatment [1]. Development of restorative treatment requires efficient tools to screen for new therapeutic approaches. Current *in vitro* methods mostly rely on random cell cultures that lack the biological complexity necessary to generate any translatable results. Thus, engineered nerve-on-a-chip models have recently gained interest as they can emulate better the *in vivo* architecture [2]. However, current systems on rigid glass multielectrode arrays (MEA) lack the flexibility to apply mechanical stress, which is known to induce neuropathy above a critical threshold, and which is believed to be a useful regenerative strategy for nerve damage [3] at moderate cyclic strains. To address this, we aim to establish a stretchable *in vitro* nerve model platform.

The platform consists of a polydimethylsiloxane (PDMS) microstructure [4] with seeding wells connected to 8- μm wide directional axon guidance channels that all converge into a mm size nerve-forming output channel. The PDMS microstructure is designed to be compatible with our in-house, customized, stretchable MEAs.

When seeding rat dorsal root ganglion (DRG) spheroids, we could grow several mm long DRG axons within our PDMS microstructure on glass. Within 30 days, cells have already formed an axon fascicle in the *in vitro* nerve channel and were viable over 100 days. Moreover, co-cultured Schwann cells elicited myelination around some axonal segments (see Figure 1).

Overall, our initial feasibility experiments demonstrate the potential of the proposed methodology to facilitate the understanding of the role of tensile stress in neuropathy.

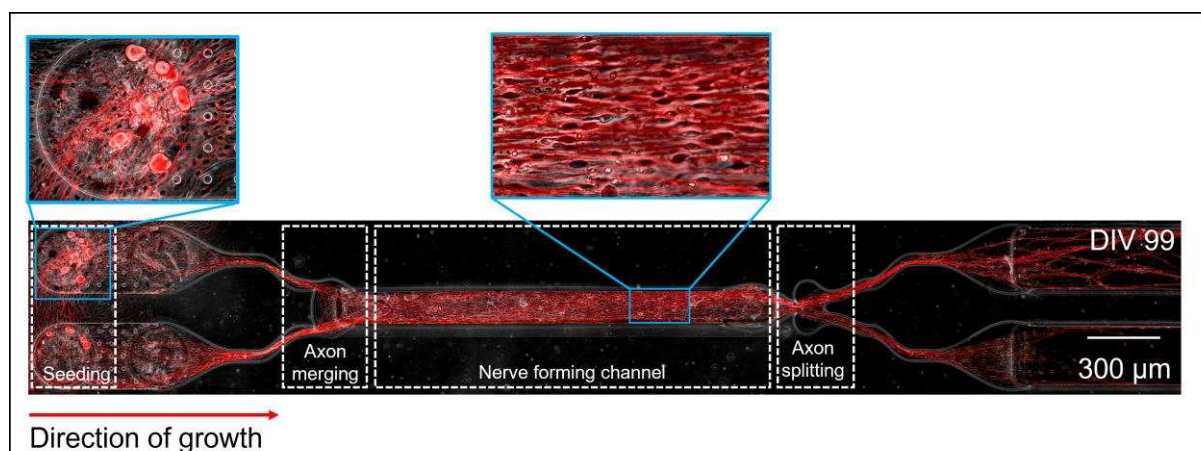


Figure 1: Dorsal Root Ganglion (DRG) cells spheroids co-cultured with Schwann cells, grew 3 mm long axons unidirectionally (from left to right) in a PDMS guidance microstructure. DRG cells were transduced to express red fluorescent protein (RFP) and imaged at DIV99. Cultured in half Neurobasal Medium, half DMEM, supplemented with growth factors and 50 $\mu\text{g}/\text{mL}$ ascorbic acid.

References

1. "Peripheral Neuropathy Fact Sheet", NINDS, (2018). NIH Publication No. 18-NS-4853
2. Anderson, WA et al. (2021). Advances in 3D neuronal microphysiological systems: towards a functional nervous system on a chip. *In Vitro Cell Dev Biol Anim.* 57(2):191-206.
3. Shah, S et al. (2014). Peripheral nerve lengthening as a regenerative strategy. *Neural Regeneration Research*, 9(16): 1498-1501
4. Forró, C et al. (2018). Modular microstructure design to build neuronal networks of defined functional connectivity. *Biosensors and Bioelectronics*, 122, 75-87.

Concepts for multi-layer flexible microelectrode arrays with active electrode addressing for future epiretinal implants

Eashika Ghosh,^a Wilfried Mokwa,^a Sven Ingebrandt^{a,*}

a. Institute of Materials in Electrical Engineering 1, RWTH Aachen University,
Sommerfeldstr. 24, 52074 Aachen

*: ingebrandt@iwe1.rwth-aachen.de

More than 260 different inherited retina diseases are known to affect the human eye. One of the most prominent ones is Retina Pigmentosa (RP) with approximately 1.5 million cases worldwide [1, 2]. RP damages the photoreceptors in the retina gradually leading to complete blindness. In addition, a functional degeneration and morphological re-organization of the neuronal layers of the retina occurs with distinct pathology in each patient. Therefore, restoring the loss of vision with generic devices, as it was done in past generations of retinal implants, is very challenging. Although many attempts and concepts were developed in the past, most of them remained unsuccessful. Some of the visual prosthetics showed optimistic results, however, with a strongly limited resolution and field of vision [3].

In the newly established research-training group InnoRetVision¹ (GRK2610) we address the limitations of our previous epiretinal implants with innovative concepts and state-of-the-art materials and technologies. One of the new ideas is to develop and fabricate a multifunctional, flexible microelectrode array with an active addressing and a high electrode count. In previous projects of our institute, different designs of “very large electrode arrays for epiretinal stimulation (VLARS)” and retina implants including photodiode arrays (projects Optoepiret) with a maximum of 250 electrodes were targeted, but only a lower electrode count was successfully realized on a flexible polyimide (PI) substrate with a maximum field of view of 18.8° (**figure 1a**) [4]. There, application-specific integrated circuits (ASICs) containing photodiodes, wireless communication elements and active stimulation electronics were fabricated in a CMOS process, thinned and flip-chipped onto flexible multilayer carriers realized in multi-layer PI. The iridium oxide (IrOx) microelectrodes of the stimulation array were addressed 1:1 from the ASIC side.

In this work, we aim to develop new implant concepts allowing for a higher amount of stimulation electrodes with the option to include recording electrodes for a closed-loop stimulation concept, adaptable to each patient’s pathology (**figure 1b**). To reach this goal, the electrode array embedded in the flexible multilayer materials needs to be actively addressable [5, 6]. The addressable array will be realized in a multi-layer PI or in a multilayer Parylene-C substrate. As a first step, we realized a design for a flexible array with hexagonal structures, which should include an active microelectrode concept to accommodate a large number of stimulation electrodes. The implant should be foldable like the former VLARS designs to allow insertion into the eye via small incision of 5 mm in the cornea, avoiding a major surgical operation as shown for earlier designs in **figure 1c**. The flexible arrays are fabricated in a multilayer process established in our institute including 3-layer gold interconnects through the flexible PI structure to contact the sputtered IrOx microelectrodes.

In later steps, we aim to include active elements like thin-film silicon transistors for active switching of the microarray and photodiodes for energy harvesting to supply the energy for the switching elements (**figure 1d**). We will present the first concepts and test structures for these different functional elements. The different concepts addressed and tested in this project will be the foundation for the next-generation retina implants in a later period of InnoRetVision.

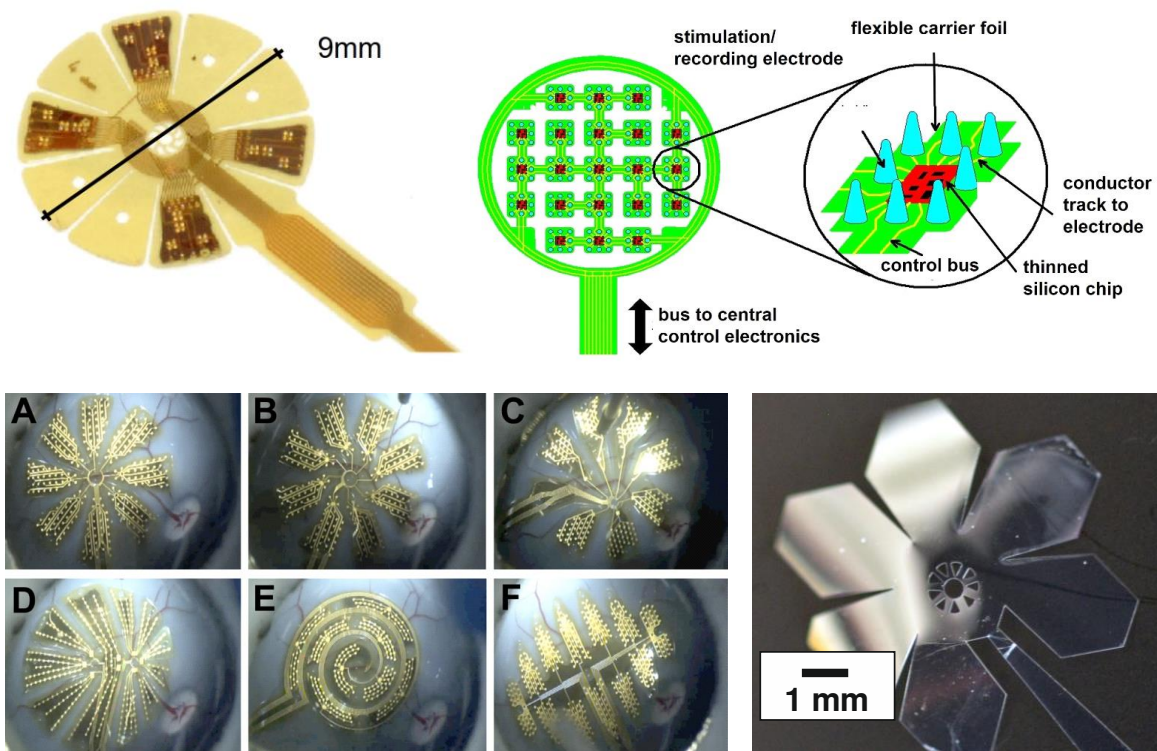


Figure 1: **a)** Former implant of project Optoeipret 3, which included ASICs in a PI multilayer structure. Microelectrodes were addressed 1:1 from the silicon chips side. **b)** Concept of an active microelectrode array with embedded thin silicon chips for active electrode addressing and stimulation and recording functionality. **c)** (A-F) Implantation tests of former electrode designs of the project VLARS. **d)** New, flexible implant carrier structure based on 10 µm thick Parylene-C.

References

1. Duncan, J. L., Pierce, E. A., Laster, A. M., Daiger, S. P., Birch, D. G., Ash, J. D., Iannaccone, A., Flannery, J. G., Sahel, J. A., Zack, D. J. and Zarbin, M. A. (2018). Inherited Retinal Degenerations: Current Landscape and Knowledge Gaps. *Transl. Vis. Sci. Technol.*, 7, 1-15. doi:10.1167/tvst.7.4.6
2. Occelli, L. M., Pasmarter, N., Ayoub, E. E. and Petersen-Jones, S. M. (2020). Changes in retinal layer thickness with maturation in the dog: an in vivo spectra domain - optical coherence tomography imaging study. *BMC Vet. Res.*, 16, 11. doi:10.1186/s12917-020-02390-8
3. Behrend, M. R., Ahuja, A. K., Humayun, M. S., Chow, R. H. and Weiland, J. D. (2011). Resolution of the Epiretinal Prosthesis is not Limited by Electrode Size. *IEEE Trans. Neural Syst. Rehabil. Eng.*, 19, 436-442. doi:10.1109/tnsre.2011.2140132
4. Waschowski, F., Hesse, S., Rieck, A. C., Lohmann, T., Brockmann, C., Laube, T., Bornfeld, N., Thumann, G., Walter, P., Mokwa, W., Johnen, S. and Roessler, G. (2014). Development of very large electrode arrays for epiretinal stimulation (VLARS). *Biomed. Eng. Online*, 13, 15. doi:10.1186/1475-925x-13-11
5. Feili, D., Schuettler, M. and Stieglitz, T. (2008). Matrix-addressable, active electrode arrays for neural stimulation using organic semiconductors - cytotoxicity and pilot experiments in vivo. *J. Neural Eng.*, 5, 68-74. doi:10.1088/1741-2560/5/1/007
6. Li, J. H., Song, E. M., Chiang, C. H., Yu, K. J., Koo, J., Du, H. N., Zhong, Y. S., Hill, M., Wang, C., Zhang, J. Z., Chen, Y. S., Tian, L. M., Zhong, Y. D., Fang, G. H., Viventi, J. and Rogers, J. A. (2018). Conductively coupled flexible silicon electronic systems for chronic neural electrophysiology. *Proc. Natl. Acad. Sci. U. S. A.*, 115, E9542-E9549. doi:10.1073/pnas.1813187115

Thin CMOS-compatible silicon scaffold for interfacing with 3D cell culture models

Aaron Delahanty^{a,b,*} Idris Salmon^c, Sohail Faizan Shaikh^{a,b}, Alexandru Andrei^a, Liesbet Lagae^{a,b}, Adrian Ranga^c, Dries Braeken^a

- a. IMEC vzw, Kapeldreef 75, B-3001, Leuven, Belgium
- b. KU Leuven, Department of Physics and Astronomy, Laboratory for Soft Matter and Biophysics, Leuven, Belgium
- c. KU Leuven, Department of Mechanical Engineering, Laboratory of Bioengineering and Morphogenesis, Biomechanics Section, Leuven, Belgium

* aaron.delahanty@imec.be email of corresponding author

Cerebral Organoids are self-patterning 3D neural cultures capable of mimicking some features of *in vivo* neurogenesis and disease states [2]. Spontaneous electrical activity arises in these models over prolonged culture [1,5]. Various electrode-based approaches exist to interface electrically with these cultures, however current solutions lack the combination of high-density electrode sites and accessibility to the entire volume of the biological model [3]. Here, a thin, stackable, 17 μm porous silicon scaffold has been developed that allows for the expansion of the outer layer of the organoid to infiltrate through, and absorb, the scaffold. Individual cells migrate through the open pores of the scaffold, extending the organoid tissue in a continuous manner. After 3 days of continuous culture, the tissue extends above the scaffold with an average apical point of 47 μm (n=5) and exhibits calcium transients (see Figure 1). This scaffold offers an all-silicon structure compatible with both metal electrodes with off-chip ADC, as well as CMOS-based electrodes for electrical stimulation, recording, and impedance measurements [4].

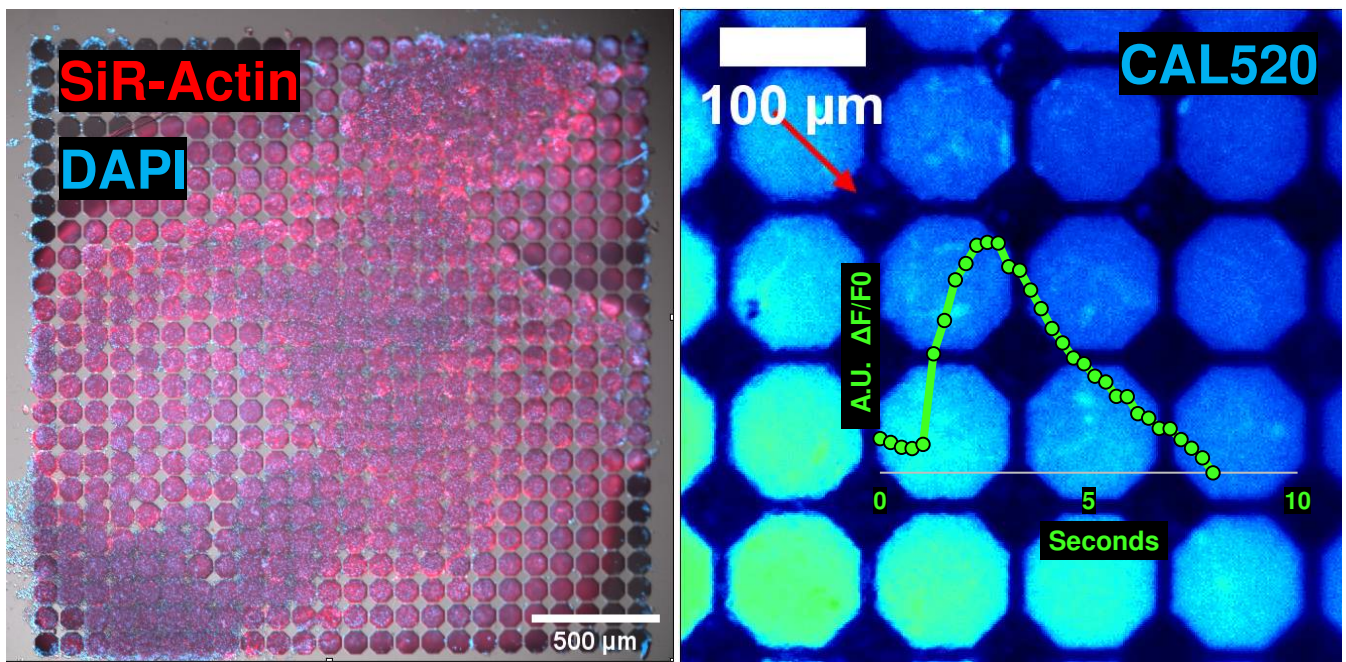


Figure 1: Left Panel – A Cerebral Organoid cultured in bulk medium on orbital shaker, subsequently transferred to the backside of the silicon scaffold for 3 days of continued culture. Image is taken from frontside via epifluorescent microscope. Right Panel – Calcium Transient imaging at 4Hz sampling. Individual cells migrate to the topside of the scaffold and exhibit calcium transients as indicated by the dF/F_0 trace.

References

1. Fair, S. R., Julian, D., Hartlaub, A. M., Pusuluri, S. T., Malik, G., Summerfied, T. L., Zhao, G., Hester, A. B., Ackerman, W. E., Hollingsworth, E. W., Ali, M., McElroy, C. A., Buhimschi, I. A., Imitola, J., Maitre, N. L., Bedrosian, T. A., & Hester, M. E. (2020). Electrophysiological Maturation of Cerebral Organoids Correlates with Dynamic Morphological and Cellular Development. *Stem Cell Reports*, 15(4), 855–868. <https://doi.org/10.1016/j.stemcr.2020.08.017>
2. Lancaster, M. A., Renner, M., Martin, C.-A., Wenzel, D., Bicknell, L. S., Hurles, M. E., Homfray, T., Penninger, J. M., Jackson, A. P., & Knoblich, J. A. (2013). Cerebral organoids model human brain development and microcephaly. *Nature*, 501(7467), 373–379. <https://doi.org/10.1038/nature12517>
3. Passaro, A. P., & Stice, S. L. (2021). Electrophysiological Analysis of Brain Organoids: Current Approaches and Advancements. *Frontiers in Neuroscience*, 14(January), 1–13. <https://doi.org/10.3389/fnins.2020.622137>
4. Putzeys, J., Lopez, C. M., Berti, L., Firrincieli, A., Van Den Bulcke, C., Wang, S., Chun, H. S., Van Helleputte, N., Braeken, D., Weijers, J.-W., & Reumers, V. (2018). A Multimodal CMOS MEA for High-Throughput Intracellular Action Potential Measurements and Impedance Spectroscopy in Drug-Screening Applications. *IEEE Journal of Solid-State Circuits*, 53(11), 3076–3086. <https://doi.org/10.1109/jssc.2018.2863952>
5. Trujillo, C. A., Gao, R., Negraes, P. D., Gu, J., Buchanan, J., Preissl, S., Wang, A., Wu, W., Haddad, G. G., Chaim, I. A., Domissy, A., Vandenberghe, M., Devor, A., Yeo, G. W., Voytek, B., & Muotri, A. R. (2019). Complex Oscillatory Waves Emerging from Cortical Organoids Model Early Human Brain Network Development. *Cell Stem Cell*, 1–12. <https://doi.org/10.1016/j.stem.2019.08.002>

Low-distortion CMOS neural preamplifier for high-channel-count neuroelectronic interfaces

Beata Trzpil-Jurgielewicz,^a Władysław Dąbrowski,^a Paweł Jurgielewicz,^a Ewa Kublik,^b Piotr Wiącek,^a Paweł Hottowy^{a,*}

- a. Faculty of Physics and Applied Computer Science, AGH University of Science and Technology, al. A. Mickiewicza 30, 30-059 Krakow, Poland
- b. Nencki Institute of Experimental Biology, Polish Academy of Sciences, ul. Pasteura 3, 02-093 Warszawa, Poland

* hottowy@agh.edu.pl

Multichannel CMOS neural amplifiers use high-value pseudoresistors for the high-pass filters to remove the electrode DC voltages [1]. The pseudoresistors are highly nonlinear and can cause large distortion for signals with high amplitudes and frequencies near the cutoff frequency of the filter [2]. Here we present electrical and electrophysiological measurements of a novel neural preamplifier with significantly improved pseudoresistor linearity that enables low-distortion amplification of the full spectrum of extracellular neural signals.

In our design, the pseudoresistor is built from two PMOS transistors. The gate-source voltages (V_{gs}) for both transistors are kept constant independently of the voltage drop across the pseudoresistor (figure 1a). Such a solution removes the main cause of the nonlinearity. The specific value of V_{gs} controls the cutoff frequency. It is generated as a voltage drop across 1 M Ω polysilicon resistor in contrast to MOSFET-based voltage shifters proposed before [2]. By changing the DC current in the polysilicon resistor between 300 and 450 nA one sets the cutoff frequency in the range 0.1 Hz-10 Hz. The preamplifier gain is 26 dB. Details of the circuit design and analysis of circuit distortion and noise have been presented in [3].

The test ASIC (Application Specific Integrated Circuit) was designed in 180 nm SOI CMOS technology (figure 1b). The measured characteristics of THD (Total Harmonic Distortion)-vs-frequency for 14 channels are shown in the figure 1c. Each curve shows a single maximum near the cutoff frequency which was set at 1 Hz. The height of the maximum increases for higher signal amplitudes and reaches 0.9% for the largest tested signal amplitude (10 mV peak-to-peak). The noise measured with Neuronexus A16 probe (177 μm^2 iridium sites) in 0.9% NaCl was 6.5 μV and 7.2 μV in the 1-300 Hz, 300 Hz–10 kHz frequency ranges respectively. These values are comparable with the current state-of-the-art performance reported in the literature [4]. The basic parameters of the preamplifier are summarized in figure 1d.

In a pilot electrophysiological experiment we used the test chip and Neuronexus A16 probe to record wide-band activity from the rat barrel cortex. We recorded high-amplitude (up to 5 mV) Local Field Potential in response to tactile whisker stimulation (figure 2a). Spontaneous spikes (up to about 1 mV) were also clearly visible (figure 2b).

The presented preamplifier offers low distortion (<1% THD) for the wide range of frequencies and amplitudes of neuronal signals. This feature is combined with competitive noise performance, low power consumption and small silicon area (figure 1c) is suitable for integration in high-channel-count neuroelectronic interfaces. The complete amplifier with a second gain stage and analog/digital converter is currently under development.

This work was supported by Polish National Science Centre grant DEC-2013/10/M/NZ4/00268 (PH). B.T.-J, P.J. have been partially supported by the EU Project POWR.03.02.00-00-I004/16. B.T.-J. has been partly supported by the EU Project POWR.03.03.00-IP.08-00-P13/18 PROM NAWA.

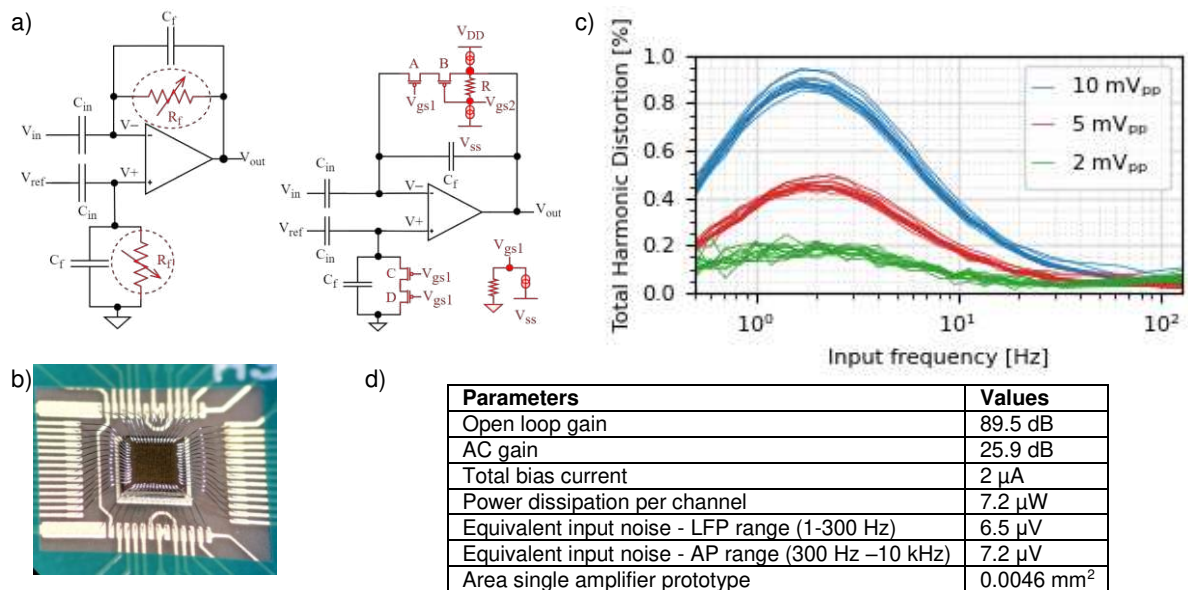


Figure 1: a) Architecture of an AC-coupled amplifier and design of the preamplifier with fixed- V_{gs} architecture using polysilicon resistor; b) Photograph of the ASIC mounted on the evaluation board c) Measured THD vs. frequency with 1 Hz cutoff frequency for various input signal amplitudes; d) Measured basic parameters of the amplifier.

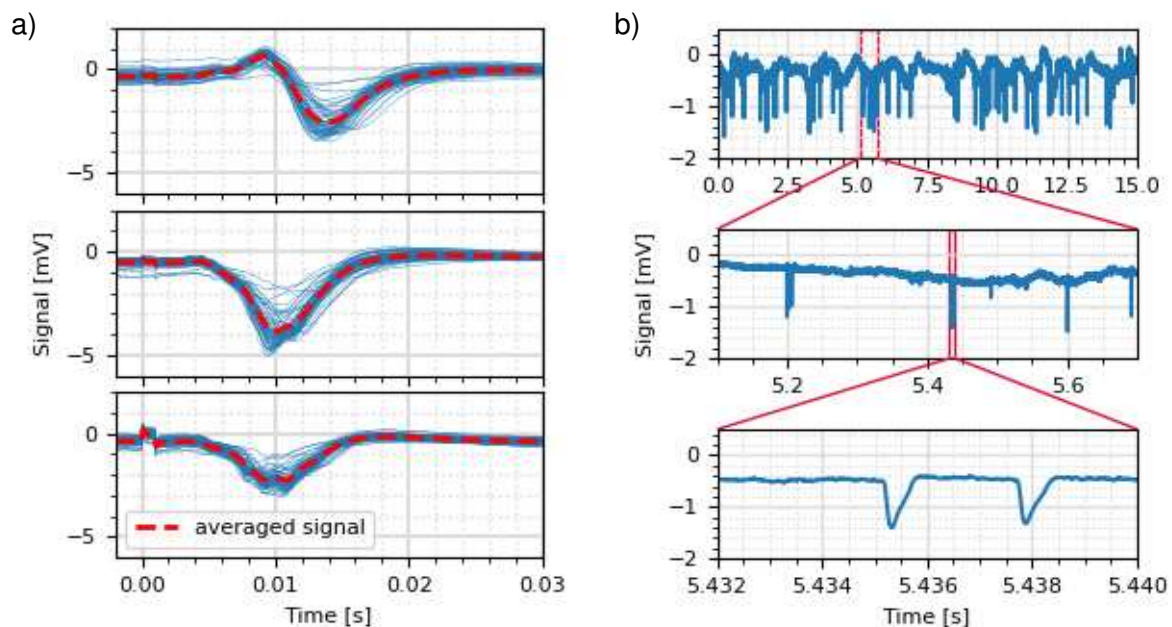


Figure 2: a) Data from three channels showing LFP signals evoked by tactile whisker stimulation in in upper, middle and deep cortical layers; b) Spontaneous data from one channel showing slow waves and spiking activity.

References

- Harrison, R. R., & Charles, C. (2003). A low-power low-noise CMOS amplifier for neural recording applications. *IEEE Journal of solid-state circuits*, 38(6), 958-965.
- Kassiri, H., Abdelhalim, K., & Genov, R. (2013, October). Low-distortion super-GOhm subthreshold-MOS resistors for CMOS neural amplifiers. In *2013 IEEE Biomedical Circuits and Systems Conference (BioCAS)* (pp. 270-273). IEEE.
- Trzpił-Jurgielewicz, B., Dąbrowski, W., & Hottowy, P. (2021). Analysis and Reduction of Nonlinear Distortion in AC-Coupled CMOS Neural Amplifiers with Tunable Cutoff Frequencies. *Sensors*, 21(9), 3116.
- Jun, J. J., Steinmetz, N. A., Siegle, J. H., Denman, D. J., Bauza, M., Barbarits, B., ... & Harris, T. D. (2017). Fully integrated silicon probes for high-density recording of neural activity. *Nature*, 551(7679), 232-236.

CMOS-compatible fabrication of vertical nanoneedles for an optimized intracellular in vitro cell contact

Sonja Allani,^a [Andreas Pickhinke](mailto:Andreas.Pickhinke@uni-due.de),^{a,b*} Karsten Seidl,^{a,b,**} Holger Vogt^{a,b}

- a. Fraunhofer Institute for Microelectronic Circuits and Systems, Duisburg, Germany
- b. Department of Electronic Components and Center for Nanointegration Duisburg-Essen (CENIDE), University Duisburg-Essen, Duisburg, Germany

* Andreas.Pickhinke@uni-due.de, ** Karsten.Seidl@ims.fraunhofer.de

Motivation

The use of vertical hollow nanostructures can provide intracellular access for various biomedical applications such as drug delivery or recording of electrical activity. The combination of CMOS circuitry with vertical nanoelectrodes enables a time and spatially resolved visualization of large cell networks in vitro. Due to the large seal resistance of the penetrating electrodes, signals generation and propagation can be observed with single cell resolution and sub-threshold sensitivities. To achieve an adhesion-based penetration and stability of the electrode-cell contact, a sub-micrometer nanostructure diameter is necessary due to the resulting bending of the cell membrane [1,2]. It has been shown that hollow geometry of the nanoelectrodes favors the long-term stability of the electrode-cell coupling [3]. Here, a CMOS-compatible fabrication approach for an optimized intracellular contact made in vertical hollow nanoelectrodes with a partially encapsulated shaft.

Materials and Methods

Hollow geometry structures are formed by a combination of deep reactive ion etching (DRIE) in sacrificial silicon and atomic layer deposition (ALD) in the generated template (see Figure 1). A planar (CMOS)-MEA is covered with undoped silicon glass (USG) and Ta₂O₅ by using chemical vapor deposition (CVD) and ALD, respectively. A CVD-deposited sacrificial layer stack consisting of two silicon layers and an oxide separation layer is structured via DRIE. The resulting template is matched via highly conformal ALD of Ta₂O₅ as a passivation material. After physical removal of the surface and bottom dielectric, the electrode material Ru is deposited by ALD. The removal of the horizontal metal surface results in vertical nanoelectrodes with an oxide encapsulation embedded in a sacrificial layer. The release of the embedded electrodes is performed in three steps to chemically remove the upper part of the encapsulation while the lower part is protected by the sacrificial layer. Furthermore, this process approach can be adapted to enable drug delivery. By leaving out the planar MEA, the physical removal of the bottom dielectric can be used to access the silicon substrate below the structures, where cavities can be etched as microfluidic channels from both sides.

Results and Discussion

The described method uses standard microsystem technology processes on 200-mm silicon wafers and i-line lithography. It could be shown that the developed method is suitable to fabricate the desired structures (see Figure 2) in a highly reproducible manner. Furthermore, the general feasibility for drug delivery with a simplified structure can be shown.

Conclusion and Outlook

The developed technique combines standard semiconductor techniques to create vertical hollow nanostructures. Utilizing etching properties of different materials during chemical release allows the nanostructures to be encapsulated at a precisely defined height. The monolithically integrated process can be easily adjusted to tune the height, size, shape and encapsulation of the nanoelectrodes. This allows future work to investigate the geometry for optimized nanoelectrode-cell contact.

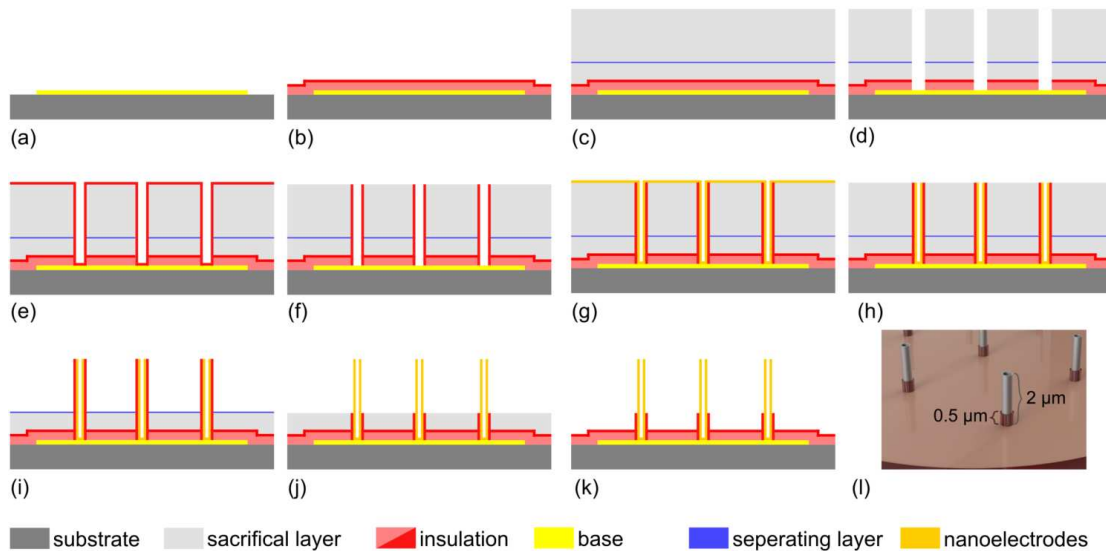


Figure 1 Scheme of the fabrication process for vertical nanoelectrodes. (a) Planar base electrode, (b) CVD and ALD of insulation, (c) CVD of sacrificial layer stack (d) DRIE, generating cylindrical holes in sacrificial layer stack, (e) ALD of the shaft insulation material, (f) oxide DRIE results in remaining oxide cylinders, embedded in sacrificial layer stack, (g) ALD of the electrode material, (h) ICP of the metal surface, (i)-(k) isotropic removal of sacrificial silicon and oxides, respectively, (l) 3D-scheme of the resulting vertical nanostructures.

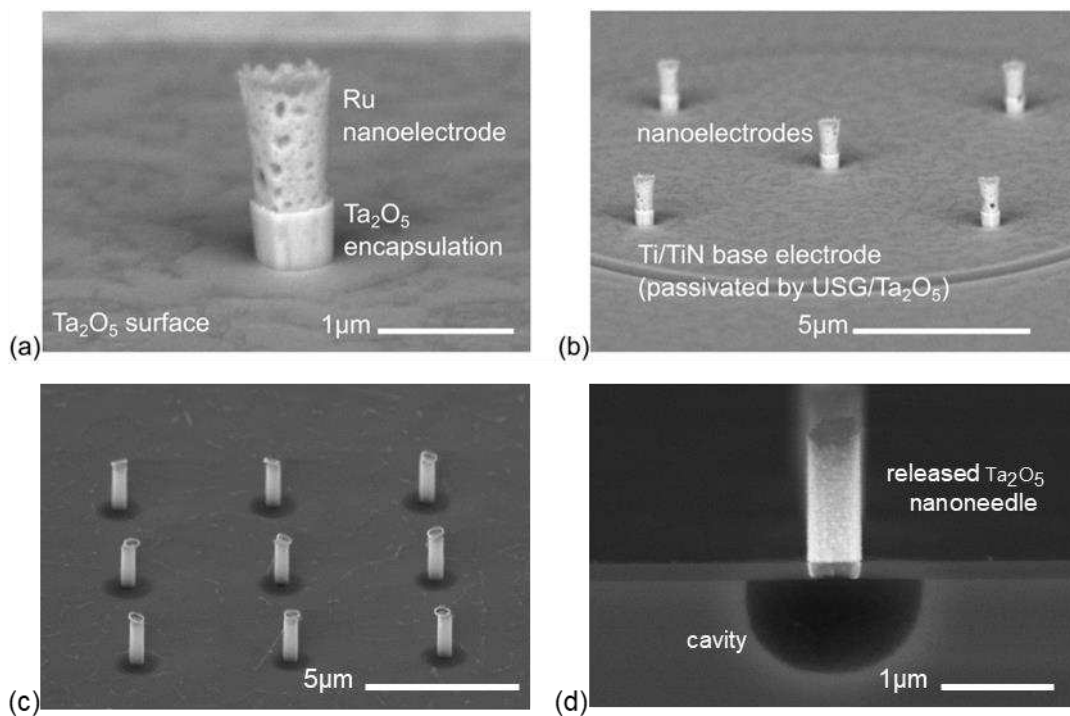


Figure 2 SEM images of (a) a vertical Ru nanoelectrode which is partially encapsulated by a Ta_2O_5 passivation layer, (b) an array of five nanoelectrodes, precisely aligned on a planar Ti/TiN base electrode which is electrically decoupled by USG/ Ta_2O_5 passivation layers, (c) array of passive Ta_2O_5 nanoneedles with an underlying cavity, (d) cross section through the cavity below a nanoneedle for the feasibility study on drug delivery.

References

1. Capozza R et al. 2018. Cell membrane disruption by vertical micro-/nanopillars: Role of membrane bending and traction forces. *ACS Appl Mater Interfaces*. 10:29107-29114.
2. Dipalo M et al. 2018. Cells adhering to 3D vertical nanostructures: Cell membrane reshaping without stable internalization, *Nano Lett*. 18:6100-6105.
3. Lin ZC et al. 2014. Iridium oxide nanotube electrodes for sensitive and prolonged intracellular measurement of action potentials, *Nat Commun*. 5, 3206.

A Low-Noise CMOS MEA with 4k Recording Sites, 4k Recording Channels, and 1k Stimulation Sites

Timo Lausen^a, Stefan Keil^a, Norman Dodel^a, Andrea Corna^{b,c},
Andreea-Elena Cojocaru^{b,c}, Thoralf Hermann^b, Peter Jones^b, Andreas Grall^d,
Peter Jesinger^d, Dieter Patzwahl^d, Jannis Meents^d, Christoph Jeschke^d, Günther Zeck^{b,c},
and Roland Thewes^a

- a. Chair of Sensor and Actuator Systems, Faculty of EECS, TU Berlin, Berlin, Germany
- b. NMI Natural and Medical Sciences Institute at the University of Tübingen, Reutlingen, Germany
- c. Institute of Biomedical Electronics, TU Wien, Vienna, Austria
- d. Multi Channel Systems MCS GmbH, Reutlingen, Germany

timo.lausen@tu-berlin.de

In [1], a user-friendly system was published to operate CMOS MEAs with 65 x 65 recording sites and 32 x 32 stimulation sites. There, the array sizes of the respective CMOS MEAs are 1 x 1 mm² and 2 x 2 mm², respectively. Directly underneath each recording site two MOSFETs are located, one for voltage-to-current conversion of the recorded signals, the other one for biasing purposes. This approach forms the recording array which is controlled and supported by some additional circuitry outside the active area. A second array for stimulation purposes is overlaid consisting of a daisy chain of D-Flip-Flops to shift and provide the logic information concerning the application of stimulation signals to the respective stimulation sites. By means of stimulation site related transmission gates one out of three stimulation signals can be applied to the respective site or the site can be left floating.

Aiming for CMOS MEAs which are compatible to the current system but provide larger active areas at lower recording noise levels, modified designs have been fabricated. Electrically they behave identically to the devices published in [1], have the same electrical, mechanical, and fluidic interfaces, the same electrical instruction set, but internally they use a different architecture and a different circuit design approach for the recording part. Whereas the stimulation array is copied from [1], recording circuitry is now arranged outside the active array. This provides more area per recording channel and allows for increased design freedom. The recorded signals from the active area are guided by metal interconnect lines to two arrays of low-noise amplifiers located left and right of the active recording array (Fig. 1). To avoid cross-talk between neighboring signal interconnects an on-chip shielding method is applied. At the outputs of the respective amplifiers (operated in the voltage domain) V-to-I conversion is performed to achieve electrical compatibility with the available system [2]. An assembled device – looking very similar to the devices from [1] - is shown in Fig. 2.

The new chips are fabricated in a 180 nm standard CMOS process with six metal layers as in [1], however, additionally here low-noise (buried channel) MOSFETs are used which had not been available earlier. Two versions of devices are available with an active area of 2.3 x 2.3 mm² resp. 4.1 x 4.1 mm², a recording site pitch of 36 μm resp. 64 μm, and a stimulation site pitch of 72 μm resp. 128 μm.

Measured noise in the LFP band from 1Hz to 300Hz and in the AP band from 300 Hz to 3 kHz is below 11 μVrms in both cases (n=6 chips). Interfacing and recording of ex vivo retina or of brain slices leads to measured noise in the AP band of 15.6 μVrms still providing excellent signal-to-noise ratios of the recorded action potentials.

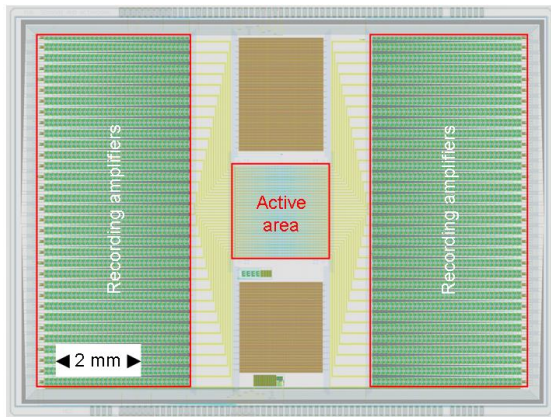


Fig. 1: Floor plan of one of the new CMOS MEA chips with an active recording / stimulation area of 2.3 x 2.3 mm². The major blocks, the active recording and stimulation array and the two arrays with recording amplifiers, are highlighted.

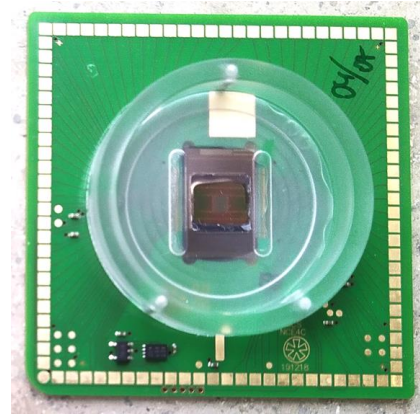


Fig. 2: Assembled chip with an active recording / stimulation area of 2.1 x 2.1 mm². Assembly technique and electrical interface same as in [1].

References

1. G. Bertotti et al., "A CMOS-based sensor array for in-vitro neural tissue interfacing with 4225 recording sites and 1024 stimulation sites", 2014 IEEE Biomedical Circuits and Systems Conference (BioCAS) Proceedings, 2014, pp. 304-307, doi: 10.1109/BioCAS.2014.6981723.
2. <https://www.multichannelsystems.com/products/cmos-mea5000-system>

Acknowledgements

Funding of this project by the German Ministry for Education and Research (FKZ: 161L0059), European Union's Horizon 2020 program (grant agreement No 861423), and by the State Ministry of Baden-Wuerttemberg for Economic Affairs, Labor and Tourism is gratefully acknowledged.

Memristive device integration on CMOS MEA chips for neural activity detection

Onur Toprak^{a,b}, Florian Maudet^a, Roland Thewes^b, Catherine Dubourdieu^{a,c}, and Veeresh Deshpande^a

- a. Institute Functional Oxides for Energy-Efficient Information Technology (EM-IFOX), Helmholtz-Zentrum Berlin für Materialien und Energie, 14109 Berlin, Germany
- b. Chair of Sensor and Actuator Systems, Faculty of EECS, Technische Universität Berlin, Berlin, Germany
- c. Freie Universität Berlin, Physical Chemistry, Berlin, Germany

onur.toprak@helmholtz-berlin.de

The recording of neural activity plays a key role in understanding the brain's functionality. Recent developments in CMOS MEA technology have enabled recording neural signals with high spatiotemporal resolution as well as electrical stimulation. They have opened new avenues for neuroscience research and development of neuroprosthetics. Further advancements in neuroprosthetics require CMOS MEA chips that are energy efficient, can perform high throughput signal processing in real-time (such as spike detection and sorting), and provide feedback stimulation. Recently, FPGA-based signal processing has been demonstrated for this purpose [1]. However, this approach suffers from high power consumption and large area requirements due to a large number of RAM blocks. Therefore, it is necessary to develop energy efficient CMOS MEA chips with a huge amount of on-chip memory. In recent years, memristive devices have attracted significant attention as power efficient, highly scalable memories providing the potential for in-memory computing. Their intrinsic ability of gradual resistance change can be utilized to perform logic operations as well as data storage. By combining memristive device arrays with CMOS MEAs, one can envision a low power platform for real-time neural activity detection and stimulation. Our research project entitled 'MEMMEA' is aiming to demonstrate such a platform by integration of memristive devices in back-end-of-line (BEOL) processes of CMOS MEA chips. We intend exploiting the resistive state modulation of memristive devices to perform on-chip spike sorting and spike summation. The resistance of a memristor can be changed by applying a sequence of write pulses. By optimizing pulse width and voltage amplitude, one can obtain multiple stable resistance states. Therefore, the neural spikes can be adapted (by amplifying their amplitude to the required write voltage level) and applied to the memristor to change its resistance. By measuring the resistance change, one can detect the number of spikes, thus achieve signal summation. The occurrences in time of the resistance changes can be utilized for spike sorting. This concept was first introduced by I. Gupta et al. [2], where a CMOS MEA chip was used for signal recording while the signals to a single memristor device were applied externally.

In this work, we will discuss concepts and strategies to develop a hybrid memristor-CMOS MEA by fabricating the memristor device on top of a CMOS chip in order to build a platform for neural activity detection. One of the major steps is the development of the BEOL integration of memristive devices, as well as optimization of their electrical characteristics for spike sorting. The memristive devices usually consist of metal/insulator/metal (MIM) sandwich structures. We will discuss memristive devices based on Cu/SiO₂/W (conductive bridge random access memory, CBRAM) and Ti/HfO₂/W (oxide random access memory, OxRAM) stacks as they are compatible with BEOL integration. Cu/SiO₂/W CBRAM devices can switch under very low voltage conditions ($V_{\text{set}} \sim 250$ mV, $V_{\text{reset}} \sim 80$ mV) and therefore exhibit low power operation [3]. Likewise, HfO₂ based OxRAM devices exhibit reliable switching performance at operation voltages below 1 V as well and fast switching speed (<100 ns) [4]. Fig. 1 (a) shows an optical microscope image of a typical HfO₂ based OxRAM device, Fig. 1 (b) depicts typical resistance

switching characteristics of such a device. The electrical characteristics and intrinsic switching mechanisms of both stacks will be highlighted. The critical parameters required for neural signal processing, such as endurance, retention time, memory window, and switching time will be considered for both types of memristive devices. As the recorded neural signals consist of extremely low voltage (few μV to mV), they need to be converted to appropriate amplitudes and pulse widths to trigger resistance changes in memristive devices. The required programming conditions to achieve spike sorting in the two stacks will also be discussed.

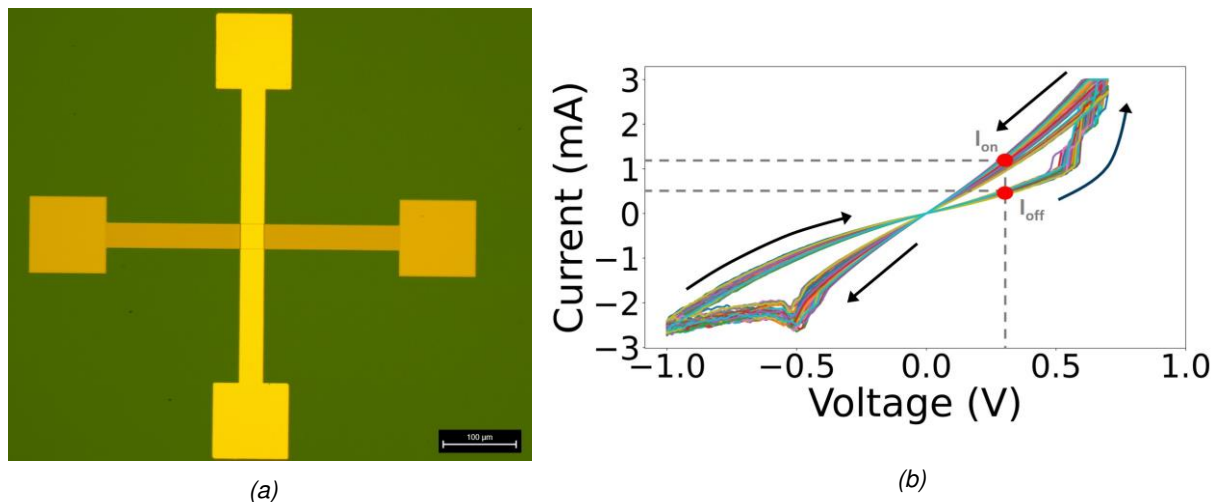


Figure 1a: Optical microscope image of typical HfO_2 based OxRAM device. Figure 1b: The I-V measurements carried out for 100 switching cycles are shown. The arrows represent the direction of the voltage sweep in each full cycle. ON and OFF current levels are marked to show the memory window.

References

1. Schäffer, L., Nagy, Z., Kincse, Z., Fiáth, R. and Ulbert, I (2021), Spatial Information Based OSort for Real-Time Spike Sorting Using FPGA, *IEEE Transactions on Biomedical Engineering*, 68(1), 99-108, Doi: 10.1109/TBME.2020.2996281
2. Gupta, I., Serb, A., Khiat, A., Zeitler, R., Vassanelli, S., & Prodromakis, T. (2016). Real-time encoding and compression of neuronal spikes by metal-oxide memristors. *Nature communications*, 7(1), 1-9. Doi: 10.1038/ncomms12805
3. Nandakumar, S. R., Minvielle, M., Nagar, S., Dubourdieu, C., & Rajendran, B. (2016). A 250 mV $\text{Cu}/\text{SiO}_2/\text{W}$ memristor with half-integer quantum conductance states. *Nano letters*, 16(3), 1602-1608. Doi:10.1021/acs.nanolett.5b04296
4. Daniele Ielmini (2016), Resistive switching memories based on metal oxides: mechanisms, reliability and scaling, *Semiconductor Science and Technology*, 31, 063002. Doi: 10.1088/0268-1242/31/6/063002

Electrochemical Measurement Platform within Multi-functional High-density Microelectrode Array

Chloe Magnan^a, [Hasan Ulsan](#)^a, Roland Diggelmann^a, and Andreas Hierlemann^a

^aETH Zürich, Department of Biosystems Science and Engineering, Switzerland

hasan.ulsan@bsse.ethz.ch

Many neuroscientific questions can be addressed by studying highly interdependent processes, such as the exact timing and occurrence of single-cell action potentials, their propagation speed and trajectories along axons, the release of neurotransmitters at synapses, cell densities, tissue properties and surface adhesion. Measuring these properties simultaneously at sufficient spatial and temporal resolution poses a major challenge. Our group has developed a multi-functional high-density microelectrode array that can be used to simultaneously perform impedance imaging, electrophysiological recordings and electrochemical measurements (EMs) [1]. Here we present a graphical user interface (GUI) that gives experimenters access to all these functionalities in an intuitive way. We demonstrate the performance through EMs of known concentrations of sulfuric acid.

To perform EMs, a voltage is applied between a working and a reference electrode. By sweeping the voltage, a redox reaction is induced at the electrode, and the Faradaic current at the electrode-liquid interface is detected by reading out current variations at the working electrode. Cyclic Voltammetry (CV) and Fast Scan Cyclic Voltammetry (FSCV) can be applied for electrochemical characterization. During CV, the potential difference is ramped up linearly. CV is optimized to measure analyte concentrations, oxidation and reduction potentials. FSCV is based on the same principle but includes a faster scan rate ($>100 \text{ Vs}^{-1}$) to provide high resolution and, potentially, chemical specificity.

To measure interdependent phenomena with multifunctional devices, experimenters need an easy-to-use application to test many parameters in a limited time. With a GUI, coded with the pyqt5 library of Python (Fig. 1), the user has the possibility to change: (i) hardware parameters, such as amplifier gain, (ii) electrode arrangement or (iii) input voltage. In addition, the GUI can be used to visualize cyclic voltammogram curves. This data representation is essential for a convenient interpretation of CV and FSCV results. In the window "Pulse Generator" (Fig. 1 A) the experimenter can select input voltage parameters and create command sequences. These are then displayed at the right side where the user can select them to run an experiment, stop it and save the data and parameters. In the application "Results Window", electrode arrangements (Fig. 1 C), recorded raw data (Fig. 1 D) and cyclic voltammograms (Fig. 1 B) can be displayed and saved. Various outputs can be displayed in the same plot to compare and detect concentration changes.

Fig. 2 shows the results obtained during a measurement of 0.5 M sulfuric acid (H_2SO_4) solution. In this experiment, the 28 EM units of the multifunctional chip are connected to randomly selected electrodes. A potential difference is varied at a constant rate of 5 Vs^{-1} , between -1.2 V and 0.7 V. The CV curves show two reactions that are known to occur at the interface between platinum and an acidic electrolyte [2]: first, a redox reaction between hydrogen and platinum and then, a redox reaction between oxygen and platinum.

We present an easy-to-use method to perform EM experiments with a multi-functional HD-MEA. In our experiments we observed electrode-to-electrode variations and drift over time. These effects have to be characterized and further improved in order to detect very small concentration changes that are biologically relevant. The multi-functional HD-MEA will be used to detect neurotransmitters with electroactive properties, such as dopamine or serotonin, which are essential to the proper functioning of our brain. The detection of these neurotransmitters in conjunction with electrophysiological recordings and impedance imaging will provide new insights into their role in network interactions.

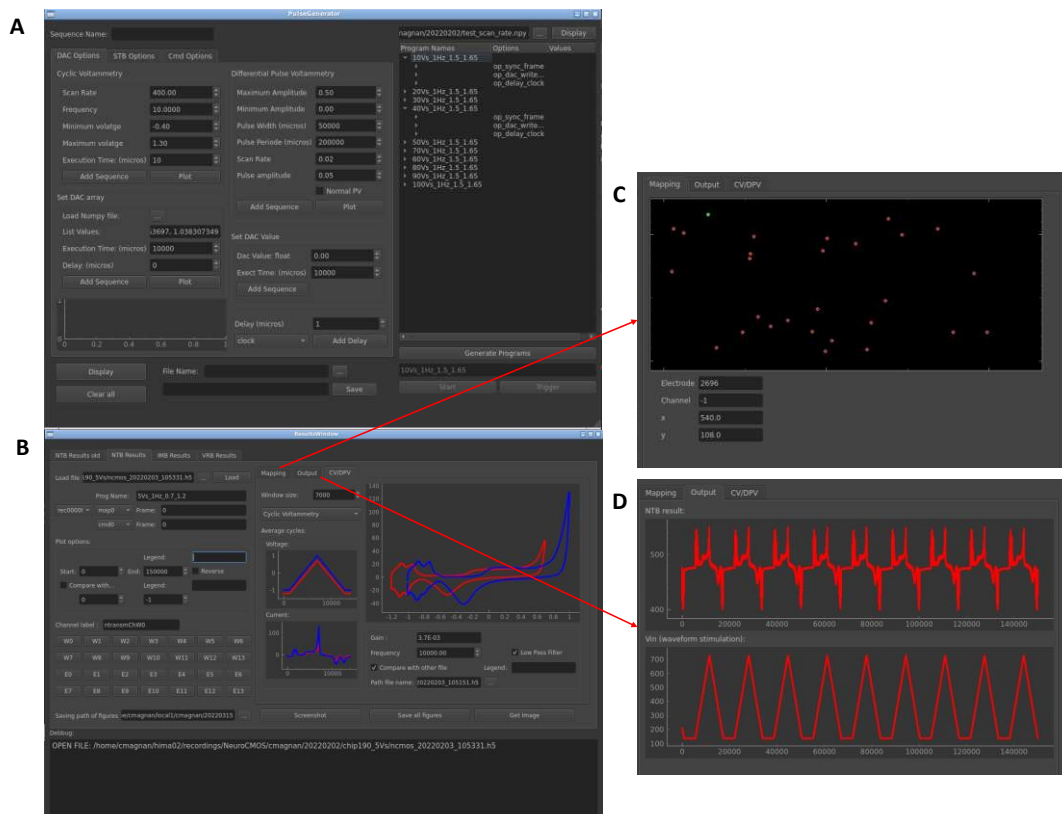


Figure 1: Graphical user interface for the control and analysis of electrochemical measurements. (A) "Pulse Generator" application used to set experimental parameters. (B) "Result Reader" application used to visualize the recorded data (right plot: cyclic voltammogram), (C) selected electrode configuration and (D) raw data traces.

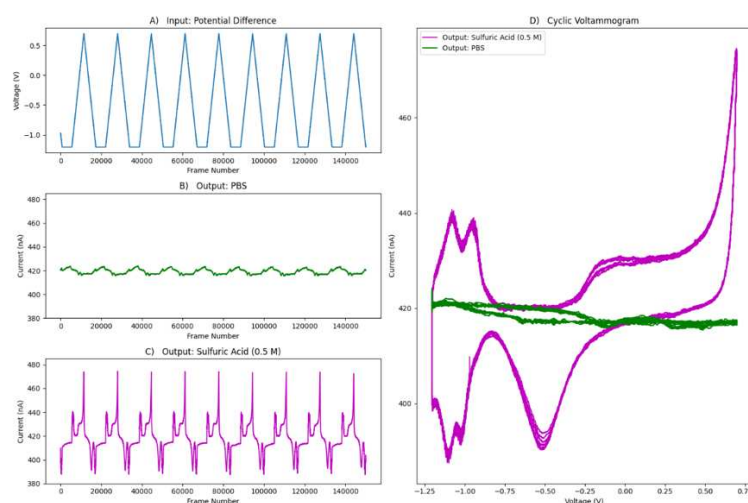


Figure 2: CV signals measured at one electrode at a scan rate of 5Vs^{-1} and a potential ranging between -1.2V and 0.7V . (A) Applied input voltage. (B) Measured current in buffer solution PBS. (C) Measured current in 0.5 M sulfuric acid (H_2SO_4). (D) Cyclic voltammogram of data from (A) to (C).

Acknowledgements

This work was supported by the European Union through the European Research Council (ERC) Advanced Grant 694829 'neuroXscales' and the Swiss National Science Foundation under contract 205320_188910 / 1.

References

- [1] J. Dragas et al., in JSSC, vol. 52, no. 6, pp. 1576-1590, Jun 2017.
- [2] P. Daubinger et al. in Royal Society of Chemistry, vol. 16, pp. 8392, Mar 2014.

A new CMOS-electrode-array-based impedance sensor integrated into an open microfluidic platform

Raziyeh Bounik ^a, Fernando Cardes ^a, Vijay Viswam ^b, Mario M. Modena ^a, Andreas Hierlemann ^a

a. Department of Biosystems Science and Engineering, ETH Zurich, Basel, Switzerland

b. MaxWell Biosystems AG, Zürich, Switzerland

* Raziyeh.bounik@bsse.ethz.ch

Motivation

Compared to traditional two-dimensional (2D) cell cultures, three-dimensional (3D) microtissues and organoids more accurately replicate in-vivo physiological conditions, e.g., cell-cell interaction and density gradients [1]. Open microfluidic hanging-drop platforms are used to culture microtissues or organoids at the air-liquid interface, while the nutrients are supplied through microfluidic channels interconnecting the hanging droplets [2]. However, tissue monitoring in the drops relies on microscope-image acquisition to characterize tissue size and growth. To provide continuous characterization of the tissue size and properties, we integrated a new complementary metal oxide semiconductor (CMOS) impedance sensor platform into the hanging-drop network for in-situ measurements.

Materials and Methods

The microfluidic hanging-drop system was fabricated from PDMS by using a double-sided molding process. To integrate the CMOS sensor into the hanging-drop platform, we first glued the CMOS chip onto a glass substrate featuring metal contact traces. We then plasma-bonded the microfluidic structure onto the substrate and connected the metal traces on the glass substrate to the CMOS chip via bond wires, which were then covered with epoxy for protection and stability. Finally, inlet and outlet holes were drilled into the glass substrate and metallic needles were aligned and affixed for fluidics inlet and outlet [3].

Results

To characterize the performance of the CMOS impedance sensor platform, we loaded a 700 μm -diameter glass bead in the hanging drop below the sensor (Figure 1.a) We then acquired impedance measurements at 100 kHz using two pseudo electrodes, which were formed from the electrodes of the array at the side and at the center using a reference electrode, placed along one side of the electrode array. Impedance measurements were taken at different drop heights (Figure 1.b). As depicted in Figure 1.c, impedance values recorded from the side electrode remained essentially constant for all drop sizes, as they mostly depended on the medium conductivity. In contrast, the impedance between the center and reference electrodes significantly increased as the drop height was reduced, as the dielectric bead affected the current distribution between the electrodes.

Summary and conclusion

Here we showed the integration of a CMOS impedance sensor platform in an open-microfluidic hanging-drop network. Impedance measurements from sensing electrodes at the side and center of the array enabled us to sense the medium conductivity and the electrode-to-sample distance.

Acknowledgements

Financial support through MHV Grant 171267 and ERC Advanced Grant 694829 “neuroXscales” are acknowledged.

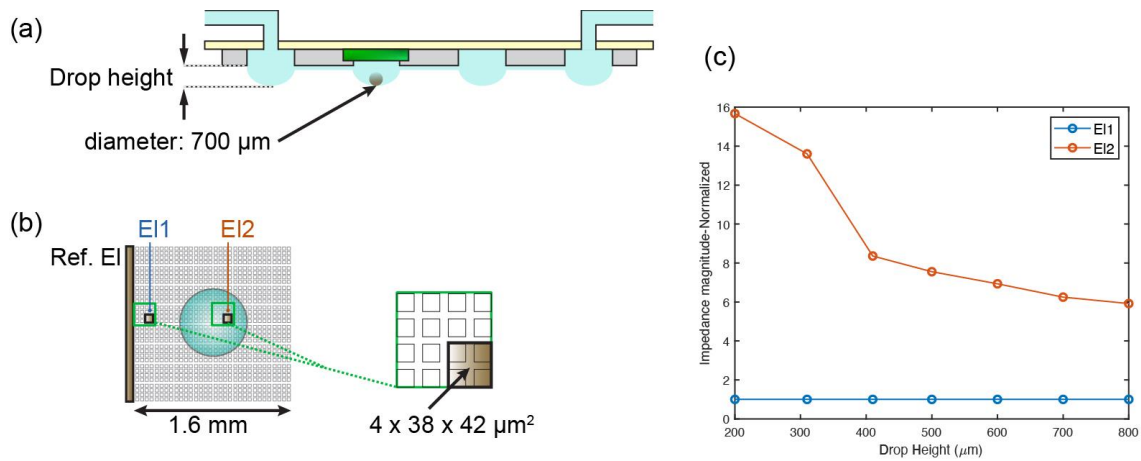


Figure 1: (a) Hanging-drop platform with a glass bead in the sensing droplet, (b) bottom view of the electrode array indicating reference and sensing pseudo-large electrodes, used for the impedance measurements, (c) impedance measurements conducted at 100 kHz at different drop heights

References

1. H. Clevers, "Modeling Development and Disease with Organoids," *Cell*, vol. 165, no. 7, pp. 1586–1597, 2016, doi: 10.1016/j.cell.2016.05.082.
2. O. Frey, P. M. Misun, D. a Fluri, J. G. Hengstler, and A. Hierlemann, "Reconfigurable microfluidic hanging drop network for multi-tissue interaction and analysis.," *Nat. Commun.*, vol. 5, no. May, p. 4250, 2014, doi: 10.1038/ncomms5250.
3. R. Bounik, M. Gusmaroli, P. M. Misun, V. Viswam, A. Hierlemann, and M. M. Modena, "Integration of Discrete Sensors and Microelectrode Arrays into Open Microfluidic Hanging-Drop Networks," *Proc. IEEE Int. Conf. Micro Electro Mech. Syst.*, vol. 2019-Janua, no. January, pp. 441–444, 2019, doi: 10.1109/MEMSYS.2019.8870732.

Tracking Axon Initial Segment Plasticity using high-density microelectrode arrays: A Computational Study

Tobias Gänswein,^{a*} Sreedhar S Kumar,^{a*} Alessio P Buccino,^a Vishalini Emmenegger,^a Andreas Hierlemann^a

- a. Bio Engineering Laboratory, Department of Biosystems Science and Engineering, ETH Zürich, Basel, Switzerland

* tobias.gaenswein@bsse.ethz.ch; sreedhar.kumar@bsse.ethz.ch

Despite being composed of highly plastic neurons with extensive positive feedback, the nervous system maintains stable overall function. To keep activity within bounds, the nervous system relies on mechanisms collectively termed “homeostatic plasticity”. Homeostatic changes involve the regulation of synaptic inputs and/or intrinsic neuronal excitability. Homeostatic changes of neuronal excitability were recently found to be concomitant with structural changes at the axon initial segment (AIS), a microdomain located at the proximal end of the axon and the initiation site of action potentials (AP) [1]. Studies have shown that the position and length of the AIS may vary in an activity-dependent manner, thereby suggesting that they could play a crucial role in regulating intrinsic neuronal excitability and – consequently – in fine-tuning activity in the network [2,3].

Current approaches to investigate structural plasticity of the AIS have major limitations [4]. Most studies compare the statistics of the AIS’s structural metrics between snapshots of control networks and networks that have been perturbed and allowed to homeostatize over a fixed duration. The use of global or summary measures fails to account for neuronal heterogeneity present in each population – in terms of cell types, somato-dendritic morphologies, and initial AIS locations – and obscures the contribution of individual neurons to network effects. High-density microelectrode arrays (HD-MEAs) with their high spatiotemporal resolution constitute a promising tool to overcome these limitations at increased experimental throughput. Extracellular electrical activity, recorded by these arrays, first needs to be analyzed using spike-sorting algorithms to assess the contributions of individual neurons. The high resolution of the array enables detailed spatial reconstruction of the extracellular electrical footprint (template) of single units (identified during spike-sorting) within which the AIS is in most cases localized near the electrodes recording high signal amplitudes [5]. However, tracking unit templates over hours and reliably inferring subtle microstructural changes from changes in a unit’s template is a formidable data-analysis challenge. Template changes arising from structural modifications of the AIS are difficult to predict, since the morphology of the proximal axon and its distance and orientation relative to the electrodes play crucial roles. Further, confounding factors like neuronal drift relative to the electrodes may also lead to template changes that could potentially be misleading.

In this study, we used sophisticated computational models to address these challenges by systematically elucidating the association between the AIS and extracellular footprints. We characterized changes in the extracellular electrical-potential landscape arising from structural changes of the AIS and explored the feasibility of reliably inferring structural changes from electrical extracellular multi-unit recordings. To this end, we used detailed multi-compartment models of single neurons with varying morphologies. The models featured AIS-specific ion-channel conductances, whose position within the neuron morphology was systematically altered. We generated APs by stimulating each model with constant currents and generated the corresponding extracellular recordings for the HD-MEA model using the LFPy package (Figure 1). We expect our *in silico* characterization to yield salient signatures of AIS plasticity in extracellular footprint changes. They may then be used to infer structural changes of the AIS in extracellular electrical recordings and facilitate high-throughput studies of AIS plasticity.

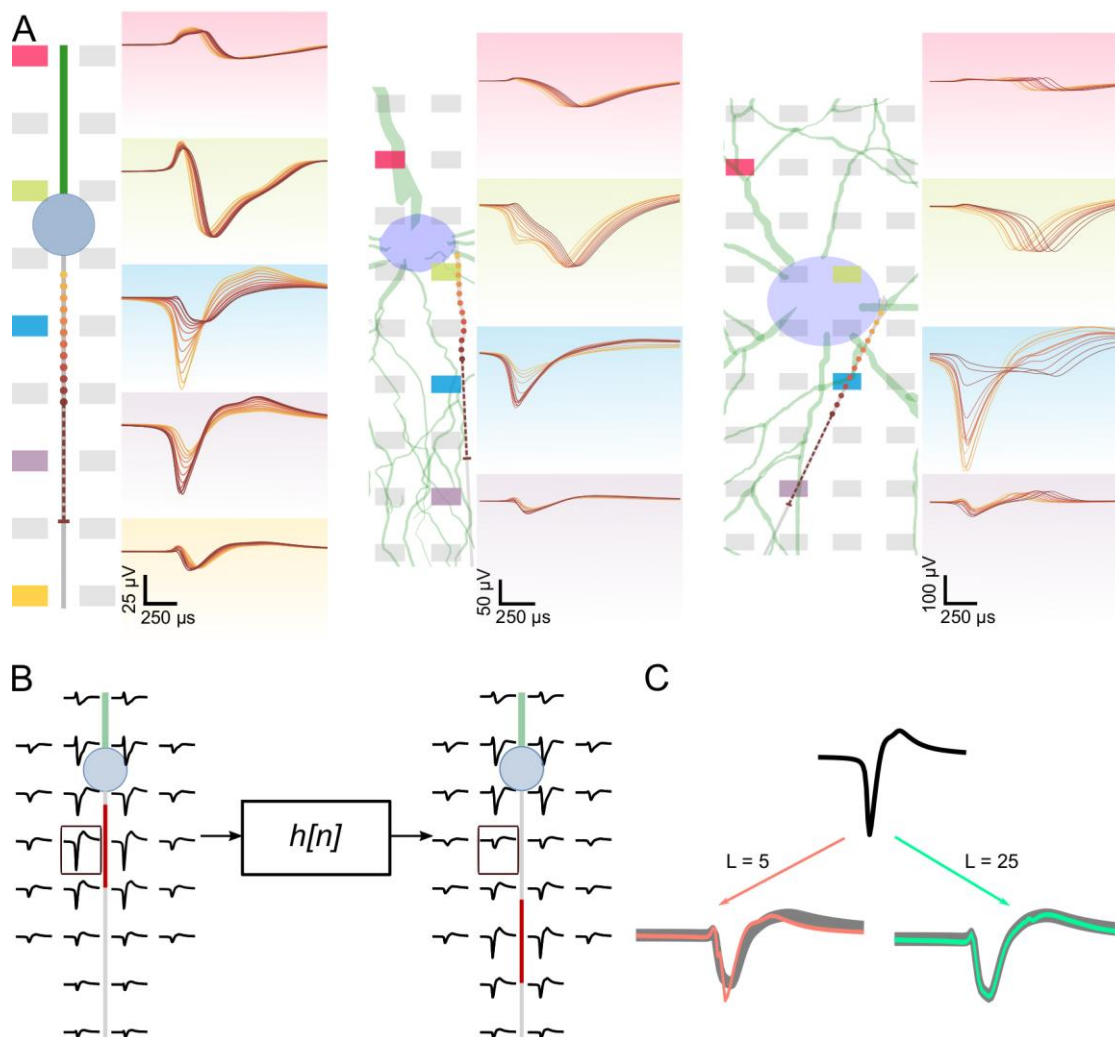


Figure 1. Action potential waveforms in the extracellular footprint of various neuronal models exhibited systematic changes as a result of AIS relocation. (A) Waveform cutouts at selected electrodes (colored pink, green, blue, purple and yellow) along the different neuronal models are shown for various AIS locations. Proximal AIS locations are indicated as colored dots along the axon (gray) and the colors represent distances to the soma. The dotted line represent the extent of the 30 μm long AIS for the most distal AIS position. (B) Footprint changes associated with AIS relocation were modeled as a set of m linear transformations each with an impulse response, $h_m[n]$, where m is the number of electrodes included in the footprint. Electrode-wise impulse responses of length $L = 25$ were estimated by computing the pseudo-inverse of the respective convolution matrices. (C) Waveform transformations mediated by AIS plasticity may be estimated using the corresponding impulse response functions. This is illustrated for a single electrode marked (black box) in (B). The baseline and transformed waveforms are shown in black and gray respectively. Overlays of transformed waveforms estimated using impulse response of lengths $L=5$ and 25 are shown in salmon and green respectively.

References

- [1] L.M. Palmer, G.J. Stuart, Site of Action Potential Initiation in Layer 5 Pyramidal Neurons, *J. Neurosci.* 26 (2006) 1854–1863. <https://doi.org/10.1523/JNEUROSCI.4812-05.2006>.
- [2] J. Lezmy, M. Lipinsky, Y. Khrapunsky, E. Patrich, L. Shalom, A. Peretz, I.A. Fleidervish, B. Attali, M-current inhibition rapidly induces a unique CK2-dependent plasticity of the axon initial segment, *Proc. Natl. Acad. Sci. U. S. A.* 114 (2017) E10234–E10243. <https://doi.org/10.1073/pnas.1708700114>.
- [3] M.S. Grubb, J. Burrone, Activity-dependent relocation of the axon initial segment fine-tunes neuronal excitability, *Nature.* 465 (2010) 1070–1074. <https://doi.org/10.1038/nature09160>.
- [4] A.S. Dumitrescu, M.D. Evans, M.S. Grubb, M. Engelhardt, P.M. Jenkins, K. Bender, Evaluating tools for live imaging of structural plasticity at the axon initial segment, *Front. Cell. Neurosci.* 10 (2016). <https://doi.org/10.3389/fncel.2016.00268>.
- [5] D.J. Bakkum, M.E.J. Obien, M. Radivojevic, D. Jäckel, U. Frey, H. Takahashi, A. Hierlemann, The Axon Initial Segment is the Dominant Contributor to the Neuron’s Extracellular Electrical Potential Landscape, *Adv. Biosyst.* 3 (2019) 1800308. <https://doi.org/10.1002/adbi.201800308>

High-throughput ground-truth validation of neuronal spike sorting algorithms

Xiaohan Xue,^{*} Alessio Paolo Buccino, Sreedhar Saseendran Kumar, Andreas Hierlemann¹ and Julian Bartram¹

ETH Zürich, Department of Biosystems Science and Engineering, Switzerland

*xiaohan.xue@bsse.ethz.ch

1. shared senior authorship

Spike sorting is an essential procedure to extract single-neuron spiking activity from extracellular electrical recordings, which is a mixture of signals from multiple neurons. To assess the performance of spike sorting algorithms, ground-truth data – where the true spiking times of individual underlying neurons are known – are necessary. However, existing strategies that rely on paired recordings via patch clamp and extracellular electrodes are low-throughput and provide ground-truth access only to a limited number of neurons [1, 2]. Here, we propose a high-throughput validation method that enables robust benchmarking of spike sorting tools by combining high-density microelectrode array (HD-MEA) recordings with fast voltage imaging. While the latter allows to monitor intracellular potentials from several neurons simultaneously, the HD-MEA technology provides the respective spontaneous extracellular spike times in a large-scale network. The proposed multimodal approach has unique advantages as i) it can provide simultaneous ground-truth access to numerous neurons, ii) it records complex network events (e.g., network bursts) that are required to address the well-known spike collision issue and iii) the non-invasive nature of the proposed method allows for long-term recording.

The complementary-metal-oxide-semiconductor (CMOS)-based HD-MEA recording unit was mounted under an upright spinning-disk confocal microscope equipped with a gated intensified high-speed camera (Lambert Instrument). The HD-MEA system employs 26'400 electrodes at pitch of 17.5 μm and allows simultaneous recording from up to 1'024 electrodes at 20 kHz. We plated primary rat hippocampal neurons onto the sensing area of the HD-MEA chip and expressed the chemigenetic voltage indicator (Voltron_{stg}) [3]. Typically, we recorded extracellularly from over 90% of the electrodes in the field of view at 20X magnification, while optically monitoring more than 10 neurons simultaneously. The acquired imaging and HD-MEA data were aligned using TTL pulses sent from the high-speed camera to the HD-MEA system. Voltage signals were extracted from regions of interest (ROI) around individual neurons, and the intracellular spikes were detected from the $\Delta F/F$ voltage traces. We then spike sorted the extracellular recordings with multiple spike sorters, and used the obtained ground-truth data to evaluate their performance (Figure 1).

We anticipate that with our proposed method and a standardized framework, the spike sorting developer community will be able to systematically benchmark the performance of existing spike sorters, in order to make spike sorting tools more reliable, robust, and efficient.

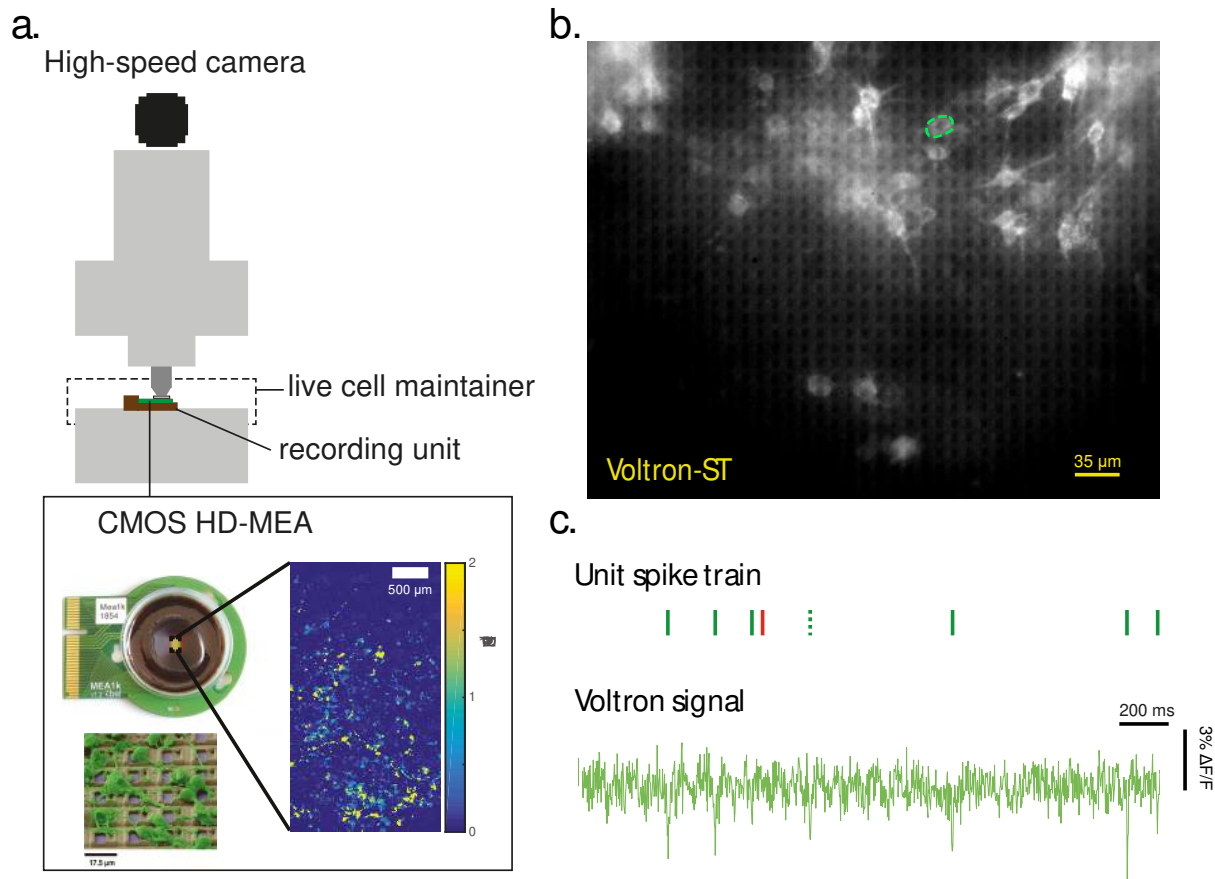


Figure 1. Method illustration. a) The experimental setup that we used to perform simultaneous large-scale voltage imaging and HD-MEA recordings. b) The intracellular voltage signals from multiple well-isolated neurons can be captured in the optical readout; an example neuron is highlighted in dashed green. c) Illustration of the validation of a unit identified after spike sorting the electrical readouts acquired at electrodes in the proximity of the example neuron. A direct comparison of the unit spike train and the voltage signal allowed us to identify spikes that were correctly assigned (solid green line), missed (dashed green line), or erroneously assigned to the neuron of interest (red line).

Acknowledgements: This work was supported by the ERC Advanced Grant 694829 'neuroXscales', the China Scholarship Council and the ETH Zurich Postdoctoral Fellowship 19-2 FEL-17.

References

1. Carlson, David, and Lawrence Carin. "Continuing progress of spike sorting in the era of big data." *Current opinion in neurobiology* 55 (2019): 90-96. doi: 10.1016/j.conb.2019.02.007
2. Buccino, Alessio, Samuel Garcia, and Pierre Yger. "Spike sorting: new trends and challenges of the era of high-density probes." (2022). doi: 10.31219/osf.io/jhau2
3. Abdelfattah, Ahmed S., et al. "Bright and photostable chemigenetic indicators for extended in vivo voltage imaging." *Science* 365.6454 (2019): 699-704. doi: 10.1126/science.aav6416

Spatiotemporally Resolved Neurogenic Computational Model

Erdem Altuntac^a, Xin Hu^a, Brett Addison Emery^a, Lorenzo Maugeri^a, Shahkrukh Khanzada^a, and Hayder Amin^{a*}

a. Biohybrid Neuroelectronics Laboratory (BIONICS), German Center for Neurodegenerative Diseases (DZNE), Tatzberg 41, 01307, Dresden, Germany

* Corresponding author: Hayder.Amin@dzne.de

The dentate gyrus (DG) in the hippocampus continuously produces new neurons throughout the lifetime of mammals [1]. However, the implication of adult hippocampal neurogenesis on memory encoding and information processing during learning has remained ambiguous. To decipher these complex biological processes, computational models and theoretical studies were reported to explore the computation implication of newly-generated neurons in the DG network [2]. These early established models can be categorized as abstract models that explore the neural function with restricted structural details and biologically based models with extended underlying anatomical and functional complexities. However, existing models only represent an abstraction of the underlying biological processes and conceal the large-scale spatiotemporal impact of the DG on the global hippocampal network; thus, outperforming the realistic circuit operation. We here present a novel feedforward computational model based on a multilayer perceptron oscillatory neural network (MLP-ONN) that incorporates interconnected hippocampal-cortical regions (i.e., DG, Hilus, CA3, CA1, and EC). The model architecture and its data construction are adapted from our empirical results obtained from large-scale recordings of a high-density microelectrode sensing array [3]. The computational framework encodes sparse temporal non-linear oscillatory patterns generated by the Kuramoto model [4] and projected serially in each hippocampal layer, adjusted to the empirical large-scale recordings data using a constrained learning algorithm [5]. Using these features, the model demonstrates the impact of changing DG network size on memory encoding, recall performance, and network synchrony. Hence, the model paves the way to investigating the computational implications of neurogenic impact in the hippocampal network with biologically plausible features.

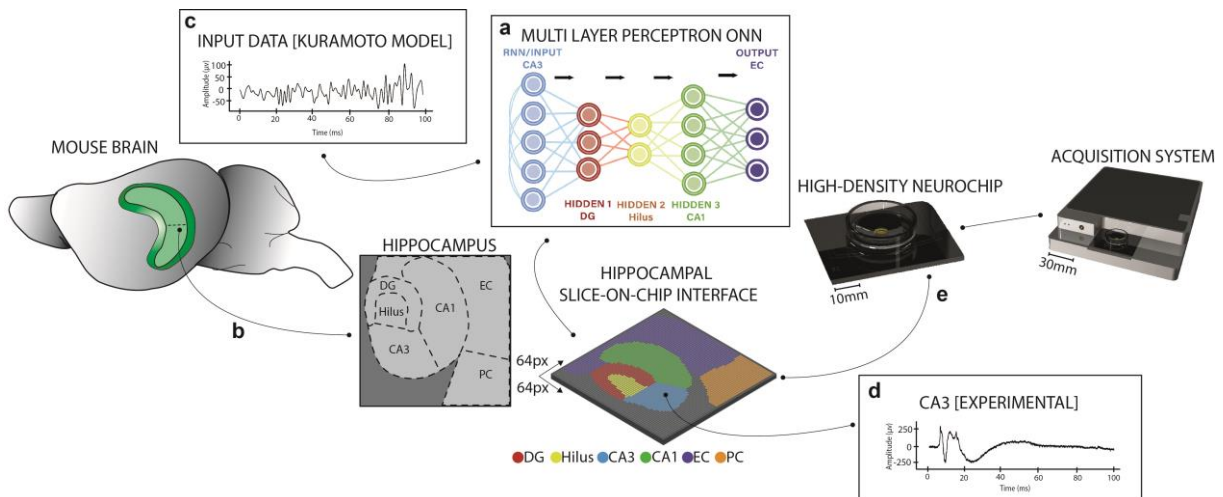


Figure 1. Representative schematic showing the spatiotemporal model architecture (a) of the hippo-cortical network (b) and the non-linear oscillatory activity generated by the Kuramoto model (c) and benchmarked to the experimental large-scale recordings (d) obtained from high-density microelectrode neurochip (e).

References

- [1] G. Kempermann, L. Wiskott, and F. H. Gage, “Functional significance of adult neurogenesis,” *Curr. Opin. Neurobiol.*, vol. 14, no. 2, pp. 186–191, 2004, doi: 10.1016/j.conb.2004.03.001.
- [2] J. B. Aimone and F. H. Gage, “Modeling new neuron function: A history of using computational neuroscience to study adult neurogenesis,” *Eur. J. Neurosci.*, vol. 33, no. 6, pp. 1160–1169, 2011, doi: 10.1111/j.1460-9568.2011.07615.x.
- [3] B. A. Emery, X. Hu, S. Khazada, G. Kempermann, and H. Amin, “Rich experience boosts the hippocampal connectome and high-dimensional coding,” *bioRxiv*, 2022, doi: <https://doi.org/10.1101/2022.02.23.480123>.
- [4] Y. Kuramoto, “Self-entrainment of a population of coupled non-linear oscillators,” *Int. Symp. Math. Probl. Theor. Phys.*, pp. 420–422, Oct. 1975, doi: 10.1007/BFB0013365.
- [5] E. Altuntac, “Choice of the Parameters in A Primal-Dual Algorithm for Bregman Iterated Variational Regularization,” *Numer Algor*, vol. 86, no. 2, pp. 729–759, 2021, doi: 10.1007/s11075-020-00909-6.

Understanding electrical signals in volume conductor on MEA

Timo Salpavaara^{a,*}, Akseli Nummi^a, Jarmo Verho^a, Tomi Ryyänen^{a,b}, Jari Väliaho^a, Antti Mäki^a, Jukka Lekkala^a, Pasi Kallio^a

- a. Faculty of Medicine and Health Technology, Tampere University, Finland
- b. Tampere Institute for Advanced Study, Tampere University, Finland

* timo.salpavaara@tuni.fi

The magnitude, shape and polarity of electrophysiological signals measured with the microelectrode arrays (MEAs) are dependent on the orientation and magnitude of the signal source, the overall spatial arrangement of the measurement, the properties of the medium and the limitations of the electrode surfaces and the amplifier. The effects of the mutual geometry of the signal source and the electrodes (measurement and ground) are emphasized when measuring tissue samples or 3D cell cultures *in vitro*. This makes the measurement arrangement and the problematics more analogous to those in a conventional biopotential measurement where the electrical currents and potentials are analyzed in a volume conductor [1]. In addition, if a cell culture device on the top of a MEA constricts the flow of the electrical currents in the volume conductor such as in tunnel devices [2], the analysis of the signals becomes even more complicated.

We are developing methods for studying how the electrical signals are coupled from a source to the electrodes in cell culture medium on the top of MEAs. These methods consist of a test environment and its COMSOL Multiphysics model (see Figure 1). The objective in the development of the custom-made test environment was to have a system where the electrophysiological measurement using MEAs can be emulated and reliably repeated. The COMSOL model was created to get a better understanding of the measurement system and to test alternative configurations such as different electrode layouts. The test environment consists of a custom-made interchangeable low-noise MEA amplifier (16 channels) and its data acquisition unit (DAQ), a fully configurable signal generator and a needle-like source electrode setup that can be moved freely with microactuators in 3D space above MEAs. The implementation of the movable signal source was inspired by the setup proposed by Nisch et al. in [3]. The sample-based signal generator, synchronized to measurement, can produce bipolar waveforms. Furthermore, an external electrically isolated amplifier is used to convert the generator's output to currents or voltages in a desired range to better emulate typical biological signal sources.

Initial results that were gathered with a scaled-up version (diameter 300 μm) of MEA electrodes suggest that our COMSOL model is able to predict the measurement data (see Figure 2). In addition, the results are in a reasonable agreement with the earlier experiments by Nisch et al. Furthermore, our results suggest that the location of the ground electrode on the MEA and the possible signal sources around it have an effect on the measured data. The combination of the test environment and the corresponding COMSOL model provides an excellent tool for developing MEA technology and increases the understanding of how electrical signaling of cells in cell cultures is transferred to field potentials (FPs) measured with MEAs especially when using complex 3D arrangements.

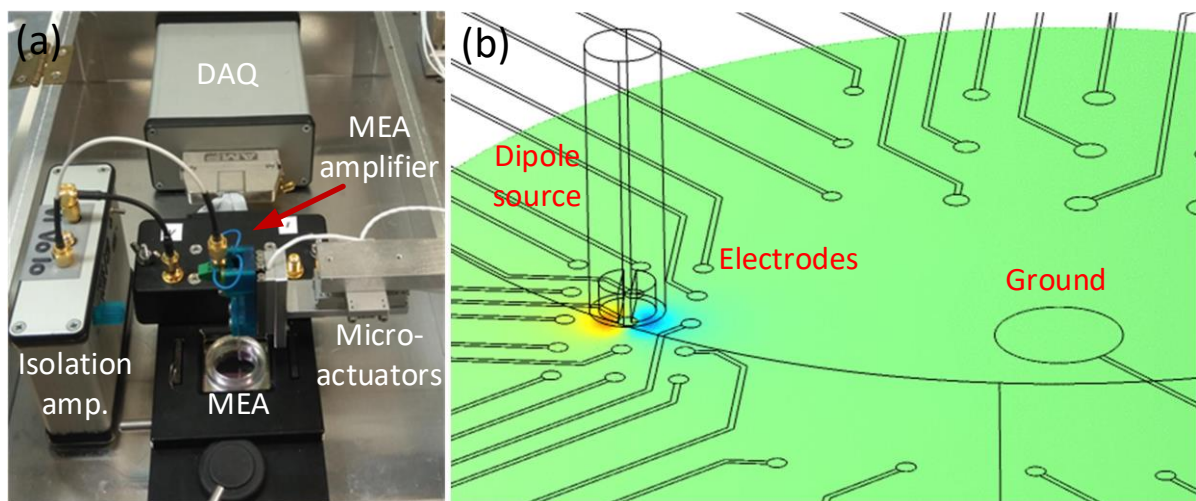


Figure 1: a) A photograph of the test arrangement. b) The model of the simulated measurement.

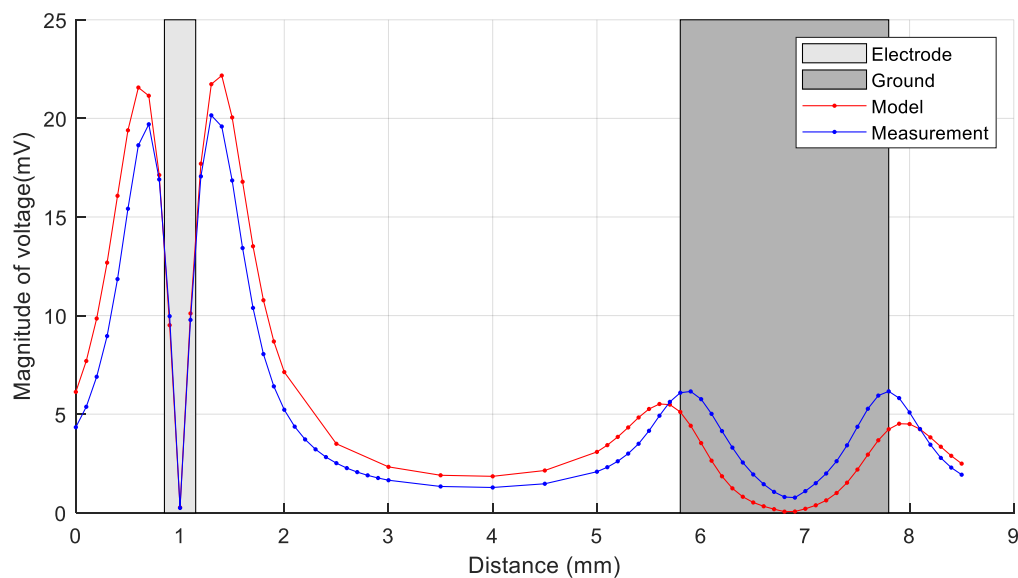


Figure 2: The modelled and the measured signals when the pipette was moved above the MEA.

References

1. Malmivuo, J. and Plonsey, R. (1995) Bioelectromagnetism: Principles and Applications of Bioelectric and Biomagnetic Fields. doi:10.1093/acprof:oso/9780195058239.001.0001.
2. Toivanen, M., Pelkonen, A., Mäkinen, M., Yli-Outinen, L., Sukki, L., Kallio, P., Ristola, M., and Narkilahti, S. (2017). Optimised PDMS tunnel devices on MEAs increase the probability of detecting electrical activity from human stem cell-derived neuronal networks. *Frontiers in Neuroscience* 11, 606. doi:10.3389/fnins.2017.00606.
3. Nisch, W., Böck, J., Egert, U., Hämmerle, H., and Mohr, A. (1994). A thin film microelectrode array for monitoring extracellular neuronal activity in vitro. *Biosensors and Bioelectronics* 9, 737–741. doi:10.1016/0956-5663(94)80072-3.

Prediction in in-vitro neural networks

Martina Lamberti,^a Joost le Feber^{a,*}

a. Department of Clinical Neurophysiology, University of Twente, Enschede, PO Box 217 7500AE, The Netherlands

* j.lefeber@utwente.nl

Several studies have hypothesized that networks of neurons should be able to predict [1,2]. Prediction has been recognized as relevant and beneficial for different aspects of information processing, like motor and cognitive control, decision making and perception, and has been associated with registration of recent sensory inputs [1,2,3]. Recent studies showed that retinal cells are able to predict external visual stimuli [4], but no proof has been provided that prediction is a general capability of neuronal networks. Our goal was to determine whether *in vitro* neural networks have the ability to predict external stimulation, and how this ability depends on memory.

We used rat primary cortical neurons plated on multi electrodes arrays (MEAs) with 59 recording electrodes, and we subjected them to 20 hours of electrical stimulation through one of the electrodes shown to induce a clear stimulus response. All cultures were about the same age (21.7 ± 3.9 DIV). We applied stochastic interstimulus intervals (ISIs) taken from a known distribution, and recorded network activity. Repeated stimulation at one electrode has been shown to induce memory traces within one or a few hours [5,6]. We calculated mutual information (MI) to determine whether recorded neuronal activity provided information on future stimuli [4]. MI quantifies how much one signal can reduce the uncertainty of another signal [4,7,8]. MI was calculated between the recorded and binarized activity of all electrodes and the binarized stimulation signal. Activity was binarized per 100ms bin by a 59 element vector. For each electrode the associated vector element was 1 if there was at least one spike recorded in that bin, and 0 otherwise. Similarly, we created a stimulation vector with one element per (100ms) bin, which was set to 1 if there was a stimulus in that bin and to 0 otherwise. To calculate MI between recorded activity and future stimuli, the stimulation vector was time-shifted with steps of 100ms to a maximum of 2s backwards.

MI curves showed a highly reproducible shape, with an elevated plateau between 0 and 1s, a clear peak around 1.1s and then a smooth decrease to ~ 0 (Fig 1A). The shape probably reflected the ISI distribution (Fig 1D), with the plateau corresponding to latencies up to the minimum possible ISI and the peak corresponding to the most probable ISI. We calculated MI between current and future stimuli (MI_{self} , Fig 1B) and subtracted MI_{self} from MI curves. This largely reduced the peak at 1.1s, suggesting that most information on future stimuli lies in the presence of clearly recognizable stimulus responses (Fig 1C). Such responses outlast the duration of the stimulus and thus reflect a form of short-term memory. We quantified short-term memory as the summed mutual information between activity and past stimulation in 300 ms intervals (MI_{past}), and prediction as the summation of MI curves (between activity and future stimulation) in 2s intervals (MI_{future}). MI_{future} and MI_{past} showed good correlation, which was maintained over time ($R > 0.5$, Fig. 1F,G). The slope of this relationship decreased with time ($p < 0.03$), while the offset increased ($p < 0.03$), indicating that prediction became less dependent on induced stimulus responses during the 20 hours of stimulation. These results indicate that neuronal activity does provide information on the upcoming stimulation, and that the amount of information initially depends on short term memory. This dependency decreased with time. We speculate this might be related to the formation of long-term memory traces during the 20h of stimulation.

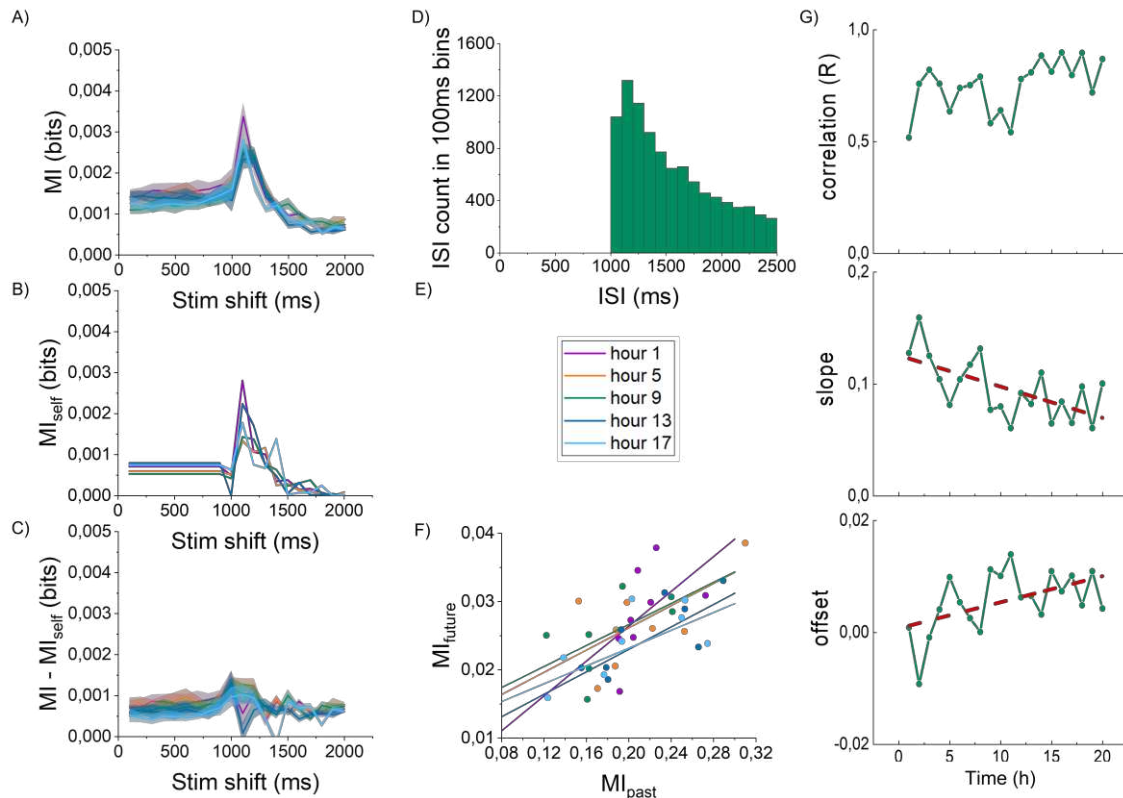


Figure 1: Predictive information in recorded activity in $n=8$ experiments. A) MI curves between activity and future stimulation. B) MI_{self} curves, describing MI between current and future stimulation. C) $MI - MI_{self}$ becomes flatter but tends to remain above 0. In panel A, B and C, horizontal axes indicate time difference between current activity and future stimuli. E) color coding of time for panel A,B,C and F. D) ISI distribution. D) MI_{self} curves, describing MI between current and future stimulation. F) relationship between MI_{future} and MI_{past} . Lines represent linear fit. G) Time courses of correlation coefficient (R), offset and slope of MI_{future} relation to MI_{past} . Red dashed lines represent linear fit.

Acknowledgement

This study was supported by the US AFOSR, grant number FA9550-19-1-0411.

References

1. Bubic, A., Von Cramon, D. Y., & Schubotz, R. I. (2010). Prediction, cognition and the brain. *Frontiers in human neuroscience*, 4, 25.
2. Pitkow, X., Liu, S., Angelaki, D. E., DeAngelis, G. C., & Pouget, A. (2015). How can single sensory neurons predict behavior?. *Neuron*, 87(2), 411-423.
3. Barron, H. C., Aukstulewicz, R., & Friston, K. (2020). Prediction and memory: A predictive coding account. *Progress in neurobiology*, 192, 101821.
4. Palmer, S. E., Marre, O., Berry, M. J., & Bialek, W. (2015). Predictive information in a sensory population. *Proceedings of the National Academy of Sciences*, 112(22), 6908-6913.
5. le Feber, J., Witteveen, T., van Veenendaal, T. M., & Dijkstra, J. (2015). Repeated stimulation of cultured networks of rat cortical neurons induces parallel memory traces. *Learning & memory*, 22(12), 594-603.
6. Dias, I., Levers, M. R., Lamberti, M., Hassink, G. C., Van Wezel, R., & Le Feber, J. (2021). Consolidation of memory traces in cultured cortical networks requires low cholinergic tone, synchronized activity and high network excitability. *Journal of neural engineering*, 18(4), 046051.
7. Thomas, M. T. C. A. J., & Joy, A. T. (2006). *Elements of information theory*. Wiley-Interscience. 2nd edition.
8. Archer, E. W., Park, I. M., & Pillow, J. W. (2013). Bayesian entropy estimation for binary spike train data using parametric prior knowledge. *Advances in neural information processing systems*, 26.

Studying the information processing of small patterned neural networks *in vitro*

Benedikt Maurer^a, Jens Duru^a, Stephan J. Ihle^a, Ciara Giles Doran^a, Joël KÜchler^a, Robert John^a, János Vörös^{a,*}

- a. Laboratory of Biosensors and Bioelectronics, Institute for Biomedical Engineering, ETH Zürich, 8092 Zürich, Switzerland

* janos.voros@biomed.ee.ethz.ch

Understanding information processing and memory formation of neural networks in the brain poses one of the greatest challenges in neuroscience. To gain insights, neurons are studied under great effort *in vivo*. However, the applied methods often only enable monitoring a subset of neurons embedded in a complex network. Whole brain imaging methods on the other hand lack the spatiotemporal resolution for single-cell based analysis. The fundamentals of neural processing are difficult to study in such environments.

To overcome such limitations, we are following the approach of bottom-up neuroscience, in which small engineered neural networks are studied *in vitro*. Primary cortical neurons are seeded into polydimethylsiloxane (PDMS) microstructures to spatially confine the location of their soma and guide neurite growth, which reduces the complexity of the network architecture (as shown in Figure 1A and 1B) [1,2]. In order to study the neural information encoding and processing, the microstructures are placed on high-density microelectrode arrays (HD-MEAs), where network interaction is enabled by means of stimulating and recording from the network [3,4].

Single-electrode stimulation on every network electrode elicits partially deterministic responses with stable traces over thousands of trials [5]. These traces can be tracked and analysed depending on stimulus timing and location following a constant stimulation paradigm (see Figure 1C). Combination of multiple, simultaneously applied stimuli could elucidate how neural networks process multiple inputs and prioritise information. Furthermore, we conduct sensitivity assays of single-electrode resolution, which could support identifying structural components of the network.

The combination of microstructures with HD-MEAs enables comparison of network responses with respect to stimulus location. With these tools we aim to describe the complex input-output relationship of small neural networks and link the functional to physical network structure. We believe that this could validate fundamental neuroscience postulates, inform the design of *in silico* models and one day enable performing computational tasks on biohybrid systems.

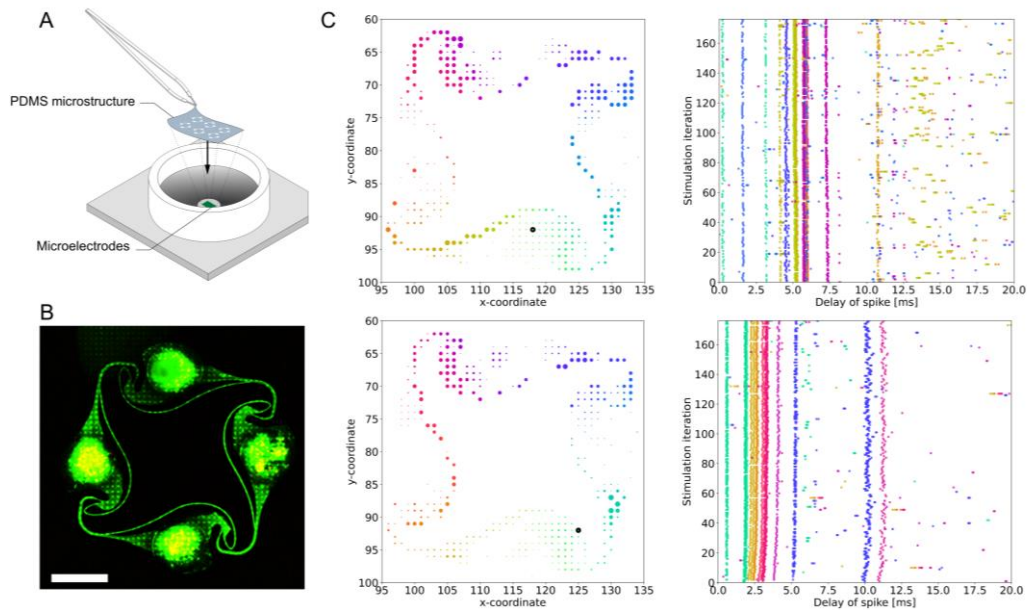


Figure 1: A) PDMS microstructures are placed on HD-MEA [4]. B) Fluorescent image of neurons growing in a directional microstructure. Scale bar corresponds to 200 μm . C) Example results from repeated stimulation on two different electrodes. The stimulation electrode (black circle) and spike raster plot colour-coding are shown on the left. Dot size corresponds to average spiking frequency. The raster plots of spikes recorded in the first 20 ms after stimulation of the 20 most active electrodes are shown on the right. The cultures are primary rat cortical neurons at DIV 20.

References

1. Forro, C., Thompson-Steckel, G., Weaver, S., Weydert, S., Ihle, S., Dermutz, H., . . . Voros, J. (2018). Modular microstructure design to build neuronal networks of defined functional connectivity. *Biosensors & Bioelectronics*, 122, 75-87. doi:10.1016/j.bios.2018.08.075
2. Mateus, J. C., S. Weaver, D. van Swaay, A. F. Renz, J. Hengsteler, P. Aguiar and J. Vörös (2021). Nanoscale patterning of in vitro neuronal circuits. *bioRxiv*: 2021.2012.2016.472887.
3. Muller, J., Ballini, M., Livi, P., Chen, Y., Radivojevic, M., Shadmani, A., . . . Hierlemann, A. (2015). High-resolution CMOS MEA platform to study neurons at subcellular, cellular, and network levels. *Lab Chip*, 15(13), 2767-2780. doi:10.1039/c5lc00133a
4. Duru, J., Küchler, J., Ihle, S.J., Forró, C., Bernardi, A., Girardin, S., Hengsteler, J., Wheeler, S., Vörös, J., Ruff, T. (2022) Engineered biological neural networks on high density CMOS microelectrode arrays. *Frontiers in Neuroscience*, 16. doi:10.3389/fnins.2022.829884
5. Ihle, S. J., Girardin, S., Felder, T., Ruff, T., Hengsteler, J., Duru, J., . . . Vörös, J. (2021). An experimental paradigm to investigate stimulation dependent activity in topologically constrained neuronal networks. *Biosensors and Bioelectronics*, doi:10.1016/j.bios.2021.113896

Interface development to facilitate measurement of neuronal activity using micro electrode arrays

Gerco Hassink^{a*}, Maria Carla Piastra^a, Joost Le Feber^a

- a. Dep. Clinical Neurophysiology, University of Twente, Drienerlolaan 5, 7522 NB Enschede, The Netherlands

* g.c.hassink@utwente.nl

Micro Electrode Arrays (MEAs) are useful tools to study activity in networks of dissociated neurons, which can be applied to model various brain disorders [1]. Although most MEA recording hardware is equipped with dedicated software, the flexibility of such tools is limited. Data storage, for example, does not allow the user to select the format and time-consuming (offline) conversions are often necessary. Furthermore, it is not possible to fine-tune the recording setup for specific experiments nor perform more real-time sophisticated processing of the recorded data.

To address this, we designed a new flexible, open-source, MATLAB-based interface software for MEA2100 based on the API provided by Multi Channel Systems [2]. The main features are:

- Core program:
 - No data loss while the interface is running.
 - Threshold based spike detection based on continuously updated noise estimates
 - Storage in a MATLAB compatible format with a minimal conversion time
 - Time stamps and channel numbers
 - 6 ms of waveshape (2ms before the spike to 4ms after)
 - The estimated noise (rms) of that channel at the time of recording
 - Controllable hardware settings (AD conversion, filters, etc.)
- Data visualization:
 - Raster plot
 - Waveshapes indicating reproducibility
 - Raw signals, showing used detection thresholds
 - Noise estimates per electrode
- Data storage:
 - Storage of full raw data at regular intervals.
- Stimulation:
 - Flexible stimulation, triggered by recorded activity, or read from file

The interface consists of a core program that takes care of the most essential data storage, and estimates the time left for additional functions without the risk of data loss. Data are read from the interface board ring buffer (100,000 frames) in blocks of 25,000 frames (1s of data). After reading the data, the number of frames remaining in the buffer is displayed to indicate the time that remains for additional plug-in functions. Channel-specific noise estimates are continuously updated for threshold-based detection of action potentials. Timestamp, channel number, waveshape, and noise level at the time of an event are stored in a .mat file.

Additional functions, including visualization, raw data storage, and stimulation are available as separate modules that can be switched on as long as processing time allows. The interface is made modular to facilitate further future extension. We plan to share the code with the community, e.g., on GitLab.

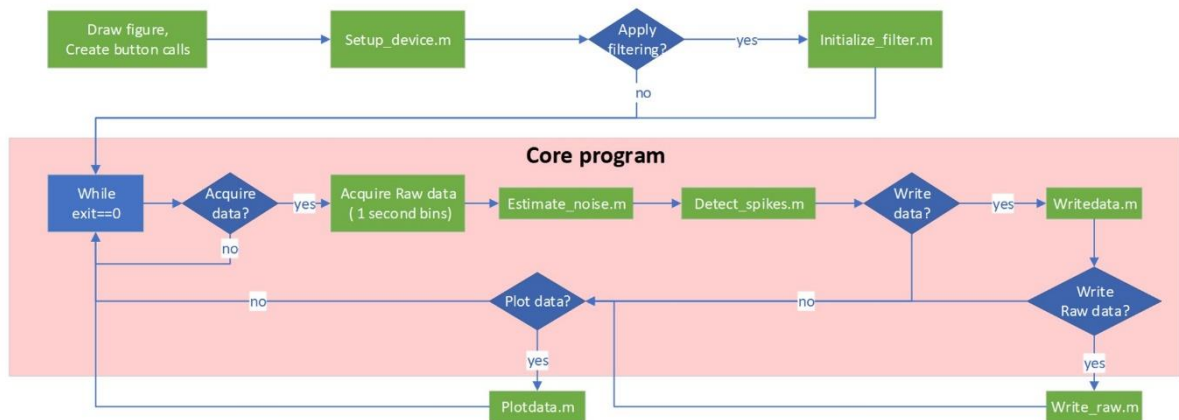
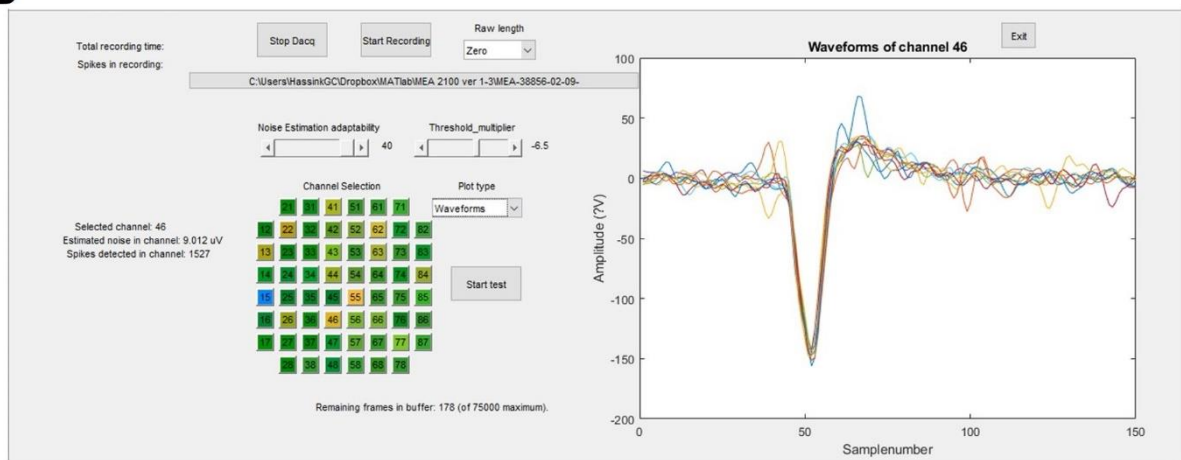
A**B**

Figure 1: A) The program, consists of an initialization phase in which filters etc. are set, and a core program which ensures data storage. Additional functionality like plotting and grounding of electrodes are placed outside the core program. B) Screen shot of the interface. At the left panel basic data like estimated noise, file name, noise threshold, buffer usage, and color coding of average- (green) and actual activity (red) are indicated. In the right panel the selected type of plot is displayed.

References

1. Le Feber, J. (2019). In vitro models of brain disorders, in In vitro neuronal networks: from culturing methods to neuro-technological applications, M. Chiappalone, V. Pasquale, and M. Frega, Editors., Springer: Cham. p. pp31.
2. <https://github.com/multichannelsystems/McsUsbNet>

Polymer Microelectrode Array Interfaces to the Nervous System

Ellis Meng, PhD, Professor

Departments of Biomedical and Electrical and Computer Engineering

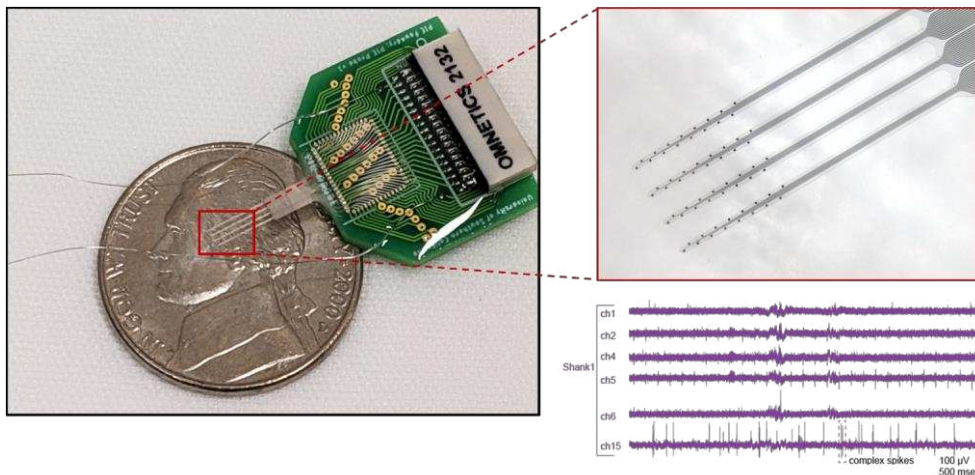
Biomedical Microsystems Laboratory

University of Southern California

<http://biomems.usc.edu>

Extracellular electrodes provide convenient access to neural information via electrophysiological recordings and can achieve both cellular resolution as well as scale when constructed using micro- and nanofabrication. Early miniaturized microelectrodes and microelectrode arrays first adopted silicon as a structural building material to support individual or multiple electrode recording sites. Significant advances over several decades have resulted in mature penetrating silicon-based electrode arrays that can be placed into tissue to access targeted sites. However, the disparate mechanical stiffness between the rigid silicon and soft tissue has been attributed to instability of the electrode-tissue interface which may provoke a chronic, unwanted foreign body response. More recently, interest in accessing information across multiple regions of the brain, different parts of the nervous system, and acquiring recordings for long periods of time have motivated research efforts to advance polymer-based microelectrode arrays which are constructed using thin film polymer substrates that are not only flexible and softer but also optically transparent. This combination of features and their compatibility with micro- and nanofabrication methods allows a wide range of different polymer-based microelectrode arrays to be realized as surface or penetrating neural interfaces.

Significant advances in developing robust fabrication processes have improved the yield and sophistication of polymer microelectrode arrays [1]. To achieve large scale recording, the increased channel counts required have led to complementary advances in packaging and integration technology that enable low profile connections to bare die or packaged integrated circuits, especially multiplexers that enable conductive traces to be shared among large numbers of electrodes [2]. The overall progress has enabled a new model for disseminating polymer microelectrode arrays to the neuroscience research community. This new resource, the Polymer Implantable Electrode Foundry [3], offers custom or generic electrode arrays, testing services, and training to the neuroscience research community worldwide.



References

1. K. Scholten, C. E. Larson, H. Xu, D. Song and E. Meng, "A 512-Channel Multi-Layer Polymer-Based Neural Probe Array," in *Journal of Microelectromechanical Systems*, vol. 29, no. 5, pp. 1054-1058, 2020, doi: 10.1109/JMEMS.2020.2999550.
2. J. Yoo and E. Meng, "Bonding methods for chip integration with Parylene devices," in *Journal of Micromechanics and Microengineering*, vol. 31, no. 4, 045011, 2021, doi: 10.1088/1361-6439/abe246.
3. <http://piefoundry.usc.edu/>

A Flexible 3D Microelectrode Array for Bioelectronic Interfacing

Helen Steins^{a,b,*}, Michael Mierzejewski^a, Lisa Brauns^a, Angelika Stumpf^a, Alina Kohler^a, Gerhard Heusel^a, Andrea Corna^c, Thoralf Herrmann^a, Peter D. Jones^a, Günther Zeck^{a,c}, Rene von Metzen^{a,¶} & Thomas Stieglitz^{b,d,e,¶}

- a. NMI Natural and Medical Sciences Institute at the University of Tübingen, Reutlingen, Germany
- b. Department of Microsystems Engineering, University of Freiburg, Freiburg, Germany
- c. Institute of Biomedical Electronics, TU Wien, Vienna Austria
- d. Bernstein Center Freiburg, University of Freiburg, Freiburg, Germany
- e. BrainLinks BrainTools, University of Freiburg, Freiburg, Germany

¶ These authors contributed equally to this work.

* Corresponding author: helen.steins@nmi.de

In recent years, the bioelectronic approach of targeting neural structures in the peripheral as well as central nervous system has increasingly gained significance for the treatment of various neurological disorders [1]. Especially the development of flexible neural interfaces with low-impedance microelectrodes is highly important to measure low-amplitude neural signals from fine and delicate nervous structures [2]. As the signal quality is improved by decreasing the distance between axon and electrode [3], neural interfaces with three-dimensional microelectrodes are promising devices to record from micrometre-sized neural structures.

The project NEPTUN targets the treatment of bowel disorders, like obstipation or incontinence, by electrical intervention in pathological neuronal circuits of the complex visceral neural network in the small pelvis.

For this purpose, we designed a polyimide-based 3D microelectrode array with 32 pillar-shaped electrodes. These microstructures (\varnothing 20 μm or 50 μm) were fabricated by electrodeposition of gold on a seed layer using a thick photoresist as template. Each pillar was insulated with a 4- μm -thick parylene C layer, which was only opened at the pillar head. To decrease the electrodes' impedance, pillar heads were modified by wet etching or by a coating with titanium nitride (TiN). An insulated pillar of diameter 50 μm with a 15- μm -high TiN coated head exhibited an impedance of \sim 11 k Ω at 1 kHz.

The performance of the 3D MEA was evaluated in ex vivo mouse retina experiments. The pillars proved to be stable during the experiments and slightly pierced the retina resembling a velcro-like behaviour. Spontaneous action potentials emanating from retinal ganglion cells were recorded.

Our developed thin-film MEA with 3D low-impedance microelectrodes allowed the recording of neural signals from peripheral nerves, making it an interesting tool to be used in various neurologic approaches as well as for in vitro cell culture and tissue preparations.

Acknowledgements

This work was financed by the German Federal Ministry of Education and Research (BMBF) in the project NEPTUN (grant 13GW0271). The work received financial support from the State Ministry of Baden-Wuerttemberg for Economic Affairs, Labour and Housing Construction.

References

1. Famm, K., Litt, B., Tracey, K. J., Boyden, E. S. and Slaoui M. (2013). A jump-start for electroceuticals. *Nature* 496, 159-161. doi: 10.1038/496159a.
2. Larson, C. E. and Meng, E. (2020) A review for the peripheral nerve interface designer. *Journal of neuroscience methods* 332, 108523. doi: 10.1016/j.jneumeth.2019.108523
3. Zijlmans, M., Worrell, G. A., Dümpelmann, M., Stieglitz T., Barborica, A., Heers, M., Ikeda, A., Usui, N. and Le Van Quyen, M. (2017). How to record high-frequency oscillations in epilepsy: a practical guideline. *Epilepsia* 58, 1305-1315. doi: 10.1111/epi.13814

Rapid prototyping of soft electrode arrays for implantable, wearable and cell culture applications

Ivan Minev^{a,*}

- a. Department of Automatic Control and Systems Engineering, University of Sheffield, Mappin St, Sheffield S1 3JD, United Kingdom

* i.minev@sheffield.ac.uk

The design of electrode arrays continues to evolve pursuing improved biointegration, mechanical softness, higher channel counts, miniaturisation, reliability and modalities extending beyond electrical interfacing. This motivates the need for novel materials and methods for fabrication and integration.

Here I will describe our efforts to adapt direct ink writing (3D printing) for the fabrication of electrode array systems that are soft, multimodal and application tailored. We employ a set of functional silicones with appropriate rheological and electrical properties. For example flexible and stretchable contacts and interconnects are printed from composites consisting of platinum nanoparticles and silicone. This enables a good compromise between electrical and mechanical properties at physiologically relevant strains. Direct ink writing yields well to integration of multiple interfacing modalities because various silicones (e.g. with tuned optical properties) can be processed in parallel. Finally designs can be easily iterated to fit a specific anatomical niche or application. I will illustrate these points with some examples (Fig. 1): a library of implants for various nodes of the neuromuscular system, wearable sensors of hand function and a cell culture platform with electrodes, microfluidics and optical fibre [1-3]. While direct ink writing cannot achieve miniaturisation competing with photolithography methods, sub-mm array integration can be achieved reliably which for many applications is sufficient. Next steps will focus on the reliability and long-term performance of printed devices.

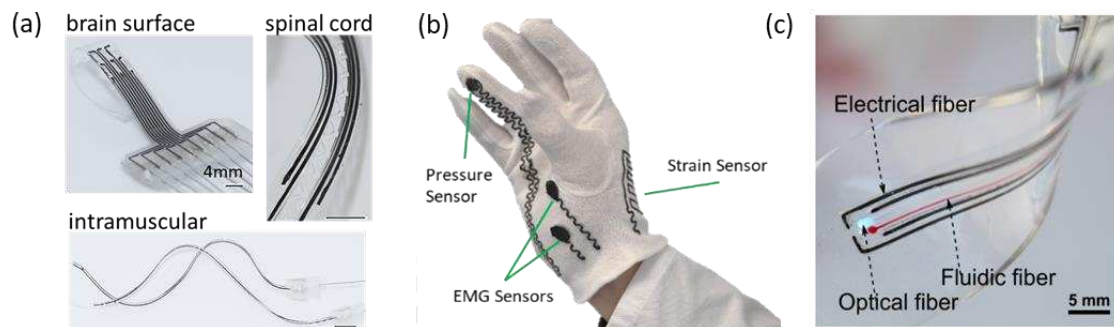


Figure 1: Printed bioelectronic devices. (a) implantable arrays (adapted from [1]), (b) sensor glove (unpublished), (c) multimodal membrane for cell culture interfacing (adapted from [2]).

References

- [1] D. Afanassenkau, D. Kalinina, V. Lyakhovetskii, C. Tondera, O. Gorsky, S. Moosavi, N. Pavlova, N. Merkul'yeva, A.V. Kalueff, I.R. Minev, P. Musienko, Rapid prototyping of soft bioelectronic implants for use as neuromuscular interfaces, *Nature Biomedical Engineering* 4(10) (2020) 1010-1022.
- [2] M. Athanasiadis, D. Afanassenkau, W. Derks, C. Tondera, F. Murganti, V. Busskamp, O. Bergmann, I.R. Minev, Printed elastic membranes for multimodal pacing and recording of human stem-cell-derived cardiomyocytes, *npj Flexible Electronics* 4(1) (2020) 16.
- [3] B. Habelt, C. Wirth, D. Afanassenkau, L. Mihaylova, C. Winter, M. Arvaneh, I.R. Minev, N. Bernhardt, A Multimodal Neuroprosthetic Interface to Record, Modulate and Classify Electrophysiological Biomarkers Relevant to Neuropsychiatric Disorders, *Front Bioeng Biotechnol* 9 (2021) 770274-770274.

Physiological and pathological synchronisations in the human cortex

Katharina T. Hofer^{1,3}; Ágnes Kandrás^{1,3}; Kinga Tóth¹; Estilla Z. Tóth¹; Gábor Nagy², Attila G. Bagó²; Loránd G. Erőss²; László Entz²; Dániel Fabó²; István Ulbert^{1,2,3} and Lucia Wittner^{1,2,3}

1. Institute of Cognitive Neuroscience and Psychology, Research Center for Natural Sciences, Budapest, Hungary
2. National Institute of Mental health, Neurology and Neurosurgery, Budapest, Hungary
3. Faculty of Information Technology and Bionics, Pázmány Péter Catholic University, Budapest, Hungary

Most of the brain's cognitive functions are based on neuronal synchronisation processes. Knowledge about the coordinated firing of neuronal populations is essential in understanding the generation mechanisms of physiological and pathological synchronies. In focal epilepsies, the human neocortex generates hypersynchronous convulsive activity between seizures, classified as interictal spikes. The initiation of these paroxysmal events has been linked to hyperexcitability and to bursting behaviour of neurons in animal models. Despite the importance of interictal spikes in epilepsy diagnostics, little is known about their cellular mechanisms in humans. We investigated spontaneously occurring physiological synchronous population activity and interictal spikes in epileptic patients with the aid of chronically implanted intracortical linear microelectrodes and with intraoperative acute hippocampal recordings. Furthermore, we explored physiological and epileptic population events emerging in postoperative human neocortical tissue derived from epileptic and non-epileptic tumour patients with multiple channel linear microelectrodes adapted to in vitro conditions. Physiological neocortical activity was characterised by the complex interactions of excitatory and inhibitory cells. Spontaneously emerging interictal-like spikes also involved both excitatory and inhibitory circuits, however, excitatory cells, and especially intrinsically bursting neurons had a leading role in the generation of these hypersynchronous events. In contrast, in our in vitro disinhibition model of epileptiform activity, both interictal spikes and seizures were mainly initiated by the synchronous and intense discharge of inhibitory cells. Our data suggest the importance of the finely tuned balance of excitation and inhibition in the generation of physiological synchronisation, which is shifted towards an enhanced excitability in epilepsy. Spontaneously occurring and disinhibition-induced epileptic activity are generated by different cellular mechanisms, which draws attention to the differences between pharmacological models and the human disease.

Investigating Multimodal Neurogenesis: Olfactory Bulb and Hippocampal Networks on a High-density Neurochip

Brett Addison Emery^a, Xin Hu^a, Shahrukh Khanzada^a, Lorenzo Maugeri^a, Gerd Kempermann^{b,c}, Hayder Amin^{a*}

- Biohybrid neuroelectronics laboratory, German Center for Neurodegenerative Diseases (DZNE), Dresden, Germany
- Adult neurogenesis laboratory, German Center for Neurodegenerative Diseases (DZNE), Dresden, Germany
- Genomics of regeneration, Center for Regenerative Therapies TU Dresden (CRTD), Dresden, Germany

* hayder.amin@dzne.de

The mammalian brain exhibits profound complexity and synaptic plasticity through its continuous addition of new neurons to a circuit in a process called neurogenesis [1]. Two brain regions exhibit multiscale circuit remodeling through this process – the olfactory bulb and hippocampus. The local tissue-level changes have been widely investigated; however, the alterations at a network level remain inaccessible [2]. Specifically, how changes in a local subregion influence global circuit rewiring and dynamic network features have remained largely unexplored due to the lack of high-spatiotemporal resolution technology and large-scale electrophysiological recordings. We here demonstrate multimodal circuit-wide oscillatory firing patterns and layer-specific functional connectivity in the olfactory bulb and hippocampal networks obtained from large-scale recordings using a high-density (HD) microelectrode sensing array [3, 4]. This slice-neurochip interface allowed examination of slow and fast oscillatory activity from each firing electrode and its spatial relationship to the defined regions in the circuit. Our findings illustrate simultaneous recordings from the entire network, which allows us to quantify synchronous electrophysiological parameter differences and layer-specific waveform markers. We employed several methods of time-course correlation, multivariate Granger causality, directed transfer function (DTF), and graph-theoretic analysis to characterize the local and global network behaviors. Examining the pairwise cross-covariance between active electrode pairs reveal individual neuronal ensemble contributions to synchronous activation between layers and hub microcircuits, demonstrating a network-wide rewiring. Further investigations into large-scale functional connectivity and graph-theoretic analysis unveil regional interactions, functional adaptability, and global communication contributing to the overall network topology [6]. Our study suggests a novel tool to decipher network topologies and the computational implications of large-scale activity patterns in functional multimodal neurogenic circuits.

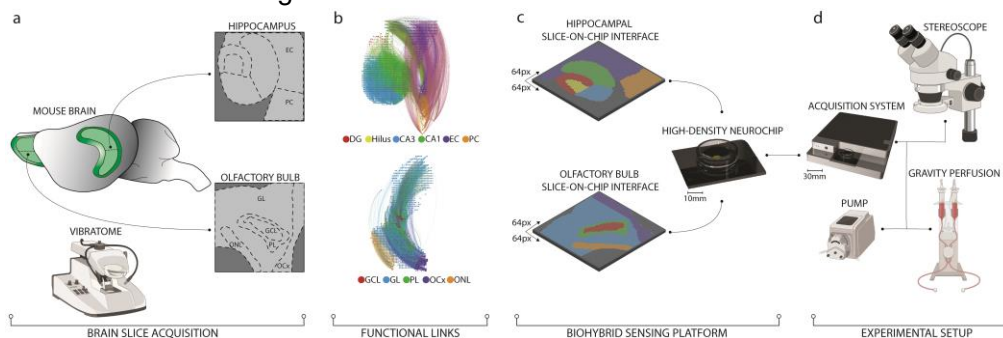


Figure 1. Representative schematic showing acquisition of olfactory bulb and hippocampal slices (a), and their functional connectivity maps obtained from corresponding slices (b) obtained from large-scale on-chip recordings using a biohybrid sensing platform (c), and custom-designed experimental setup (d).

References

1. G. Kempermann, L. Wiskott, and F. H. Gage, "Functional significance of adult neurogenesis," *Curr. Opin. Neurobiol.*, vol. 14, no. 2, pp. 186–191, (2004).
2. Tuncdemir, S. N., Lacefield, C. O. & Hen, R. Contributions of adult neurogenesis to dentate gyrus network activity and computations. *Behav. Brain Res.* 374, (2019).
3. Hu, X., Khanzada, S., Klütsch, D., Calegari, F. & Amin, H. Implementation of biohybrid olfactory bulb on a high-density CMOS-chip to reveal large-scale spatiotemporal circuit information. *Biosens. Bioelectron.* 198, 113834 (2022).
4. Emery, B.A., Hu, X., Khanzada, S., Kempermann, G., & Amin, H. Rich experience boosts functional connectome and high-dimensional coding in the hippocampal network. *bioRxiv*, preprint. (2022).
5. Bassett, D. S. et al. Efficient physical embedding of topologically complex information processing networks in brains and computer circuits. *PLoS Comput. Biol.* 6, (2010).
6. Rubinov, M. & Sporns, O. Complex network measures of brain connectivity: Uses and interpretations. *Neuroimage* 52, 1059–1069 (2010).

Neuroprotective role of lactate release from astrocytes in a human *in vitro* model of the ischemic penumbra

Marta Cerina^a, Eva Voogd^a, Marloes Levers^a, Monica Frega^{a*}

- a. Department of Clinical Neurophysiology, University of Twente, 7522 NB Enschede, the Netherlands

* m.frega@utwente.nl

In cerebral ischemic stroke, there is an urgent need to uncover new treatments to protect brain cells from ischemic damage. In the past decades, hundreds of neuroprotective strategies have been successfully tested on animal models [1,2]. Nevertheless, among them only a few have proved to be effective in clinical use [3]. This failure of translation poses doubts on the validity of animal models for the study of human stroke. Recently, Pires Monteiro et al. established a human *in vitro* model of the cerebral ischemic penumbra consisting of neuronal networks derived from human induced pluripotent stem cells (hiPSCs) cultured on Micro Electrode Arrays (MEAs) and exposed to controlled hypoxic conditions [4]. Using this model, they showed that a treatment strategy based on activation of neuronal activity (i.e. optogenetic stimulation) resulted in neuroprotection [4].

Here, we used the same hiPSCs-based *in vitro* model of the ischemic penumbra to investigate the biological mechanisms underlying the neuroprotective effect mediated by optogenetic stimulation. We hypothesized that optogenetic stimulation might maintain or trigger the astrocyte-to-neuron lactate shuttle (ANLS) [5, 6], i.e. lactate release from astrocytes in support of neurons, resulting in neuroprotection. Our hypothesis was supported by studies suggesting that lactate could have, along with a physiological role in the brain as a supplementary energy source and as a signaling molecule [7, 8], a neuroprotective role in several pathological conditions, including ischemic stroke [9-11].

In our study, we generated hiPSCs-derived neuronal networks and we cultured them on MEAs [12]. We measured the electrophysiological activity and cell viability under controlled hypoxic conditions to investigate (i) whether the ANLS contributed to the neuroprotective effect mediated by optogenetic stimulation and (ii) whether lactate could be neuroprotective in our model. We found that the inhibition of two transporters involved in the ANLS partially impaired the optogenetic stimulation-mediated neuroprotective effect on synchronized electrophysiological activity (Fig. 1a). Moreover, we showed that lactate administration before the onset of hypoxia had a neuroprotective effect on cell viability during the first 24 hours of hypoxia (Fig. 1b).

Our results indicate that the ANLS plays a role in neuroprotection and highlight the paramount role of astrocytes in support of neurons in pathological contexts. Therefore, we suggest that considering treatment strategies targeting astrocytes, along with neurons, may represent a successful approach to develop clinically relevant therapies for ischemic stroke. Moreover, according to recent literature, our findings suggest that lactate might have a neuroprotective role in ischemic stroke. Since lactate exerts its effect on multiple therapeutic targets (e.g.. glutamate excitotoxicity [13,14], oxidative stress [15,16], neuronal death [17,18]) and it could be easily translated into patients [19], we argue that it may represent a valid candidate for neuroprotection, undoubtedly worthy of further investigation. Lastly, our study supports the validity of hiPSCs-derived neuronal networks cultured on MEAs as a tool to model neurological diseases, such as ischemic stroke, in order to study the underlying pathophysiological mechanisms and to test new candidate drugs and treatments.

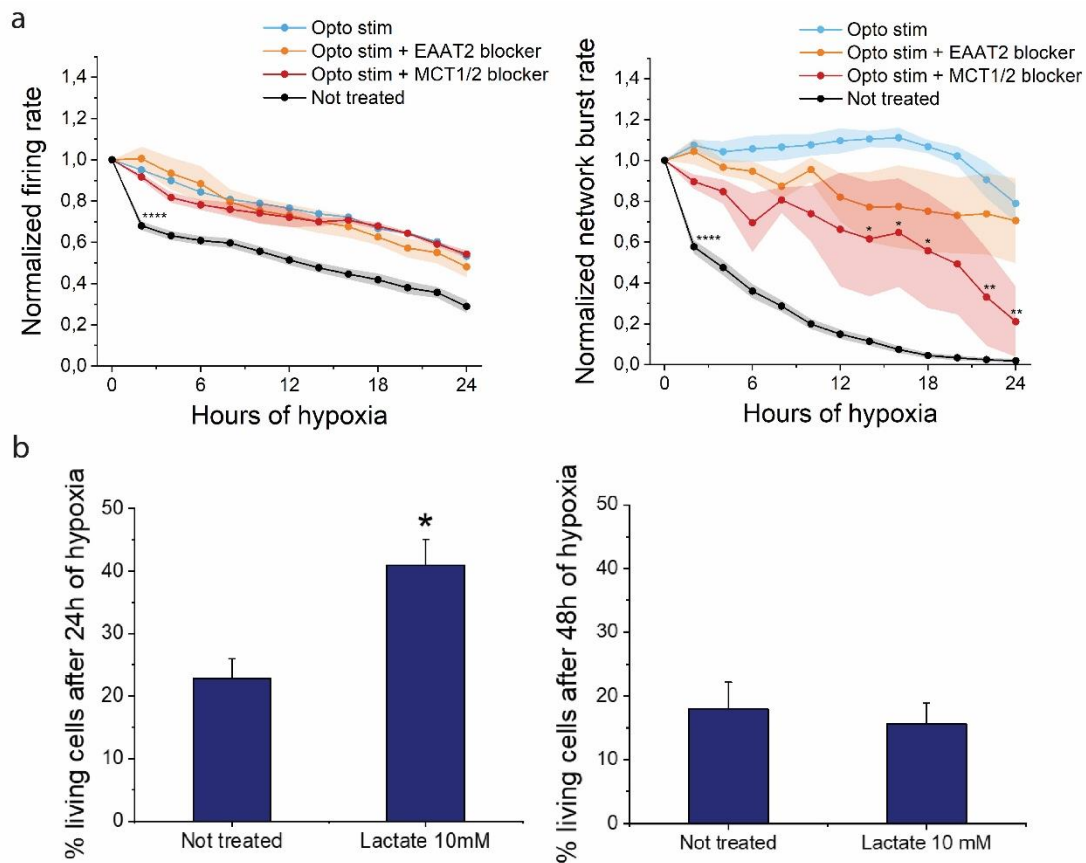


Figure 1. a) Graphs showing the mean firing rate and the network burst rate of neuronal networks exposed to 24 hours of hypoxia treated with optogenetic stimulation without blockers (blue line), treated with optogenetic stimulation and EAAT2 blocker (orange line), treated with optogenetic stimulation and MCT1/2 blocker (red line) and not treated (black line). The values are normalized to the data of the baseline phase. Two-way ANOVA test and post hoc Bonferroni correction was performed between neuronal networks treated with optogenetic stimulation without blockers and other conditions. * $p < 0.05$, ** $p < 0.005$, **** $p < 0.0001$. Asterisks corresponding to $p < 0.0001$ are not shown after the first timepoint this p-value was found. **b)** Bar graphs showing the percentage of living cells in neuronal networks exposed to hypoxia not treated and treated with lactate 10 mM after 24 and 48 hours of hypoxia. Mann Whitney test was performed between conditions. * $p < 0.05$.

References

- [1] R. N. Auer, "Neuroprotection in the Treatment of Brain Ischemia," *Progress in Cardiovascular Diseases*, pp. 271–282, 2017.
- [2] Z. Zhou *et al.*, "Advances in stroke pharmacology," *Pharmacology and Therapeutics*, vol. 191, pp. 23–42, 2018, doi: 10.1016/j.pharmthera.2018.05.012.
- [3] A. Moretti, F. Ferrari, and R. F. Villa, "Neuroprotection for ischaemic stroke: Current status and challenges," *Pharmacology and Therapeutics*, vol. 146, pp. 23–34, 2015, doi: 10.1016/j.pharmthera.2014.09.003.
- [4] S. Pires Monteiro *et al.*, "Neuroprotective effect of hypoxic preconditioning and neuronal activation in a in vitro human model of the ischemic penumbra," *Journal of Neural Engineering*, vol. 18, no. 3, 2021, doi: 10.1088/1741-2552/abe68a.
- [5] L. Pellerin and P. J. Magistretti, "Glutamate uptake into astrocytes stimulates aerobic glycolysis: A mechanism coupling neuronal activity to glucose utilization," *Proceedings of the National Academy of Sciences of the United States of America*, vol. 91, no. 22, pp. 10625–10629, 1994, doi: 10.1073/pnas.91.22.10625.
- [6] L. Pellerin and P. J. Magistretti, "Sweet sixteen for ANLS," *Journal of Cerebral Blood Flow and Metabolism*, vol. 32, no. 7, pp. 1152–1166, 2012, doi: 10.1038/jcbfm.2011.149.
- [7] V. Mosienko, A. G. Teschemacher, and S. Kasparov, "Is L-lactate a novel signaling molecule in the brain?," *Journal of Cerebral Blood Flow and Metabolism*, vol. 35, no. 7, pp. 1069–1075, 2015, doi: 10.1038/jcbfm.2015.77.
- [8] P. J. Magistretti and I. Allaman, "Lactate in the brain: From metabolic end-product to signalling molecule," *Nature Reviews Neuroscience*, vol. 19, no. 4, pp. 235–249, 2018, doi: 10.1038/nrn.2018.19.
- [9] A. Schurr, R. S. Payne, J. J. Miller, and B. M. Rigor, "Brain lactate, not glucose, fuels the recovery of synaptic function from hypoxia upon reoxygenation: An in vitro study," *Brain Research*, vol. 744, no. 1, pp. 105–111, 1997, doi: 10.1016/S0006-8993(96)01106-7.
- [10] C. Berthet, H. Lei, J. Thevenet, R. Gruetter, P. J. Magistretti, and L. Hirt, "Neuroprotective role of lactate after cerebral ischemia," *Journal of Cerebral Blood Flow and Metabolism*, vol. 29, no. 11, pp. 1780–1789, 2009, doi: 10.1038/jcbfm.2009.97.
- [11] H. L. Cater, C. D. Benham, and L. E. Sundstrom, "Neuroprotective role of monocarboxylate transport during glucose deprivation in slice cultures of rat hippocampus," *Journal of Physiology*, vol. 531, no. 2, pp. 459–466, 2001, doi: 10.1111/j.1469-7793.2001.0459i.x.
- [12] M. Frega *et al.*, "Rapid neuronal differentiation of induced pluripotent stem cells for measuring network activity on micro-electrode arrays," *Journal of Visualized Experiments*, vol. 2017, no. 119, pp. 1–10, 2017, doi: 10.3791/54900.
- [13] J. Ros, N. Pecinska, B. Alessandri, H. Landolt, and M. Fillenz, "Lactate reduces glutamate-induced neurotoxicity in rat cortex," *Journal of Neuroscience Research*, vol. 66, no. 5, pp. 790–794, 2001, doi: 10.1002/jnr.10043.

- [14] I. Llorente-Folch, C. B. Rueda, I. Pérez-Liébana, J. Satrústegui, and B. Pardo, "L-lactate-mediated neuroprotection against glutamate-induced excitotoxicity requires ARALAR/AGC1," *Journal of Neuroscience*, vol. 36, no. 16, pp. 4443–4456, Apr. 2016, doi: 10.1523/JNEUROSCI.3691-15.2016.
- [15] A. Schurr and E. Gozal, "Aerobic production and utilization of lactate satisfy increased energy demands upon neuronal activation in hippocampal slices and provide neuroprotection against oxidative stress," *Frontiers in Pharmacology*, vol. 3 JAN, no. January, pp. 1–15, 2012, doi: 10.3389/fphar.2011.00096.
- [16] A. Tauffenberger, H. Fiumelli, S. Almustafa, and P. J. Magistretti, "Lactate and pyruvate promote oxidative stress resistance through hormetic ROS signaling," *Cell Death and Disease*, vol. 10, no. 9, 2019, doi: 10.1038/s41419-019-1877-6.
- [17] J. Yang *et al.*, "Lactate promotes plasticity gene expression by potentiating NMDA signaling in neurons," *Proceedings of the National Academy of Sciences of the United States of America*, vol. 111, no. 33, pp. 12228–12233, 2014, doi: 10.1073/pnas.1322912111.
- [18] M. B. Margineanu, H. Mahmood, H. Fiumelli, and P. J. Magistretti, "L-Lactate Regulates the Expression of Synaptic Plasticity and Neuroprotection Genes in Cortical Neurons: A Transcriptome Analysis," *Frontiers in Molecular Neuroscience*, vol. 11, no. October, pp. 1–17, 2018, doi: 10.3389/fnmol.2018.00375.
- [19] F. Annoni, L. Peluso, E. Gouv, J. Creteur, E. R. Zanier, and F. S. Taccone, "Brain Protection after Anoxic Brain Injury : Is Lactate Supplementation Helpful ?," *Cells*, pp. 1–11, 2021.

Towards personalized neurostimulation strategies to restore brain function after lesion

Marta Carè^{a,b}, Federico Barban^{a,b}, Alberto Averna^c, Vinicius R. Cota^{a,d}, Rosaria Greco^e, Cristina Tassorelli^e, Lorenzo De Michieli^a, Randolph J. Nudo^{f,g} David J. Guggenmos^f and Michela Chiappalone^{a,b*}

- a. Rehab Technologies, Istituto Italiano di Tecnologia, 16163 Genoa, Italy.
- b. Department of Informatics, Bioengineering, Robotics System Engineering (DIBRIS), University of Genova, 16145, Genoa, Italy.
- c. Department of Neurology, Bern University Hospital and University of Bern, Bern, Switzerland.
- d. Department of Electrical Engineering, Universidade Federal de São João Del-Rei, São João Del-Rei, 36307-352, Brazil
- e. Fondazione Istituto Neurologico Casimiro Mondino, 27100 Pavia, Italy.
- f. Department of Rehabilitation Medicine, University of Kansas Medical Center, Kansas City 66160, USA.
- g. Landon Center on Aging, University of Kansas Medical Center, Kansas 66160, USA.

* michela.chiappalone@unige.it

Stroke is a major contributor of long-term disability worldwide, but effective therapies remain limited. One of the major contributions to observed motor impairment is the disruption of communication between spared brain areas. The reestablishment of this communication is likely to drive motor recovery. Closed-loop neurostimulation approaches have shown efficacy in reconnecting brain regions that have become disconnected as a result of an acquired brain injury. One technique, Activity-Dependent Stimulation (ADS), uses the timing of detected single-unit action potentials in one brain region to trigger an intracortical microstimulation pulse in a different area to entrain their activity. Recently, ADS was used in a model of traumatic brain injury localized to primary motor cortex (caudal forelimb area; CFA) in rats to reconnect a premotor (rostral forelimb area; RFA) with primary somatosensory cortex (S1) [1] to induce rapid behavioral recovery. To further characterize ADS, we have investigated its ability to rapidly alter firing characteristics in both anesthetized and ambulatory healthy rats [2, 3]. However, the extent ADS has on the ability to induce changes in spiking activity within the trigger and target regions in injured animals remains unclear. Therefore, we had the goals of investigating i) the global impact of a focal lesion on the neuronal activity of spared premotor and somatosensory areas and ii) the ability of ADS to significantly alter these lesion-induced changes. We performed acute experiments in anesthetized rats using a model of focal ischemic lesion in CFA using microinjections of Endothelin-1 (ET-1) [4]. As shown in Fig. 1, we implanted microelectrode arrays to record neurophysiological activity in RFA and trigger intracortical microstimulation in S1. Spiking activity from RFA and S1 was recorded and analyzed off-line. We found [5] that the lesion induced a differential change of spiking activity in RFA and S1, while ADS increased the firing level in both areas. Further experiments will be necessary to correlation between these neurophysiological changes and possible behavioral improvements. As further advancement of our work, beyond ADS, it would be possible to design new stimulation strategies which can benefit from the interplay between low and high frequency components of the signals (i.e. spikes and LFP). This would provide individually tailored stimulation paradigms, which may be more effective in driving functional recovery than simple spike pairing alone. Understanding the shifts in the neural response following brain injury and coupling this response to personalized stimulation paradigms would offer novel therapeutic strategies to treat invalidating neural disorders.

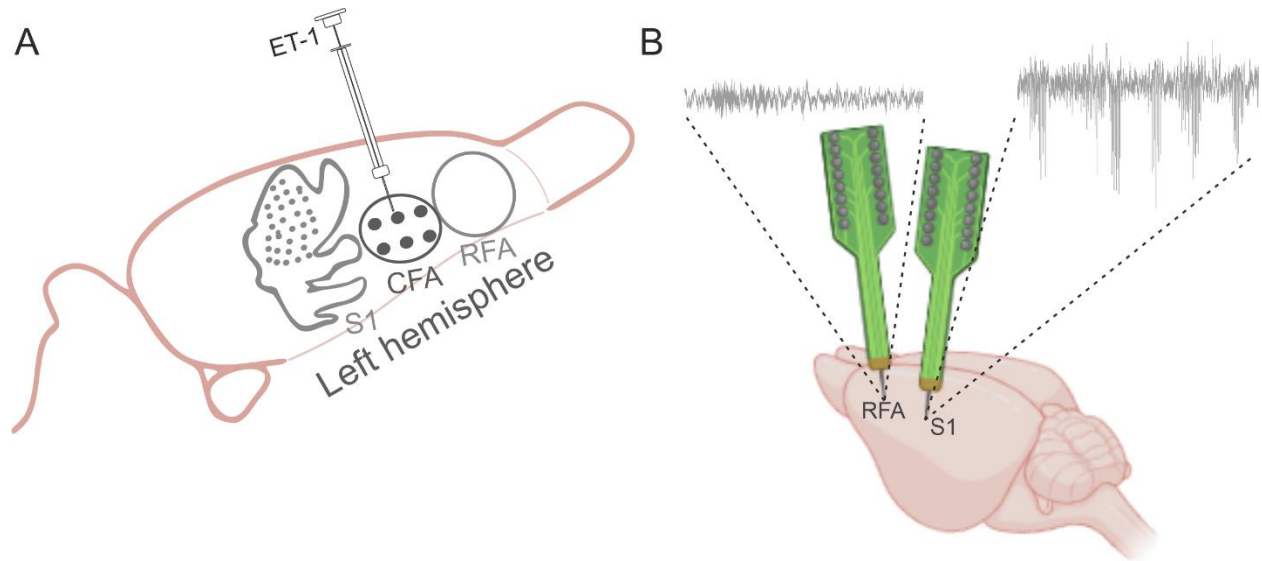


Figure 1. Experimental set-up. A) Areas of interest were stereotaxically located under anesthetized conditions. Two multisite MEAs (see B for details) were placed in the left hemisphere, i.e. in the Rostral Forelimb Area – RFA for recording, and in the Primary Somatosensory area - S1 for recording and stimulation. B) Schematic representation of the setup (created with BioRender.com). Two 4 shank, 16 contact site MEAs were inserted into the cortex. Top: raw signals of spontaneous activity in the recording sites (i.e., RFA and S1).

References

1. Guggenmos, D.J., et al., Restoration of function after brain damage using a neural prosthesis. *Proc Natl Acad Sci U S A*, 2013. 110(52): p. 21177-82.
2. Avena, A., et al., Differential Effects of Open- and Closed-Loop Intracortical Microstimulation on Firing Patterns of Neurons in Distant Cortical Areas. *Cereb Cortex*, 2020. 30(5): p. 2879-2896.
3. Avena, A., et al., Entrainment of Network Activity by Closed-Loop Microstimulation in Healthy Ambulatory Rats. *Cereb Cortex*, 2021. 31(11): p. 5042-5055.
4. Frost, S.B., et al., An animal model of capsular infarct: endothelin-1 injections in the rat. *Behavioural brain research*, 2006. 169(2): p. 206-211.
5. Carè, M., et al., The impact of closed-loop intracortical stimulation on neural activity in brain-injured, anesthetized animals. *Bioelectron Med*, 2022. 8(1): p. 4.

Openly available MEA dataset from hPSC-derived and rat cortical networks and associated data analysis pipeline

Andrey Vinogradov^a, Fikret Emre Kapucu^a, Tanja Hyvärinen^a, Susanna Narkilahti^{a*}

a. Faculty of Medicine and Health Technology, Tampere University, Tampere, Finland

* susanna.narkilahti@tuni.fi

We introduce a comparative dataset (over 2 TB) of microelectrode array (MEA) recordings from human pluripotent stem cell (hPSC)-derived and rat embryonic cortical neurons [1,2]. The data include extracellularly recorded spontaneous activity during the functional development of these neuronal networks and pharmacological experiments at their mature stage. The dataset is openly available for scientific community [2].

Furthermore, we developed a comprehensive analysis pipeline for MEA recordings. Our pipeline includes efficient tools for the analysis of spikes (extracellular action potentials), single channel bursts (dense time series of spikes) and network bursts (bursts synchronously occurring in multiple electrodes) (see Figure 1). The part of the analysis code is published together with the dataset [2] to replicate the key scientific findings of the original publication [1].

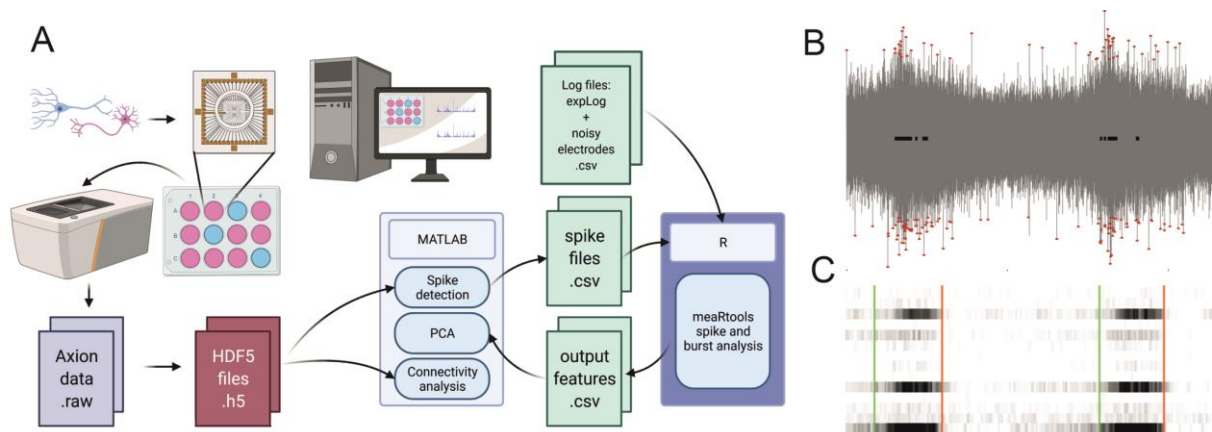


Figure 1: A. The data acquisition and analysis pipeline scheme. B. Raw signal from single MEA electrode with the detected spikes shown with red circles and single-channel bursts shown with black bars in the center. C. The raster plot with network bursts detected among many channels: green and red lines indicate network burst start and end times respectively.

References

1. Hyvärinen, T., Hyysalo, A., Kapucu, E., Aarnos, L., Vinogradov, A., Eglen, S., Ylä-Outinen, L., and Narkilahti, S. (2019). Functional characterization of human pluripotent stem cell-derived cortical networks differentiated on laminin-521 substrate: comparison to rat cortical cultures. *Sci Rep* 9, 17125. doi: 10.1038/s41598-019-53647-8.
2. Kapucu, E., Vinogradov, A., Hyvärinen, T., Ylä-Outinen, L. and Narkilahti, S. (2022). Comparative microelectrode array data of the functional development of hPSC-derived and rat neuronal networks. *Sci Data* 9, 120. doi: 10.1038/s41597-022-01242-4.

In silico modeling to unravel human neuronal network phenotypes on microelectrode arrays

Nina Doorn^{a,*}, Eline van Hugte^c, Nael Nadif Kasri^{c,d}, Monica Frega^{a,e}, Michel van Putten^{a,b,e}

- a. Department of Clinical Neurophysiology, University of Twente, 7500 AE Enschede, The Netherlands
- b. Department of Neurology and Clinical Neurophysiology, Medisch Spectrum Twente, 7500 KA Enschede, The Netherlands
- c. Department of Human Genetics, Radboudumc, Donders Institute for Brain, Cognition, and Behavior, 6500 HB Nijmegen, the Netherlands
- d. Department of Cognitive Neuroscience, Radboudumc, Donders Institute for Brain, Cognition and Behavior, 6500 HB Nijmegen, the Netherlands
- e. *Shared last author*

* n.doorn-1@utwente.nl

Neuronal networks derived from patients' induced pluripotent stem cells (iPSCs), cultured on microelectrode arrays (MEA), may show unique spontaneous electrical activity compared to healthy networks, reflecting particular clinical phenotypes [1–3]. For example, neuronal networks derived from patients with Dravet Syndrome (DS), a severe and intractable epileptic encephalopathy caused by a mutation in a gene encoding the voltage-gated sodium channel, show a robust phenotype on MEA [4,5]. However, in these assays, it is challenging and time consuming to identify the cellular and network mechanisms that explain the distinct neuronal network dynamics.

In silico modeling is a valuable tool to complement *in vitro* research with neuronal networks on MEA. Specifically, such models can be used to drive hypothesis testing, interpretation, and prediction of underlying disease mechanisms.

Here, we used an *in silico* model to elucidate the role of voltage-gated sodium channel mutations and network dynamics in explaining the *in vitro* observations of neuronal networks derived from patients with DS.

We constructed a biophysically detailed neuronal network model consisting of one hundred Hodgkin-Huxley type neurons, sparsely connected via plastic AMPA and NMDA receptor mediated synapses into a network placed on virtual MEA electrodes. We calibrated and validated the model using MEA-data from excitatory neuronal networks derived from iPSCs from a healthy subject (control). The *in silico* model faithfully replicated physiological network behaviour (Figure 1). To transition to a model of DS, we modified the sodium channel dynamics to simulate the DS mutation. However, we found that sodium channel dysfunctions alone were not sufficient to simulate the DS “MEA-phenotype”. Extending the model with changes in synaptic strengths did result in network dynamics showing satisfactory agreement with experimental data (Figure 1).

Our model thus predicts that, in addition to changes in the sodium channel, altered synaptic strengths are an essential component of abnormal network dynamics in DS. This hypothesis can be experimentally tested and may explain some of the clinical features of DS, such as the phenotype variability and developmental delay. This illustrates how the *in silico* model can support the development of new mechanistic hypotheses. In addition, the model can be calibrated to MEA-data from other genetic pathologies, to assist in unraveling these disorders.

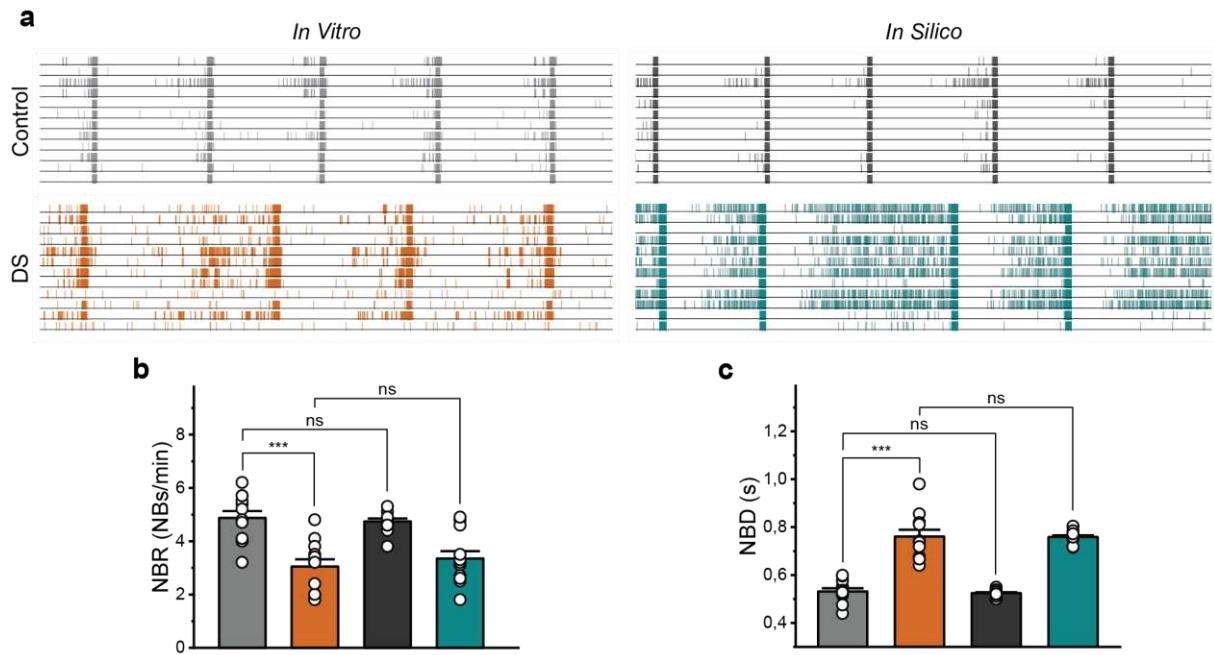


Figure 1: *In silico* model reproduces *in vitro* MEA measurements from neuronal networks derived from iPSCs of a healthy control and a patient with Dravet Syndrome (DS). **a)** Representative raster plots from *in vitro* MEA recordings from a healthy control network (grey) and a DS network (orange), and *in silico* network simulations with the control model (black) and DS model (blue). **b)** Quantification of network burst rate (NBR) and **c)** network burst duration (NBD) for 12 wells per condition *in vitro* and 12 simulated networks per model *in silico*. NBR and NBD were always calculated over 600 seconds of recording/simulation. Data represent means \pm SEM. There were no significant differences between *in vitro* and *in silico* for both Control and DS. ns $P > 0.05$, *** $P < 0.0005$, Welch's t-test was performed between two groups.

References

1. Mossink B, Verboven AHA, van Hugte EJH, Klein Gunnewiek TM, Parodi G, Linda K, et al. (2021) Human neuronal networks on micro-electrode arrays are a highly robust tool to study disease-specific genotype-phenotype correlations in vitro. *bioRxiv* 2021.01.20.427439. Available from: <https://doi.org/10.1101/2021.01.20.427439>
2. Marchetto MC, Belinson H, Tian Y, Freitas BC, Fu C, Vadodaria KC, et al. (2017) Altered proliferation and networks in neural cells derived from idiopathic autistic individuals. *Mol Psychiatry* 22(6):820–35. doi: 10.1038/mp.2016.95
3. Frega M, Linda K, Keller JM, Gümüş-Akay G, Mossink B, van Rhijn JR, et al. (2019) Neuronal network dysfunction in a model for Kleefstra syndrome mediated by enhanced NMDAR signaling. *Nature Communications* 10:1. 2019 Oct 30;10(1):1–15. doi: 10.1038/s41467-019-12947-3
4. Dravet C. (2011) The core Dravet syndrome phenotype. *Epilepsia*. 52(SUPPL. 2):3–9. doi: 10.1111/j.1528-1167.2011.02994.x
5. Marini C, Scheffer IE, Nabbout R, Suls A, de Jonghe P, Zara F, et al. (2011) The genetics of Dravet syndrome. *Epilepsia* 52 Suppl 2(SUPPL. 2):24–9. doi: 10.1111/j.1528-1167.2011.02997.x

DeePhys, a machine learning-driven platform for electrophysiological phenotype screening of human stem-cell derived neuronal networks

Philipp Hornauer^{a,*}, Gustavo Prack^a, Nadia Anastasi^b, Silvia Ronchi^a, Taehoon Kim^a, Christian Donner^c, Michele Fiscella^{a,d}, Karsten Borgwardt^a, Verdon Taylor^e, Ravi Jagasia^b, Damian Roqueiro^{a,b}, Andreas Hierlemann^a, and Manuel Schröter^a

- a. Department of Biosystems Science and Engineering, ETH Zürich, Basel, Switzerland
- b. Roche Pharma Research and Early Development, Neuroscience and Rare Diseases, Roche Innovation Center Basel, F. Hoffmann-La Roche Ltd., Basel, Switzerland
- c. Swiss Data Science Center, ETH Zürich, Zürich, Switzerland
- d. MaxWell Biosystems AG, Zürich, Switzerland
- e. Department of Biomedicine, University of Basel, Basel, Switzerland

* philipp.hornauer@bsse.ethz.ch

Despite several decades of research, key pathophysiological mechanisms of Parkinson's disease (PD) remain poorly understood, and PD as of today is not curable. Since animal models cannot capture the full extent of the pathology, there is a desperate need for human-based model systems to study disease etiology and to develop new therapies [1]. Patient-derived and genetically engineered human induced pluripotent stem cells (hiPSCs) represent exciting new tools to investigate fundamental aspects of the mechanisms and underlying pathways of neurological disorders in a clinically relevant setting [2].

Today's high-density microelectrode arrays (HD-MEAs) provide researchers the opportunity to probe the development of disease-specific electrophysiological phenotypes at great spatiotemporal detail and scale [3]. However, in contrast to genomic or proteomic analysis frameworks, there are currently no standardized procedures for the functional characterization of human neurons. Novel analysis approaches are, therefore, urgently needed to fully capitalize on the rich data sets provided by HD-MEAs.

Here we introduce *DeePhys*, a modular analysis workflow particularly suited to probe the electrophysiological phenotype of developing hiPSC-derived neuronal networks (see Figure 1). *DeePhys* enables the inference of cellular and network-level electrophysiological features from spike-sorted HD-MEA data (Figure 1D) and provides classification models to systematically estimate their importance in differentiating between different cell lines (Figure 1E). Treatment efficacy then can be evaluated using pretrained models based on features with the highest predictive power (Figure 1F).

In this proof-of-concept study, we applied *DeePhys* to hiPSC-derived dopaminergic (DA) neuron-astrocyte co-cultures harboring a well-known genetic mutation associated with early-onset PD (*SNCA*^{A53T}) and an isogenic control line (Figure 1A). We find that the electrophysiological features inferred by *DeePhys* proved to be specific for the A53T phenotype across all scales, enabled to predict the genotype and the age of individual cultures with high accuracy, and revealed a mutant-like phenotype after downregulation of α -synuclein (α -syn). This finding may be linked to previous results regarding the role of α -syn in the maintenance of the neuronal synaptic vesicle pool [4]. Our results show that *DeePhys* provides an easy-to-use, scalable, quantitative analysis platform for functional phenotype screening and for addressing important biomedical questions in the development of novel treatments.

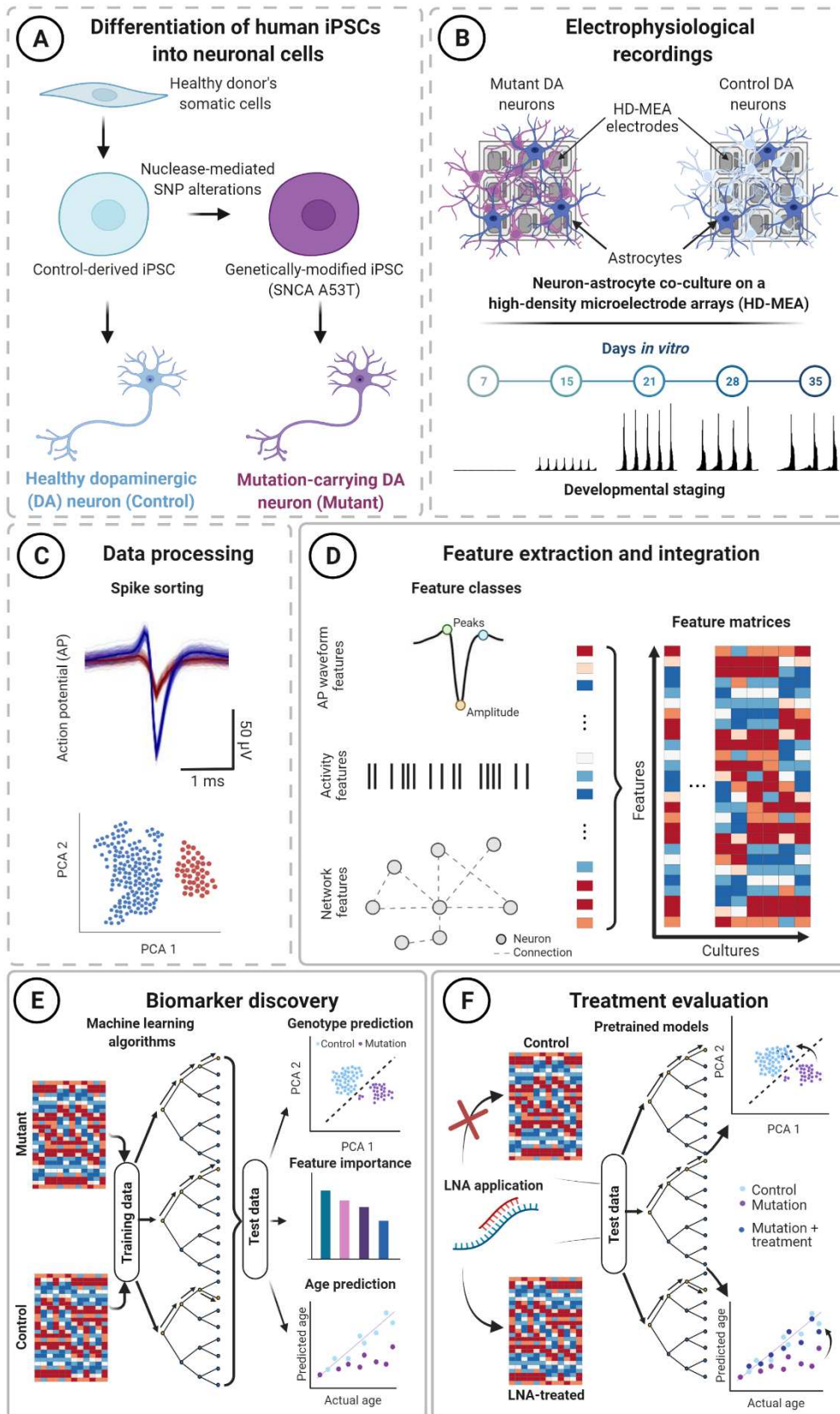


Figure 1: Schematic of the DeePhys analysis pipeline. Panels with dashed outlines represent steps that precede the analysis with DeePhys (Figure 1A-C), while a solid outline indicates the core steps of the DeePhys pipeline (Figure 1D-F).

References

1. Dawson, T. M., Golde, T. E., & Lagier-Tourenne, C. (2018). Animal models of neurodegenerative diseases. *Nature Neuroscience*, *21*(10), 1370–1379.
2. Mertens, J., Reid, D., Lau, S., Kim, Y., & Gage, F. H. (2018). Aging in a Dish: iPSC-Derived and Directly Induced Neurons for Studying Brain Aging and Age-Related Neurodegenerative Diseases. *Annual Review of Genetics*, *52*, 271–293.
3. Pelkonen, A., Pistono, C., Klecki, P., Gómez-Budia, M., Dougalis, A., Konttinen, H., Stanová, I., Fagerlund, I., Leinonen, V., Korhonen, P., & Malm, T. (2021). Functional Characterization of Human Pluripotent Stem Cell-Derived Models of the Brain with Microelectrode Arrays. *Cells*, *11*(1). <https://doi.org/10.3390/cells11010106>
4. Cabin, D. E., Shimazu, K., Murphy, D., Cole, N. B., Gottschalk, W., McIlwain, K. L., Orrison, B., Chen, A., Ellis, C. E., Paylor, R., Lu, B., & Nussbaum, R. L. (2002). Synaptic vesicle depletion correlates with attenuated synaptic responses to prolonged repetitive stimulation in mice lacking α -synuclein. *The Journal of Neuroscience: The Official Journal of the Society for Neuroscience*, *22*(20), 8797–8807.

Neuroprostheses for artificial vision

Diego Ghezzi

Medtronic Chair in Neuroengineering, École polytechnique fédérale de Lausanne (EPFL),
Geneva, Switzerland

Implantable neural prostheses are devices exploited to recover impaired or lost functions, such as vision. In this talk, I will present our effort to develop novel visual prostheses. I will cover aspects spanning from materials to manufacturing methods and preclinical validation. In particular, I will focus on wireless solutions for stimulation.

A common design constraint in neural implants is the presence of cables connecting the electrode-tissue interface to implantable electronic units. The presence of wires and connectors is a significant disadvantage for neural prostheses. They are weak points often leading to failure, they exert mechanical forces and tractions on the implant and the tissue, and they might lead to post-surgical complications, such as infection. Also, the use of implantable electronic units is another disadvantage due to constraints in power consumption, heat generation, and the high risk of failure in a wet environment due to leakage. In neurotechnology, truly wireless electrodes are highly desirable.

POLYRETINA is a wireless retinal prosthesis allowing wide-field and high-resolution stimulation of the retina. First, I will describe our recent results related to POLYRETINA testing. Then, I will discuss how materials and solutions adopted for POLYRETINA are now applied to new devices for artificial vision and other applications.

Direct measurement of oxygen reduction reactions at neurostimulation electrodes

Jiri Ehlich,^{a*} Ludovico Migliaccio,^a Ihor Sahalianov,^a Marta Nikić,^{a,b} Jan Brodský,^a Imrich Gablech,^a Xuan Thang Vu,^c Sven Ingebrandt,^c Eric Daniel Głowacki^a

- Bioelectronics Materials and Devices Laboratory, Central European Institute of Technology, Brno University of Technology, Purkyňova 123, 612 00 Brno, Czech Republic
- Institute of Neuroelectronics, Technical University of Munich, Germany
- Institute of Materials in Electrical Engineering 1, RWTH Aachen University, Germany

* Jiri.Ehlich@ceitec.vut.cz

During electrical neural stimulation, charge-balanced biphasic current pulses are typically used to trigger action potentials in excitable tissues. Cathodic pulses depolarize cells, evoking action potentials, meanwhile subsequent anodic pulses are meant to reverse the products of possible electrochemical processes back to their original form. Balanced biphasic current pulses are thus generally considered to be safe for chronic applications [1]. However recently it has been found, that not all reactions that could possibly happen at the electrode-tissue interface during the stimulation are perfectly reversible. Products of these reactions can be possibly toxic to the tissue or otherwise affect physiology. The identity and the scale of such reactions still remains an unexplored area [2].

Our work examines oxygen reduction reactions (ORRs) at the electrodes made out of commonly used materials used for neural stimulation electrodes (platinum, platinum-iridium alloy, gold, tungsten, nichrome, iridium oxide, titanium, titanium nitride, ITO and PEDOT:PSS). Oxygen can be reduced either to water or hydrogen peroxide by 4- or 2-electron process. Both reactions can significantly reduce the quantity of dissolved oxygen near the electrode, creating hypoxic conditions which may be harmful to neurons. Peroxide, meanwhile, can induce toxic reactions or act as a signaling molecule. We have examined the amount of reduced oxygen and produced peroxide by various biphasic stimulation protocols using amperometric sensors (Clark electrodes) and compared electrocatalytic activities of studied materials.

Main finding is that typical charge-balanced biphasic pulse protocols do not prevent irreversible ORRs. Some electrode materials induce highly hypoxic conditions near electrode surface, others additionally produce an accumulation of hydrogen peroxide into the mM range.

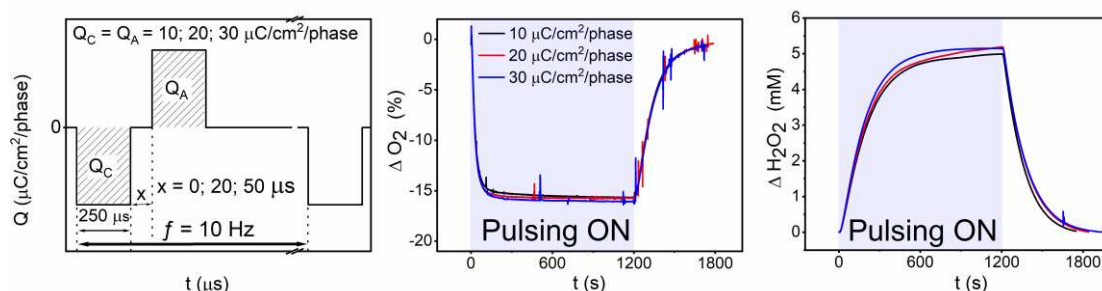


Figure 1: Example of charge-balanced cathodic-leading current pulses and subsequent amperometric sensor response 200 μm above the electrode surface. Gold electrode was used for this demonstration..

References

- Boehler, C., Carli, S., Fadiga, L., Stieglitz, T. & Asplund, M. Tutorial: guidelines for standardized performance tests for electrodes intended for neural interfaces and bioelectronics. Nat. Protoc. 15, 3557–3578 (2020).
- Cogan, S. F., Ehrlich, J., Plante, T. D., Gingerich, M. D. & Shire, D. B. Contribution of oxygen reduction to charge injection on platinum and sputtered iridium oxide neural stimulation electrodes. IEEE Trans. Biomed. Eng. 57, 2313–2321 (2010).

***In-vitro* evaluation of artificial vision restoration in the retina using high density micro-electrode arrays**

Andrea Corna^{a,b*}, Poornima Ramesh^d, Florian Jetter^b, Meng-Jung Lee^b, Jakob H Macke^{c,d}
Günther Zeck^{a,b}.

- a. Institute of Biomedical Electronics, TU Wien, Vienna, Austria
- b. Neurophysics, Natural and Medical Sciences Institute, University of Tübingen, Reutlingen, Germany
- c. Machine Learning in Science, University of Tübingen, Tübingen, Germany
- d. MPI for Intelligent Systems, Tübingen, Germany.

* andrea.corna@tuwien.ac.at

Photoreceptor degeneration pathologies affect millions of people worldwide with severe consequences, ranging from partial vision loss to blindness. Retina implants aim to restore vision in degenerated retinas via artificial stimulation of the inner retina cell layers [1,2]. To date, however, an agreement on the optimal retina stimulation strategy has not been reached. A key to understanding and optimizing retina artificial stimulation is bidirectional stimulation and recording of the retina activity. *In-vitro* experiments using Micro-Electrode Arrays (MEA) technology, via optimal electrode design and low noise electronics, enable high signal to noise ratio recording, enhancing data quality and providing a deeper understanding of artificial stimulation [3]. In this work we characterized sinusoidal stimulation as an alternative to standard pulsatile stimulation approaches using a CMOS based High Density (HD) MEA [4]. The sensor arrays comprise 4225 recording electrodes intermingled with 1024 stimulation electrodes within 1, 4 or 5.3 mm². The electrode density (pitch:16, 32 or 36 μm) allows electrical imaging and precise localization of cell soma and axons in combination with the possibility of arbitrary selection of the stimulation waveform and stimulation area. We exploited these features to investigate spatial and contrast discrimination of artificial shapes by stimulation with sinusoidal waveforms in epiretinal configuration. Stimulation was performed in adult photoreceptor degenerated mouse retina (rd10) and adult healthy retina. We demonstrated efficient stimulation at low charge densities (40 nC mm⁻²) and discrimination of 32 μm spatial jitter [5]. In order to further understand the potential of sinusoidal stimulation we expanded the work to study the response to different frequencies up to 100 Hz. The results were evaluated in terms of stimulation efficacy, in relation to stimulation charge, and response reliability. In summary, continuous electrical imaging of stimulated activity at subcellular scales allows identification of optimal stimuli with respect to spatial and temporal specificity up to the frequency range of 100 Hz.

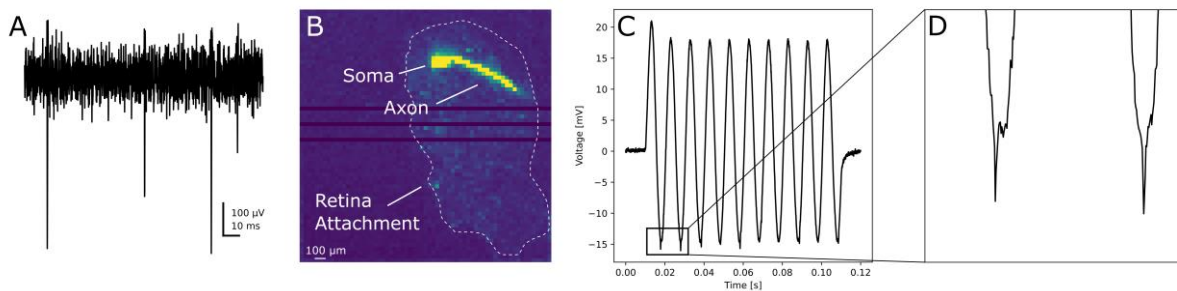


Figure 1: CMOS HD MEA bidirectional *in-vitro* interface. A) Example of low noise CMOS recording of retinal ganglion cell's (RGC) extracellular action potential. B) Electrical imaging of the axon path: Low noise recording allows localization of soma and axon's position and estimation of retina attachment on the 5.3 mm² sensor array of the CMOS MEA. C) Simulation artifact visible in a raw electrode recording during sinusoidal stimulation (100 Hz). D) insert from C showing induced spikes during the cathodic phase of the sinusoidal stimulation.

1. Zrenner, E. (2013). Fighting blindness with microelectronics. *Science translational medicine*, 5(210), 210ps16-210ps16.
2. Palanker, D., Le Mer, Y., Mohand-Said, S., Muqit, M., & Sahel, J. A. (2020). Photovoltaic restoration of central vision in atrophic age-related macular degeneration. *Ophthalmology*, 127(8), 1097-1104.
3. Obien, M. E. J., Deligkaris, K., Bullmann, T., Bakkum, D. J., & Frey, U. (2015). Revealing neuronal function through microelectrode array recordings. *Frontiers in neuroscience*, 8, 423.
4. Bertotti, G., Velychko, D., Dodel, N., Keil, S., Wolansky, D., Tillak, B., ... & Thewes, R. (2014, October). A CMOS-based sensor array for in-vitro neural tissue interfacing with 4225 recording sites and 1024 stimulation sites. In *2014 IEEE Biomedical Circuits and Systems Conference (BioCAS) Proceedings* (pp. 304-307). IEEE.
5. Corna, A., Ramesh, P., Jetter, F., Lee, M. J., Macke, J. H., & Zeck, G. (2021). Discrimination of simple objects decoded from the output of retinal ganglion cells upon sinusoidal electrical stimulation. *Journal of Neural Engineering*, 18(4), 046086.

Delayed feedback control as a closed-loop stimulation protocol to disrupt oscillatory network bursting *in vitro*

Domingos Castro^a, Miguel Aroso^a, A. Pedro Aguiar^b, David B. Grayden^c, Paulo Aguiar^{a,*}

- a. Neuroengineering and Computational Neuroscience Lab, i3S – Institute for Research and Innovation in Health, University of Porto
 - b. Department of Electrical and Computer Engineering, University of Porto
 - c. Department of Biomedical Engineering, University of Melbourne
- * pauloaguiar@i3s.up.pt

Oscillatory neuronal activity, generated by collective and periodic neuronal discharges, is thought to play an important role in brain function. However, excessive synchronization may become pathological, being often associated with neurological disorders such as Parkinson's disease, essential tremor, epilepsy and dystonia [1]. Direct brain stimulation has shown remarkable success in mitigating the symptoms of such diseases when drug therapy is not effective. However, stimulation is typically applied in an open-loop paradigm, which might lead to excessive stimulation and burdensome side effects [2]. To achieve effective control with minimum side effects, stimulation should be handled by a closed-loop controller that actuates according to the current state of the brain.

Computational studies have focused on developing closed-loop stimulation protocols to ablate pathological neuronal synchronization. Delayed feedback control (DFC) is a method known to control chaotic systems and has been extensively explored to desynchronize neuronal networks *in silico* [3-6]. Briefly, DFC applies a feedback signal proportional to the difference between the current oscillation and the oscillation delayed by a fixed period. Theoretically, DFC should lead to desynchronization if the considered delay corresponds to the half-cycle duration. Despite its multiple applications in computational studies, there is still controversy in the literature regarding its efficacy, with reports suggesting that synchronization may actually be amplified under certain conditions [7].

To the best of our knowledge, we present here for the first time, an implementation of DFC to disrupt periodic synchronization in biological neuronal networks. We used hippocampal neurons cultured on microelectrode arrays that, after several days *in vitro*, exhibit periodic synchronous bursts. We developed two different versions of the DFC algorithm: non-adaptive DFC (or simply DFC), which assumes a fixed bursting periodicity (black loop in Figure 1.A, analogous to what has been proposed in the literature); and adaptive DFC (aDFC), which adapts to the ongoing periodicity in real-time (Figure 1.A, black and blue loops). The electrical pulses have fixed amplitude and stimulation frequency that is defined by the resulting feedback signal (the positive part only). We show that, at least with our biological neuronal networks, traditional DFC does not desynchronize the neuronal firing, but rather promotes a new oscillatory regime (Figure 1.B, top). On the other hand, aDFC is capable of disrupting the basal neuronal oscillation (Figure 1.B, bottom).

We show that different stimulation protocols (DFC, aDFC and random Poisson stimulation) only produced consistent distinguishable effects on the neuronal dynamics for a subset of the networks tested, here termed *controllable networks*. Interestingly, these controllable networks had intermediate levels of basal firing rate and synchrony, suggesting that controllability may only be achievable if the basal network dynamics are at the “edge of chaos”, i.e., at the borderline between order and disorder. We then showed that *in silico* networks also display a controllability subspace associated with intermediate levels of firing rate and synchrony, which could be modulated as a function of network properties such as the fraction of excitatory to inhibitory neurons or the level of synaptic strength.

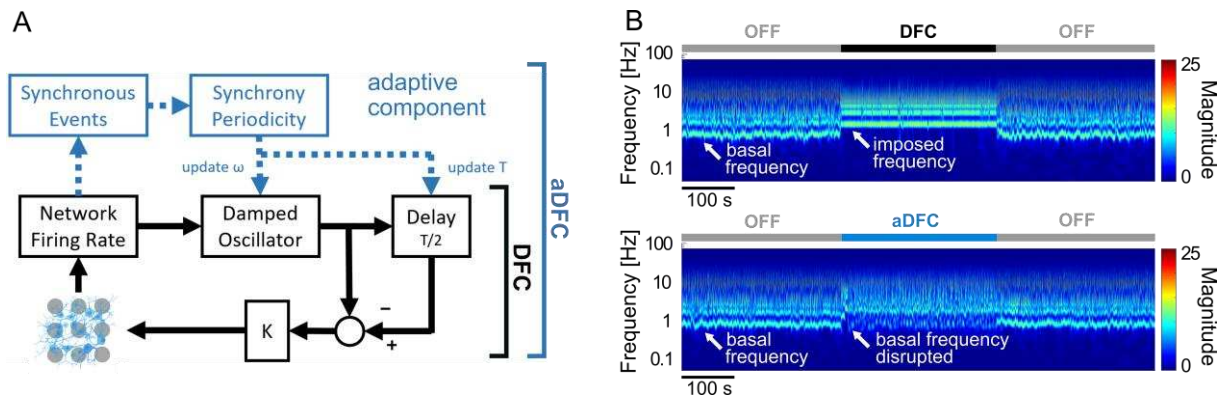


Figure 1: Delayed Feedback Control (DFC) in vitro. (A) Schematic representation of the non-adaptive DFC (DFC, black loop) and adaptive DFC (aDFC, black and blue loops) algorithms. (B) Wavelet transform of the instantaneous firing rate of a given neuronal network under DFC (top) and aDFC (bottom) stimulation protocols.

References

1. Uhlhaas, P.J., Singer, W. (2006). Neural Synchrony in Brain Disorders: Relevance for Cognitive Dysfunctions and Pathophysiology. *Neuron* 52 (1): 155–68. <https://doi.org/10.1016/j.neuron.2006.09.020>.
2. Kuo, C.H., White-Dzuro, G.A., and Ko, A.L., (2018). Approaches to Closed-Loop Deep Brain Stimulation for Movement Disorders. *Neurosurgical Focus* 45 (2): E2. <https://doi.org/10.3171/2018.5.FOCUS18173>
3. Rosenblum, M., Pikovsky, A. (2004). Delayed Feedback Control of Collective Synchrony: An Approach to Suppression of Pathological Brain Rhythms. *Physical Review E* 70 (4): 041904. <https://doi.org/10.1103/PhysRevE.70.041904>.
4. Vlachos, I., Deniz, T., Aertsen, A., Kumar, A. (2016). Recovery of Dynamics and Function in Spiking Neural Networks with Closed-Loop Control. *PLOS Computational Biology* 12 (2): e1004720. <https://doi.org/10.1371/journal.pcbi.1004720>.
5. Daneshzand, M., Miad, F., Barkana, B.D. (2018). Robust Desynchronization of Parkinson's Disease Pathological Oscillations by Frequency Modulation of Delayed Feedback Deep Brain Stimulation. *PLOS ONE* 13 (11): e0207761. <https://doi.org/10.1371/journal.pone.0207761>
6. Popovych, O.V., Tass, P.A. 2019. Adaptive Delivery of Continuous and Delayed Feedback Deep Brain Stimulation - a Computational Study. *Scientific Reports* 9 (1): 10585. <https://doi.org/10.1038/s41598-019-47036-4>.
7. Dovzhenok, A., Park, C., Worth, R.M., Rubchinsky L.L. 2013. Failure of Delayed Feedback Deep Brain Stimulation for Intermittent Pathological Synchronization in Parkinson's Disease. *PLoS ONE* 8 (3): e58264.

Acknowledgments

This work was partially financed by FEDER - Fundo Europeu de Desenvolvimento Regional funds through the COMPETE 2020 - Operational Programme for Competitiveness and Internationalisation (POCI), Portugal 2020, and by Portuguese funds through FCT - Fundação para a Ciência e a Tecnologia/Ministério da Ciência, Tecnologia e Ensino Superior in the framework of the project PTDC/EMD-EMD/31540/2017 (POCI-01-0145-FEDER-031540). Domingos Castro is a recipient of a FCT Ph.D. fellowship (SFRH/BD/143956/2019).

Network function in human cerebral organoids as a platform for mechanistic and therapeutic advances in cognitive disorders

Susanna B. Mierau, MD, Dphil

Division of Cognitive and Behavioral Neurology, Brigham & Women's Hospital, Boston, MA, USA; Lurie Center for Autism, Massachusetts General Hospital, Boston, MA, USA; Harvard Medical School, Boston, MA, USA

Human cerebral organoids offer an extraordinary *in vitro* cellular model for studying human brain development and early disturbances in neurologic disease. Microelectrode array (MEA) recordings are commonly used to compare neuronal activity in 2D and 3D cultures. Yet, MEA recordings can also reveal cellular-scale network activity (Schroeter et al., 2017), including patterns or motifs in network function seen across spatial scales from cellular to whole brain networks. We have used MEA recordings from human air-liquid interface cerebral organoids (ALI-COs; Giandomenico et al., 2019) to study network function and maturation. We have also demonstrated intact neuronal network function development with MEA recordings in a human cerebral organoid model of amyotrophic lateral sclerosis with frontotemporal dementia (ALS/FTD; Szenbenyi et al., 2021). To facilitate investigations of network development in ALI-COs and the impact of disease-causing perturbations, we created a MATLAB network analysis pipeline (MEA-NAP) for batch analysis of MEA experiments to compare network function over time and conditions (e.g., genetic mutation or drug treatment). This user-friendly, open-source diagnostic tool can process raw voltage time-series acquired from single- (Multichannel System) or multi-well MEAs (Axion) and automatically infer key network properties from organoids or 2D human (or murine) neuronal cultures. Our pipeline enables users to perform MEA analysis beyond standard measures of activity or correlation alone to identify differences in network topology and roles of individual nodes in network activity. Our analyses of network function in ALI-COs demonstrate that they can serve as a platform for investigating disease mechanisms and screening new therapies.

Kirigami-like mesh-electrode-arrays for integration with human electrogenic organoids

Csaba Forro,^a Tommy Li,^a Xiao Yang^a, Ching-Ting Tsai^a, Yang Yang^a, Francesca Santoro^{b,c,d}, Sergiu Pasca^a, Bianxiao Cui^a

- a. Stanford University, Stanford, CA, USA
- b. Tissue Electronics, Istituto Italiano di Tecnologia, Naples, 80125 Italy
- c. Faculty of Electrical Engineering and Information Technology, RWTH Aachen, 52072 Aachen, Germany
- d. Institute of Biological Information Processing – Bioelectronics, IBI-3, Forschungszentrum Juelich, 52428 Juelich, Germany

* bcui@stanford.edu, cforro@stanford.edu

Brain organoids are enabling the non-invasive study of human neural development and capturing phenotypes of disease. Cardiac organoids pave the way for regenerative medicine. Accessing the electrical activity of these electrogenic organoids is central to understanding the development and biological faithfulness of these novel tissue platforms.

Mesh electrode arrays are low footprint devices that are flexible and conformable. [1,2] Owing to these features, organoids can integrate the device [3,4] during its development in vitro which results in electrodes distributed all throughout and allow long-term recording of electrical activity.

Using lithography, we designed micron-thin polymer structures into a mesh which unfolds into a basket in aqueous solution, accommodating organoids in its center point. We have designed devices that are flexible by exploring rotational degrees of freedom of the design.

Using this design, we can culture and record from organoids on these meshes for long time periods.

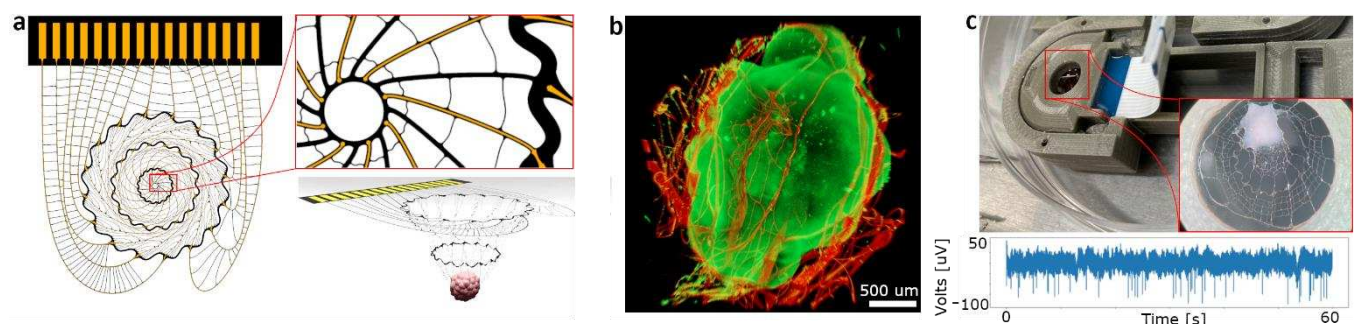


Figure 1 **a)** Mesh-like multi-electrode array design optimized for mechanical robustness by rounding edges. The inset shows tightly packed electrodes at the center of the mesh (round part of the golden lines). It unfolds into a basket to accommodate an organoid. **b)** Volumetric rendering of fluorescent z-stack microscopy. The organoid material is labeled with green fluorescent protein and the mesh has rhodamine incorporated in it (red fluorescence). The reconstruction shows the mesh is fully embedded inside the organoid **c)** 3D-printed chamber design to minimize stress on the organoid during culture. The central hole supports the unfolding of the mesh with the organoid in its center (see inset). The smaller holes on either side allow medium exchange without disturbing the organoid. The blue-and-white strip is a flat-flexible-cable that sends measured data to the computer. A typical time trace of neural activity is shown, demonstrating that the electrodes are embedded inside the organoid and in proximity of cells.

References

1. Yang, Xiao, et al. "Bioinspired neuron-like electronics." *Nature materials* 18.5 (2019): 510-517.
2. Hong, Guosong, et al. "Mesh electronics: a new paradigm for tissue-like brain probes." *Current opinion in neurobiology* 50 (2018): 33-41.
3. Kireev, Dmitry, et al. "N3-MEA probes: scooping neuronal networks." *Frontiers in neuroscience* 13 (2019): 320.
4. McDonald, Matthew, et al. "A mesh microelectrode array for non-invasive electrophysiology within neural organoids." *bioRxiv* (2021): 2020-09.

Micro Electrode Array for the monitoring of inner electrical activity of cerebral organoids

Oramany Phouphetlinthong^{a,c}, Emma Partiot^{b,c}, Audrey Sebban^{a,c}, Raphael Gaudin^{b,c}, Benoit Charlot^{a,c}.

- a. IES, Institut d'Electronique et des Systèmes UMR 5214 CNRS, Montpellier, France
- b. IRIM, Institut de Recherche en Infectiologie de Montpellier, UMR 9004 CNRS, Montpellier, France
- c. University of Montpellier, Montpellier, France
- * Benoit.charlot@umontpellier.fr

Cerebral organoids derived from stem cells are artificially grown miniature organs mimicking embryonic brain architecture. They show a 3D organization made of multiple neural cell types. Measuring the extracellular electrical activity of cerebral organoids with conventional planar microelectrode arrays is particularly challenging due to the spheroidal shape and 3D architecture of cerebral organoids.

One common solution is to cut in half the organoids[1] to expose inner cells to planar electrodes, but this is detrimental to the viability of the organoid. On the device levels there has been several attempts to build either conical electrodes[2][1], use neuropixel shanks[3] or grid like electrode arrays [4][5], to either penetrate or fit the spheroidal shaped organoids.

In order to monitor the extracellular activity of thick spheroid-shaped samples, we developed long protruding microelectrode array, curvy and spiky, able to penetrate in the inner regions of cerebral organoids in order to measure local extracellular potential of neurons.

A new microfabrication process has been developed on the base of standard process of planar MEAs. In order to obtain vertical microelectrodes we have used the relaxation of internal stresses of a stack of silicon nitride and silicon dioxide materials deposited over a sacrificial layer. These materials having opposite stress, tensile and compressive, the release of a clamped/free beam induces a backward deflexion of the latter. A patterned metal layer included between these stressed materials allows to obtain an electrode near the apex of the spiky beams which rise vertically, over two hundred microns.

Cortical organoids were derived from hESC H9 cells (female, WA09, WiCell) as previously described [6]. After analyzing by microscopy the effectiveness of the impalement and penetration of the protruding electrodes inside the organoids we performed spontaneous extracellular measurements. These experiments were carried out using MultiChannel Systems (MCS) amplifier system and compared with standard planar and conical MEAs. The results, (fig.1) shows typical extracellular traces and cutouts of spikes recorded with conical and our curvy spiky MEAs. While the planar electrodes gives no results, the conical electrode can retrieve small amplitude activities while the penetrating electrodes shows larger amplitude spikes.

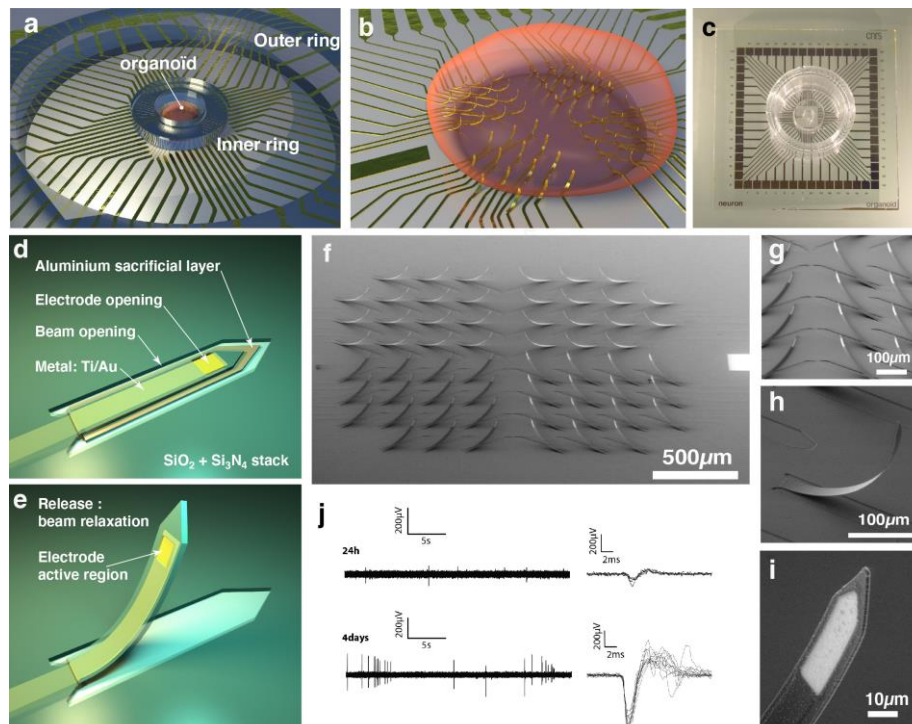


Figure 1: (a,b) 3D schematic representation of a cerebral organoid impaled on the MEA (c) Photograph of the functional MEA showing the PDMS inner and outer rings. (d) Schematic of the principle of microfabrication of the spiky electrodes, (e) once etched the beam sporting one electrode relaxes its internal stress and straighten (f) SEM picture of the whole csMEA array, and (g,h) details of curved beams and of the active region at the end of one beam (i). (j) Traces and cutouts of extracellular signal recorded with one electrode at 24h and 4 days after impalement of the organoid. 30s long acquisition and superposition of several detected spikes. The recorded signal becomes stronger with time and goes up to several hundreds of μV .

This work has shown the development of a technique to produce curved and spiky microelectrode arrays that are used to monitor the extracellular electrical activity inside of cerebral organoids. With the increase in studies of brain organoids, which are a much more relevant model than dissociated cell cultures, this device provides an effective solution for measuring the internal extracellular electrical activity of these 3D cell clusters. This work has demonstrated the ability of curved and spiky MEA to measure action potentials with relatively strong signals.

References

- [1] S. L. Giandomenico, S. B. Mierau, G. M. Gibbons, L. M. D. Wenger, L. Masullo, T. Sit, M. Sutcliffe, J. Boulanger, M. Tripodi, E. Derivery, O. Paulsen, A. Lakatos, M. A. Lancaster, *Nature Neuroscience* 2019, 22, 669.
- [2] M. O. Heuschkel, M. Fejtl, M. Raggenbass, D. Bertrand, P. Renaud, *J. Neurosci. Methods* 2002, 114, 135.
- [3] T. Sharf, T. van der Molen, E. Guzman, S. M. K. Glasauer, G. Luna, Z. Cheng, M. Audouard, K. G. Ranasinghe, K. Kudo, S. S. Nagarajan, K. R. Tovar, L. R. Petzold, P. K. Hansma, K. S. Kosik, 2021, 2021.01.28.428643.
- [4] Y. Park, C. K. Franz, H. Ryu, H. Luan, K. Y. Cotton, J. U. Kim, T. S. Chung, S. Zhao, A. Vazquez-Guardado, D. S. Yang, K. Li, R. Avila, J. K. Phillips, M. J. Quezada, H. Jang, S. S. Kwak, S. M. Won, K. Kwon, H. Jeong, A. J. Bhandodkar, M. Han, H. Zhao, G. R. Osher, H. Wang, K. Lee, Y. Zhang, Y. Huang, J. D. Finan, J. A. Rogers, *Science Advances* 2021, 7, eabf9153.
- [5] M. McDonald, D. Sebinger, L. Brauns, L. Gonzalez-Cano, Y. Menuchin-Lasowski, O.-E. Psathaki, A. Stumpf, T. Rauen, H. Schöler, P. D. Jones, *bioRxiv* 2020, 2020.09.02.279125.
- [6] N. V. Ayala-Nunez, G. Follain, F. Delalande, A. Hirschler, E. Partiot, G. L. Hale, B. C. Bollweg, J. Roels, M. Chazal, F. Bakoa, M. Carocci, S. Bourdoulous, O. Faklaris, S. R. Zaki, A. Eckly, B. Uring-Lambert, F. Doussau, S. Cianferani, C. Carapito, F. M. J. Jacobs, N. Jouvenet, J. G. Goetz, R. Gaudin, *Nat Commun* 2019, 10, 4430

Microelectrode array recording of midbrain organoid slices cultured in air-liquid interface

Anssi Pelkonen ^{a#}, Sara Kälvälä ^{a#}, Antonios Dougalis ^a, Mireia Gómez-Budia ^a, Šárka Lehtonen ^{aa*}, Tarja Malm ^{aa}

- a. A. I. Virtanen Institute for Molecular Sciences, Faculty of Health Sciences, University of Eastern Finland, Neulaniementie 2, 70211 Kuopio, Finland

#, ^{aa} equal contribution

* sarka.lehtonen@uef.fi

Human pluripotent stem cell (hPSC) derived organoids are an important tool for studying physiological and pathological neuronal network function of the whole brain or in distinct brain regions [1]. hPSC-derived dopaminergic (DAergic) neurons carrying Parkinson's disease (PD) associated mutations have also been shown to display pathological network activity in microelectrode array (MEA) recordings [2]. However, organoids can be slow to mature in terms of network function, and large organoids ($\varnothing > 2$ mm) develop necrotic cores due to poor nutrient/oxygen diffusion to deeper parts of the organoid [1]. These issues can be addressed by creating air-liquid-interface (ALI) slice cultures of organoids (Fig. 1A) as shown by experiments with cerebral organoids [3]. Our aim was to establish an ALI culture of DAergic midbrain organoids that can also display network activity on MEA.

The midbrain organoid differentiation was performed as described by Fiorenzano et al. [4] (with slight modifications). Immunocytochemical staining against tyrosine hydroxylase (TH) was used to verify the presence of DAergic neurons. After 2.5 mo of differentiation, the organoid was embedded in 2 % agarose gel, sliced to 500 μ m thick slices in ice-cold Dulbecco's phosphate-buffered saline using a vibratome (Campden 7000smz, Campden Instruments, UK). The slices were transferred to Millicell Cell Culture Inserts (PIHP01250, \varnothing 12 mm, pore size 0.4 μ m, Merck Millipore, UK). The slices were maintained in the inserts in ALI for 1.5 mo in standard cell culture conditions, after which network activity was recorded using 60-3DMEA250/12/100iR-Ti MEAs (Multichannel Systems [MCS], Germany) and MEA2100-Mini-60-System (MCS). MEA recordings were performed under constant perfusion with carboxynated artificial cerebro-spinal fluid. In order to evoke maximal network responses, 3 slices were subjected to high concentration of N-methyl-D-aspartate (NMDA; 200 μ M, 2 min). The effect of DA (100 μ M, 2 min) on continuous activity evoked by low NMDA (20 μ M) was studied in one of the slices. MEA data was analyzed using in-house made scripts and pipeline in NeuroExplorer (Nex Technologies, USA).

The midbrain organoid ALI cultures had TH positive cells, suggesting them to possess DAergic capacity (Fig. 1B). On MEA (Fig. 1C) the organoid slices showed little spontaneous activity, but the high NMDA treatment induced slice-wide synchronous delta- and theta-band activity (Fig. 1D-G) as well as synchronous bursts in all slices indicating presence of a neuronal network with synaptic connections. The slices appeared activated throughout with no indications of necrotic or otherwise silent areas. The lower concentration of NMDA also induced clear, continuous network activity (Fig. 1H-K). This activity was reversibly altered by DA, suggesting presence of functional DA receptors. While the MEA recording protocol can be further optimized, we conclude that ALI is a viable strategy for producing midbrain organoids slice cultures with functional neuronal networks.

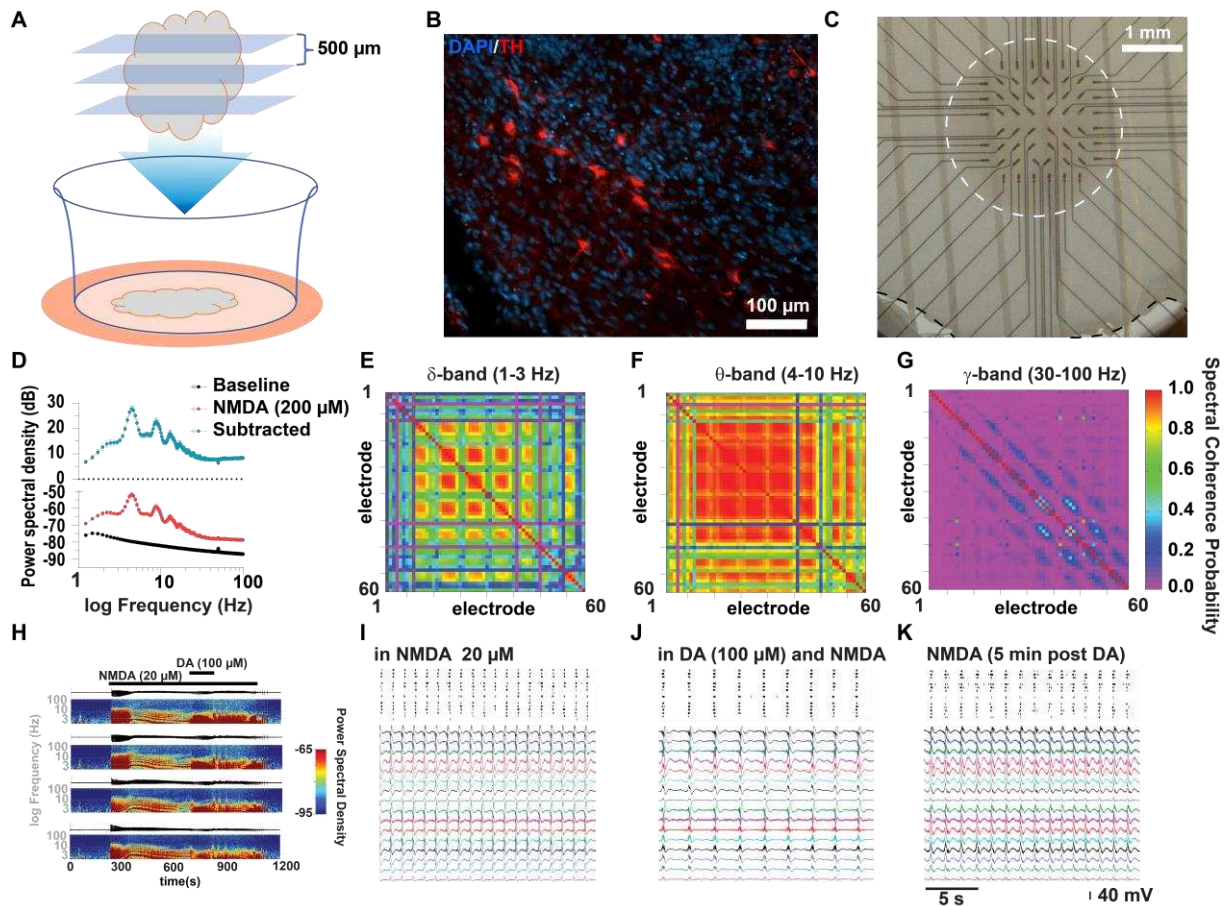


Figure 1: A: The organoids were cut to 500 μm slices and placed in cell culture inserts after 2.5 mo of differentiation. B: The ALI cultures contained tyrosine hydroxylase (TH) positive neurons. C: The membrane (edge highlighted with black dashed line) was cut out of the insert and the organoid slice (highlighted with white dashed line) was recorded on MEA after 1.5 mo at ALI. D: Baseline subtracted NMDA-induced power spectral density (PSD) of local field potentials (LFPs; low-pass filtered at 200 Hz) and the raw PSDs before and during high (200 μM) NMDA treatment. E, F, G: Functional connectivity during high (200 μM) NMDA treatment expressed as coherence probability between each electrode pair in the array at the delta (E), theta (F) and gamma bands (G). H: PSDs and representative LFP traces from four electrodes during low NMDA (20 μM) and DA (100 μM) treatment. I, J, K: Raster plots and corresponding LFP traces of activity induced by low NMDA (20 μM) before (I), during (J) and after (K) application of DA (100 μM).

References

1. Pelkonen, A., Pistono, C., Klecki, P., Gómez-Budia, M., Dougalis, A., Konttinen, H., Stanová, I., Fagerlund, I., Leinonen, V., Korhonen, P., Malm, T. (2021). Functional Characterization of Human Pluripotent Stem Cell-Derived Models of the Brain with Microelectrode Arrays. *Cells* 11, doi:10.3390/cells11010106.
2. Ronchi, S., Buccino, A.P., Prack, G., Kumar, S.S., Schröter, M., Fiscella, M., Hierlemann, A. (2021). Electrophysiological Phenotype Characterization of Human iPSC-Derived Neuronal Cell Lines by Means of High-Density Microelectrode Arrays. *Adv Biol* 5, e2000223, doi:10.1002/adbi.202000223.
3. Giandomenico, S.L., Mierau, S.B., Gibbons, G.M., Wenger, L.M.D., Masullo, L., Sit, T., Sutcliffe, M., Boulanger, J., Tripodi, M., Derivery, E., et al. (2019). Cerebral organoids at the air-liquid interface generate diverse nerve tracts with functional output. *Nat Neurosci* 22, 669–679, doi:10.1038/s41593-019-0350-2.
4. Fiorenzano, A., Sozzi, E., Birtele, M., Kajtez, J., Giacomoni, J., Nilsson, F., Bruzelius, A., Sharma, Y., Zhang, Y., Mattsson, B., et al. (2021). Single-cell transcriptomics captures features of human midbrain development and dopamine neuron diversity in brain organoids. *Nat Commun* 12, 7302, doi:10.1038/s41467-021-27464-5.

Brain, copy and paste

Donhee Ham^{a,b,*}

- a. Harvard University, USA.
- b. Samsung Advanced Institute of Technology, Samsung Electronics, South Korea.

* donhee@g.harvard.edu

Massively parallel intracellular recording of a large number of mammalian neurons forming a network is a great technological pursuit in neurobiology, but it has been difficult to achieve. For example, the intracellular recording by the patch clamp achieves a high sensitivity that can measure down to sub-threshold synaptic events, but it lacks massive parallelism, for it cannot be scaled into a dense array. For another example, the microelectrode array can record many more neurons, but the sensitivity of this extracellular technique is not high enough to easily measure synaptic activities. In this talk, I would like to present our CMOS electrode array technology that massively parallelizes the intracellular neuronal recording [1,2]. With this unprecedented ability, it can help 'copy' the functional synaptic connectivity map of mammalian neuronal networks, a celebrated problem in neuroscience [1,3]. I will also discuss how this technology can bring us a step closer to the original goal of neuromorphic engineering to create a solid-state electronic platform that can better approximate the unique computing traits of the brain [3,4].

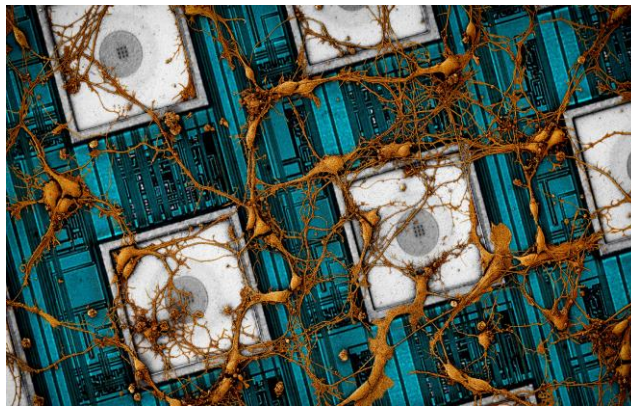


Figure 1: CMOS platform for massively parallel intracellular recording.

References

1. Abbott, J., Ye, T., Krenek, K., Gertner, R., Ban, S., Kim, Y., Qin, L., Wu, W., Park, H., and Ham, D. (2020). A nanoelectrode array for obtaining intracellular recordings from thousands of connected neurons. *Nature Biomedical Engineering* 4, 232-241.
2. Abbott, J., Ye, T., Krenek, K., Qin, L., Kim, Y., Wu, W., Gertner, G., Park, H., and Ham, D. (2020). The design of a CMOS nanoelectrode array with 4096 current-clamp/voltage-clamp amplifiers for intracellular recording/stimulation of mammalian neurons. *IEEE Journal of Solid-State Circuits* 55, 2567-2582.
3. Ham, D., Park, H., Hwang, S., and Kim, K. (2021). Neuromorphic electronics based on copying and pasting the brain. *Nature Electronics* 4, 635-644.
4. Jung, S., Lee, H., Myung, S., Kim, H., Yoon, S., Kwon, S-W., Ju, Y., Kim, M., Yi, W., Han, S., Kwon, B., Seo, B., Lee, K., Koh, G-H., Lee, K., Song, Y., Choi, C., Ham, D., and Kim, S. (2022). A crossbar array of magnetoresistive memory devices for in-memory computing. *Nature* 601, 211-216.

Impedance Measurements and Electrophysiological Recordings of Mouse Retinae on a Multifunctional HD-MEA Platform

Hasan Ulusan^a, Roland Diggelmann^a, Chloe Magnan^a, Matej Znidaric^a, Vijay Viswam^{a,b}, Felix Franke^{a,c}, and Andreas Hierlemann^a

^aETH Zürich, Department of Biosystems Science and Engineering, Switzerland

^bMaxWell Biosystems, Switzerland

^cInstitute of Molecular and Clinical Ophthalmology Basel, Switzerland

hasan.ulusan@bsse.ethz.ch

Keywords: HD-MEAs, multifunctional, impedance measurements, electrophysiology, retina

Impedance measurements on high-density microelectrode arrays (HD-MEAs) can be used to study the morphology of neuronal cells and to image biological tissue, such as the retina. Impedance imaging is a non-invasive method to visualize the position and attachment of the retina on the HD-MEA and can be used in conjunction with electrophysiological recordings of live tissue. It allows for studying the correlation between tissue-to-electrode adhesion, tissue properties and the measured spiking activity of retinal ganglion cells on the HD-MEA.

Material and Methods

The multi-functional HD-MEA chip, developed by our group, features 59,760 electrodes at a pitch of 13.5 μm [1]. The electrodes can be arbitrarily connected to several different functional units on-chip, including 2048 units for voltage recordings, 32 units for impedance measurements, 28 units for neurotransmitter detection and 16 units for extracellular voltage- or current stimulation (Figure 1A). We used a dedicated experimental setup (Figure 1B) to project light stimuli onto the photoreceptor layer of mouse retinae while simultaneously recording ganglion-cell activity. Impedance imaging was performed by applying a sinusoidal voltage signal of 50 kHz and 0.1 V_{peak} to the reference electrode and measuring the magnitude and phase shifts of the resultant currents at the individual electrodes. We built an impedance image using 32,000 randomly distributed electrodes on the array by scanning through 1000 different electrode configurations; the image was then completed with spatial interpolation.

Results

Figures 2A-D show the electrophysiological voltage recordings obtained from a high-density recording area, which contained 2025 electrodes arranged in a square of 600 μm x 600 μm . We extracted the single-cell activity of individual retinal ganglion cells (RGCs) through automatic spike-sorting [2]. Light responses of the RGCs were evoked with a chirp light stimulus. We assessed the tissue location and attachment to the HD-MEA by optical microscopy (Figure 2E) and impedance imaging (Figure 2F). The retinal tissue caused changes in the impedance magnitude on the electrodes over which it extended; better attachment of the tissue led to higher impedance magnitudes. The impedance image shows that the edges of the retina piece were pressed more strongly onto the array, which led to more electrical activity in these regions as could be seen in the spiking activity (Figure 2G). Moreover, the optic disc of the retina could be identified with both, light and impedance imaging.

Discussion and Conclusion

The orientation and location of the retinal tissue on the HD-MEA chip could be visualized through impedance imaging and could be used to guide electrophysiological recordings. Moreover, smaller structures, like the optical disc of retina, could be identified with light- and impedance imaging. With further improvements of the HD-MEA platform, we will be able to perform impedance imaging of full HD-MEA within less than 30 min and to also measure impedance values at different frequencies to perform impedance spectroscopy of the cells. We then expect to see additional retinal features, such as blood vessels, and to accurately locate those on the chip.

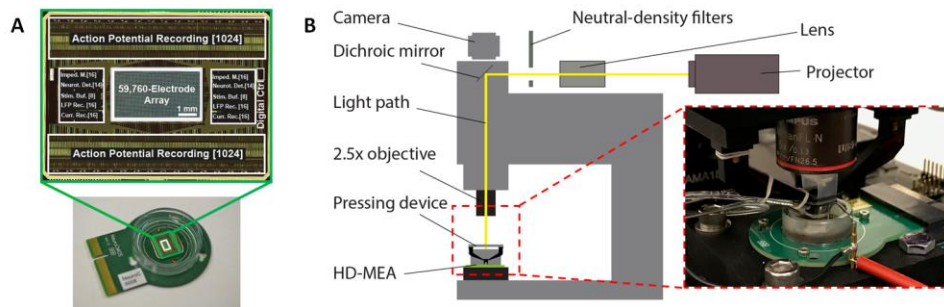


Figure 1: (A) Multi-functional HD-MEA chip micrograph. (B) Experimental setup to apply light stimuli to retina.

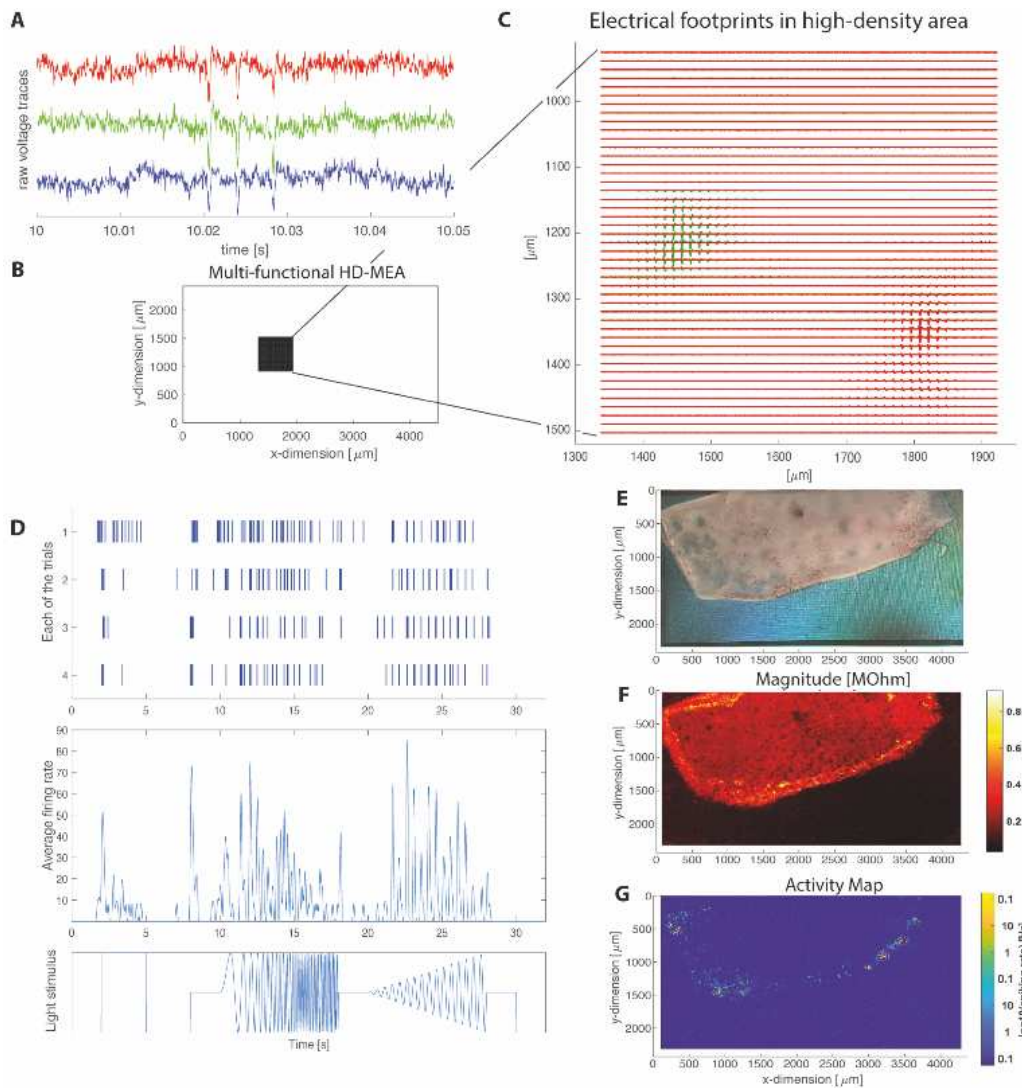


Figure 2: (A) Voltage traces on three example electrodes showing spikes of an RGC. (B) Schematic of the multi-functional HD-MEA depicting the 45x45-electrode high-density recording area. (C) Electrical footprints of two RGCs located in the high-density recording area in (B). (D) Spiking activity of 4 trials of a light stimulus of a single light sensitive neuron where the light stimulus contains a full-contrast flash, a frequency and a contrast modulation chirp. (E) Microscopy image of the mouse retina on the NeuroCMOS HD-MEA chip. (F) Difference in impedance magnitude values measured by the electrodes. (G) Activity map of the RGC neurons.

Acknowledgements

This work was supported by the European Union through the European Research Council (ERC) Advanced Grant 694829 ‘neuroXscales’ and the Swiss National Science Foundation under contract 205320_188910 / 1.

References

- [1] J. Dragas *et al.*, *IEEE JSSC*, vol. 52, no. 6, pp. 1576-1590, Jun. 2017.
- [2] R. Diggelmann *et al.*, *J. Neurophysiol.*, vol. 120, no. 6, pp. 3155–3171, Dec. 2018.

Microstimulation in the rat barrel cortex using custom ASIC-based 512-channel system and high-density silicon probes

Paweł Jurgielewicz,^a Małgorzata Szypulska,^a Piotr Wiącek,^a Andrzej Skoczeń,^a Tomasz Fiutowski,^a Władysław Dąbrowski,^a Bartosz Mindur,^a Ewa Kublik,^b Paweł Hottowy^{a,*}

- a. Faculty of Physics and Applied Computer Science, AGH University of Science and Technology, Krakow, Poland
 - b. Nencki Institute of Experimental Biology, Polish Academy of Sciences, Warsaw, Poland
- * hottowy@agh.edu.pl

We tested the efficiency of the custom-designed 512-channel stimulation/recording system and high-density silicon probes in evoking neuronal responses within a barrel column of a rat cerebral cortex. The system is based on a dedicated 64-channel ASIC for stimulation, recording and artifact reduction (Figure 1). Each channel is equipped with 7-bit DAC that sets the amplitude of the stimulation pulse (up to 15 μA) and an additional 5-bit bipolar DAC that controls the pulse waveform. The temporal resolution of the stimulation signal is 25 μs when all channels are active but can be reduced to 1 μs if a single channel is generating a stimulation signal at the given moment. The recording amplifiers are routinely disconnected from the electrodes for the duration of the stimulation pulse to avoid saturation of the recording circuit. The system can control up to four probes with a total of 512 electrodes. The system design was described in more detail elsewhere [1,2].

For the tests, we used 128-electrode probes from Masmanidis Lab (<https://masmanidislab.neurobio.ucla.edu>). The electrodes were gold-plated for impedance reduction to 0.1-0.2 $\text{M}\Omega$. Probes were inserted into the barrel cortex of an adult, anesthetized rat. Stimulation pulses with amplitudes of 1-4 μA were applied simultaneously to clusters of 1-7 electrodes at up to 80 locations in the barrel column. Neuronal signals were continuously recorded at all channels.

In response to the microstimulation, we recorded action potentials (APs) and electrically evoked local field potentials (EELPs). APs from the stimulated cells had average latencies as low as 1 ms (Figure 2). The latency jitter was below 0.1 ms for some responses but significantly larger for other cells (Figure 2B), suggesting different mechanisms of stimulation. Slow EELPs waves, similar in shape to the LFP evoked by tactile whisker stimulation, were visible on multiple shanks of the stimulating probe (Figure 3A). The amplitudes of the EELPs increased monotonically with the intensity of the applied current. Stimulation in lower cortical layers induced high-frequency oscillations typical for strong multi-whisker responses (Figure 3B) [3].

In the pilot experiments, we successfully evoked subcomponents of natural sensory responses. Future plans include stimulation with complex spatio-temporal patterns of stimulation pulses, investigation of stimulation efficacy as a function of stimulation current waveform (using the high temporal resolution mode) and reduction of the stimulation artifacts by means of low-amplitude correction pulses [4].

Funding: This work was supported by the Polish National Science Centre grant DEC-2013/10/M/NZ4/00268 (PH). PJ has been partially supported by the EU Project POWR.03.02.00-00-I004/16.

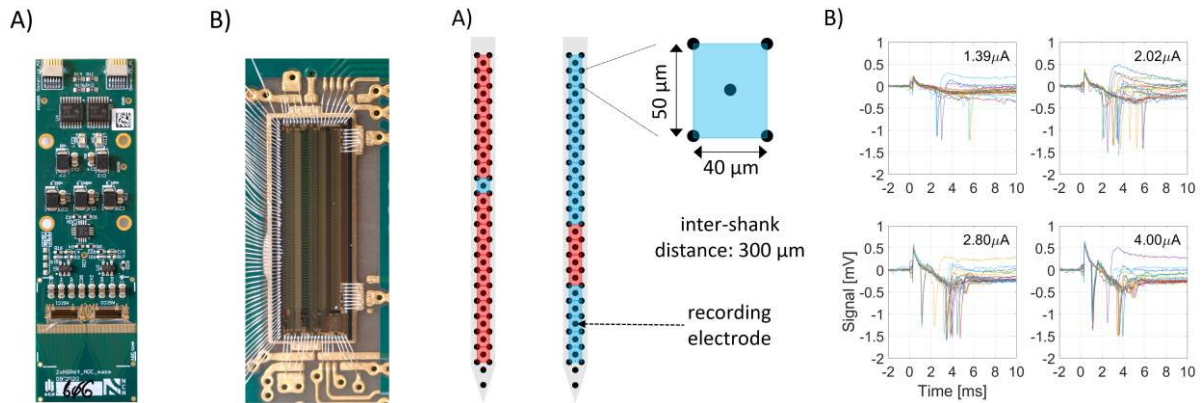


Figure 1: A) 128-channel Head-board. Two 64-pin Molex connectors matching the Masmanidis Lab probes are mounted at the bottom. B) 64-channel ASIC.

Figure 2: Stimulation of an individual neuron. A) Layout of the 128AxN probe used for stimulation and recording. Stimulation was applied to 40 clusters of 5 neighbouring electrodes. Clusters marked with red rectangles stimulated the cell, clusters marked with blue rectangles did not. The black arrow marks the electrode that recorded the spiking activity shown in B. B) The recorded spiking activity for a range of current amplitudes. The stimulation was repeated 20 times for each electrode cluster and each current amplitude. The stimulation pulses were applied at Time=0.

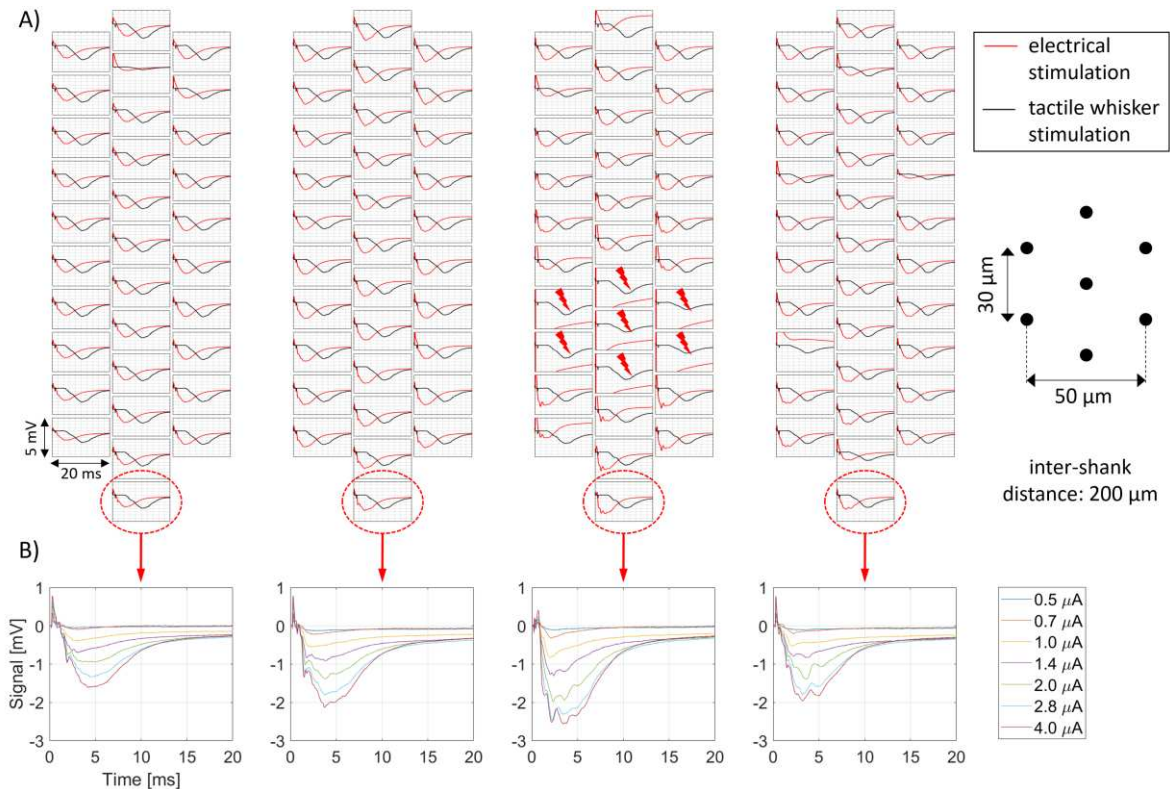


Figure 3: Local Field Potential and high-frequency oscillations evoked by microstimulation. A) Averaged signals evoked by tactile whisker stimulation (black traces) and electrical stimulation (red traces) recorded with a 128K silicon probe. Electrical stimulation was applied to a cluster of 7 electrodes marked with red thunders. All the subplots have the same horizontal and vertical scale (20 ms and 5 mV respectively). B) Averaged signals evoked by electrical stimulation, shown at 4 electrodes as a function of the stimulation amplitude.

References

1. Szypulska M et al 2019, *Acta Neurobiologiae Experimentalis* 79 (59-60).
2. Jurgielewicz P et al 2021, *Sensors* 21 (4423), doi: 10.3390/s21134423
3. Barth DS 2003, *Journal of Neuroscience* 23 (2502-2510).
4. Kołodziej K et al, Conference Abstract: MEA Meeting 2018, doi: 10.3389/conf.fncl.2018.38.00122

3D Printed Customizable Neural Probes

Rahul P. Panat^{1,†,*}, Sandra M. Ritchie¹, Mohammad Sadeq Saleh¹, Hailey L. Gordon³, Mark A. Nicholas², Bin Yuan¹, Chunshan Hu¹, Sanjida Jahan¹, Rriddhiman Bezbaruah¹, Jay W. Reddy³, Maysamreza Chamanzar³, Eric A. Yttri^{2,†,*},

Affiliations:

¹Department of Mechanical Engineering, Carnegie Mellon University, Pittsburgh, Pennsylvania, 15213, USA

²Department of Biological Sciences, Carnegie Mellon University, Pittsburgh, Pennsylvania, 15213, USA

³Department of Electrical and Computer Engineering, Carnegie Mellon University, Pittsburgh, Pennsylvania, 15213, USA

† Carnegie Mellon Neuroscience Institute, Carnegie Mellon University, Pittsburgh, Pennsylvania, 15213, USA

* Correspondence and requests for materials should be addressed to R.P.P.

(rpanat@andrew.cmu.edu) and E.A.Y. (eyttri@andrew.cmu.edu)

Abstract:

Neural probes that can be customized to record electrophysiological signals from the 3D volume of the brain are needed for study-specific neuroscience experiments. In this research, we present a new class of structurally robust, customization, low-cost, high-density microelectrode array, capable of recording from several mm³ volume of tissue. An advanced nanoparticle printing method we developed (Saleh et al., Sci Adv 2017) is used to fabricate individual shanks in the array. The probes are fully customizable with the individual shanks having arbitrary heights controlled by a CAD program. We also demonstrate 3D printing of multi-layer, multi-material electrical wiring to carry the signals from the high-density probes, opening the possibility of custom probe layouts on arbitrary substrates. The 3D printed array shanks have low impedance

and high ductility without losing strength despite high aspect ratios. Spiking activity from individual neurons of anesthetized mice have been isolated with signal to noise ratios comparable to that of the current microelectrode technologies. The diameter of each shank - as small as 10um - also help reduce tissue damage and facilitate insertion. This advance in neural activity sampling will enable new experimental paradigms that will establish the micro-to-macroscale interactions of individual neurons across the brain.

A multimodal 3D neuro-microphysiological system with neurite-trapping microelectrodes

Beatriz Molina-Martínez^a, Laura-Victoria Jentsch^a, Fulya Ersoy^a, Matthijs van der Moolen^a, Stella Donato^b, Torbjørn V. Ness^c, Peter Heutink^b, Peter D. Jones^a and Paolo Cesare^{a,*}

- a. NMI Natural and Medical Sciences Institute at the University of Tübingen, 72770 Reutlingen, Germany Department 2, University 2, Address 2
- b. German Center for Neurodegenerative Diseases (DZNE) & Hertie Institute for Clinical Brain Research, 72076 Tübingen, Germany
- c. Faculty of Science and Technology, Norwegian University of Life Sciences, 1432 Ås, Norway

* paolo.cesare@nmi.de

Three-dimensional cell technologies as pre-clinical models are emerging tools for mimicking the structural and functional complexity of the nervous system. The accurate exploration of phenotypes in engineered 3D neuronal cultures, however, demands morphological, molecular and especially functional measurements. Particularly crucial is measurement of electrical activity of individual neurons with millisecond resolution. Here we describe a novel approach (see Figure 1), using multiwell glass microfluidic microelectrode arrays, allowing non-invasive electrical recording from engineered 3D neuronal cultures.

A core innovation [1] is represented by the addition of insulating caps on substrate-integrated microelectrodes (capped microelectrodes, CME), inspired by tunnels which enable neurite recordings from adherent neurons [2, 3]. Our system enables 3D cell culture in a hydrogel scaffold with unguided extension of neurites into the CME. We investigated this new capability to use a 2D MEA to record the electrical activity of 3D neuronal circuits with calcium imaging and optogenetic stimulation. We validated the nMPS as a screening platform with the neurotoxins picrotoxin and tetrodotoxin; recorded data showed excellent sensitivity and experimental reproducibility. Electrophysiological read-out identified effects of rotenone, a neurotoxic insecticide that induces a Parkinson's disease (PD) phenotype in animal models [4], with superior sensitivity and at earlier time-points than morphological or metabolic *in vitro* assays. In addition, we have demonstrated how its microplate-compatibility enables automated handling for improved throughput of cell culture and high-content imaging. We further evaluated the system with neurons derived from human induced pluripotent stem cells (hiPSC), supporting its use for modelling human physiology and disease.

Enabling the engineering of cell type, density and 3D organization of neuronal networks in a high-throughput platform for functional and structural analysis represents a major step towards more predictive preclinical models to facilitate the translation of therapies for human neurodegenerative disorders.

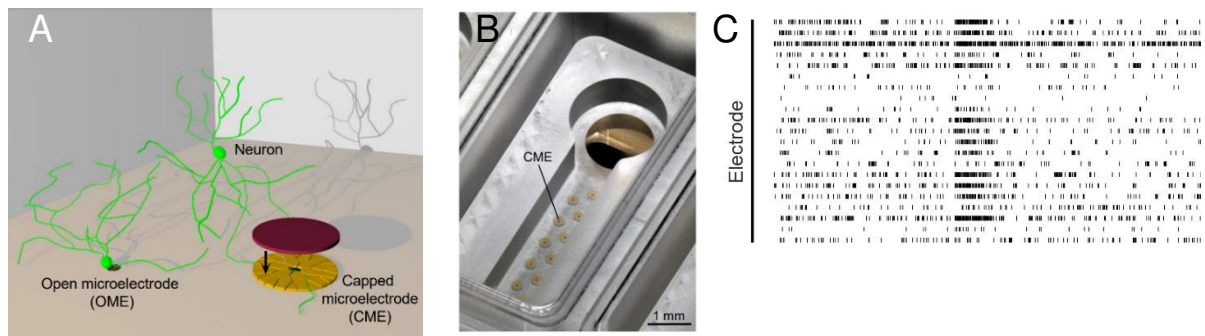


Figure 1: A microphysiological system for the recording of excitability in 3D neuronal networks A) Schematic drawing of the capped microelectrodes used for recording action potential along individual neurites extending in 3D. B) Picture of a recording unit, composed by a glass compartment for the cultivation of dissociated 3D neurons, and multiple capped microelectrodes integrated into the glass substrate. C) Representative recordings obtained from a 10 days old hippocampal neuronal culture.

References

1. Molina-Martínez B., et al. A multimodal 3D neuro-microphysiological system with neurite-trapping microelectrodes. *Biofabrication*. 2022;14(2):10.1088/1758-5090/ac463b. 2022 Jan 24. doi:10.1088/1758-5090/ac463b.
2. N Taylor, A.M., et al. A microfluidic culture platform for CNS axonal injury, regeneration and transport. *Nature Methods*, 2005. 2(8): p. 599–605. doi: 10.1038/nmeth777.
3. Pan, L., et al. Propagation of action potential activity in a predefined microtunnel neural network. *J Neural Eng*, 2011. 8(4): p. 046031. doi: 10.1088/1741-2560/8/4/046031.
4. Pan-Montojo, F., et al. Environmental toxins trigger PD-like progression via increased alpha-synuclein release from enteric neurons in mice. *Sci Rep*, 2012. 2: p. 898. doi: 10.1038/srep00898.

Development of functional in vitro model in Dravet syndrome patient hiPSC-derived cortical neurons

Ropafadzo Mzezewa¹, Tanja Hyvärinen¹, Jens Schuster², Niklas Dahl², Susanna Narkilahti^{1*}

1. Neurogroup, Faculty of Medicine and Health Technology, Tampere University, Tampere, Finland
2. Department of Immunology, Genetics and pathology, Uppsala University, Uppsala, Sweden

* susanna.narkilahti@tuni.fi

Intractable epilepsies that emerge in childhood, such as Dravet syndrome (DS), have limited response to current antiepileptic drugs (AEDs). DS patients are often typified by temperature sensitive seizures, along with other complexities like intellectual disability, sleep decline and sudden unexpected death in epilepsy, SUDEP[1]. New therapeutic drugs are therefore needed, as most patients are unresponsive to current AEDs. However, to obtain this, relevant preclinical models are needed. DS is mainly caused by a mutation in the SCN1A gene which is crucial for generating and propagating action potentials. Heterozygous mutation in SCN1A gene leads to loss of sodium currents and action potentials, resulting in reduced neural excitation and ultimately seizure formations [2]. Mouse models and in vitro based human induced pluripotent stem cell (hiPSCs) models have shown that the reduced sodium current density and impaired excitation due to the mutation, primarily affects the GABAergic inhibitory interneurons[2] [3]. Thus far most of the electrophysiological findings have been performed using whole-cell patch clamp [4], and only few have studied this phenomenon at the network level. Here we investigated the functional alteration in hiPSCs of Dravet Syndrome using microelectrode arrays (MEAs). We generated two different subtypes of neural cultures: glutamatergic [5] and GABAergic [6] enriched cultures from DS patient lines and control lines (*Figure 1A*). When cultured on MEAs we observe that DS neurons display a distinctive neuronal activity pattern compared to control neurons (*Figure 1B*). Furthermore, preliminary data reveals that DS neurons portray more sensitivity in response to specific pharmacological treatments. This study highlights the applicability of disease modelling with hiPSCs and MEAs as a valuable platform to reveal underlying disease mechanisms.

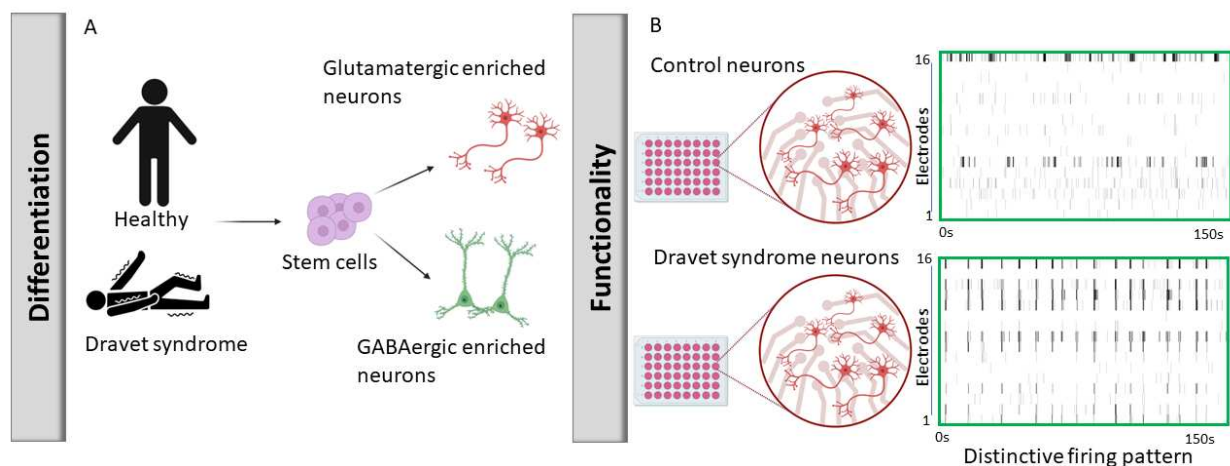


Figure 1: Graphical abstract highlighting the proposed model of DS in vitro. (A) Two sub-population of neurons generated from hiPSCs of DS neurons and healthy controls. (B) Preliminary functional studies with raster plots showing 2min segments of neuronal activity from both control and DS lines. DS neurons portray a more rapid and distinctive network firing pattern in comparison to control cultures. Representative raster is from days in vitro (DIV83).

References:

- [1] J. Ding *et al.*, 'SCN1A Mutation-Beyond Dravet Syndrome: A Systematic Review and Narrative Synthesis', *Front. Neurol.*, vol. 12, p. 743726, 2021, doi: 10.3389/fneur.2021.743726.
- [2] N. Higurashi *et al.*, 'A human Dravet syndrome model from patient induced pluripotent stem cells', *Mol. Brain*, vol. 6, no. 1, p. 19, May 2013, doi: 10.1186/1756-6606-6-19.
- [3] M. Favero, N. P. Sotuyo, E. Lopez, J. A. Kearney, and E. M. Goldberg, 'A Transient Developmental Window of Fast-Spiking Interneuron Dysfunction in a Mouse Model of Dravet Syndrome', *J. Neurosci. Off. J. Soc. Neurosci.*, vol. 38, no. 36, pp. 7912–7927, Sep. 2018, doi: 10.1523/JNEUROSCI.0193-18.2018.
- [4] Y. Sun *et al.*, 'A deleterious Nav1.1 mutation selectively impairs telencephalic inhibitory neurons derived from Dravet Syndrome patients', *eLife*, vol. 5, p. e13073, Jul. 2016, doi: 10.7554/eLife.13073.
- [5] T. Hyvärinen *et al.*, 'Functional characterization of human pluripotent stem cell-derived cortical networks differentiated on laminin-521 substrate: comparison to rat cortical cultures', *Sci. Rep.*, vol. 9, no. 1, p. 17125, Dec. 2019, doi: 10.1038/s41598-019-53647-8.
- [6] J. Schuster *et al.*, 'Transcriptomes of Dravet syndrome iPSC derived GABAergic cells reveal dysregulated pathways for chromatin remodeling and neurodevelopment', *Neurobiol. Dis.*, vol. 132, p. 104583, Dec. 2019, doi: 10.1016/j.nbd.2019.104583.

Development of a microelectrode array with embedded microfluidic inputs for electroporation of retinal slices

Lena Hegel,^a Andrea Kauth,^a Sandra Johnen,^b Sven Ingebrandt,^a

- a. Institute of Materials in Electrical Engineering 1, RWTH Aachen University, Sommerfeldstr. 24, 52074 Aachen
 - b. Department of Ophthalmology, RWTH Aachen University, Pauwelsstr. 30, 52074 Aachen
- * ingebrandt@iwe1.rwth-aachen.de

Worldwide, about three million people suffer from one of the various forms of Retinitis pigmentosa (RP). It describes an inherited eye diseases that result in gradual loss of the photoreceptors and hence a degeneration of the retina. Worldwide, there have been intensive activities to develop various forms of retinal implants to restore vision to these patients. However, the performance of current retinal prostheses is limited in terms of the resolution of objects and the size of the field of view [1]. In addition to an insufficient number of stimulation electrodes, previous versions of retinal prostheses did not take into account that the photoreceptors degenerate during the progression of RP and that a functional reorganization of the remaining neuronal cells takes place [2]. Therefore, basic research in the field of retinal implants is being restarted in the interdisciplinary research-training-group InnoRetVisionⁱ (GRK2610). The focus is on developing novel stimulation methods and improving the accessibility of different ganglion cells for stimulation in the retina. One characteristic of RP studied in rd10-mouse retinae are oscillations in the range of 3 to 6 Hz that were recorded in retinal ganglion cell spiking and in local field potentials. These oscillations need to be suppressed for successful stimulation [3]. Electroporation is a promising research approach for potential treatment of the inhibitory degeneration [4] and to suppress oscillations in neuronal retina cells. Electroporation uses electric fields generated by short voltage pulses to create reversible pores in the membrane of cells. Plasmid DNA encoding genes or therapeutic sequences can then be introduced through these pores to initiate the production of neuroprotective substances from the transfected cells [5, 6].

In previous projects, a microelectrode array (MEA) was developed for *in-vitro* electroporation. The electrode design was optimized in terms of shape, size and spacing such that the electric field is as homogeneous as possible. With low voltages (1-2V) to protect the electrode surface, sufficiently high field strengths (15-100 kV/m) are generated to electroporate cells [7].

In the present study, local chemical addressing by a chip-embedded microfluidics is added to the optimized MEA design. The electrodes are lithographically patterned with a lift-off process on the glass wafer from a 30 nm chromium and 100 nm gold layer. With the help of SUEXTM hard resist (K25, micro resist technology GmbH, Berlin), an integrated microfluidic system is lithographically structured above the electrode layer. For better compatibility in cell culture, the chip is passivated with parylene-C. After the chip has been bonded to a customized PCB carrier, the fluidic channels are contacted from above with tubes and 3-d-printed connectors (figure 1A, B). For successful electroporation, the amount of plasmid will be applied as locally and temporally precise as possible. In addition, the fluid ports could press the retina slices closer to the MEA due to a slight negative pressure in the fluid system to improve the contact between the electrode array and the slice (figure 1C, D).

With this technological development, we aim to lay the foundation of a next generation of retinal implants for genetic modification and function adaptation during retinal degeneration.

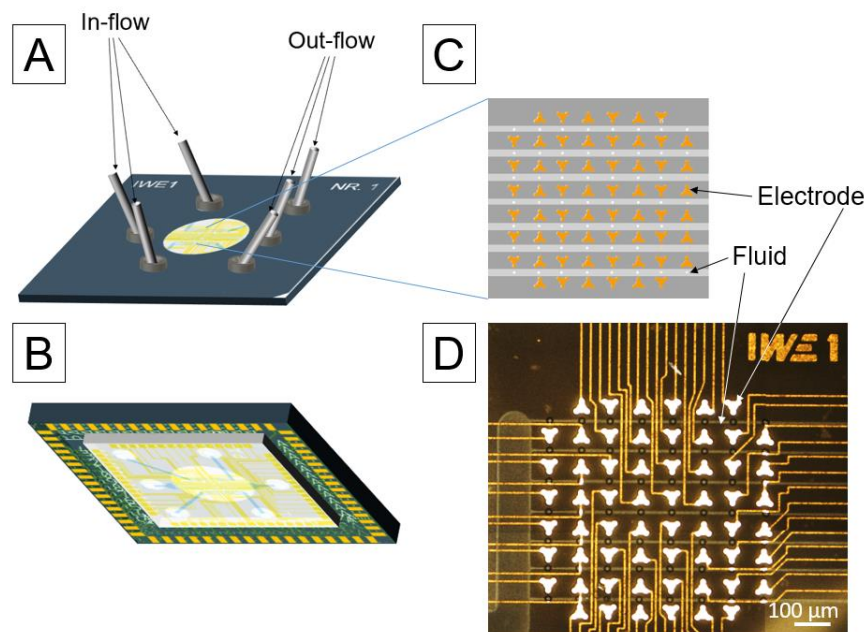


Figure 1: Schematic representation of the fluidics MEA: A) top view of the chip bonded to the PCB carrier with fluidic connections, B) bottom view of the PCB carrier with electrical connections and chip, C) closer view of the electrode design with fluidic outputs, D) Microscope image of the electrode array with microfluidic channels.

References

1. Ayton, L. N., Barnes, N., Dagnelie, G., Fujikado, T., Goetz, G., Hornig, R., Jones, B. W., Muqit, M. M. K., Rathbun, D. L., Stingl, K., Weiland, J. D., and Petoe, M. A., (2020), An update on retinal prostheses. *Clin Neurophysiol.* 131(6): 1383-1398. doi:10.1016/j.clinph.2019.11.029.
2. Haselier, C., Biswas, S., Rosch, S., Thumann, G., Muller, F., and Walter, P., (2017), Correlations between specific patterns of spontaneous activity and stimulation efficiency in degenerated retina. *PLoS One.* 12(12): 1-16. doi:10.1371/journal.pone.0190048.
3. Gehlen, J., Esser, S., Schaffrath, K., Johnen, S., Walter, P., and Muller, F., (2020), Blockade of Retinal Oscillations by Benzodiazepines Improves Efficiency of Electrical Stimulation in the Mouse Model of RP, rd10. *Invest Ophthalmol Vis Sci.* 61(13): 37. doi:10.1167/iovs.61.13.37.
4. Johnen, S., Kazanskaya, O., Armogan, N., Stickelmann, C., Stocker, M., Walter, P., and Thumann, G., (2011), Endogenous regulation of proliferation and zinc transporters by pigment epithelial cells nonvirally transfected with PEDF. *Invest Ophthalmol Vis Sci.* 52(8): 5400-7. doi:10.1167/iovs.10-6178.
5. Thumann, G., Stocker, M., Maltusch, C., Salz, A. K., Barth, S., Walter, P., and Johnen, S., (2010), High efficiency non-viral transfection of retinal and iris pigment epithelial cells with pigment epithelium-derived factor. *Gene Ther.* 17(2): 181-189. doi:10.1038/gt.2009.124.
6. Neumann, E., (1992), Membrane Electroporation and Direct Gene-Transfer. *Bioelectrochemistry and Bioenergetics.* 28(1-2): 247-267. doi:10.1016/0302-4598(92)80017-B.
7. Diarra, S., Waschkowski, F., Moreno, A. G., Haselier, C., Hesse, S., Izsvák, Z., Ivics, Z., Thumann, G., Muller, F., Mokwa, W., Johnen, S., and Walter, P., (2017), Efficient electrotransfer-mediated transfection of rd10 retinas using the non-viral Sleeping Beauty transposon system. *Investigative Ophthalmology & Visual Science.* 58(8).

ⁱ Funded by the Deutsche Forschungsgemeinschaft (DFG, German Research Foundation), GRK2610/1 - project number 424556709

Evaluation of a novel *in vitro* neurocardiac cellular model for the study of heart disorders.

Cattelan Giada^{a*}, Gentile Giovanna^{a,b}, Laura Sophie Frommelt^a, Alexandros Lavdas^a, Luisa Foco^a, De Bortoli Marzia^a, Katarina Mackova^a, Giulio Ciucci^c, Serena Zacchigna^c, Peter P Pramstaller^a, Pichler Irene^a, Zanon Alessandra^a, Rossini Alessandra^a.

- a. Eurac Research, Institute for Biomedicine (Affiliated institute of the University of Lübeck), Bolzano, Italy
- b. Faculty of science and technology, University of Bolzano, Bolzano (BZ) Italy
- c. Cardiovascular Biology Laboratory, International Centre for Genetic Engineering and Biotechnology (ICGEB), Trieste (TS), Italy

* giada.cattelan@eurac.edu

The cardiac autonomic nervous system (CANS) is widely recognized as an important player in many cardiac disorders, such as arrhythmogenic cardiomyopathy, catecholaminergic polymorphic ventricular tachycardia, ventricular tachyarrhythmia and heart failure [1]. The mechanisms of neuronal control of cardiac disease remain elusive, largely due to the lack of proper human cell models. To overcome this limitation, we have created an *in vitro* neurocardiac model system by using a silicon-based two-wells insert (Ibidi) with a defined cell-free gap for the co-culture of human iPSC-derived cardiomyocytes (iPSC-CMs) and sympathetic neurons (iPSC-SNs). Here we describe the assessment of the physiological activity of this co-culture model, using a Maestro Edge Multi-Electrode Array (MEA, Axion Biosystems) (see Figure 1). In particular, by evaluating the 3D surface reconstruction of the expression of the presynaptic marker protein Synapsin 1 (Syn1) and the sarcomeric protein α -actinin, we observed a punctate staining of varicosities suggesting multiple synaptic connections between the iPSC-CMs and the iPSC-SNs. In addition, to verify whether the iPSC-SNs were forming functional connections with the iPSC-CMs and therefore affect their activity, we have evaluated the electrical properties of iPSC-CMs after nicotine treatment, that specifically stimulates sympathetic neurons. Preliminary evidence indicates that in the presence of iPSC-SNs the beating rate of iPSC-CMs is selectively increased after nicotine stimulation. Furthermore, it has been observed that through electrical stimulation of iPSC-SNs it is also possible to modulate the beating rate of iPSC-CMs. This neurocardiac model provides a promising tool to model a wide range of cardiac but also neurological pathologies, as well as for drug screening and personalized approaches.

Funding acknowledgements:

Funded by the European Regional Development Fund and Interreg V-A Italy-Austria 2014-2020 and by the Department of Innovation, Research and University of the Autonomous Province of Bolzano-South Tyrol (Italy).

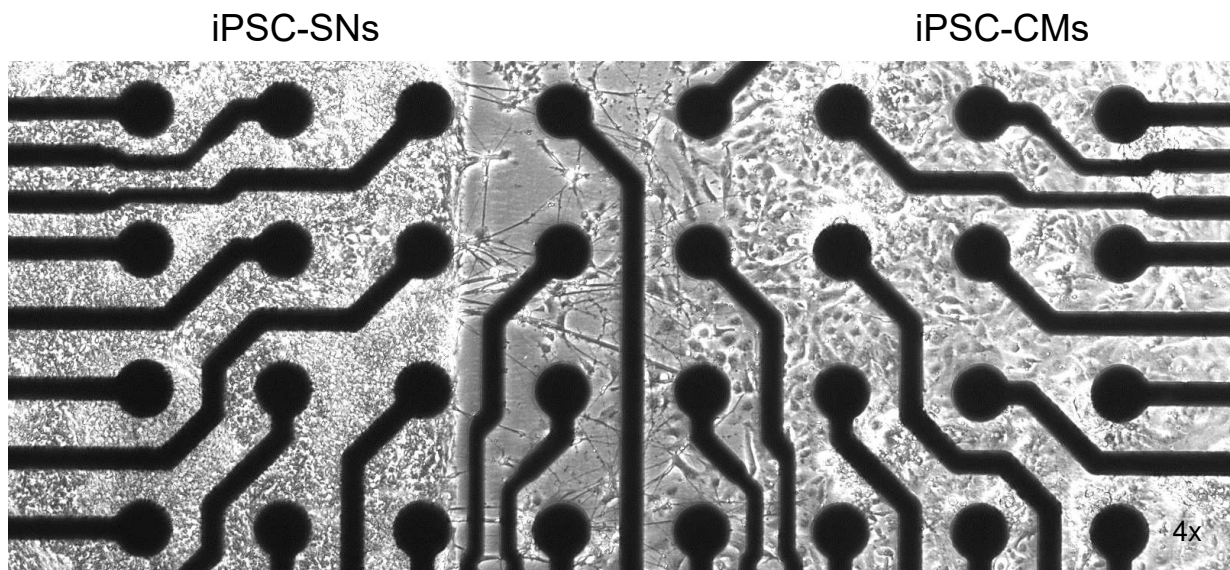


Figure 1: A brightfield image of a neurocardiac co-culture plated on MEA-plate. iPSC-SNs are plated on the left side and iPSC-CMs on the right side. In the middle it is possible to observe the interconnection between the two cell populations, with axons extending and reaching the iPSC-CMs.

References

1. Fedele, L. and T. Brand, *The Intrinsic Cardiac Nervous System and Its Role in Cardiac Pacemaking and Conduction*. *Journal of cardiovascular development and disease*, 2020. 7(4): p. 54